

# **TECHNICS. TECHNOLOGY. EDUCATION. SAFETY.**

VELIKO TARNOVO, 01-03.06.2016



# **PROCEEDINGS**

ISSN 1310-3946 ISSUE 8 (194) JUNE 2016 YEAR XXIV

## **VOLUME 1**

**TRANSPORT TECHNICS AND TECHNOLOGIES. SECURITY AND ECOLOGY.  
MECHANICS, DYNAMICS, STRENGTH. ANALYSIS OF ELEMENTS.**



Published by  
Scientific technical  
Union of Mechanical Engineering



**НАУЧНИ  
ИЗВЕСТИЯ**

**SCIENTIFIC TECHNICAL UNION OF MECHANICAL ENGINEERING**

**YEAR XXIV**

**ISSUE 8 (194)**

**JUNE 2016.**

**INTERNATIONAL SCIENTIFIC TECHNICAL CONFERENCE**

**TECHNICS. TECHNOLOGIES.  
EDUCATION. SAFETY '16**

**PROCEEDINGS**

**VOLUME 1**

**TRANSPORT TECHNICS AND TECHNOLOGIES. SECURITY AND ECOLOGY.  
MECHANICS, DYNAMICS, STRENGTH. ANALYSIS OF ELEMENTS.**

**01-03 JUNE, 2016  
VELIKO TARNOVO**

**Publisher:** Scientific technical union of mechanical engineering

**ISSN: 1310 – 3946**

# CREATION OF ACCUMULATION AND STORAGE OF ELECTRICAL ENERGY FOR DRIVERLESS ELECTRIC VEHICLES OF RUSSIAN PRODUCTION

## СОЗДАНИЕ СИСТЕМЫ НАКОПЛЕНИЯ И ХРАНЕНИЯ ЭЛЕКТРИЧЕСКОЙ ЭНЕРГИИ ДЛЯ БЕСПИЛОТНЫХ ЭЛЕКТРИЧЕСКИХ ТРАНСПОРТНЫХ СРЕДСТВ РОССИЙСКОГО ПРОИЗВОДСТВА

Ph.D., Ass. Prof. Kurmaev R.Kh.<sup>1</sup>, Ph.D. Karpukhin K.E.<sup>2</sup>, Ph.D. Terenchenko A.S.<sup>3</sup>, D.Sc. Saykin A.M.<sup>4</sup>, Struchkov V.S.<sup>5</sup>  
Head of Department <sup>1,2</sup>, Head of Centre <sup>3,4</sup>, Head of sector <sup>5</sup> –NAMI Russian State Research Center (FSUE “NAMI”), Moscow, Russia  
rinat.kurmaev@nami.ru, k.karpukhin@nami.ru, terenchenko@nami.ru, a.saykin@nami.ru, v.struchkov@nami.ru

**Abstract:** In recent years, many researches in the field of electromobile transport using as driverless vehicle are carried out in Russia as in the world. Operation electromobile transport in Russia has specific features, among which are the cold climate and heavy traffic conditions. One of the key elements of the functioning of electromobile transport is an energy storage system, the characteristics of which are highly dependent on how and under what conditions the vehicle is operated. The life of the energy storage system is also adversely affected by high temperature and short overvoltage on its elements. To increase the mileage of vehicles on the electric energy storage provides an improved system design, and in this article the experience of creating such an energy storage system for the driverless vehicle, taking into account including the Russian operating conditions. In the process of creating energy storage system were carried out calculations, mathematical and natural layout the basic elements of the system.

**KEYWORDS:** VEHICLE, DRIVERLESS VEHICLE, ELECTRIC VEHICLE, THE DRIVE OF THE ELECTRIC ENERGY, ENERGY EFFICIENCY

### 1. Introduction

International experience, based on the trends of increasing safety, reducing toxicity and fuel consumption, and, consequently, improve energy efficiency of vehicles, shows the priority of development for the creation of driverless vehicles [1]. In recent years, Russia, as well as studies conducted worldwide, associated with the use electromobile transport as driverless vehicles.

### 2. Preconditions and means for resolving the problem

Operation electromobile transport in Russia has specific features. The main factor that distinguishes the Russian operating conditions - a cold climate. Russia is located in the vast territory of the Eurasian continent and has a variety of climatic conditions. For the Russian Federation as a whole number of days per year with an average daily temperature of 0 °C or less - an average of 171 days, ie, 47% of calendar time of the year [2]. It should be noted that manufacturers claimed electric performance indicators, in particular the power reserve and the required charging time is often not focused on the realities of Russia, and the Central European climate zone, excellent road and charging infrastructure. At the same time these figures are a measure of the applicability of electric transport in the conditions of everyday life. The above-mentioned Russian conditions will undoubtedly affect the initial stated performance values.

One of the key elements of the functioning of electric vehicle is an energy storage system (high voltage battery), the characteristics of which are highly dependent on how and under what conditions is operated by the vehicle on which it is installed [3]. The Center test "NAMI" were conducted bench tests of the effect of ambient temperature on the operational performance electric car. The electric vehicle Nissan Leaf was taken as the test vehicle. Its electric power is 80 kW, and the capacity of the rechargeable Lithium-battery 24 kWh. At the same time declared maximum cruising range of 160 km. As a result of the test [2] found that the lowering of the outdoor temperature to + 25 °C to minus 7 °C causes a reduction in power reserve of 9% and 44% when consumers.

The challenge of operating energy storage system in terms of working for them is extremely important. Research results depending on the battery temperature gradient [4] shown in Figure 1. As shown, the battery power reaches a maximum when charging in the temperature range from + 20 °C to plus 40 °C. To avoid heat problems and achieve better battery performance, it is necessary to

maintain the temperature range that affects the battery and its life cycle.

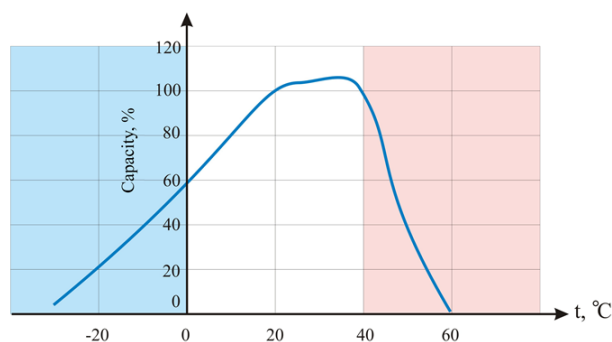


Fig. 1 Dependence of battery charge on the temperature changes

To increase the mileage of vehicles on the electric energy storage provides an improved system design, and in this article the experience of creating such an energy storage system for driverless vehicles, taking into account the Russian operating conditions. In the process of creating energy storage system were carried out calculations, mathematical and natural layout the basic elements of the system.

Currently there are many different types of batteries (chemical sources of electrical energy).

Using rechargeable batteries in electric transport places demands on them: a large energy consumption; high rate of resource; relatively low cost [5]. Further, the way these requirements are the main products manufactured and preparing for mass production of the types of batteries (rechargeable battery):

- Traction lead-acid batteries;
- Nickel-metal hydride batteries;
- Lithium - ion battery (Li-Ion);
- Lithium-polymer battery;
- Lithium-iron-phosphate and lithium-iron-phosphate sodium batteries;
- Lithium-cobalt batteries;
- Batteries with lithium titanate anode;
- Battery modified lithium titanate;
- Supercapacitors.

Modern battery systems and electric vehicles with the combined power plants are based on lithium-ion batteries of different types of electrochemical systems.

Comparative characteristics of the main types of battery are shown in Table 1, and the characteristics of the most widely represented in the battery world market are shown in Table 2.

**Table 1. Characteristics of the main types of batteries**

Parameter	Lithium-ion battery ALTAIR-NANO (50 Ah)	lead acid battery	Prism AMP20M 1HD-AA-123 systems	Lithium-ion (modified titanate) SSK
Operating temp. range, °C	-40...+55	+5...+50	-30...+55	-40...+55
Recommended storage temp., °C	-40...+55	-5...+50	-40...+55	-40...+55
Rated voltage, V	2.3	2.0	3.3	3.7
Rated capacity (1C charge / discharge 1C), Ah	50	72	20	25
Weight cell, kg	1,6r	17r	0,496	0,6
Dimensions (LxWxH, mm)	256x259x13	134x219x274	245x160x7,25	227x226x4,2
Nominal energy, 1C at 25 °C, Wh/kg	72	30	130	254
Life (25°C), year	20	10	15	15
The number of cycles at a charge 2C, a discharge 2C, at 100% depth of discharge at 25 °C	>12000	1500	3000	8000

**Table 2. Characteristics of produced batteries**

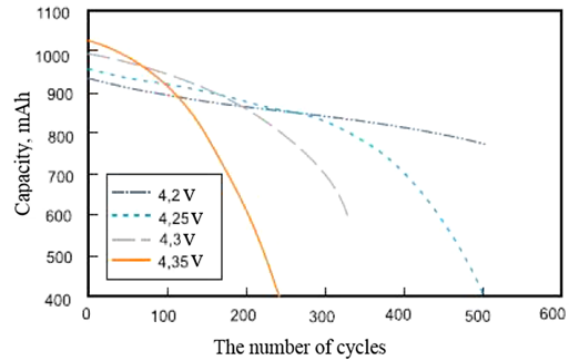
Manufacturer	Capacity, Ah	Rated voltage, B	The number of cycles	Specific energy capacity, Wh / kg	Temperature range, C
A123 Systems	20	3,3	≤3000	130	-30/+55
Altair Nano	50	2,3	≤16000	72	-40/+55
Ener1 Battery	16,7/40	3,3-3,7	-	150	0/+45
Dow Kokam	5/200	3,6	>800	125/185	0/+40
Saft Batteries	41	3,2	>1500	136	-25/+60
BYD	40/1000	3,2	>3000	100/120	-45/+85
International Bat	40/160	3,2	>3000	88/97	0/+50
Valence Tech.	40/138	12,8	>2500	19/91	-10/+50
AK Riegel	15/260	3,6	<1000	100/120	-30/+50

When using the battery must take into account the following factors. Modern batteries at nominal operating lithium - reactive element in its pure form is not available, however, when emergency situations (excessive charge or discharge current, short-circuit currents, overcharge or above overcharging below certain voltage levels on batteries) can be allocated to the internal battery electrodes that in certain cases can lead to fire and explosion.

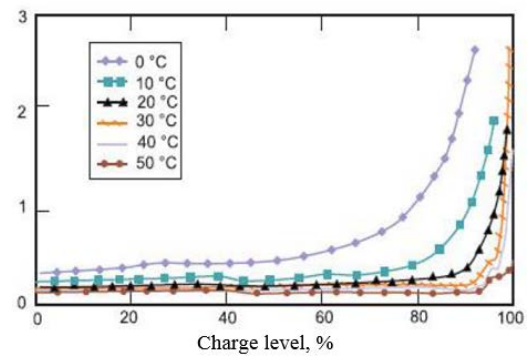
Battery allow the formation of parallel chains of n batteries to provide the necessary capacity. Required battery voltage is provided by a serial connection of individual cells or strings of n parallel-connected batteries. Thus, when connecting the battery by parallel-series connection can construct a given battery capacity and voltage. At the same time, however, each battery or each chain of parallel connected batteries requires strict control. When charging the battery of the series-connected battery charge individual elements is uneven, owing to technological scatter internal resistance of batteries, or an uneven decrease in battery capacity due to aging in service. Batteries with reduced capacity or high internal resistance tend to be large fluctuations of voltage during charge and discharge. When strictly fixed final charge voltage and discharge for a separate battery, increasing from cycle (charge-discharge) to cycle the charge difference will lead to gradually increasing imbalance of battery cells, that is, in fact, a decrease of given capacity [6.7].

Also, during charging and discharging is necessary to protect the battery from overheating. High temperatures and at short overvoltage element can cause a significant reduction in lifetime [8]. Figure 2 shows that the charge element even at 50 mV above

the maximum service life decreases to 50% of this for him. Figure 3 shows that the elements discharged more than 80% show a fivefold increase of the internal resistance (milliohms from 0,3 ohm to greater than 1.5 ohm) when the temperature changes from room temperature to 0 °C.



**Fig. 2 The effect of the charging voltage at the battery service life**



**Fig. 3 The dependence of the internal resistance of the lithium - ion battery temperature and depth of discharge**

Thus, for safety reasons, and improve performance of the batteries should include monitoring and control system, which provides control of the parameters of batteries during the operation of the battery.

Monitoring and control system is compulsorily provide control voltages and battery charge-discharge currents; introduction of other functions is not mandatory, but it can improve the performance of the battery. Alignment voltages of series-connected batteries, the battery allows to operate with the greatest possible impact capacity, capacity calculation system allows the dedicated charging device to control the battery and allows the user to estimate the time remaining until the end of charge or discharge.

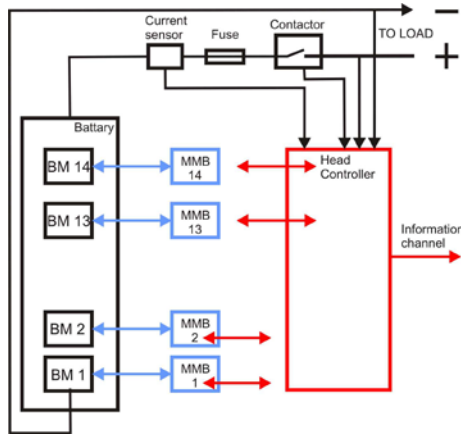
NAMI Russian research centre is currently underway to establish an experimental sample of driverless electric vehicle. For the vehicle (Figure 4), and developed the electric power storage system designed for inspection and research developed technical solutions in the field of electric power traction unit, the monitoring algorithms and active balancing of individual batteries and battery, taking into account Russian conditions.

In the process of creating energy storage system were carried out calculations, mathematical and natural layout the basic elements of the system. The use of modern software systems in the development of the battery allows you to automate the design process and perform optimization effectively. Numerical modeling has allowed to determine the required capacity of the energy storage system developed for the driverless vehicle's electric range, which should be at the level of 12 kWh.



**Fig. 4** Appearance a driverless vehicle on electric

Structural and functional diagram of the developed electric power storage system is shown in Figure 5.



**Fig. 5** Structural and functional power storage system scheme. BM - battery module; MMB - module monitoring and balancing

The circuit operates as follows. Head controller and MMB are powered by an external power supply of 12 V. When this power head controller polls all blocks MMB and in the absence of extraordinary events include the contactor. Battery ready for use. According to information channel information on the state of individual battery cells, BM temperature and charge level of the battery supplied to external observation device. In that case, if the voltage at the individual battery cells are different by more than 5 mV, the circuit includes an active cell balancing voltage is above average across the battery.

Monitoring and balancing module is built in a modular fashion. Each MMB module allows you to balance up to 12 cells.

To implement the power storage system prismatic batteries AMP20M1HD-A were selected having the following characteristics:

- nominal capacity of 20 Ah (at + 25 °C);
- the specific energy consumption of 130 Wh / kg;
- rated voltage: 3.3 V;
- maximum voltage: 3.65 V;
- the internal resistance of 0.6 milliohms;
- nominal direct current discharge: 3-5S (up to 100 A);
- maximum pulse discharge current: 20C (400A);
- the maximum allowable charge current: 3c;
- service temperature range: - 30 ... + 55 °C;
- the number of working cycles of at least 2000, at 80% depth of discharge.

Developed electric power storage system is comprised of eight modules 12 containing batteries AMP20M1HD-A - only 96 storage locations.

Voltage rating - 316.8 V. The total internal resistance – 0.576 ohm or 0.0576 ohm. The charging current from the on-board charger - 12.5 A. Power battery heat is 9 W.

Lithium batteries, as previously mentioned above have the disadvantage, as the negative effect of increasing the battery temperature during operation with an intense impact on the current

period of battery operation. It affects all hybrid and electric cars. At constant overheating, the duration of use of the battery is reduced from 5-6 years to 2-4.

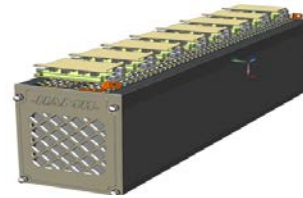
In the design of the power storage system is necessary to determine the need for cooling [9,10].

Calculation of heat energy is advantageously carried out with the assistance of mathematical modeling. For the computational simulation studies the mathematical model of the car VAZ - 1117, taken as a basis for development, developed with battery, used AVL CRUISE package.

According to calculations conducted by Regulation №83 of the UNECE to fast charge mode for cycle developed system power savings without forced cooling, heat up by only 5,0 °C and 2,46 °C respectively. Experience has shown that the resulting heat will be compensated through the housing wall of the battery.

Developed by the original electric power storage system due to new technical solutions for system charge redistribution between the battery cells can significantly extend the life of the batteries, which greatly improves the reliability and cost-effectiveness.

Based on the calculations and analysis of the design features of the construction of electricity storage systems based on lithium batteries, it was carried out development of conceptual design documentation for the experimental model of the power storage system. Figure 6 shows general 3D model developed type power storage systems (without cover).



**Fig. 6** 3D model of the general form of the developed electric power storage system

### 3. Results

On the basis of preliminary modeling of the main functional units and developed design documentation were made experimental rechargeable traction battery module samples in the amount of two copies of the total power consumption of 13 kWh.

The experimental sample of the traction battery module is shown in Figure 7.



**Fig. 7** The experimental sample storage module of the traction battery

The experimental sample rechargeable traction battery module has a plastic housing. The sides of the body have vent holes. Within each housing 48 placed on the battery cells, each battery cell is mounted in a cradle.

Battery cells are arranged in such a way that a number of positive findings of odd cells are arranged even negative findings. Quality contact had polar conclusions of storage cells provide a copper plate that secure the output terminals and tighten the three screws. One of the screws used to attach information - balancing conductor. The form framework provides a natural convection

ventilation. According to calculations, confirmed by the practice of this heatsink is sufficient for normal operation of the battery in the operating conditions of the developed vehicle.

Monitoring and control system battery is placed in the upper part, above the copper contacts. It represents four payment. Each board operates 12 cells. Monitoring and control system battery is shown in Figure 8.



*Fig. 8 Balancing boards*

Designed monitoring and control system battery allows monitoring and balancing of the battery cells, to determine the integrity of the battery state circuits, voltage and cell temperature. The transmission of information takes place in the unit Battery Management System (BMS), which provides communication, configuration and diagnosis of the battery control unit or with a PC via COM port or through the CAN. Designed traction battery module design experimental prototype driverless vehicle provides reliable internal block contacts and the necessary noise immunity control system.

Figure 9 shows an experimental model of a driverless vehicle with the established in the luggage compartment of the traction unit batteries.



*Fig. 9 Experimental model of a driverless vehicle with the energy storage system*

#### 4. Conclusion

Currently, experimental studies of a driverless vehicle with a developed energy storage system, which should confirm or refute the effectiveness of the design of the battery. This scientific study was conducted with the financial support of the state in the face of Russian Ministry of Education, the project unique identifier RFMEF162514X0006.

#### 5. References

- [1] John Wiley & Sons Ltd. Encyclopedia of Automotive Engineering, Online © 2014, p.2696.
- [2] Terenchenko A., Karpukhin K., Kurmaev R. Features of operation of electromobile transport in the conditions of Russia. Paper of EVS 28 International Electric Vehicle Symposium and Exhibition, KINTEX, Korea, 2015.
- [3] Slabosritsky R.P., Khazhmuradov M.A., Lukyanova V.P. Studying of battery cooling system. Radioelectronics and informatics, 2012, No.2, pp. 5-8.
- [4] Kurmaev R.H., Terenchenko A.S., Karpukhin K.E., Struchkov V.S., Zinov'ev E.V. Maintaining the required temperature of high-voltage batteries in electric cars and hybrid vehicles. Russian engineering research, 2015, vol. 35, No. 9, pp. 666-669.1. S.A.
- [5] Karpukhin K.E., Kozlov A.V., Terenchenko A.S., Bakhmutov S.V. Comprehensive life cycle analysis of different types of energy storage for electric or hybrid vehicle. ICAT 2015. Proceeding the international conference on automobile technology for VIETNAM, 2015. pp. 7-14.
- [6] Abdullah AL-Refai, Osamah Rawashdeh, Rami Abousleiman. An Experimental Survey of Li-Ion Battery Charging Methods. SAE International Journal of Alternative Powertrains, 2016, No. 5 (1)
- [7] Karpukhin K.E., Terenchenko A.S., Shorin A.A. Balancing parameters for a storage battery. Russian engineering research, 2016, vol. 36, No. 2, pp. 86-88.
- [8] Karpukhin K.E., Terenchenko A.S., Shorin A.A., Bakhmutov S.V., Kurmaev R.H. Temperature control of the battery for hybrid or electric vehicle. Biosciences biotechnology research Asia, Vol. 12 (2), 2015. P. 1297-1301.
- [9] Pesaran A. Battery Thermal Management in EVs and HEVs: Is-sues and Solutions. National Renewable Energy Laboratory. 1617 Cole Blvd. Golden, Colorado 80401. Advanced Automotive Battery Conference. Las Vegas, Nevada, 2001.
- [10] Slabosritsky R.P., Khazhmuradov M.A., Lukyanova V.P. Analysis and calculation of battery cooling system. Radioelectronics and informatics, (2011), No.3, pp. 3-8.

# ALTERNATIVE FUELS FOR DIESEL ENGINES AND THEIR IMPACT ON ENGINE EMISSIONS. A LITERATURE REVIEW

Zbarcea O. PhD student, Prof. Scarpete D.  
"Dunarea de Jos" University of Galati, Romania

dan.scarpete@ugal.ro

**Abstract:** Today, there is a significant interest in alternative energy sources for vehicles, as a result of continuous concern for the environmental impact and for consumption of the primary energy sources, which are limited. Diesel engines present particularly significant emission like nitrogen oxides, particulate matter, hydrocarbons and black smoke. This paper present a literature review on some alternative fuels for diesel engines, as pure plant oil, biodiesel and compressed natural gas, and their impact on diesel engine emissions.

**Keywords:** DIESEL ENGINE, PURE PLANT OIL, BIODIESEL, CNG, EMISSIONS

## 1. Introduction

Compression ignition (CI) engines are the most popular prime-movers for transportation sector as well as for stationary applications [1]. Global increasing demands for energy, declining fossil fuel reserves, environmental concerns, and rising prices have resulted in a growing interest in the development of alternative renewable energy source [2].

Petroleum reserves are rapidly and continuously depleting at an alarming pace and there is an urgent need to find alternative energy resources to control both, the global warming and the air pollution, which is primarily attributed to combustion of fossil fuels [1].

In order to meet the energy requirements, there has been growing interest in alternative fuels like vegetable oils, biodiesels, biogas, LPG, CNG to provide a suitable diesel oil substitute for internal combustion engine [3].

Biodiesel production is not something new, because the concept of using vegetable oil as fuel dates back to 1895. Rudolf Diesel developed the first diesel engine which has run with vegetable oil in 1900. The first engine has run using groundnut oil as fuel [4].

The promotion of biofuels as energy for transportation in the industrialized countries is mainly driven by the perspective of oil depletion, the concerns about energy security and global warming. However due to sustainability constraints, biofuels will replace only 10 to 15% of fossil liquid fuels in the transport sector [5].

Fossil fuels are expected to continue supplying much of the energy used worldwide. Although liquid fuels remain the largest source of energy, their share of world marketed energy consumption is projected to fall from 35% in 2007 to 30% in 2035 (Fig. 1). The decline is due to projected high world oil prices that lead energy users to switch away from liquid fuels when possible [6].

Although diesel engines are more efficient than gasoline engines

of the same power, and this results in lower fuel consumption and thus in lower carbon dioxide emissions [7], the problem associated with the emissions of smoke, PM, sulfur oxide ( $SO_x$ ), PAHs, and odor from the exhaust of diesel engines has been widely been a concern in many countries [8].

Diesel engine exhaust is a complex mixture of carbon dioxide, oxygen, nitrogen, nitrogen compounds, carbon monoxide, water vapor, sulfur compounds and numerous low and high molecular weight hydrocarbons, and particulate matter [9].

Exhaust gas emissions of IC engines have been considered a very serious issue regarding air quality and the environment [10] and, therefore, developing and seeking alternative diesel fuels, without modifying engines, has become an important issue [8].

To this context, this paper presents a review of some alternative fuel, like pure plant oil, biodiesel and compressed natural gas, and their impact on diesel engine emissions.

## 2. Pure plant oil as fuel for diesel engine

As an alternative fuel for compression ignition engines, plant oils are in principle renewable and carbon neutral. However, their use raises technical, economic and environmental issues. A comprehensive and up-to-date technical review of using both edible and non-edible plant oils (either pure or as blends with fossil diesel) in CI engines, based on comparisons with standard diesel fuel, has been carried out [4].

Pure plant oil (PPO), also referred as PVO (Pure Vegetable Oil) or SVO (Straight Vegetable Oil), is the use of plant and vegetable oils without any modification to their chemical structure as a fuel to be combusted inside a diesel engine. This method should not be confused with biodiesel, which is a fuel derived from pure plant oils through a transesterification process that splits fatty acids from glycerin to reduce the viscosity of the pure plant oil similar to that of mineral diesel [11].

Vegetable oils represent a ready, renewable and clean energy source that has shown promise as a substitute to petroleum diesel fuel for diesel engines. There are different ways of utilizing vegetable oils as a substitute for petroleum diesel: (i) crude or refined neat oil; (ii) mixture of oil with diesel fuel with appropriate dilutions; and (iii) alkyl ester products from the transesterification process [12].

Since the most of European biodiesel is made from vegetable oil, this has led to a rapid increase in demand, with a significant impact on European vegetable oil markets [13].

Because the population is constantly growing and also food need is increasing, it is important to focus our attention on non-edible crops. Non-edible oils are not suitable for human food due to the presence of some toxic components in the oil [14].

As indicated by Table 1, numerous plant oils have been tried in diesel engines at some time or other. Relatively few, however, have been systematically evaluated and used [4].

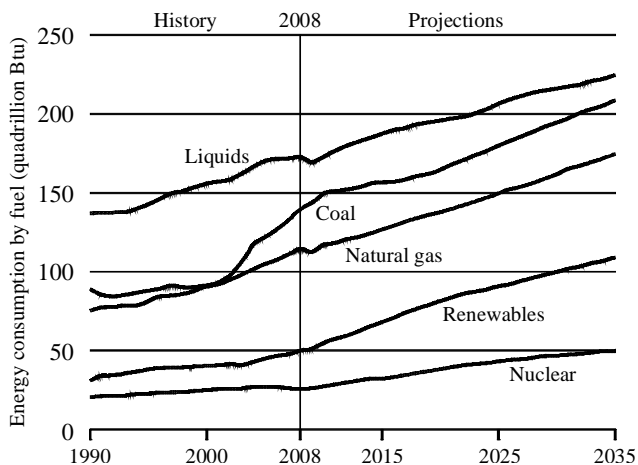


Fig. 1 World energy consumption by fuel, from 1990 to 2035 [6].

**Table 1:** Potential edible and non-edible plant oils for use in CI engines [4].

Edible oil	Non-edible oil
Sunflower oil, Rapessed oil, Rice oil, Soybean oil, Coconut oil, Corn oil, Palm oil, Olive oil, Pistachia Ol, Sesame seed oil, Peanut oil, Poppy oil, Safflower oil	Jatropha oil, Karanji or Pongamia oil, Neem oil, Jojoba oil, Cottonseed oil, Deccan hemp oil, Kusum oil, Orange oil, Rubber seed oil

Advantages of non-edible crops are ready availability, renewability, higher heat content, lower sulfur content, lower aromatic content and biodegradability, adaptability of cultivating non-edible oil feedstock in marginal land and non-agricultural areas with low fertility and moisture demand, eliminate competition for food and feed [14].

There are 350 species of oil-producing plants and thousands of sub-species [15]. Table 2 gives the average annual oil yield for the common oil plants cultivated in Europe.

**Table 2:** Oil producing crops in European Union [adapted from 13]

Oil producing crops in European Union	kg oil/ hectare
Corn	145
Oat	183
Cotton	273
Hemp	305
Linseed	402
Pumpkin seed	449
Sunflower	800
Rapessed	1000
Olive tree	1019

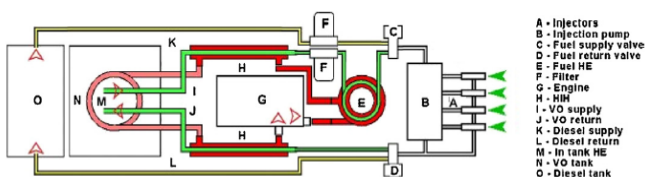
Diesel engines are designed to burn diesel fuel, which has a lower viscosity than vegetable oil. Therefore the direct usage of pure plant oil in the engine leads to poor fuel atomisation and incomplete combustion, which can rapidly damage the engine. Pure vegetable oil thickness is the central problem for their use since it is 11–17 times thicker than conventional fuel [11].

In the process of converting an engine, adaptations may need to be made to the fuel lines, combustion chamber and fuel injectors. The engine modifications necessary to run a diesel engine with vegetable oils can be divided into two categories: one tank systems and two tank systems. The best way is to fit a professional kit to the diesel engine which includes replacement injectors and glow plugs optimised for vegetable oil, as well as fuel heating [16,8].

The major components of a professional kit are: electrical switching unit (switching to the gas, rinse/ventilation) and an integrated heater (Diesel-Therm), control electronics (diesel - quick rinse, warning when off on vegetable oil), heat exchanger for water / oil circuit, fuel lines, fuel filter, cockpit panel for plant oil / diesel with LED's all operating conditions signal and audible warning when off mode in vegetable oil, complete manufactured cable set with relay sockets, plugs and fuses, various small material (hose clamps), detailed installation manual [17].

With two-tank PPO kits (Fig. 2), one tank holds the vegetable oil and the other petro-diesel (or biodiesel). The engine is started on the petro-diesel tank and runs on petro-diesel for the first few minutes while the vegetable oil is heated to lower the viscosity [11].

Items “O” and “N” represent the two tanks, which are installed inside a vehicle. Heating systems include “M” which is a heater located inside in the vegetable oil tank and “E” which is normally a



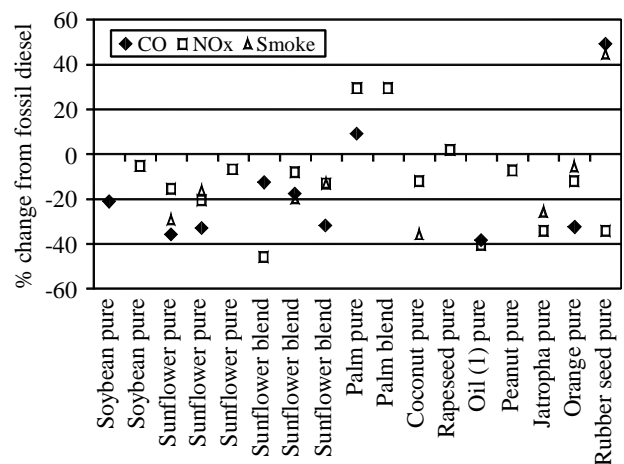
**Fig. 2** Illustration of a two tank system, which allows a vehicle to run on PPO [11].

special type of heat exchanger. The operation of this system is that upon shut down of the engine the mineral diesel or biodiesel from the smaller tank “O” is feed into the engine until all the vegetable oil is purged out [11].

Literature on using vegetable oils as fuel for diesel engine shows that exhaust gas temperature and smoke intensity may either increase or decrease in comparison to fossil diesel.

Wang et al. [18] carried out a series of experimental tests to evaluate the performance and gaseous emission characteristics of a diesel engine when fuelled with vegetable oil and its blends of 25%, 50%, and 75% of vegetable oil with ordinary diesel fuel separately. The engine works at a fixed speed of 1500 rpm, but at different loads respectively, i.e. 0%, 25%, 50%, 75% and 100% of engine full loads. The experimental results show that power output and fuel consumption are comparable to diesel when fueled with vegetable oil and its blends. The emission of nitrogen oxides (NO<sub>x</sub>) from vegetable oil and its blends are lower than that of pure diesel fuel. This emission character found in the tests to some extent is of significance for the practical application of vegetable oil to replace ordinary diesel fuel.

A technical review and life-cycle analysis [4] revealed that when the engine runs on plant oil, emissions of CO and HC may either increase or decrease (Fig. 3). At low load operation using plant oil, CO emission is almost the same as for fossil diesel. Whereas at higher loads, the mixture becomes richer thus more CO is produced due to the lower oxygen content of plant oil. Emissions of NO<sub>x</sub> tend to increase with the nitrogen content of the oil. Most literature reports a decrease in NO<sub>x</sub> emission with plant oil (or blends) compared to fossil diesel (Fig. 3).



**Fig. 3** CO, NO<sub>x</sub> and smoke emission of CI engines running on plant oil (or blends with fossil diesel) as compared to fossil diesel (Oil (1): unknown) [4].

One can observe that the CO emitted by all biodiesel blends of various origins is lower than that by the corresponding neat Diesel fuel case, with the reduction being higher the higher the percentage of the biodiesel in the blend [19].

Emissions of NO<sub>x</sub> tend to increase with the nitrogen content of the oil. The NO<sub>x</sub> emissions were slightly reduced with the use of biodiesel or vegetable oil blends of various origins with respect to that of the neat Diesel fuel, with this reduction being higher the higher the percentage of biodiesel or vegetable oil in the blend [4,19].

The smoke density was significantly reduced with the use of biodiesel blends of various origins with respect to that of the neat Diesel fuel, with this reduction being higher the higher the percentage of biodiesel in the blend. On the contrary, it was increased with the use of vegetable oil blends of various origins, with this increase being higher the higher the percentage of vegetable oil in the blend [19].



In other experiment [20], Rakopoulos et al. have evaluated the use of sunflower, cottonseed, corn and olive straight vegetable oils of Greek origin, in blends with diesel fuel at proportions of 10 vol.% and 20 vol.%, in a six-cylinder, turbocharged and after-cooled, heavy duty, direct injection, Mercedes-Benz diesel engine.

Fig. 4 shows, for the speed of 1500 rpm, the emitted nitrogen oxides ( $\text{NO}_x$ ) for the neat diesel fuel, and the 10% and 20% blends of the four vegetable oils with diesel fuel, at the three loads. One can observe that the  $\text{NO}_x$  emitted by all vegetable oil blends are equal or slightly higher than the ones for the corresponding diesel fuel case, with this increase being higher the higher the percentage of the vegetable oil in the blend [20].

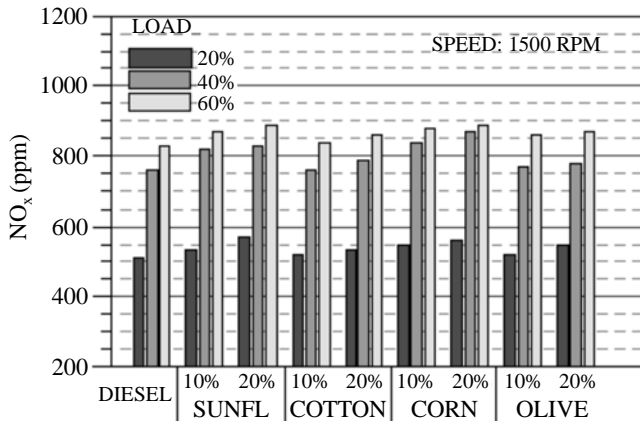


Fig. 4 Emissions of nitrogen oxides ( $\text{NO}_x$ ) for neat diesel fuel, and the 10% and 20% blends of the four vegetable oil with diesel fuel [20].

For the same experiment [20], it can be observed that the soot emitted by all vegetable oil blends is lower than the ones for the corresponding neat diesel fuel case, with this reduction being higher the higher the percentage of the vegetable oil in the blend. This is attributed to the combustion being mixing controlled for these vegetable oil blends, as it is also the case for the neat diesel fuel case, which is however now assisted by the presence of the fuel bound oxygen even in locally rich zones [20].

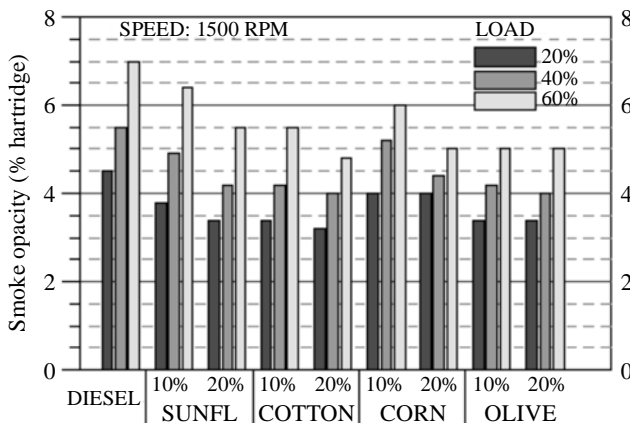


Fig. 5 Emissions of smoke for neat diesel fuel, and the 10% and 20% blends of the four vegetable oil with diesel fuel [20].

### 3. Biodiesel

Crude vegetable oils are inferior as fuel in terms of viscosity, heating value, freezing point, etc. [21]. In order to reduce viscosity, vegetable oils are converted into esters by transesterification

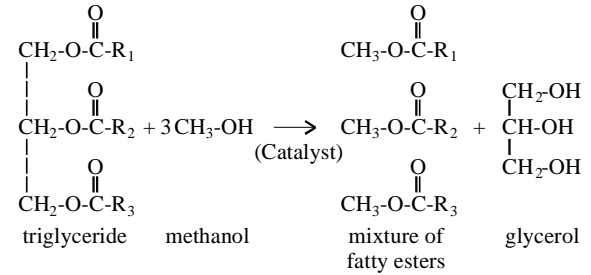


Fig. 6 Transesterification reaction [22].

reaction [1]. The result of transesterification reaction (Fig. 6) is biodiesel, as a fuel comprised of mono-alkyl esters of long chain fatty acids derived esters from vegetable oils or animal fats, designated B100 [23].

Because the biodiesel viscosity is almost twice higher than the diesel fuel viscosity (according to Standard EN 14214:2003, the biodiesel viscosity at  $40^\circ\text{C}$  is  $3.5\text{-}5.0 \text{ mm}^2/\text{s}$  [24]), biodiesel is currently used in blends with diesel fuel.

Biodiesel can be produced from various vegetable oils, waste cooking oils or animal fats. The fuel properties of biodiesel may be changed when different feedstocks are used [25]. However, biodiesel production is highly dependent on many local variables such as feedstock and land availability, costs associated with feedstock procurement, government subsidies and tax reductions as well as interactions with the food industry [26].

The main stages of the fuel systems for biodiesel from vegetable oil and waste cooking oil are shown in Figure 7.

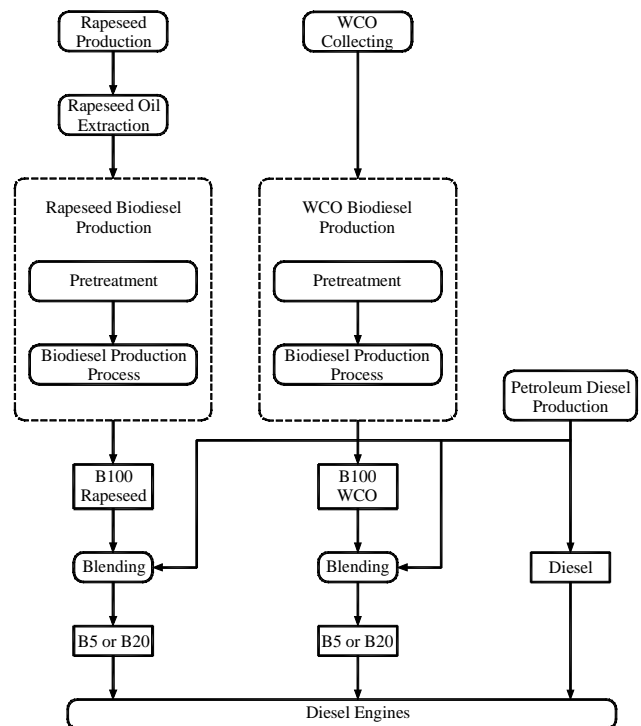


Fig. 7 Fuel systems for biodiesel from vegetable oil (rapeseed oil) and waste cooking oil (WCO) (adapted from [26]).

A survey on 27 literatures [27], to study the effect of pure biodiesel on engine power, showed that 70.4% of them agreed that, with biodiesel (especially with pure biodiesel), engine power will

Table 3: Statistics of effects of pure biodiesel on engine performances (adapted from [27])

	Total number of references	Increase	%	Similar	%	Decrease	%
		Number		Number		Number	
Power performance	27	2	7.4	6	22.2	19	70.4
Economy performance	62	54	87.1	2	3.2	6	9.7

drop due to the loss of heating value of biodiesel (Table 3). However, the results reported show some fluctuation. Some authors found that the power loss was lower than expected (the loss of heating value of biodiesel compared to diesel) because of power recovery.

Due to the increasing interest in the use of biodiesel, the Environmental Protection Agency (USA) has conducted a comprehensive analysis of the emission impacts of biodiesel using publicly available data [28]. This investigation made use of statistical regression analysis to correlate the concentration of biodiesel in conventional diesel fuel with changes in regulated and unregulated pollutants. Since the majority of available data was collected on heavy-duty highway engines, this data formed the basis of the analysis. The average effects are shown in Figure 8. One may observe that due to higher content of oxygen in biodiesel, CO, PM and HC emission are reduced, but the NO<sub>x</sub> emission is higher than that of diesel fossil fuel.

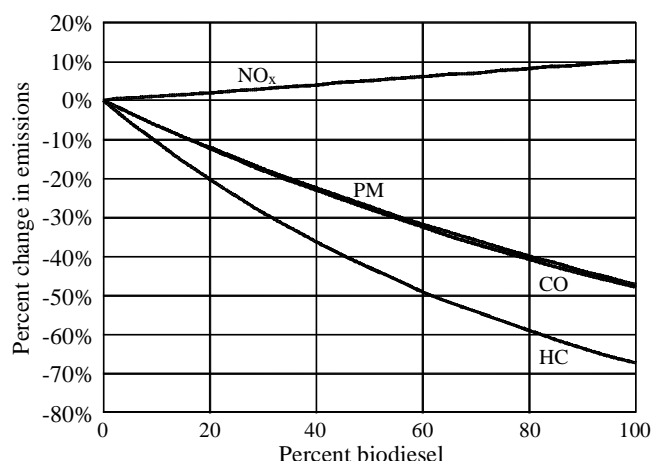


Fig. 8 Average emission impacts of biodiesel for heavy-duty highway engines [28].

The results of an experimental investigation [29], using two different samples of B10 blend of eucalyptus biodiesel, showed that smoke opacity improves for both samples, smoke is found to be 64.5% and 62.5% cleaner than that of diesel. Out of all blends B10 was found to be a suitable alternative to conventional diesel fuel to control air pollution without much significant effect on engine performance.

As for the vegetable oils as alternative fuel for diesel engines, the literature on biodiesel emission is not uniform.

In this respect, some available results of Light-Duty diesel vehicle test data for some rapeseed biodiesel blends (a minimum of 20 measurements of a particular blend were required to assess the significance of the effect) allow one to explore the differences in the effects on emissions of the different biodiesel feedstocks [30]. The emission data are discussed as follows:

- HC lower for B20 and B100, but no correlation between biodiesel content in the blend and level of HC emission;
- NO<sub>x</sub> higher than for diesel fuel for all blends, the higher content of biodiesel, the higher NO<sub>x</sub> emission;
- CO emission is random, lower for B20, but higher for B30;
- Particulate matter (PM) emission is not significant versus diesel fuel. However, a very slight increase of PM for biodiesel blends is observed.

The heterogeneous and uncorrelated data from [27] could be due to the use of biodiesel and biodiesel blends on diesel engines tuned only for pure diesel fuel or for B5-B7 blends. Using higher percentage biodiesel blends, or even B100 fuel, on existing unmodified engines, could cause an inappropriate response of the engine in respect of torque (power) and emission.

#### 4. CNG as fuel for diesel engine

International communities are seeking reliable and alternative fuel sources and technologies to reduce environmental stresses, air pollution, increase fuel availability, decrease the use of and dependence on foreign oil, and optimize the performance of existing fuel supply infrastructures [31].

Natural gas (NG) is one of the most important energy carriers today because it is available in large quantities and its reserves are of the same magnitude as the crude oil reserves [32]. The use of natural gas as a fuel has garnered considerable interest since the beginning of the 1990s.

Italy was the first country in which the use of natural gas as fuel for the propulsion of road vehicles was successful [33]. In the last decade the number of NG vehicles has risen to over a million in several countries around the globe. One reason for this evolution is economic: in many countries NG is considerably less expensive than conventional fuels such as gasoline and diesel. The other advantage is the fact that natural gas burns in a cleaner, less polluting way. Natural gas sources are spread throughout the world, which reduces the risk of an energy crisis [32].

CNG/NG, is a mixture of hydrocarbons in gaseous form, consists of approximately 80-90% of methane along with some percentage of ethane, propane, nitrogen [34]. A gaseous form of natural gas, clearly has some substantial benefits compare to petrol and diesel.

According to [32], the main constituent of NG is methane (80–98%, depending on the extraction source). Other (about 2%), butane and pentane (less than constituents are ethane (1–8%), propane 1%). NG also contains nitrogen and carbon dioxide (0.2–1.5%) and small quantities of sulfur compounds (hydrogen sulphide and mercaptans). Of all hydrocarbon compounds used as motor fuels, methane has the highest knock resistance [32]. Its octane number is ca. 130. NG is non-toxic, odourless and non-corrosive. It is lighter than air and is slightly soluble in water.

Amrouche et al. [35] have found that CNG:

- Is composed of 85 to 99% methane;
- Has the highest energy/carbon ratio of any fossil fuel, and has a high octane (110/130) (against 95 and 98 for gasoline and 92/96 for the diesel). His feature helps the increase of the compression ratio engines and thus the efficiency;
- Is safely: It is lighter than the air, in the case of gas leak, it goes to the atmosphere;
- Auto-ignite above 540°C (450°C for LPG, 220°C for unleaded gasoline and 225°C for diesel).
- Doesn't freeze until below -165°C, which makes it insensitive with the climatic conditions.

One of the reasons to use NG as an alternative fuel was the ecological consideration [32], NG having the potential to mitigate CO<sub>2</sub> emissions due to its lower carbon content [36].

Natural gas is used as a fuel in two forms [32]:

1. In its gaseous form (at ambient temperature and under a high pressure of 20 MPa) it is called compressed natural gas (CNG).
2. In its liquid form (cooled to a temperature of -161°C at atmospheric pressure) it is called liquefied natural gas (LNG).

In the case of using CNG, vehicle engines should be modified (dedicated/retrofitted) at the same time with changing fuels [36]. Dedicated vehicles are preferable but there are a few light-duty CNG vehicles available. For applying to a specific type of vehicle, retrofitting is an option. However, the efficiency of retrofitted vehicles is questionable on reduction of CO<sub>2</sub> emissions [36].

In order to ensure smooth transportation life cycle and sustainability, it is important to synchronize CNG fuel supply, CNG refueling stations and CNG fuel vehicles [31]. Recent studies show that the proper implementation with reasonable ratio of refueling stations to alternative fuel vehicle is of great importance [31].

Many investigations were carried out in order to use of CNG as an alternative fuel according to their fuel usage and they are [34]:

- Dual fuel: like the CNG buses the mixture of CNG and diesel introduced in the engine. As natural gas will not ignite under combustion chamber alone so diesel is required.
- Bi-fuel: like cars and light motor vehicle, convention petrol engine where the fuel system has been modified to operate either petrol gas.
- Mono-fuel: this is specialized engine type which has been designed and optimized to operate only on natural gas.

The natural gas vehicle is currently one of least polluting vehicles available on the market [35]. In fact, compared to others vehicles powered with petroleum products, the CNG vehicles have shown a very strong reduction of the polluting emissions (-100 % of lead, the Non-Methane Hydrocarbons are reduced by approximately 50%, - (50-87%) of  $\text{NO}_x$ , - (20-30%) of  $\text{CO}_2$ , - (70-95%) of CO. And the combustion of natural gas produces almost no fine particulate matter). Natural gas vehicles have significantly low noise levels and engine vibration, it reduce noise about -5 to -8 decibels by vehicle [35].

Introducing vehicles that run on CNG can significantly reduce black carbon emissions from on-road vehicles [37].

The use of natural gas as a vehicle fuel is claimed to provide several benefits to engine components and effectively reduce maintenance requirements [34]. It does not mix with or dilute the lubricating oil and will not cause deposits in combustion chambers and on spark plugs to the extent that the use of petrol does, thereby generally extending the piston ring and spark plug life. In diesel dual-fuel operation evidence of reduced engine wear is reported, leading to expected longer engine life [34].

Development of the CNG dual-fuel turbocharged CI engine was described in reference [32]. NG was introduced into the engine cylinder in the gaseous state through a honeycomb mixer. The pilot ignition fuel was diesel fuel. The following results on emissions were obtained (Fig. 9):

- An increase in pilot diesel fuel extends the lean burning limit and decreases HC and CO emissions (while  $\text{NO}_x$  emissions increase), which is generally higher than for diesel fuelling.
- Smoke emission is considerably reduced for dual fuelling.
- $\text{NO}_x$  emission is also reduced.

## 5. Conclusions

To meet the energy requirements and environmental concerns, there has been growing interest in alternative fuels like vegetable

oils, biodiesel and CNG to provide a suitable diesel oil substitute for internal combustion engine.

As an alternative fuel for compression ignition engines, plant oils are in principle renewable and carbon neutral, but their use raises technical, economic and environmental issues.

There are different ways of utilizing vegetable oils as a substitute for petroleum diesel: (i) crude or refined neat oil; (ii) mixture of oil with diesel fuel with appropriate dilutions; and (iii) alkyl ester products from the transesterification process.

Since diesel engines are designed to burn diesel fuel, which has a lower viscosity than vegetable oil, using only vegetable oil as fuel needs to fit a professional kit to the diesel engine, which includes replacement injectors and glow plugs optimised for vegetable oil, as well as fuel heating.

Literature on using vegetable oils as fuel for diesel engine shows that CO emission is decreasing, while emissions of  $\text{NO}_x$  tend to increase.

To reduce the viscosity of vegetable oils, vegetable oils are converted into esters by transesterification reaction. Because the biodiesel viscosity is almost twice higher than the diesel fuel viscosity, biodiesel is currently used in blends with diesel fuel.

Using pure biodiesel, engine power drops due to the loss of heating value of biodiesel. In some cases, the power loss was lower than expected because of power recovery.

Due to higher content of oxygen in biodiesel, CO, PM and HC emission are reduced, but the  $\text{NO}_x$  emission is higher than that of diesel fossil fuel.

One of the reasons to use natural gas as an alternative fuel was the ecological consideration, NG having the potential to mitigate  $\text{CO}_2$  emissions due to its lower carbon content.

In the case of using CNG, vehicle engines should be modified at the same time with changing fuels. Dual fuel, bi-fuel or mono-fuel fuel systems have been designed and optimized to allow diesel and spark ignition engines to operate only on natural gas.

Compared to others vehicles powered with petroleum products, the CNG vehicles have shown a very strong reduction of the polluting emissions.

The use of natural gas as a vehicle fuel is claimed to provide several benefits to engine components and effectively reduce maintenance requirements .

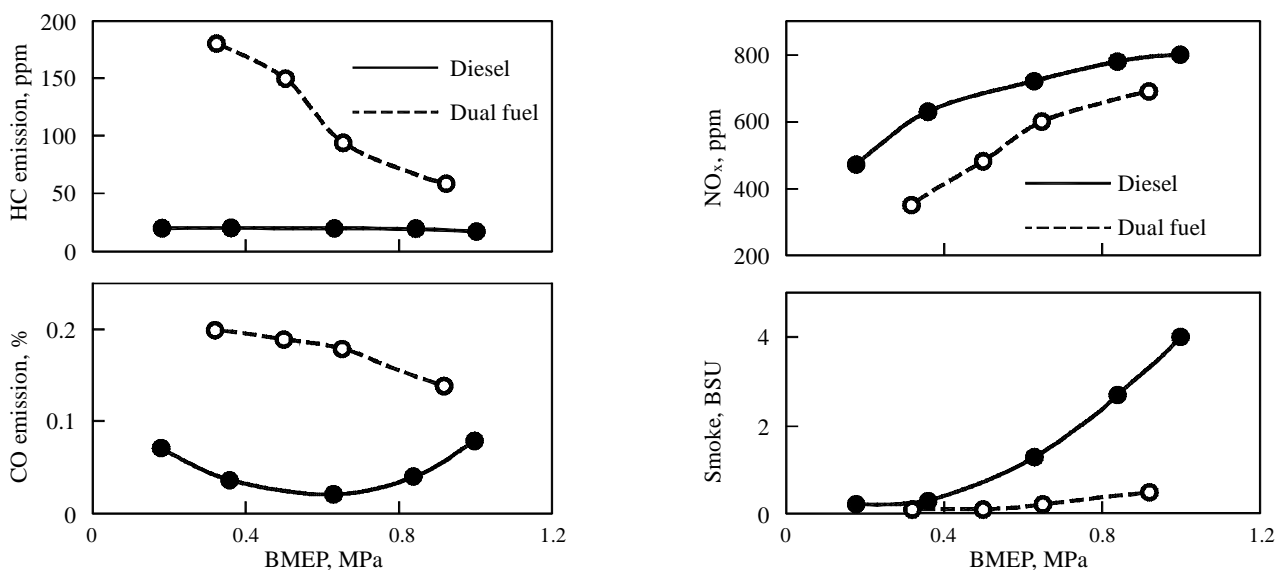


Fig. 9 HC, CO,  $\text{NO}_x$  and smoke emissions versus b.m.e.p. for dual and diesel fuelling of a turbocharged engine at  $n=1600$  r/min [32].

## 6. References

- [1] Agarwal, A. K. et al. Particulate emissions from biodiesel fuelled CI engines. *Energy Conversion and Management* 94 (2015) 311–330.
- [2] Atadashi, I. M. Crude biodiesel refining using membrane ultra-filtration process: An environmentally benign process. *Egyptian Journal of Petroleum* (2015) 24, 383–396.
- [3] De, B., R. S. Panua. An experimental study on performance and emission characteristics of vegetable oil blends with diesel in a direct injection variable compression ignition engine. *Procedia Engineering* 90 (2014) 431–438
- [4] Hossain, A. K., P.A. Davies. Plant oils as fuels for compression ignition engines: A technical review and life-cycle analysis. *Renewable Energy* 35 (2010) 1–135.
- [5] Palit, S., A. K. Chowdhuri, B. K. Mandal. Environmental impact of using biodiesel as fuel in transportation: a review. *Int. J. Global Warming*, Vol. 3, No. 3, 2011.
- [6] Promoting Green Energy for Better Tomorrow. Pakistan Renewable Energy Society. <http://www.pres.org.pk/category/energy/>
- [7] Alfieri, E. Emissions-Controlled Diesel Engine. A dissertation submitted to the Swiss Federal Institute of Technology Zurich for the degree of Doctor of Sciences. 2009. <http://e-collection.library.ethz.ch/eserv/eth:41539/eth-41539-02.pdf>
- [8] Lin, Y.-C. et al. Approach for Energy Saving and Pollution Reducing by Fueling Diesel Engines with Emulsified Biosolution/Biodiesel/Diesel Blends. [https://www.researchgate.net/publication/5309993\\_Approach\\_for\\_Energy\\_Saving\\_and\\_Pollution\\_Reducing\\_by\\_Fueling\\_Diesel\\_Engines\\_with\\_Emulsified\\_Biosolution/Biodiesel\\_Diesel\\_Blends](https://www.researchgate.net/publication/5309993_Approach_for_Energy_Saving_and_Pollution_Reducing_by_Fueling_Diesel_Engines_with_Emulsified_Biosolution/Biodiesel_Diesel_Blends)
- [9] McClellan, R. O., T. W. Hesterberg, J.C. Wall. Evaluation of carcinogenic hazard of diesel engine exhaust needs to consider revolutionary changes in diesel technology. *Regulatory Toxicology and Pharmacology* 63 (2012) 225–258.
- [10] Sane, H. et al. Emission reduction of IC engines by using water-in-diesel emulsion and catalytic converter. *IJRET: International Journal of Research in Engineering and Technology*, Volume: 03 Issue: 08 | Aug-2014, pp. 378–383.
- [11] Russo, D. et al. State of the art of biofuels from Pure Plant Oil. *Renewable and Sustainable Energy Reviews* 16 (2012) 4056–4070.
- [12] Z. Franco, Q. D. Nguyen. Flow properties of vegetable oil–diesel fuel blends. *Fuel* 90 (2011) 838–843.
- [14] Atabani, A. E. et al. Non-edible vegetable oils: A critical evaluation of oil extraction, fatty acid compositions, biodiesel production, characteristics, engine performance and emissions production. *Renewable and Sustainable Energy Reviews* 18 (2013) 211–245.
- [13] Vegetable oil markets and the EU biofuel mandate. The International Council on Clean Transportation, February 2013, [http://www.theicct.org/sites/default/files/publications/ICCT\\_vegoil\\_and\\_EU\\_biofuel\\_mandate\\_20130211.pdf](http://www.theicct.org/sites/default/files/publications/ICCT_vegoil_and_EU_biofuel_mandate_20130211.pdf)
- [15] Joshua and Kaia Tickell, *From the Fryer to the Fuel Tank. The complete guide to using vegetable oils as an alternative fuel.* Second Edition. GreenTeach Publishing, USA. 1999, ISBN 0-9664616-1-4.
- [16] Pure plant oil as fuel. Technical aspects and legislative context. [https://ec.europa.eu/energy/intelligent/projects/sites/iee-projects/files/projects/documents/agriforenergy\\_2\\_pvo\\_handbook\\_en.pdf](https://ec.europa.eu/energy/intelligent/projects/sites/iee-projects/files/projects/documents/agriforenergy_2_pvo_handbook_en.pdf)
- [17] Conversion from Diesel Engines to run with Pure Plant vegetable Oil. <http://heipro.com/>
- [18] Wang, Y. D. et al. An experimental investigation of the performance and gaseous exhaust emissions of a diesel engine using blends of a vegetable oil. *Applied Thermal Engineering* 26 (2006) 1684–1691.
- [19] Rakopoulos, C. D. et al. Comparative performance and emissions study of a direct injection Diesel engine using blends of Diesel fuel with vegetable oils or biodiesels of various origins, *Energy Conversion and Management* 47 (2006) 3272–3287.
- [20] Rakopoulos, C. D. et al. Comparative environmental behavior of bus engine operating on blends of diesel fuel with four straight vegetable oils of Greek origin: Sunflower, cottonseed, corn and olive, *Fuel* 90 (2011) 3439–3446.
- [21] Arbab, M. I. et al. Fuel properties, engine performance and emission characteristic of common biodiesels as a renewable and sustainable source of fuel. *Renewable and Sustainable Energy Reviews* 22 (2013) 133–147.
- [22] Van Gerpen, J. et al. Biodiesel Production Technology. NREL/SR-510-36244, Contract No. DE-AC36-99-GO10337, 2004.
- [23] ASTM D 6751 – 02 Standard Specification for Biodiesel Fuel (B 100) Blend Stock for Distillate Fuels, [http://www.biofuels.coop/pdfs/12\\_astm.pdf](http://www.biofuels.coop/pdfs/12_astm.pdf)
- [24] EN 14214:2003 (E) Automotive Fuels - Fatty Acid Methyl Esters for Diesel Engines - Requirements and Test Methods
- [25] Ozsezen, A. N., M. Canakci. Determination of performance and combustion characteristics of a diesel engine fueled with canola and waste palm oil methyl esters. *Energy Conversion and Management* 52 (2011) 108–116.
- [26] Ozata, I. et al. Comparative Life Cycle Assessment Approach for Sustainable Transport Fuel Production from Waste Cooking Oil and Rapeseed. January 2009, <http://www.researchgate.net/publication/228406700>
- [27] Xue, J., T. E. Grift, A. C. Hansen. Effect of biodiesel on engine performances and emissions. *Renewable and Sustainable Energy Reviews* 15 (2011) 1098–1116.
- [28] A Comprehensive Analysis of Biodiesel Impacts on Exhaust Emissions, Draft Technical Report EPA420-P-02-001, October 2002.
- [29] Verma, P., M. P. Sharma, G. Dwivedi. Potential use of eucalyptus biodiesel in compressed ignition engine. *Egyptian Journal of Petroleum* (2015) xxx, xxx–xxx, in press.
- [30] Anderson, L. G. Effects of Biodiesel Fuels Use on Vehicle Emissions. *Journal of Sustainable Energy & Environment* 3 (2012) 35–47.
- [31] Gabbar, H. A., R. Bedard, N. Ayoub. Integrated modeling for optimized regional transportation with compressed natural gas fuel. *Alexandria Engineering Journal* (2016) 55, 533–545.
- [32] Kowalewicz, A., M. Wojtyniak. Alternative fuels and their application to combustion engines, Proceedings of the Institution of Mechanical Engineers, Part D: Journal of Automobile Engineering 2005 Vol. 219: 103–125.
- [33] Berghmans, J., M. Vanierschot. Safety aspects of CNG cars. *Procedia Engineering* 84 (2014) 33–46.
- [34] Saraswat, M. et al. Assessment of different alternative fuels for internal combustion engine: A review. *International Journal of Engineering Research & Management Technology*, May- 2015 Volume 2, Issue-3, ISSN: 2348–4039.
- [35] Amrouche, F. et al. Compressed Natural Gas: The new alternative fuel for the Algerian transportation sector. *Procedia Engineering* 33 (2012) 102–110.
- [36] Gojash, O., A. Fukuda, T. Fukuda. Estimation of CO<sub>2</sub> emissions reduction using alternative energy – Potential Application of Clean Developed Mechanism (CDM) in the Transport Sector to Developing Countries. *IATSS Research* Vol. 31 No.1, 2007, pp. 32–40.
- [37] Kholod, N., M. Evans. Reducing black carbon emissions from diesel vehicles in Russia: An assessment and policy recommendations. *Environmental Science & Policy* 56 (2016) 1–8.

# THE PARAMETRIC OSCILLATIONS OF STEEL FRICTION PLATES FOR A MULTIPLATE CLUTCHES

## ПАРАМЕТРИЧЕСКИЕ КОЛЕБАНИЯ ФРИКЦИОННЫХ ДИСКОВ В ТРАНСМИССИЯХ ТРАНСПОРТНЫХ МАШИН

Prof. Dr. Eng. Taratorkin I.<sup>1</sup>, Prof. Dr. Eng. Derzhanskii V.<sup>1</sup>, postgraduate Taratorkin A.<sup>1</sup> – Institute of Engineering Science of the Ural Branch of the Russian Academy of Sciences (IES UB RAS), Russia

**Abstract:** The article substantiates the ways of tuning parametric oscillations providing for increasing durability of steel and friction plates of vehicle transmissions. The evaluation of dynamic stability is conducted on the basis of the analysis of Mathieu equation and Ince-Strutt diagram. It is offered to restrict the parameter of rigidity modulation depth by filtering low-frequency disturbances formed in the nonlinear system by the power unit (internal combustion engine (ICE) or electric motor (EM)), by hydrodynamic processes in the hydraulic transformer (torque converter or hydraulic coupling) and in the system of its oil supply. The performance evaluation of the developed actions on plate's durability is conducted.

**KEYWORDS:** PLATE, FRICTION DESK, PARAMETRIC OSCILLATIONS, DYNAMIC STABILITY

### 1. Introduction

The advanced multi-purpose tracked and wheeled vehicles operated in super severe conditions more and more perfect designs of hydromechanical, electromechanical and hybrid transmissions are to be developed [1]. Prototypes tests show the high dynamic loading which restricts component durability, in particular, the durability of plates of multiplate clutches and conjugated components [2, 3]. The article [4] considers the type of failure insufficiently investigated - plate disruption, which is observed in transmissions being developed and in designs of worldwide automotive leaders. It should be noted that the same type of failure is observed in the vehicles equipped with stepped ratio gear transmissions without torque converter and diesel engines.

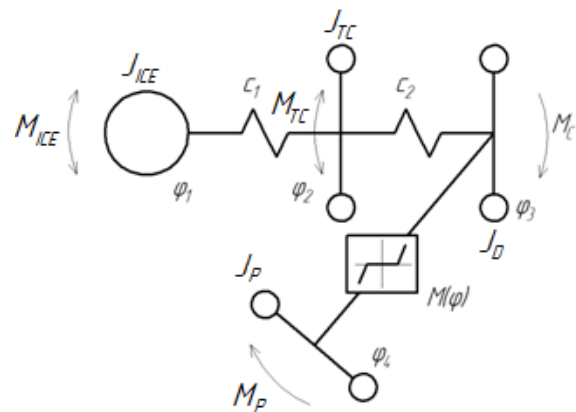
The metallographic analysis of the disrupted plates shows that crack formation has a fatigue character, which is revealed within limited time of trial operation. It occurs due to generation of high-frequency oscillation. The article [4] shows that plate disruption take place because of resonant modes which are generated by hydrodynamic processes in the impeller-turbine interblade space and by working liquid pulsation in the oil supply circuit. However, because of the nonlinear elastic characteristics of plate and drum interaction at gap opening the parametric oscillations and resonances are excited which are more dangerous and are not eliminated with usual methods.

Thus, according to the aforesaid, there are three main points of the research subject. First, to study the processes of dynamic loading formation of wet clutch plates. Second, to prove the ways of durability increasing of wet clutch elements. Third, to improve the existing method of multiplate clutches calculation considering frequency characteristics and dynamic factors of loading.

Scientific novelty of the research involves to study conditions of resonance appearance. By the way, to develop the ways for eliminating resonant modes based on dynamics research of highly nonlinear system at polyharmonic disturbances. These disturbances are formed by a ICE or EM, by hydrodynamic processes in the impeller-turbine space of the torque converter and by pulsation of working liquid pressure in the oil supply circuit.

### 2. Analytical research of nonlinear system dynamics

The dynamic problem is solved on the basis of mathematical model of the system under study "Engine unit – Torque Converter – Planetary Transmission Elements (conjugated drum and lined plate)" (Fig. 1).



**Fig. 1.** Design model of the nonlinear system: the system structure.

The scheme introduces the following notations:  $J_{ICE}$ ,  $J_{TC}$ ,  $J_D$ ,  $J_P$  are moments of inertia of the engine, torque converter, drum and plate;  $c_1, c_2$  are rigidities of the pre-torque-converter zone damper and transmission input shaft respectively;  $M(\varphi)$  is a nonlinear elastic characteristics of plate-to-drum interaction;  $\varphi_1; \varphi_2; \varphi_3; \varphi_4$  are corresponding generalized coordinates of inertia masses. The movement of the elements is described by the following system of the differential equations (1):

$$\begin{cases} J_{ICE}\ddot{\varphi}_1 + c_1(\dot{\varphi}_1 - \dot{\varphi}_2) = H_0 + H_i \sin(\omega_i t + \alpha_i) \\ J_{TC}\ddot{\varphi}_2 - c_1(\dot{\varphi}_1 - \dot{\varphi}_2) + c_2(\dot{\varphi}_2 - \dot{\varphi}_3) = H_m \sin(\omega_m t + \alpha_m) \\ J_D\ddot{\varphi}_3 + b(\dot{\varphi}_3 - \dot{\varphi}_4) - c_2(\dot{\varphi}_2 - \dot{\varphi}_3) + M(\varphi) = M_C \\ J_P\ddot{\varphi}_4 - b(\dot{\varphi}_3 - \dot{\varphi}_4) - M(\varphi) = H_D \end{cases} \quad (1)$$

In this system  $H_i$ ,  $\omega_i$ ,  $\alpha_i$  are amplitudes, frequencies and initial stages of engines harmonics respectively;  $H_j$ ,  $\omega_j$ ,  $\alpha_j$  are amplitudes, frequencies and epoch angle of harmonics respectively, being formed in the impeller-turbine space of the torque converter;  $M_C$  is a reduced torque of resistance to motion;  $H_D$  is drag torque losses.

In the design model plate and drum connection is carried out on the clearance fit centering according to the diameter of the reference circle of teeth which providing axial movement of plate relatively to the drum when engage or disengage. The design model of plate and drum gear connection is shown in Fig. 2.

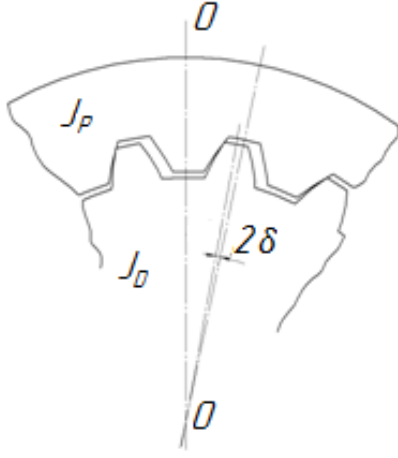


Fig. 2. Design model of the nonlinear system: drum and plate connection.

A nonlinear function - nonlinear elastic characteristics on angular coordinate, is schematized (Fig. 3) and is accepted symmetric with a gap, i.e.:

$$M(\varphi) = \begin{cases} 0 & \text{at } |\varphi| \leq \delta \\ c \cdot |\varphi| \cdot \text{sign}(\varphi) & \text{at } |\varphi| > \delta. \end{cases}$$

The parameter  $\delta$  was determined by engineering drawings ( $\delta=0,3$  degrees);  $c$  is rigidity of the couple "plate tooth - drum tooth" on the basis of modeling a stress-strain behavior of tooth gearing of a plate with a drum ( $c=6.845 \cdot 10^5$  N·m/rad). For determination of plate-to-drum rigidity it is necessary to define the uniformity factor of loading between teeth. Mutual position of drum relatively to plate has a periodic character during functioning. For a quantitative evaluation of the disturbances formed by the nonlinear system under the study, it is accepted that contact rigidity is defined by one, two, three, etc. couples of teeth, and during the parallel work of elements the rigidity is summarized.

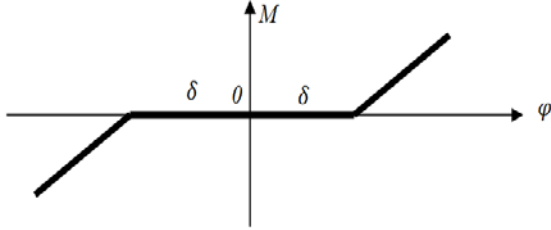


Fig. 3. Idealization of the nonlinear function, dependence of the moment on an angular coordinate (nonlinearity with a clearance).

The results of modeling the systems dynamics are shown in Fig. 4.

4.

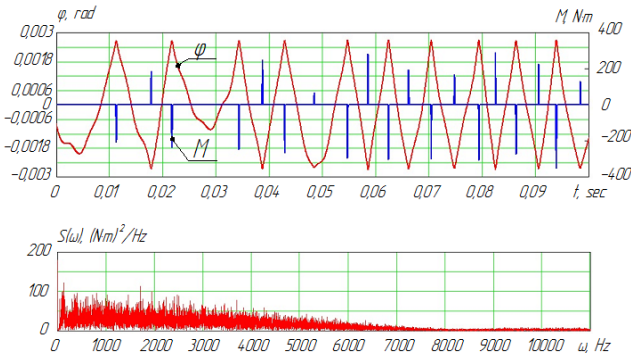


Fig. 4. Results of modeling the system dynamics.

The results of the computational solution of the system (1) show that nonlinear high-frequency interaction plate-to-drum generates a wide disturbing forced spectrum (from 0 to 6,000 Hz) with high power. Thus, the spectrum of forced frequencies crosses the spectrum of the system natural frequencies. By the way, this spectrum crosses forms of plate oscillations (if system is considered as system with the distributed parameters). This fact can provide generation of resonant oscillations of plates. The analysis for eliminating of resonances appearance was performed. This problem

is solved on the basis of studying two-mass mathematical model of the nonlinear system "Drum - Plate". This model accounts on equivalent moment of inertia of TC turbine, elements of planetary gear sets, pack of  $I$  plates, gap between plate and drum. The model was modified to a nonlinear differential equation (2) after addition a coordinate of the relative angular movement  $\varphi = \varphi_1 - \varphi_2$ :

$$J_{dr} \ddot{\varphi} + b \dot{\varphi} + M(\varphi) = M(t) \quad (2)$$

In this equation  $J_{dr}$  is a driven inertia moment

$$\left( J_{dr} = \frac{J_D \cdot J_P \cdot i}{J_D + J_P \cdot i} \right); \quad b \text{ is a dissipation factor depending on a}$$

frequency, oscillation amplitude and the hysteresis loop area (which occurs due to imperfectly elastic collision of the plate with the drum,  $b=4.5$  N·m·sec);  $M(t)$  is temporary function of the disturbing torque formed by the engine, by the hydrodynamic processes in the impeller-turbine space of the torque converter, by the pulsation of working liquid pressure in the oil supply circuit;  $J_P$  is a moment of plate inertia;  $i$  is a number of plates. The moment of inertia  $J_{dr}$  calculated with number of assumption. In this regard, the value  $J_{dr}$  is determined by experimental data in compliance with the frequency of its natural oscillations in the dynamic system.

### 3. Analysis of stability of nonlinear system periodic solutions

It is known that the solution of the nonlinear equation (2) is ambiguous and several stationary modes with various amplitudes  $\varphi_i = \varphi_i(t)$  may be existed as well as unstable.

The analysis of stability is carried out with application of parametrical oscillation approach. For this purpose the mathematical model (2) is modified to Mathieu equation [5,6]:

$$\ddot{\varphi} + 2\varepsilon \dot{\varphi} + \omega_0^2 \left[ 1 - \frac{q_{dyn} \cos(pt)}{q_{st}} \right] \varphi = 0 \quad (3)$$

The equation does not take into account the presence of dissipative forces. The moment of friction in off-mode, when plates free rotate, is considered when determining a modulation parameter in the formula  $\frac{q_{st}}{q_{cr}}$  in formula (3) and determines the value of the parameter  $h$  in the Ince-Strutt diagram. Evaluation of the numerical values of dissipation coefficient  $b$  in the system of equations (1), arising as a result of inelastic interactions of the plate with the drum, has no significant effect on the value of the natural frequency of the dynamic system and insignificantly reduces the instability area in the Ince-Strutt diagram (Fig. 5, blue line).

In this equation  $\omega_0^2 = \frac{b}{2J_{dr}}$ ;  $\omega_0^2$  is a square of natural oscillations frequency of the nonlinear system corresponding to the value of harmonic linearization factor  $q_{dyn}$ ;  $p$  is external forcing frequency.

The rigidity of nonlinear interaction «Drum-to-Plate» was taken as modulation depth  $2\mu = \frac{q_{dyn(A)}}{q_{st(A)}}$ . The numerator was determined by four-mass-model solution. The dominator was determined according to the drag torque.

For the assumed values of the amplitudes of angular oscillation values  $q_{dyn(A)}$  stiffness ( $A$ ) and  $q_{st(A)}$  ( $A$ ) determined by the method of harmonic linearization (4) for the above non-linearity (Fig. 3):

$$q(A) = c_0 - \frac{2c_0}{\pi} \left( \arcsin \frac{\delta}{A} + \frac{\delta}{A} \sqrt{1 - \frac{\delta^2}{A^2}} \right), \quad (4)$$

where  $A$  is an angular oscillation amplitude;  $\delta$  is a gap (play). It is important to note that an assumed value in computation  $q_{dyn(A)}$  gives the value  $\omega_0$  within the range between 600 and 700 Hz, which is close enough to the lowest natural frequency (the second form of oscillations of the multiplate clutch lined plate) of the transmission under study.

Next, the Mathieu equation was modified to the parameters of the Ince-Strutt diagram  $a$  and  $h$  (Fig. 5). Entering the parameters of

rigidity modulation depth  $\mu$  and the frequency of its alternation  $p$ , Mathieu equation without taking into consideration dissipation is modified to (5):

$$\ddot{\varphi} + [a - 2h\cos(2\tau)]\varphi = 0. \quad (5)$$

In this equation  $a$  and  $h$  are parameters (abscissa and ordinate)

of Ince-Strutt diagram (Fig. 5):  $a = \left(\frac{2\omega}{p}\right)^2$ ;  $h = a\mu$ ;  $2\tau =$

$p\tau$ . Such representation allows to analyze stability of parametrical oscillations according to the specified diagram and according to the positions of points with given coordinates  $a$  and  $h$ .

On the diagram the instability regions are shaded, stability regions are not shaded. In the Figure 5 a straight line 1 characterize the function  $h = a\mu$  of the dynamic system "Drum - Plate" under study, ( $p=1,200$  and  $680$  Hz,  $\mu = 1.275$ ). As it comes from the diagram practically in all the range of functioning Line 1 is in instability region. This means that parametric oscillations take place.

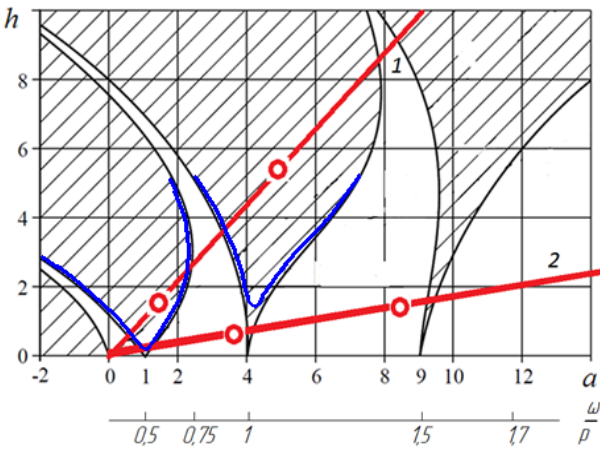


Fig. 5. Ince-Strutt diagram for the system under study.

For a simplification of data analysis in the diagram the scale of natural frequency to forcing frequency ratio is changed in addition  $\omega/p$ . For analysis simplification the diagram was redrawn in the dependence of depth rigidity on frequencies relation (see Fig. 6). Fig. 6 shows zones of the main and the second parametrical resonances (the shaded areas) with damping logarithmic decrement of attenuation  $\Delta=0.3$ .

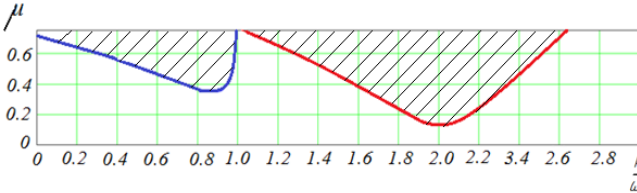


Fig. 6 - Zones of stability in relation to forcing frequency  $p$  for the main and the second parametrical resonance.

As follows from the diagram, it is possible to prevent parametric oscillations in two ways. First, to increase dissipation in the system. On the diagram it is reflected as lifting of the tips above abscissa axis. And second, to reduce rigidity depth to less than 0,1. The first way is structurally pointless. The second one is possible.

Structurally it may be realized by installation of a filter of low-frequency oscillations which will not let high-frequency disturbances generated to be transferred to the drum. This analytical conclusion received on the basis of the Ince-Strutt diagram, analysis is verified when performing computational modeling according to the model (1).

Besides, the required values of the modulation depth and natural frequency of the system providing expansion of the stability zone are established. For the system under study decrease in modulation depth parameter  $\mu$  up to the value 0.1 (Line 2 in Fig. 5) allows to narrow essentially the range of parametrical resonant oscillation. The variation of modulation depth parameter  $\mu$  is implemented by introduction of the low-frequency oscillation filter, which carries

out filtration of the high-frequency disturbances generated in the system and vibroprotection of the drum and multiplate clutch elements. As a result a low-frequency filter is synthesized. The results of the synthesis are implemented, for example, in the form of development of the torsion damper, which can be installed between a turbine wheel of the torque converter and input shaft of the planetary gearbox.

During the research an experimental test was carried out. This test proved the idea about exclusion of a high-frequency disturbance by means of low-frequency filter. The object of the research was the hydromechanical transmission, in which the plates of one of multiplate clutches in this transmission were in resonant mode at a frequency of 456 Hz due to nonlinear disturbance from electric motor and resulting torsional vibrations (Fig. 7). Two torque measurement sensors were installed in the transmission. The first one was connected with the shaft which is separated from the multiplate clutch by torsion damper (sensor A). The second sensor measured torsion torque of the shaft, which had rigid kinematical connection with the drum of the multiplate clutch under study. The electric motor was a source of vibrations in the transmission. The results of the test show that sensor A did not register oscillations at the resonant frequency of 456 Hz, but sensor B did. This proves efficiency of the suggested method of exclusion of resonant oscillations (as superharmonic) in non-linear system due to installation of torsion damper (which operates in the capacity of a low-frequency-filter).

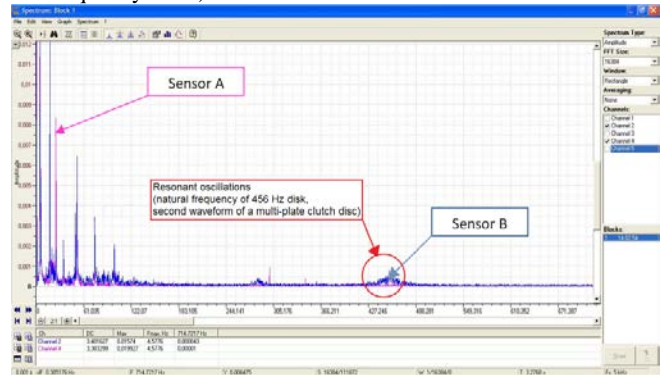


Fig. 7. Screenshot of the spectrum analyzer to confirm the idea of exclusions high-frequency perturbations due to the use of low-pass filter

Figure 8 shows the results of "Engine – Torque Converter – Drum – Plate" nonlinear system dynamics modeling after performing actions connected with tuning out parametrical resonant oscillations according to suggested way. Comparing the results of modeling (Fig. 4 and Fig. 8) it is evident that the power of disturbing spectral density generated by the system is reduced in comparison with the initial one over 2,5 times, and the amplitude of the moment decreases over 3 times. The assessment of fatigue durability of the plate design shows that if tuning parametrical resonances by the suggested way, the plate resource raises enormously.

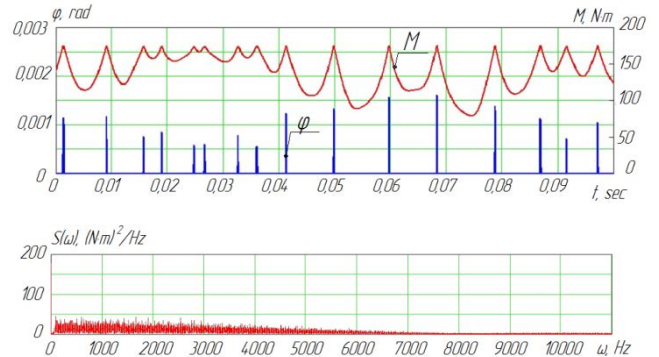


Fig. 8. The results of "Engine – Torque Converter – Drum – Lined Plate" nonlinear system dynamics modeling, after performing actions connected with tuning out parametrical resonant oscillations by suggested way.

## Summary

The new results about formation of dynamic loading of multiplate clutches plates are the basis of development of the described design calculation method and is distinguished from existing one by taking into account probability of generating parametrical resonant oscillations.

According to the research results it is established that the resonant mode in the multiplate clutch plates can be generated at various frequencies and by various disturbing sources. Resonance disturbance in the nonlinear system can be generated by oscillations of the ICE and EM torque, as well as by hydrodynamic processes in the impeller-turbine passage circulation of the torque converter, by oscillations of working liquid pressure in the system of its oil supply. Tuning out resonances at one of its frequencies can excite it on the adjacent ones. In this regard the most effective way of eliminating resonant modes is to filter oscillations generating a resonance.

Filtration of oscillations in pre- and post-converter zones can be carried out by synthesis of a high-frequency oscillation damper eliminating resonance in these zones, practically without receiving [5, 6] disturbances with frequencies significantly exceeding its natural frequency. Thus, to filter high-frequency oscillations generated in the transmission, as well as formed by a nonlinear characteristic of elastic interaction of tooth gearing of a drum and a plate, requires introduction of an additional torsion damper.

The executed assessment of the performance of the developed actions shows that elimination of resonant modes significantly increases durability of multiplate clutch plates.

## References

1. Krasnevsky L.G. Background and Prospects of Development of Automatic Transmissions of Mobile Vehicles / Krasnevsky L.G. // Topical issues of engineering science: Edited volume. OIM NAN of Belarus, Minsk – 2012, Edition. 1 – Pp. 108-114.
2. Derzhansky V. B. Forecasting of Dynamic Loading of Hydromechanical Transmissions of Transport Vehicles: Monograph / Derzhansky V. B., Taratorkin I.A. – Yekaterinburg: Ural RAN, 2010. – 176 p.
3. Design of Vehicle Transmissions/ Under the editorship of A.I. Grishkevich. – M.: Mechanical engineering, 1983. – 263 p.
4. Derzhansky Viktor, Taratorkin Igor, TaratorkinAlexandr. Decrease in Dynamic Loading of Transmission Elements of the Vehicle//Proceedings of the FISITA 2012 World Automotive Congress, Volume 10: Chassis Systems and Integration Technology. Beijing. :InstituteofTechnologyPress, Beijing – 2012, p. 495-504 .
5. Theory of oscillations: Textbook. For higher education institutions / Under a general edition of K.S. Kolesnikov. – 2nd edition, stereotyped. – M.: MG TU publishing house of N.E. Bauman, 2003. – 272 p, pic.:(Series.MechanicsatTechnicalUniversity; T. 4).
6. Panovko Y.G. Introduction in the Theory of Mechanical Oscillations: Manual. – 2nd edition. - and enlarged / Panovko Y.G. – M.: Science. Main edition of physical and mathematical literature, 1980. – 272 p.



# ОЦЕНКА СКОРОСТНЫХ СВОЙСТВ ГУСЕНИЧНЫХ МАШИН ПО ФАЗОВО-ЧАСТОТНЫМ ХАРАКТЕРИСТИКАМ

## EVALUATION OF SPEED CHARACTERISTICS OF TRACKED VEHICLES ON THEIR PHASE-FREQUENCY PROPERTIES

проф., д.т.н., Держанский В.Б., проф., д.т.н. Тараторкин И.А., к.т.н., Гизатуллин Ю.Н., инж., аспирант Тараторкин А.И. инж., аспирант Волков А.А. – Институт машиноведения Уральского отделения РАН, Россия

**Abstract:** In work the method of forecasting of mobility of high-speed tracked vehicles on their dynamic properties is resulted. The design decisions are resulted, allowing to raise average speed of passage of a test snake on 12 ... 16 % without decrease in durability of elements of caterpillars.

**KEYWORDS:** FORECASTING, MOBILITY, TRACKED VEHICLE, DYNAMIC PROPERTIES

### 1. Введение

При разработке и модернизации конструкции транспортных машин одной из важных задач является прогнозирование их быстроходности, оцениваемой средней скоростью движения. Для этого при движении в транспортном режиме по характерным дорогам используются методы прогнозирования, основанные на изучении установившихся процессов. При этом средняя скорость определяется как случайная величина на основе функции распределения скорости по пути с учетом ограничений по тяговым качествам, по предотвращению заноса на криволинейных участках, по параметрам плавности хода на неровных участках дороги. При движении по ровным дорогам скорость ограничивается тягово-динамическими качествами машины и условиями движения в повороте – условиями бокового заноса.

Эти методы разработаны и дают достаточно точные результаты для сравнительно тихоходных машин и при движении по местности на деформируемых грунтах. Для скоростных машин подвижность во многом ограничивается управляемостью. Это свойство характеризует все аспекты динамики системы «Человек – машина – внешняя среда» и оценивается динамическими, кинематическими и силовыми характеристиками. Динамические свойства определяются по фазовым частотным характеристикам, т.е по реакции машины как управляемого объекта на гармоническое возмущение.

Многочисленными работами, посвященными исследованию динамики управляемого движения быстроходных гусеничных машин (БГМ) установлено, что скоростные качества на трассах с интенсивным изменением кривизны траектории во многом ограничиваются удельной мощностью и величиной поворачивающего момента, создаваемого гидрообъемным механизмом поворота (ГОМП). Для повышения динамических качеств машин поворачивающий момент должен быть достаточным для преодоления сопротивления грунта повороту и инерционной составляющей. В противном случае проявляется действие нелинейности характеристики гидрообъемной передачи системы управления поворотом (СУП), вызванной ограничением давления или расхода рабочей жидкости. В этих условиях не обеспечивается не только динамическая устойчивость, но и статическая. Введение обратной связи в СУП не повышает управляемости.

Однако из результатов проведенного с участием автора экспериментального исследования динамики управляемого движения машины с увеличенной удельной мощностью на 33 % и поворачивающим моментом, обеспечивающим рост угловых ускорений при повороте на малодеформируемом грунте от 0,7 до 1,1 рад/с<sup>2</sup>, то есть в 1,4 раза, следует, что средняя скорость движения на дороге с интенсивным изменением кривизны траектории (тестовой «змейке», влажный бетон, дернистый грунт) гораздо ниже рассчитанной по силовым условиям поворота. Реализация потенциальных скоростных качеств с увеличением поворачивающего момента

во многом ограничивается динамическими свойствами машины – фазовым отставанием реакции на управляющее воздействие. Это приводит к тому, что продольная ось корпуса не успевает повернуться относительно касательной требуемой траектории. Для вписывания в заданный коридор необходимо снижать скорость движения. Однако существующие методы прогнозирования быстроходности гусеничных машин не учитывают их динамические свойства.

Эти свойства определяются по фазовой частотной характеристике, значение которой определяется по дифференциальному уравнению вращательного движения и динамики гидропривода.

### 2. Предпосылки и средства для решения проблемы

Динамические свойства гусеничной машины наиболее полно проявляются при движении по тестовой «змейке». В связи с этим при моделировании динамические параметры определяются по реакции гусеничной машины на гармоническое управляющее воздействие при заданных начальных условиях  $\dot{\psi}(0)$ ,  $V_X(0)$ ,  $V_Y(0)$ ,  $[x(0)]$ .

Анализ модели показывает, что реакция машины соответствует линейной системе, дополненной звеном чистого запаздывания. Динамические характеристики определяются по фазовым частотным характеристикам.

Обычно при оценке напряженности управляющей деятельности водителя в качестве основного показателя рассматривается время упреждения, при котором обеспечивается точность траектории движения. Применительно к рассматриваемому процессу, время, соответствующее требуемому опережению задающего воздействия по отношению к изменению угловой скорости, с увеличением скорости уменьшается.

Если быстроедействие рассматривать как показатель сложности регулирования направления движения, то следовало бы признать, что управлять движением машины по заданной «змейке» с неизменной длиной волны тем проще, чем выше скорость. Такое заключение противоречит опыту, так как с ростом скорости уменьшается время прохождения машиной одного цикла.

Исследования показывают, что человеку как звену замкнутого контура управления трудно компенсировать отставание выходного сигнала по фазе  $\psi_\phi$ . В приводе управления поворотом машины нет форсирующих звеньев, которые могли бы способствовать изменению угловой скорости, курсового угла (направления движения) с требуемым опережением; эта функция возлагается на водителя. Поэтому, чем больше фазовый сдвиг, тем жестче требования, предъявляемые динамической системой «машина – внешняя среда» к водителю и исполнительным механизмам системы управления поворотом. При больших значениях фазового отставания водитель вообще не сможет вписаться в заданную

кривую пути без снижения скорости. В связи с этим, критерия сложности управления выбран коэффициент фазовой напряженности регулирования направлением движения, определяемый отношением фазы реакции к числу  $\pi$ :

$$k_\phi(V) = \frac{\psi_\phi}{\pi}.$$

Для гусеничной машины массой 14 т. фазовая частотная характеристика приведена на рис. 1.

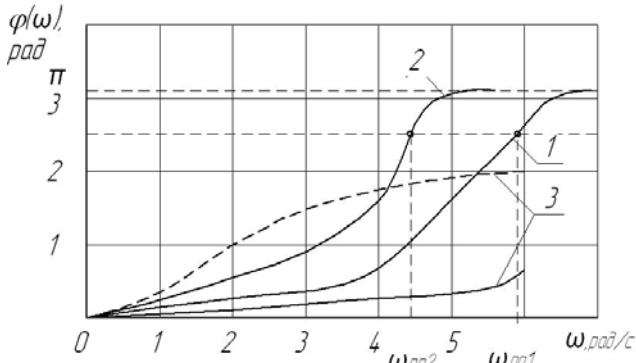


Рис. 1 - Фазовая частотная характеристика

1 – машины, как сплошного твердого тела; 2 – то же при учете упруго-инерционных свойств СУП; 3 – гидропривода СУП в зависимости от состояния рабочей жидкости: сплошная линия - номинальное состояние, пунктирная линия - двухфазное состояние

### 3. Решение рассматриваемой проблемы

В результате исследования, рассматривая движение как непрерывный марковский процесс, определена цикличность включения системы управления поворотом с непрерывными свойствами как положительное число выбросов случайной стационарной функции кривизны траектории «нулевого» уровня при движении по трассе, кривизна которой задана детерминированной или случайной функцией (в соответствии с работой В.А. Савочкина [2]).

Выполненными исследованиями установлено, что цикличность включения механизма поворота существенно превышает расчетные значения (рис. 2) и при максимальной скорости достигает 40 на километр пути при скорости 60...65 км/ч.

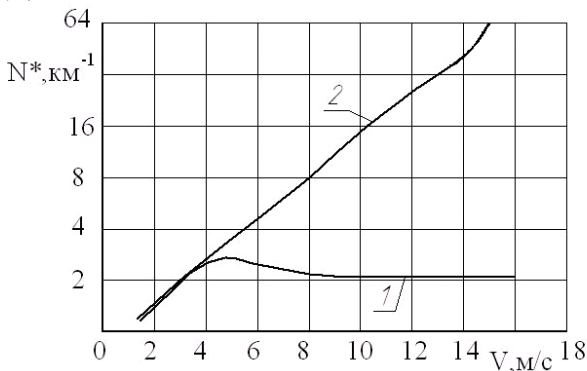


Рис. 2 - Зависимость цикличности включения механизмов поворота с непрерывными свойствами от скорости движения при случайном изменении направления траектории:

1 – прогнозируемое число включений МП по известным методикам; 2 – прогнозируемое число включений МП с учетом требуемой точности траектории движения.

Во многом это связано с принимаемыми допущениями. Параметры действительного процесса управления отличается от расчетных. Цикличность включения механизма поворота зависит не только от вероятностных свойств дорожной

кривизны, но и от требуемой точности траектории, поэтому число управляющих воздействий, их частота существенно отличается от числа поворотов дороги. При необходимости выполнения поворота машиной водитель поворачивает штурвал на некоторый угол  $\beta(k_\phi, \alpha_{ум})$ . Из-за бокового смещения действительный резерв ширины проезжей части необходимо уменьшить на величину  $\Delta Y = \int_0^t V \cdot \theta(V, t) dt$ .

Кроме того, вследствие юза и буксования гусениц фактическая кривизна отличается от расчетной:  $k_\phi = k_p \cdot B / L$ . С учетом дивергенции отклонения вектора параметров траектории движения, ограниченного быстродействием системы, действительный угол поворота машины гораздо меньше расчетного  $\beta(k_\phi, \alpha_{ум})$  и составляет:

$$\beta_\phi = \beta(k_\phi, \alpha_{ум}) - \theta - \Delta\beta_3 - \Delta\theta \quad (1)$$

В формуле приняты следующие обозначения:

$\beta(k_\phi, \alpha_{ум})$  - заданный угол поворота машины;  $\theta, \Delta\theta$  - значения бокового угла детерминированное и стохастическое соответственно;  $\Delta\beta_3$  - величина отклонения направления движения, компенсирующее запаздывание системы.

Дополнительное число включений механизма поворота, обеспечивающее требуемую точность траектории по условиям вписываемости можно определить как математическое ожидание случайной функции удельного числа поворотов  $N_{уд}(k_\phi)$ :

$$N^*_\phi(k_\phi) = m_s[N_\phi(k_\phi)] = \int_0^{k_\phi} \frac{k_\phi}{\beta_\phi} \varphi_s(k_\phi) dk_\phi \quad (2)$$

где  $\varphi_s(k_\phi)$  - плотность вероятностей модуля дорожной кривизны  $k_\phi = |k_\phi|$  ( $0 \leq k_\phi \leq k_\phi$ ), определяемая по спектральной плотности или корреляционной функции дорожной кривизны  $k_\phi = |k_\phi|$ ;  $\beta_\phi$  - действительный угол поворота машины, его определение приведено выше.

Прогнозируемое значение скорости движения можно определить по уравнению:

$$V = \begin{cases} \frac{\omega_{пр} \Delta S}{\pi} & \text{– при детерминированной} \\ & \text{функции кривизны} \\ \frac{\omega_{пр}}{2\pi(N^* + N_\phi^*)} & \text{– при стохастической} \\ & \text{функции кривизны} \end{cases} \quad (3)$$

где  $\omega_{пр}$  - значение частоты соответствующее допустимому значению коэффициента фазовой напряженности

$$k_\phi(V) = 0,75.$$

Корректность допущений при определении цикличности включения механизма поворота, адекватность математической модели реальному процессу подтверждены экспериментальным исследованием динамики управляемого движения машины.

На основе сопоставления результатов теоретического и экспериментального исследования делается вывод о необходимости корректировки математической модели введения звена «чистого запаздывания».

Одним из важных параметров, определяющих подвижность машин, является цикличность включения системы управления поворотом. Из результатов экспериментального исследования видно, что при скорости движения  $V \leq 5$  м/с фактическое

число включений соответствует расчетному. При больших значениях скорости число включений существенно возрастает и при  $V=20$  м/с составляет 42 на километр пути (0,8 Гц), и ограничивается психофизиологическими свойствами водителя как звена обратной связи системы. Существенная разность по сравнению с известными результатами расчета по известным методикам вызвана тем, что параметры действительного процесса управления отличаются от расчетных. Цикличность включения механизма поворота зависит не только от вероятностных свойств дорожной кривизны, но и от требуемой точности траектории. Число управляющих воздействий, их частота существенно отличается от количества поворотов дороги. При расчете цикличности с учетом обеспечения требуемой точности траектории расчетное значение функции цикличности включения от скорости движения удовлетворительно совпадает с экспериментальными данными.

На основе проведенных исследований предлагается следующий алгоритм прогнозирования быстроходности гусеничной машины при криволинейном движении. Исходными данными являются: геометрические и упруго-инерционные параметры машины, определяющие фазовую частотную характеристику, удельная мощность, характеристики тяговая и системы управления поворотом; спектральная плотность дорожно-грунтовых условий движения: кривизна дороги  $S_k(\omega)$  и ее ширина  $S_H(\omega)$ , а так же коэффициента сопротивления повороту  $S_\mu(\omega)$ . На основе обратного преобразования Фурье определяются параметры дорожно-грунтовых условий  $k(s), H(s), \mu(s)$  в функции пути.

В дальнейшем производится определение параметров нелинейности системы управления, динамических свойств ( $t_{3\omega}, t_{1\omega}$ ) гусеничной машины и водителя, коэффициент фазовой напряженности  $K_\phi(\omega)$ , составляющие угла поворота машины  $\beta(k_D, \alpha_{шт})$  в соответствии с уравнением (4) и таблицей 1, цикличность включения механизма поворота (3,6) и частота процесса регулирования направления движения  $\omega_{пр}$ . Кроме того, вводятся ограничения: условия вписываемости (5), психологические свойства водителя выполняющего функции звена обратной связи, перегрузки ГОП, буксование гусеницы забегающего борта, по тяговым возможностям и боковому заносу. По результатам расчетов строятся графики изменения кинематических параметров при движении по тестовой змейке (рис. 3) и по трассе со случайным изменением кривизны траектории. На основе этих данных и имитационного моделирования движения машины производится расчет скорости движения как наименьшей по вышеприведенным ограничениям.

Полученные результаты статистически обрабатываются, определяется спектральная плотность скорости движения и числовые характеристики функции распределения по пути.

#### 4. Результаты и дискуссия

Реализация такого подхода позволяет не только прогнозировать быстроходность машины по ее динамическим свойствам, но и решать обратную задачу повышения скоростных свойств дифференцированным сокращением ограничений при автоматизации управления движением. Сформулированы требования к автоматизированной системе, в частности по созданию форсирующего управления, компенсации быстрых отклонений, сокращения цикличности включения механизма поворота водителем.

Доказано, что повышение быстроходности машин в повороте при достаточном значении поворачивающего момента может быть достигнуто совершенствованием динамических свойств СУП – синтезом пропорционально

интегрирующе-дифференцирующих (ПИД) корректирующих устройств.

Обоснована необходимость сокращения податливости рабочих ветвей гусениц. Эти предложения реализованы при разработке гусениц со сплошным основанием резиновых элементов шарнира и его армированием. Это позволило повысить среднюю скорость прохождения тестовой змейки на 12...16 % без снижения долговечности гусениц. Экспериментальными исследованиями установлены приемы управления машиной при движении в повороте, без снижения скорости.

Выбор и вариация параметров конструкции машины, приемов управления движением осуществляется на основе анализа зависимостей фазового отставания реакции на возмущение управления и цикличности включения механизма поворота. Сокращение фазового отставания возможно при уменьшении момента сопротивления повороту – в режиме движения с частичным заносом ( $\chi < 0,5L, \theta(v,t) < \theta(v,\mu,H)$ ) при существенном ограничении – необходимости упреждающего управления, высокого быстродействия СУП.

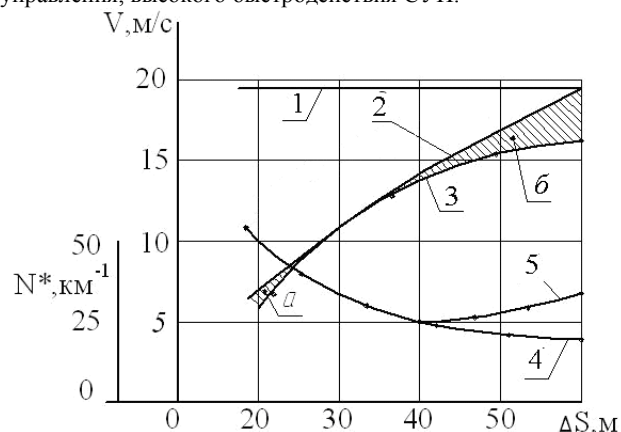


Рис. 3 - Анализ результатов исследования (тестовая змейка)

- 1 – кинематически возможная скорость по двигателю  $V(S)$ ;
- 2 – ограничение предельной скорости по фазовой частотной характеристике СУП;
- 3 – экспериментальные данные  $V(S)$ ;
- 4 - расчетное значение цикличности включений СУП  $N^*$ ;
- 5 - экспериментальное значение цикличности включений СУП  $N=N^*+N^*$ , обеспечивающих точность траектории.
- а - зона ограничения скорости по тяговым свойствам двигателя и СУП;
- в - зона ограничения по динамическим свойствам СУП.

Фазовое отставание могло бы быть существенно сокращено, если бы водитель мог изменять управляющее воздействие по производной рассогласования направляющего угла. Эти два направления снижения фазового отставания могут быть реализованы форсирующими звеньями автоматизированной системы управления движением. При этом установочная мощность гидрообъемной передачи должна быть достаточной для преодоления динамической составляющей момента сопротивления повороту. При ограниченной установочной мощности гидрообъемной передачи высокие динамические качества машины, определяющие вход в поворот, могут быть обеспечены продольным замедлением при снижении скорости поступательного движения. Эта функция осуществляется созданием конструкции механизма поворота с регулируемым кинематическим параметром или применением алгоритма управления движением, обеспечивающим переключение передачи на номер ниже, что предотвращает разблокировку ГТ при перегрузке двигателя. Повышение динамических и скоростных качеств БГМ в процессе поворота в сложных дорожных условиях с непрерывным изменением направления движения обеспечивается при работе двигателя на повышенных оборотах. Снижать скорость движения за счет уменьшения подачи топлива для вписывания в поворот

нецелесообразно, т.к. это приводит к уменьшению производительности гидронасоса ГОП.

При движении на прямолинейных участках пути, на марше или в колонне, при стабилизации скорости движения возможно обеспечить режим работы двигателя минимального расхода топлива. Заметное изменение угловой скорости поворота машины при увеличении подачи топлива в процессе поворота через 1,5...3,0 с., если двигатель работал при неполной загрузке. При этом условии увеличение подачи топлива стабилизирует движение машины на границе устойчивости.

Снижение жесткости механической характеристики ГОП, что характерно для двухфазного состояния рабочей жидкости при ее вспенивании или кипении следует отнести к фатальной ситуации. Скорость движения в этом режиме ограничивается управляемостью и устойчивостью из-за неудовлетворительного качества переходных процессов, фазового отставания реакции.

Повышение скорости прямолинейного движения по твердым дорогам с ограниченными сцепными свойствами за счет сокращения числа управлений (подруливаний), компенсирующих быстрые отклонения угловой скорости, осуществляется при синтезе оптимального управления, основанного на определении спектральной плотности случайного процесса. Другим вариантом является управление по менее зашумленной координате – курсовой угол.

Повышение скорости сокращения фазового отставания может быть достигнуто и при увеличении собственной частоты машины  $\omega^2_0 = \frac{C_M}{J_{пр}}$  по координате  $\psi$ . Этому значению

соответствует фазовый угол  $\pi/2$  и в дальнейшем резко возрастает до  $\pi$ . Гусеницы с РМШ, обладающие большей податливостью не способствуют росту собственной частоты (снижению фазового угла). Корректность основных допущений при определении ФЧХ и цикличности включения СУП, адекватность математической модели реальному процессу, позволяет обосновать основные пути повышения предельной частоты ФЧХ ( $\omega_{п}$ ) и скоростных качеств БГМ при криволинейном движении. В частности обоснована необходимость сокращения податливости рабочих ветвей гусениц. Эти предложения реализованы в конструкции гусениц со сплошным основанием резиновых элементов шарниров и их армированием. Такое решение позволило повысить линейную жесткость на 64 %, предельную частоту  $\omega_{п}$  с 4,5 до 5,4 рад/с. Это позволило повысить среднюю скорость прохождения тестовой змейки на 12...16 % и повысить долговечность шарниров гусениц.

Сокращение податливостей рабочих ветвей гусениц повысило эффективность компенсации быстрых отклонений при введении в контур управления интегрирующего звена. Такой же эффект достигается повышением сцепных свойств гусениц с опорной поверхностью при установке асфальтоходных башмаков.

В общем случае движения – при действии возмущений стохастического характера, качество переходных процессов, сокращение фазы реакции на управляющее воздействие и точность траектории при ограничении затрат мощности на компенсацию отклонений достигаются синтезированным оптимальным управлением при не полностью известных возмущающих силах.

## 5. Выводы

1. На основе проведенного исследования в данной работе научно обоснована и решена задача разработки метода прогнозирования быстроходности гусеничных машин по их динамическим свойствам, выбора параметров конструкции и системы управления поворотом, позволяющая более полно реализовать потенциальные скоростные качества многоцелевых гусеничных машин при движении по дорогам с интенсивным изменением кривизны, имеющая важное военное и народно-хозяйственное значение.
2. Испытания опытной машины с макетным образцом ПИД корректирующего устройства системы управления поворотом на тестовой змейке показали, что средняя скорость движения повысилась до 14,3 %, при сокращении числа включений с 37 до 25 на километр пути. При движении по грунтовой трассе со случайным изменением кривизны траектории средняя скорость возрастает на 12...16 %, сокращается число включений механизма поворота в 1,5...1,8 раза.
3. Обоснована необходимость сокращения податливости рабочих ветвей гусениц. Предложенные конструкторские решения реализованы при разработке гусениц со сплошным основанием резиновых элементов шарниров и их армированием. Это позволило повысить среднюю скорость прохождения тестовой змейки на 12...16 % без снижения долговечности элементов гусениц.

## 6. Литература

1. Держанский В.Б., Тараторкин И.А. Прогнозирование динамической нагруженности гидромеханической трансмиссии транспортных машин Екатеринбург: УрО РАН 2010 - с. 176
2. Савочкин В.А., Дмитриев А.А. Статистическая динамика транспортных и тяговых машин. – М.: Машиностроение, 1993. – 320 с.

# SUBHARMONIC RESONANCES IN THE HYDROMECHANICAL TRANSMISSION OF THE WHEELED CHASSIS

## СУБГАРМОНИЧЕСКИЕ РЕЗОНАНСЫ В ГИДРОМЕХАНИЧЕСКОЙ ТРАНСМИССИИ КОЛЕСНОГО ШАССИ

Prof. Dr. Eng. Derzhanskii V.<sup>1</sup>, Prof. Dr. Eng. Taratorkin I.<sup>1</sup>, postgraduate Taratorkin A.<sup>1</sup> – Institute of Engineering Science of the Ural Branch of the Russian Academy of Sciences (IES UB RAS), Russia

**Abstract:** *In the article on the basis of the developed mathematical model the dynamics of the highly nonlinear system is investigated, consistent patterns of resonant mode occurrences are established, which is experimentally confirmed. It is established that one of the main reasons for high dynamic loading and HMT elements durability reduction is subharmonic resonances caused by close agreement of frequencies of free nonlinear system fluctuations with multiple value of frequencies of diesel engine disturbances. On the basis of the new consistent patterns, the area of stability and parameter move direction is defined for its provision. The offered damper design is synthesized for significantly reducing HMT dynamic loading.*

**KEYWORDS:** *OSCILLATIONS, NATURAL FREQUENCY, SUBHARMONIC RESONANCE, DYNAMIC LOADING HYDROMECHANICAL TRANSMISSION*

### 1. Introduction

The Multiple Wheel Chassis are widely applied both as vehicles and as processing equipment in the Russia's oil and gas sector in extreme operational conditions of Far North, the Polar Urals and West Siberia. The specified chassis is equipped with single-type hydromechanical transmissions which reliability is limited in many respects, in particular, in durability of matching reduction gearboxes [1].

Allison Company offers a project for modernization of MWC by installation of the engine and transmission assembly. However, the cost of the project makes 14 million RUB, which almost four times exceeds the cost of MWC complete overhaul. An increase in durability of matching reduction gearboxes, design development, their implementation, i.e. transmission modernization in the course of chassis maintenance is an effective way of increasing its reliability.

Application of a matching reduction gearbox with several tooth gears providing kinematic match of engine and hydraulic torque converter characteristics is a peculiar feature of the transmission design under study. Strong nonlinearity of the system is caused by gear backlash opening in tooth gears and existing resonance elimination methods in this case are inefficient. In this regard, the proposed work devoted to analyzing the conditions of subharmonic resonant mode occurrences in the strongly nonlinear system and to substantiating the method of their detuning is topical.

**The objective of this work is** to define the ways of increasing durability of matching reduction gearboxes of MWC hydromechanical transmissions, to develop and implement design solutions providing detuning from subharmonic resonant oscillations on the basis of a new type torque vibration damper synthesis.

**Scientific novelty** of the work lies in studying consistent patterns of generation and provision of rationale for a method of eliminating subharmonic resonant modes in the system "Diesel Engine – Hydromechanical Transmission" on the basis of studying the dynamics of the strong nonlinear system with polyharmonic disturbances from the diesel engine.

### 2. The background of the problem and rationale for the key questions to be explored

Transmission dynamic loading is determined by influence of considerable sign-variable torques occurring in the steady-state regime under resonances, as well as under transient regime of engine start-up and dying out, acceleration and braking operation, gear shifting and torque converter lockup.

The analysis of the failure rate shows that the greatest amount of element breakage of the mechanical system "Engine – Transmission - Transport Vehicle" deals with the part between the

diesel (the activator of mechanical oscillations) and a pump wheel of the torque converter.

The solution of specific problems is hindered due to absence of an objective method for choosing a type of damper design and its parameter identification. It predetermines a large volume of experimental and test and evaluation work at the stage of developing the design when modification demands essential time, work and material expenditures.

The background for the research is scientific development of many domestic and foreign experts. Most fully the technique of tuning out resonant modes on the basis of oscillation damper synthesis is stated in the works of Grishkevich A. [1]. The results of researching the dynamic behavior of nonlinear systems leading to generation of such phenomena as clunk noise and shuffle are given in works of A. Crowther, R. Singh, Stahl, K., Pflaum, H., Meingassner, G. J., Lohmann, B. et al. [2,3,4,5]. The solution of this problem is stated in practical methods and reference books of Centa Company (Germany). The results of the company's research and its development are widely applied in mechanical engineering around the world, including Russia.

However, the existing works don't allow for considering high nonlinearity of the elastic characteristics peculiar to the system under study.

On the basis of the analysis of the scientific works devoted to research and design of oscillation dampers, the conclusion is made that reduction in dynamic loading and damper synthesis, which consider real nonlinear properties, does not seem possible due to a complex interrelation of the system elements. The article substantiates the necessity of carrying out theoretical and pilot studies with application of up-to-date methods of nonlinear mechanics, of parametrical oscillation stability assessment, of simulation modeling and of processing of experimental data.

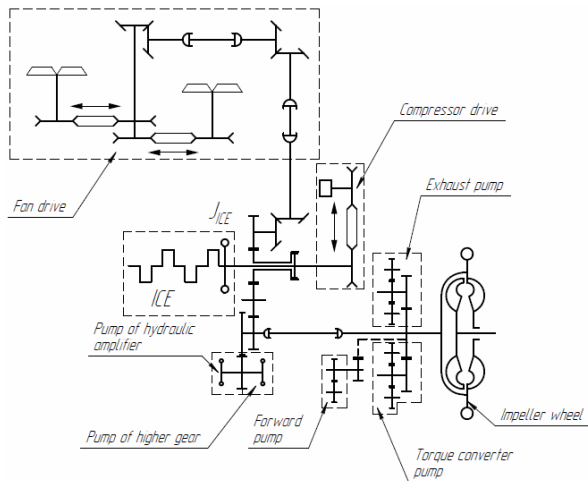
### 3. Theoretical research of dynamic loading

Hydromechanical transmission is a complex multiunit mechanical nonlinear system of a variable structure containing ring elements.

The detailed analysis of this model has allowed for drawing a conclusion that the dynamic torque on transmission shafts is formed by:

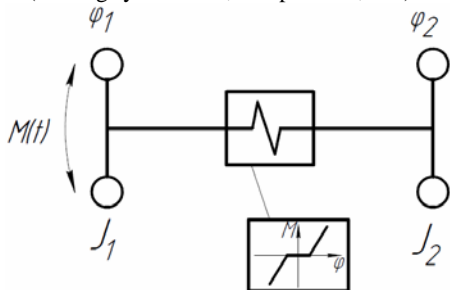
- a periodic component of the engine torque, both in steady-state and non-steady-state operating regimes;
- the dynamics of the mechanical system under transients of standing start, acceleration, gear shifting and torque converter lockup.

The dynamic loading of the matching reduction gearbox design elements (the kinematic scheme is given in Fig.1) is a defining factor limiting durability of engine and transmission assembly for the MWC family under study.



**Fig. 1.** Kinematic scheme of pre-torque-converter zone

The analysis has shown that the dynamic loading of the matching reduction gearbox design elements can be effectively defined on the basis of studying the dynamics of a two-mass system – the so-called pre-torque-converter zone [1]. This system (the computational scheme is given in Fig. 2) comprises an engine flywheel (the first mass), a torque converter impeller wheel (the second mass) with the inertial masses of a matching reduction gearbox (cooling system fans, compressors, etc.) connected to it.



**Fig. 2.** Design model of pre-torque-converter zone.

The nature of interrelation between these two masses is built up by elastic and dissipative characteristics of the torsion damper (torsion, see Fig. 2) and tooth gears of a matching reduction gearbox, which backlash opening forms nonlinearity of an elastic interaction. The analysis of the dynamic process in the system under study and predetermination of the ways for reduction in dynamic loading are made on the basis of a mathematical model of the pre-torque-converter zone of the hydromechanical transmission as a nonlinear two-mass system (1).

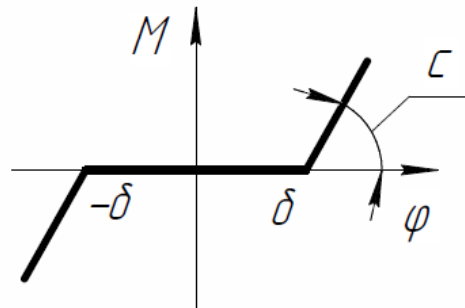
$$\begin{cases} J_1 \ddot{\varphi}_1 + M(\varphi) = M(t) \\ J_2 \ddot{\varphi}_2 - M(\varphi) = 0 \\ \varphi = \varphi_1 - \varphi_2 \end{cases} \quad (1)$$

where  $J_1, J_2$  are inertia moments of the engine and the impeller respectively;  $M(\varphi)$  is nonlinear elastic interaction function (Fig. 3);  $M(t)$  - time function of engine and impeller wheel torque.

Nonlinear function - dependence of the moment on relative angular coordinate – is schematized (Fig. 3) and is accepted as symmetric with a dead zone without saturation [7], i.e.

$$M(\varphi) = \begin{cases} 0 & \text{at } |\varphi| \leq \delta \\ c \cdot (|\varphi| - \delta) \cdot \text{sign}(\varphi) & \text{at } |\varphi| > \delta, \end{cases}$$

the parameters of which  $\delta$  and  $c$  are defined experimentally.



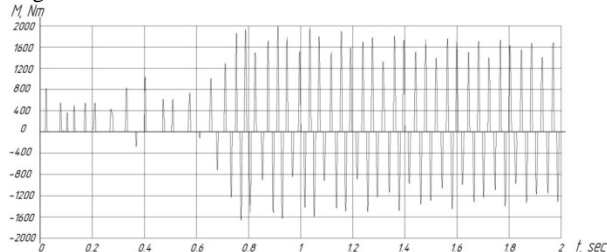
**Fig. 3.** Schematization of nonlinear function with dependence of the moment on the angular coordinate (nonlinearity with a dead band without saturation).

The time function of the engine torque  $M(t)$  is accepted in Fourier's series form, the parameters of which are defined according to the data of the manufacturing factory.

$$M(t) = M_0 + \sum_{m=1}^{\infty} M_m \cos(m\omega t + \beta_m)$$

The harmonious analysis of the engine torque shows that the most dangerous harmonics of the engines YaMZ-8401, YaMZ-240, D-12 (according to the manufacturer, JSC Avtodiesel) is the sixth, i.e. in the engine rpm range, the exciting frequency makes from 70 to 85 Hz that considerably (3 ... 4 times) exceeds the frequencies of natural oscillations of the system under study (12 ... 17 Hz).

The results of the numerical solution (1) at values of the parameters corresponding to the object of the pilot study are given in Fig. 4. As comes from this Fig. 4 oscillations of the torque occur regarding the established value with amplitude 3 ... 4 times exceeding the established value.

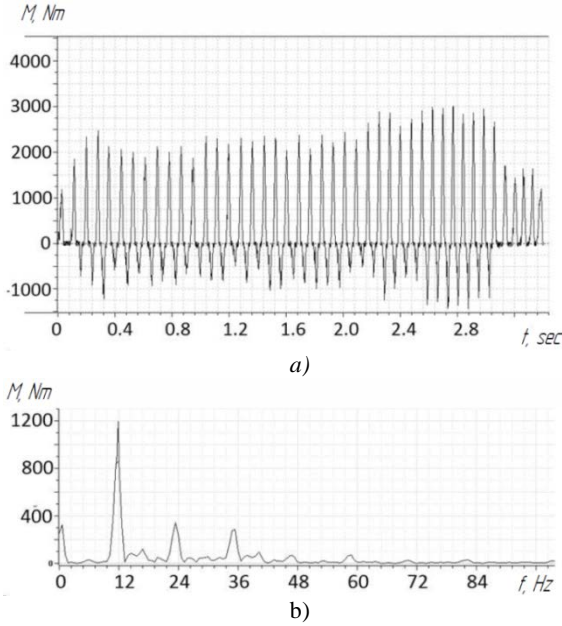


**Fig. 4.** The results of the numerical solution (1) at values of the parameters corresponding to the object of the pilot study ( $n_{ICE}=740$  rev/min)

The characteristics of the periodic process under study (moment amplitude, natural oscillations) significantly depend on the initial conditions which is characteristic for nonlinear systems. In fig. 4, two various types of movement characterized by the size of backlash opening are shown. It leads both to an amplitude change and frequency of periodic oscillations of the system under study.

The results of numerical modeling are confirmed experimentally at running trials of the wheel chassis KZKT-7428, equipped with YaMZ-8401.10. Similar results were obtained at trials of wheeled chassis KZKT-74286 with engine YaMZ-240 and MWC MAZ-537 with the engine D-12 (the trial results of KZKT-74286 and MAZ-537 are not given).

The fragment of the oscillogram of the torque changing in the steady-state mode, at the engine rpm range of 700 ... 850 rpm, is given in Fig. 5a. From the provided data, it follows that the change of the torque has an oscillatory character with an amplitude up to 2,500 Newton meters, and the process frequency makes from 10 to 19 Hz with a disturbing frequency of the engine from 70 to 85 Hz (the 6th main engine harmonics of the engine YaMZ-8401). This alternating character of the torque within the time frame (Fig. 4, Fig. 5), corresponds to subharmonic resonant oscillations in the nonlinear mechanical system with a dead zone.



**Figure 5.** The fragment of the oscillogram of the torque changing at the torsion shaft (a) and its spectrum (b) in an idle mode ( $NICE=740$  rev/min.)

The spectral analysis of the obtained numerical solution verifies the abovementioned conclusion about generation of oscillations at subharmonic frequencies multiple times smaller than the main harmonics (the 6<sup>th</sup>) of the YaMZ-8401 engine. In this case, the subharmonic resonance oscillations in nonlinear systems coexist with principal forced oscillations.

Thus, the solution of the system of nonlinear differential equations is not unambiguous. In addition, existence of several steady-state modes with various amplitudes is possible  $\varphi_i = \varphi_i(t)$ , including an unstable mode. Research of oscillation process stability and provision of a rationale for the direction of resonant modes elimination is carried out on the basis of the device of parametrical oscillations [8]. To implement this approach, an equation system of (1) by introduction of a coordinate of relative angular movement  $\varphi = \varphi_1 - \varphi_2$  is reduced to the form of nonlinear differential equation (2)

$$J_{reduced}\ddot{\varphi} + M(\varphi) = M(t), \quad (2)$$

where  $J_{reduced}$  – reduced moment of inertia. Other functions introduced into the equation (2) are given above. The complexity of the analytical determination of the reduced inertia moment is that it is necessary along with the moment of flywheel inertia to consider response time of the torque converter impeller filled with hydraulic fluid. Besides, in the design of MWC transmission, it is from the pump wheel that many mechanical devices are actuated (fans, pumps, compressors, etc.). In this regard this size is determined experimentally [6] ( $J_{ICE} = 8,5 \text{ kgm}^2$ ).

To analyze stability of the system, the mathematical (2) model is modified to Mathieu equation [8]:

$$\ddot{\varphi} + 2\varepsilon\dot{\varphi} + \omega^2 \left[ 1 - \frac{q_{dyn}\cos(\omega_6 t)}{q_{st}} \right] \varphi = 0 \quad (3)$$

In this equation  $\varepsilon = b/2J_{reduced}$  is a dissipation parameter;  $\omega^2$  is a square of natural frequencies of the nonlinear system, determined considering the constant component of the engine moment. The value of this moment is determined by losses in the matching reduction gearbox, by losses on overcoming resistance in the compressor drive, the drive of fans, etc. The frequency of natural oscillations is defined by the following response characteristics:

$$\omega = \sqrt{\frac{c - \frac{c}{\pi} \left( \arcsin \frac{\delta - x}{\varphi_d} + \arcsin \frac{\delta + x}{\varphi_d} + \frac{\delta - x}{\varphi_d} \sqrt{1 - \frac{(\delta - x)^2}{\varphi_d^2}} + \frac{\delta + x}{\varphi_d} \sqrt{1 - \frac{(\delta + x)^2}{\varphi_d^2}} \right)}{J_{reduced}}}, \quad (4)$$

where  $\varphi$  is angular amplitude at the neutral point in the transmission and at the shaft speed matching to idle speed;  $x$  is the shift of the zero line determined by a constant component of

loading. Introducing the parameters of depth of disturbance  $\mu$  and its alternation frequency  $p$ , Mathieu equation without considering dissipation is modified to

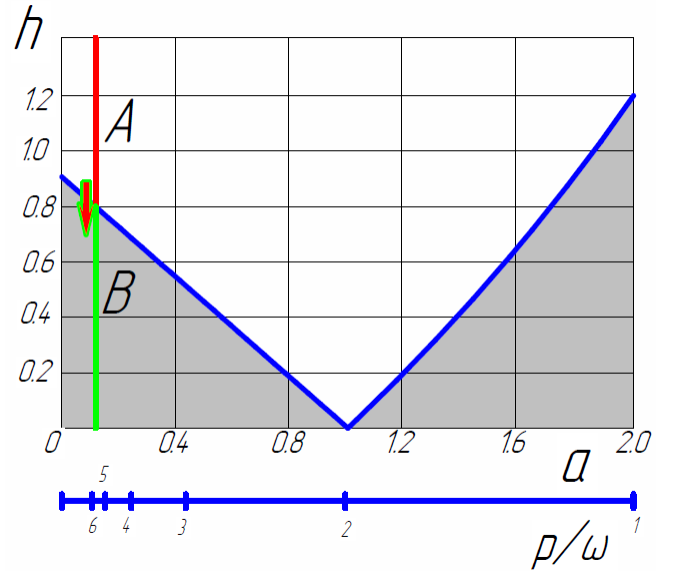
$$\ddot{\varphi} + [a - 2h\cos(2\tau)]\varphi = 0, \quad (5)$$

where  $a = \left(\frac{2\omega}{p}\right)^2$ ;  $h = a\mu$ ;  $2\tau = pt$ . Ince-Strutt diagram with the coordinates  $h(a)$  is given in Fig. 6 (stability area is shaded). The parameters of the system under study are represented by point A, being in the unstable zone. The coordinates of the point are determined as follows. The abscissa of the point A is determined according to the formula  $a = \left(\frac{2\omega}{p}\right)^2$ , where  $\omega$  is the frequency of natural oscillations of the nonlinear system, determined according to the formula (4) and corresponding to the amplitude of the moment of the main motor harmonics with a frequency  $p$  ( $p=6$ ,  $M=1,200$  Nm). To determine the parameter  $h$ , it is necessary to evaluate modulation depth  $\mu$ , characterizing the amplitude of a variable parameter of the system (relation  $q_{dyn}/q_{st}$  in formula (3)) being determined for this system according to the formula (6).

$$\mu = \frac{c - \frac{c}{\pi} \left( \arcsin \frac{\delta - x}{\varphi_d} + \arcsin \frac{\delta + x}{\varphi_d} + \frac{\delta - x}{\varphi_d} \sqrt{1 - \frac{(\delta - x)^2}{\varphi_d^2}} + \frac{\delta + x}{\varphi_d} \sqrt{1 - \frac{(\delta + x)^2}{\varphi_d^2}} \right)}{c - \frac{2c}{\pi} \left( \arcsin \frac{\delta}{\varphi_s} + \frac{\delta}{\varphi_s} \sqrt{1 - \frac{\delta^2}{\varphi_s^2}} \right)} - 1, \quad (6)$$

where  $c$  is rigidity of an elastic element (torsion),  $c = 72,000 \text{ Nm/rad}$ ;  $\varphi_d$  is the amplitude of the sixth engine harmonics;  $\varphi_s$  is the amplitude corresponding to the engine load moment (loss torque);  $\delta$  is a dead zone defined by backlashes in the gear of the matching reduction bogear ( $\delta=0.026$  rad);  $x$  is a shift of the zero line ( $x=0.029$ ).

For the given parameters at rpm engine speed of 850 rev/min, Ince-Strutt diagram parameters makes  $a = 0.07$   $h = 1.033$ .



**Fig. 6.** Ince-Strutt Diagram.

Analyzing the results of numerous calculations, corresponding to the diagram it appears that at the given parameters of the dynamic system in the range of parameter values from 0 to 0.111 (frequency range of the disturbance we are interested which is determined by the detuning factor  $\frac{p}{\omega} = 6$  at the minimum allowable speed ICE – 600 rev/min) the parameter  $h$  exceeds the value of 0.9. Therefore, all estimated values of set points in  $h$ - $a$  coordinates reside in an instability zone A (shaded) to the left from the red line. Such a situation remains unchanged up to 900 rev/min when periodic oscillations of the dynamical system have an unstable (resonance) character.

Solution of the inverse problem of choosing optimal parameters of a dynamical system, being unable to control the modulation depth  $\mu$  and to change the characteristics of the nonlinear elastic relationship (dead zone value), is possible only if to change the setting of detuning the system  $\frac{p}{\omega}$  (relation  $\frac{p}{\omega}$  is

given in Fig. 6 as an additional axis of abscissa). Thus, the stability is ensured by choosing torsion vibration damper compliance considering the condition that an operating point with coordinates  $h - a$  will get into the shaded zone **B**, located in the diagram to the left of the green line.

For example, taking the minimum allowable point of rpm engine speed at 600 rev/min and gradually reducing the rigidity of the elastic element, we determine the Ince-Strutt diagram parameters. The calculation is performed before moving the operating point with coordinates  $h - a$  from unstable zone to the stable one, i.e. from zone **A** to zone **B**. With respect to the dynamical system, the desired effect is achieved at the rigidity of the elastic element of 45,000 ... 50,000 Nm/rad. Furthermore, the Ince-Strutt diagram parameters made  $a=0.089$   $h=0.684$  at  $c=45000$  Nm/rad and  $a=0.098$   $h=0.854$  at  $c=50000$  Nm/rad.

When the reliability of the results obtained by comparison with experimental data, they can become the basis for the method of limiting torque oscillation amplitudes and, respectively, of dynamic loading.

#### 4. Analysis of the research results

Qualitative and quantitative comparison of the research results was carried out on the basis of analysis for amplitudes and frequencies of high frequency oscillations in the pre-torque-converter zone (see. Fig 3 and Fig 4). Some differences of amplitude and frequency might be explained by deviation of initial conditions when modeling.

On the basis of the research results the method of elimination of resonant modes in the nonlinear system is developed. According to nonlinear elastic characteristic parameters on the basis of the developed mathematical model, the zone of stability and probability of subharmonic resonant mode generation is defined. For their eliminating, it is necessary to vary parameters of Ince-Strutt diagram ( $h$  and  $a$ ) from a condition of getting into the stability zone. The most effective and easy way is tuning out the natural frequency of the system by changing angular rigidity of matching reduction gearbox. In particular, for reduction in dynamic loading of the HMT under study by elimination of a resonant mode, it is necessary that torsion damper angular rigidity was not higher than 50,000 Newton meters per radian.

Accordingly, a design of a matching reduction gearbox (Fig. 7) with a new type of torsion vibration damper with the rigidity of 21,000 Nm/rad. This silicone elastic element comes from the line of the Centa Company dampers and fit well into the existing design of the matching gearbox

The proposed design of the matching gearbox (Fig. 7) is produced as a three-shaft transmission with overdrive skew gears. In the case 1 on the bearing supports, there is a drive shaft-mounted gear 2, intermediate 3 and driven 4 shafts. The case 1 is fastened with the bolts to the housing 5 of the engine flywheel 6. The support 9 is connected with the engine flywheel 6. The disk 10 is connected to the support 9 with female splines. The elastic element, made as a silicone ring 11, with the help of the splines on the outside surface is connected with the disk 10, and the splines on the internal surface with multiple piece hub group 12, carried by bearings 15, installed in the support 9. The transmission shutdown mechanism made in the form of a two-stage gear coupling located in the cavity formed by the front part of the case. The gear clutch consists of a driven half coupling 8, connected by internal splines with the left end of the extended drive-shaft of the gear 2. The half-coupling 8 is connected by internal splines with the sleeve 7. Thus, the sleeve 7 provides for connection of the driven half coupling 8 with multiple piece hub group 12 on the outside surface where there are splines. At that, the sleeve 7 is fixed at two positions with ball locking mechanism 16. The driven shaft 4 through cardan shaft rotates a pump wheel of the torque converter of hydromechanical transmission of the transport vehicle (fig. 7 does not show it).

The proposed design of the matching reduction gearbox works in the following way. With steady rotation of the shaft, the

flywheel 6, the support 9, the disk 10, the elastic ring 11, the multiple hub group 12 due to the sleeve connection 7 in an operating condition, the drive shaft-mounted gear 2 rotate as one unit. As the tooth rim of the drive shaft-mounted gear 2 by means of the gear 13 of the intermediate shaft 3 is connected with the gear 14 of the driven shaft 4, the latter rotates taking into account the gear ratio transmission with an angular velocity greater than the drive shaft speed.

With unsteady rotation of the shaft, the flywheel 6, the support 9, the disk 10, can oscillate in regard to the multiple hub group 12, and respectively, to the drive shaft-mounted gear 2 within the angular allowable deformation of the elastic ring 11.

As it is shown above, the parameters of the elastic ring 11 are chosen to provide the dynamic system stability, decrease the frequency of natural oscillations of the mechanical system «Engine-Damper-Impeller Wheel» take resonant modes out of the limits of an engine rpm speed operating range. This provides the desired resource of the matching reduction gearbox.

The efficiency of research results is defined on the basis of experimental determination of torque converter loading at trial runs.

Dynamic loading of the hydromechanical transmission with an improved design of a matching reduction gearbox is evaluated at road test simulation. Efficiency of the proposed solutions was evaluated by a value of the dynamic torque on the drive shaft according to the amplitude and reverse characteristic (see Fig. 8).

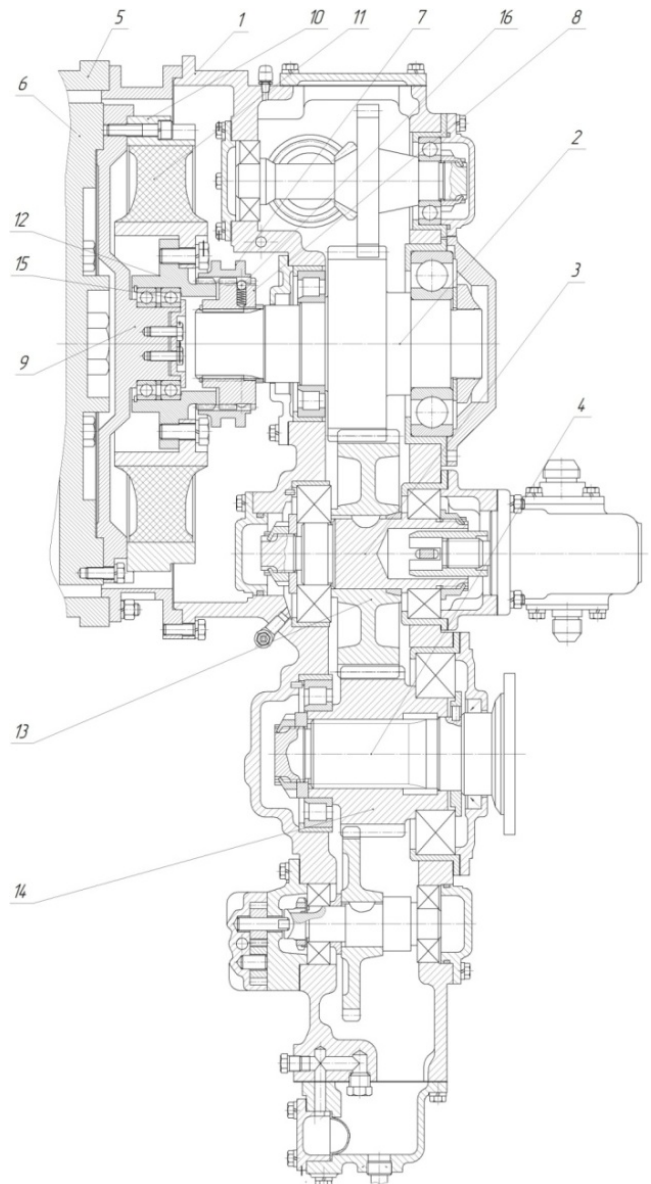
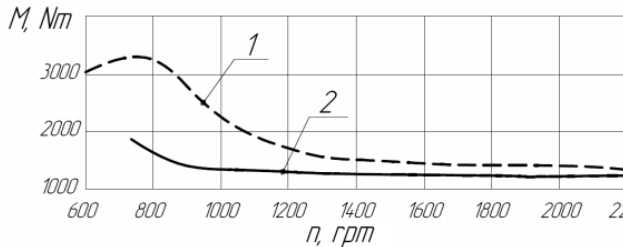


Fig. 7. Modernized design of matching reduction gearbox.





**Fig. 8.** Amplitude and reverse characteristics of the dynamic torque in the pre-torque-converter zone of the HMT: 1 – original (serial produced) version of a matching reduction gearbox; 2 – the developed sample of a matching reduction gearbox.

Comparison of the amplitude and reverse characteristics (lines 1, 2 in Fig. 5) shows that the proposed design of a matching reduction gearbox allows for tuning resonance out of engine rpm working range and reduce the dynamic torque in 5... 6 times. Thus, durability of matching reduction gearbox elements increased significantly.

### Conclusions

1. The mathematical model applied in the research and a package of computer programs give a possibility to investigate dynamics of highly nonlinear system, to determine consistent patterns of generating resonant modes, verified experimentally

2. It is substantiated that one of the main reasons for high dynamic loading and HMT element durability restriction is subharmonic resonance caused by close coincidence of natural frequencies of the nonlinear system with multiple value of diesel engine disturbing frequencies. On the basis of the determined consistent patterns the area of stability and the direction of parameter variation for its maintenance is defined.

3. The conducted pilot researches of dynamic loading of the hydromechanical transmission of three MWC models, statistical data processing confirms validity of the developed mathematical model reflecting physical processes in resonant modes and of correctness of the basic assumptions.

4. On the basis of the obtained results, the engineering solutions, allowing for reducing dynamic loading of the transmission are proposed and designs of new type dampers are developed for matching reduction gearboxes of the HMT of various models of MWC. It allows for tuning resonant modes out of engine rpm working range and for reducing dynamic loading of the transmission up to 5 ... 6 times, thus predetermining an increase of matching reduction gearbox elements durability.

### References

1. Grishkevich A.I. Design of Vehicle Transmissions: Reference book / Under general redaction of A.I. Grishkevich; M.: Mechanical engineering, 1984. – 272 pages, pic.
2. A. CROWTHER, N. ZHANG, R. SINGH, “Development of a Clunk Simulation Model for a Rear Wheel Drive Vehicle with Automatic Transmission”, SAE 2005-01- 2992
3. W. OH, R. SINGH : "Examination of Clunk Phenomena Using a Non-Linear Torsion Model of a Front Wheel Drive Vehicle with Manual Transmission", SAE 2005-01-2991
4. J. GURM, W. J. CHEN, A. KEYVANMANESH, T. ABE, A. CROWTHER, R. SINGH: "Transient Clunk Response of a Driveline System: Laboratory Experiment and Analytical Studies", SAE 2007-01-2233
5. Stahl, K., Pflaum, H., Meingassner, G. J., Lohmann, B. et al., “Testing the performance of innovative torsional vibration reduction systems”. Innovative Automotive Transmissions, Hybrid & Electric Drives, 2012
6. Derzhansky V. B. Subharmonic Oscillation Damping in Hydromechanical Transmission [An electronic resource] / Derzhansky V. B., Taratorkin I.A. // Electron. journal. "Science and Education: electronic scientific and technical edition". #03, March 2013 DOI: 10.7463/0413.0548552 Access mode: <http://technomag.bmstu.ru/doc/548552.html>, free.
7. Popov E.P. Theory of Nonlinear Systems of Automatic Control and Management: Textbook. - 2nd edition. - M.: Science, 1988. - 256 pages.
8. Panovko Y.G. Introduction in the Theory of Mechanical Oscillations: Textbook 2nd edition, revised and enlarged/ Y.G. Panovko; M.: Science. chief editorial board of physical and mathematical literature, 1980. – 272 pages, pic.

# A METHOD OF VEHICLE-PEDESTRIAN ACCIDENT RECONSTRUCTION

Eng. Lyubenov D.A., PhD

Faculty of Transport, Department of Transport – University of Ruse, Bulgaria

E-mail: dliubenov@uni-ruse.bg

**Abstract:** In this work a method of vehicle-pedestrian accident reconstruction in case of unlimited driver visibility and accelerating vehicle moving is presented. This method presents are mathematical models for determining the pedestrian visibility time, vehicle speed at the moment of impact, time to vehicle move from the moment of the hazard occurrence until the moment of impact, the vehicle distance from the place of impact, stopping distance, etc.

**Keywords:** ROAD TRAFFIC CRASHES, VEHICLE, PEDESTRIAN, ACCIDENT RECONSTRUCTION

## 1. Introduction

According to World Health Organization about 1.25 million people die each year as a result of road traffic crashes, 90% of the world's fatalities on the roads occur in low- and middle-income countries, even though these countries have approximately half of the world's vehicles and almost half of all deaths on the world's roads are among those with the least protection – motorcyclists (23%), pedestrians (22%) and cyclists (4%). Road traffic injuries are the leading cause of death among young people, aged 15–29 years [7].

In Bulgaria during the first ten months of 2015 were registered 6054 serious accidents. The distribution of accidents on main reasons shows that the highest share of these have occurred due to violations of drivers - 96.4%. The distribution of accidents by type shows that approximately 27% of accidents are vehicle-pedestrian accident [8].

Expertise is a procedural regulated activities carried out at the request of the competent authority of persons who possess special knowledge and skills to study certain subjects. Special knowledge is the knowledge that simultaneously meet the following requirements: not legal; not well known. They received the result of theoretical knowledge and practical experience in a particular discipline. Traffic accident reconstruction is an essential element of the investigation of road accidents and lawsuits.

The aim of this work is to present a method of vehicle-pedestrian accident reconstruction in case of unlimited driver visibility and accelerating vehicle moving.

## 2. Method and Discussion

Vehicle-pedestrian accident can be classified by various signs and conditions, depending on what part of the car hit the pedestrian; under the terms of visibility; according to the character of the movement of the car; according to the movement of the pedestrian in relation to the vehicle and the road and etc.

There are various approaches and methods for the vehicle-pedestrian accident reconstruction [1-6]. Many of them are focus on analysis of accident with a pedestrian when the vehicle is moving at a constant speed or deceleration vehicle moving. Sometimes in urban areas occur accident in which the car moves accelerating and hitting crossing roadway pedestrian. The reasons for such a mechanism of occurrence of accidents in which the driver does not operate the brake and the car does not start deceleration in the event of hazard are different. These can be a distraction to the driver, insufficient experience of driving fast changing road situation insufficient time for the work of the braking system technical faults of vehicle and others.

The study and analysis of such accidents required to be used different methods. Otherwise, results and reports made will be inaccurate.

Fig. 1 shows a sketch of the place of an accident between a car and a pedestrian. The sketch is prepared according to the protocol for inspecting the accident. If necessary, the expert can make additional measurements of various elements of the road infrastructure. The accident occurred at the intersection. Before the occurrence of the accident the car was stopped and waited enable traffic signal for starting and crossing the road intersection. In this traffic accident from the moment of starting to the point of impact the vehicle was acceleration moving.

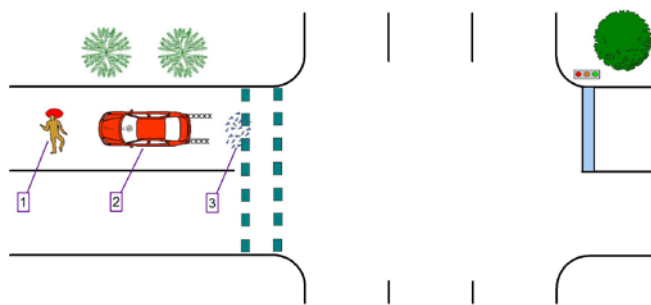


Fig. 1. Vehicle-pedestrian accident place

The positions of fig. 1 have the following meaning: position 1 – the location of a pedestrian after impact; position 2 - the location of the vehicle after the collision with the pedestrian; position 3 - scattered pieces of glass and plastic on the road.

The method of vehicle-pedestrian accident reconstruction in case of unlimited driver visibility and accelerating vehicle moving includes the following basic steps:

### 2.1. Determination of the location of the beginning of the impact

The point of impact between the pedestrian and the car is the place of a pedestrian on the road at the time of initial contact with the car. It is determined by a variety of case data - various evidence and items found at the scene of an accident, sketch of the accident scene, prepared according to the protocol of view of traffic accident, data from witnesses who were eyewitnesses to the accident, forensic medical report and other data.

The place of impact can be determined also using mathematical relationships between vehicle speed at the time of impact and the distance of the rejection of a pedestrian. If near the accident place is located traffic cameras or security cameras at different sites, records of these cameras can help to determine accurately the place of impact and the mechanism of progress of the traffic accident.

Fig. 2 shows a sketch of the same accident. On this sketch indicated the location of the vehicle (position 3) and the location of a pedestrian (position C) at the moment of impact.

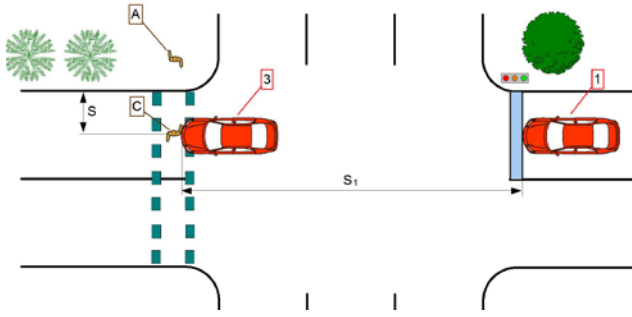


Fig. 2. Location of the vehicle (position 3) and pedestrian (position C) at the moment of impact

## 2.2. Determination of the distance, traveled by a pedestrian from the moment of occurrence of a traffic hazard until the moment of impact

The determination of the moment of occurrence of a traffic hazard is a legal question. Most often this is the moment of entry of a pedestrian on the roadway (position B, Fig. 3). It may be referred to another moment of occurrence of a traffic hazard by the investigating authority or court. This moment could be earlier, when the pedestrian has not yet reached the roadway, but the driver of the car has been able to see a pedestrian

The distance, traveled by a pedestrian from the moment of occurrence of a traffic hazard until the moment of impact is indicated by  $S$  in fig. 2. It is determined by scale sketch or the geometry of the road in accordance with the place of impact.

## 2.3. Determination of the pedestrian speed

The pedestrian speed depends mainly on their age, sex and pace of movement (normal move, running, etc.). If the case file has additional information on a pedestrian, relating to his speed of movement it should take account. In accordance with written above the pedestrian speed is determined by reference or experimental studies.

## 2.4. Determination of the pedestrian visibility time

The pedestrian visibility time is the time during which pedestrian was on the roadway at the time of occurrence of a traffic hazard until the moment of impact. The pedestrian visibility time can be calculated by the formula

$$t_p = \frac{S}{V_p}, s \quad (1)$$

where  $S$  is the distance, traveled by a pedestrian from the moment of occurrence of a traffic hazard until the moment of impact,  $m$ ;  $V_p$  - pedestrian speed,  $m/s$ ;

## 2.5. Determining the distance, traveled by a car from the moment of start until the moment of impact

The distance  $S_1$ , traveled by a car from the moment of start (position 1, Fig. 2) until the moment of impact (position 3, Fig. 2) can be determined by scale sketch. If necessary, this distance can be determined by measuring the scene of an accident.

## 2.6. Determination of vehicle speed at the moment of impact

There are various dependencies and methods for determining this speed. In this case, the vehicle speed at the moment of impact can be determined by the following relationship

$$V_{imp} = \sqrt{2S_1 a}, m/s \quad (2)$$

where  $a$  is the acceleration of the car,  $m/s^2$ ;  $S_1$  - the distance, traveled by a car from the moment of start until the moment of impact,  $m$ .

## 2.7. Determination of the time for the movement of the car to the moment of impact

This time under constant acceleration motion can be determined by one of the following relations:

$$t_{imp} = V_{imp} / a, s; \quad (3)$$

$$t_{imp} = \sqrt{2S_1 / a}, s. \quad (4)$$

## 2.8. Comparing pedestrian visibility time $t_p$ with time to move the car to the moment of impact $t_{imp}$

In this comparison are possible two practical cases:

- If  $t_p \geq t_{imp}$  follows that the pedestrian was entered on the road at the time of starting the car. For this case a traffic hazard was occurring at the time of starting the car. The accident was preventable if the vehicle has started to move after passing a pedestrian.

- If  $t_p < t_{imp}$  follows that the pedestrian was entered on the road when the car has started. This option calculations continue.

## 2.9. Determination of the time for the movement of vehicle from the moment of start until the moment of occurrence of a traffic hazard

The moment of vehicle start is shown in fig. 2, position 1. The moment of occurrence of a traffic hazard is shown in fig. 3, position 2.

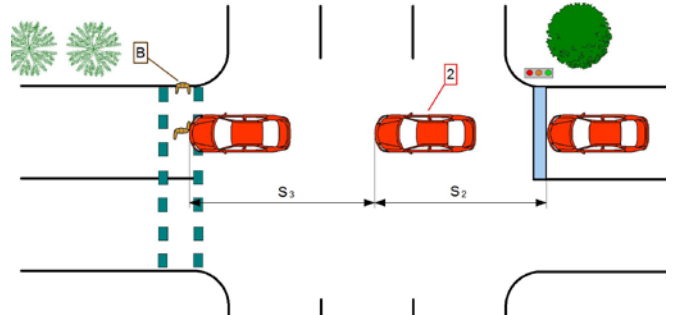


Fig. 3. Location of the vehicle and a pedestrian at the time of occurrence of a traffic hazard

The time for the movement of vehicle from the moment of start until the moment of occurrence of a traffic hazard can be determined by the following relationship

$$t_2 = t_{imp} - t_p, s \quad (5)$$

## 2.10. Determination of the vehicle speed at the time of occurrence of a traffic hazard

This vehicle position is shown in fig. 3, position 2. This speed can be determined by the following relationship

$$V_2 = at_2, m/s^2 \quad (6)$$

## 2.11. Determination of the distance of the car from the place of impact at the time of occurrence of a traffic hazard

The position of the vehicle at the moment of impact with the pedestrian is shown in fig. 2, position 3. This distance can be determined by the following relationship

$$S_3 = \left( \frac{V_{imp} + V_2}{2} \right) t_p, m \quad (7)$$

## 2.12. Determination of the vehicle speed at initiation of braking

The initiation of braking of the vehicle is the moment of occurrence of a braking deceleration. The vehicle speed at initiation of braking can be determined by the following relationship

$$V_3 = V_2 + at_{ib}, m/s \quad (8)$$

where  $t_{ib}$  is the total time which is necessary the driver to initiation of braking

$$t_{ib} = t_{drt} + t_{vrt} + 0,5t_{inc}, s \quad (9)$$

where  $t_{drt}$  is the driver reaction time, s;  $t_{vrt}$  – the vehicle reaction time, s;  $t_{inc}$  – the time for increase the braking deceleration, s;

The driver reaction time is made up of human perception time - how long the driver takes to see the hazard, and the brain realize it is a hazard requiring an immediate reaction and the human reaction time - how long the body takes to move the foot from accelerator to brake pedal. The vehicles reaction time depends on the brake pedal free-play, hydraulic properties of the brake fluid and working order of the braking system.

## 2.13. Determination of the vehicle stopping distance

The vehicle stopping distance in this case is determined by the following relationship

$$S_d = \left( \frac{V_2 + V_3}{2} \right) t_{ib} + \frac{V_3^2}{2a_{dec}}, m \quad (10)$$

where  $a_{dec}$  is the vehicle braking deceleration.

The vehicle braking deceleration depends on tyre pressures, tyre tread and grip, vehicle weight, the co-efficient of friction of the road surface, slope of road, surface smoothness, etc.

## 2.14. Determination of the opportunity to prevent the accident by stopping the vehicle

The possibility to prevent the accident by stopping the vehicle is checked by comparing the vehicle stopping distance and the distance of the car from the place of impact at the time of occurrence of a traffic hazard

If the vehicle stopping distance is less than or equal to the distance of the car from the place of impact at the time of occurrence of a traffic hazard is that the driver had the technically possible stop before the place of impact.

If the vehicle stopping distance is greater than the distance of the car from the place of impact at the time of occurrence of a traffic hazard is that the accident was unpreventable through braking. For this version of the development of the accident can be checked and the possibility pedestrian to cross in front of the car and leave his lane of travel.

## 3. CONCLUSION

In this work a method of vehicle-pedestrian accident reconstruction in case of unlimited driver visibility and accelerating vehicle moving is presented. Described a methodical sequence of work. Presented are analytical relationships for calculation of various parameters needed for vehicle-pedestrian accident reconstruction.

This method can be used by accident investigators and in the training of specialists for accident reconstruction experts.

*The article reflects the results of the work on Project No 2016 - FT - 03 on "Study of the simulator for driver training to improve*

*traffic safety", financed by fund "Scientific Research" University of Ruse.*

## REFERENCES

1. Davis G. „Relating Severity of Pedestrian Injury to Impact Speed in Vehicle-Pedestrian Crashes: Simple Threshold Model”. Transportation Research Record. Volume 1773.
2. Han, R.M. Brach. Impact throw model for vehicle-pedestrian collision reconstruction. Proc. ImechE. Part D: J. Automob. Eng., 216 (6) (2002), pp. 443–453
3. Happer, A., Araszewski, M., Toor, A., Overgaard, R. et al., „Comprehensive Analysis Method for Vehicle/Pedestrian Collisions,” SAE Technical Paper 2000-01-0846, 2000, doi:10.4271/2000-01-0846.
4. Inhwon Han, Raymond M. Brach, Throw Model for Frontal Pedestrian Collisions, SAE Paper No. 2001-01-0898, pp. 1115–1127.
5. Lyubenov D.A. “A method of vehicle-pedestrian accident reconstruction”. International journal “Machines, Technologies, Materials”. ISSUE 5/2014, p. 13 - 15. ISSN 1313-0226.
6. Wood D.P., C.K. Simms, D.G. Walsh. Vehicle-pedestrian collisions: validated models for pedestrian impact and projection. Proc. ImechE. Part D: J. Automob. Eng., 219 (2) (2004), pp. 183–195.
7. <http://www.who.int/> World Health Organization. Global status report on road safety 2015
8. <http://dokpbdp.mvr.bg/default.htm/> The State-Public Consultative Commission on the Problems of Road Safety. Statistical road safety data.

## CONTACT

Daniel A. LYUBENOV. Department of Transport – University of Ruse, 8 Studentska Str., 7017 Ruse, Bulgaria. E-mail: dliubenov@uni-ruse.bg

# CLEANING OF WATER AND SAND BEACHES FROM OIL AND OIL PRODUCTS WITH GRAPHITE SUPERSORBENT. METHODS AND EQUIPMENT.

## ОЧИСТКА ВОДНОЙ ПОВЕРХНОСТИ И ПЕСКА, ЗАГРЯЗНЕННЫХ НЕФТЬЮ И НЕФТЕПРОДУКТАМИ ГРАФИТОВЫМ СУПЕРСОРБЕНТОМ. МЕТОДЫ И ОБОРУДОВАНИЕ.

Bondarenko O., Dr. eng. Strativnov E., Dr. eng. Kozhan A., Dr. eng. Dmitriev V., Dr. eng. Khovavko A.  
 Gas Institute of National Academy of Sciences of Ukraine, Kyiv, Ukraine  
 E-mail: \_ximka\_@mail.ru, estrativnov@gmail.com

**Abstract:** Elaboration of effective ways of elimination of spilled oil and oil products are very actually now. One of the most effective methods for solving this problem is the absorption of the oil by sorbents. Supersorbent on the basis of thermally expanded graphite has unique characteristics. It is a special modification of the graphite obtained by multi-stage thermo-chemical treatment of natural flakes graphite. We have developed different methods of preliminary preparation and subsequent application of this sorbent considering a specificity of emergency spill, properties of spilled liquid, the nature of cleaning surface and weather conditions. Also, question of spent sorbent utilization has been studied. The recycling process involves the desorption process up to 85% with subsequent use of the sorbent to 10 cycles of regeneration. Obtained while desorption liquid can be used for another purpose or as an additive to fuel oil. Technology and equipment for liquidation of emergency oil spills on water surface and coastal sand have been developed and tested.

**KEYWORDS:** SUPERSORBENT, THERMALLY EXPANDED GRAPHITE, OIL SPILLAGES, REGENERATION OF SPENT SORBENT, STABLE AND MOBILE UNITS

### 1. Introduction

At the present time to eliminate pollutions on the water surfaces and sand beaches from oil, petroleum and other organic fluids spills as rule porous substances of natural and artificial origin are used. They are: peat, sawdust, shredded twigs, perlite, polystyrene foam, various fibrous materials. Sorbents are applied to the contaminated area after that the major part of spilled product is collected more often by mechanical means. Also, special bacteria that decompose organic matter into the neutral substance is used [1].

### 2. Objective and research methodologies

At liquidation of emergency spills of oil and oil products by the method of sorption the most promising method is the use as oil-absorbing sorbent thermoexpanded graphite (TEG). TEG represents by itself a special modification of the graphite obtained by multistage natural graphite thermochemical processing. This kind of graphite found in the literature also under the names of exfoliated graphite, foamed graphite and thermografenite. This product is characterized by very low bulk density (2-5 kg/m<sup>3</sup>) and high specific surface which in combination with its selectivity for oil causes a high absorption capacity relative to oil and other organic liquids. One gram of this substance can absorb 30-60 grams of oil (see Table 1). An important feature of this sorbent is its inertness, the ability to desorption up to 90% of absorbed liquids and the possibility of thermochemical regeneration for repeated use [2-4].

**Table 1.** TEG sorption characteristics for some organic liquids

The name of the substance	Sorption capacity, g/g sorbent
Acetone	30
Turpentine	30
Benzene	35
Diesel fuel	40
Kerosene	40
Vegetable oil	45
Machine oil	50
Crude oil	55

Actually liquidation process of emergency spills of oil, oil products and other organic liquids on the water surfaces and sand of coastal zone with sorbent on the basis of thermoexpanded graphite includes such stages:

- sorbent obtaining – thermo expanded graphite (if it required directly on the place of emergency spill);
- pre-treatment (preparation) of the sorbent;

- applying of a sorbent on contaminated surface;
- collecting of a saturated sorbent;
- separation and recycling of on absorbed liquid;
- regeneration of a waste sorbent and its reuse.

Scientists from Gas Institute of National Academy of Sciences of Ukraine have designed, manufactured and tested series of units with different performance, autonomy and automation for TEG manufacturing.

- pilot unit with a capacity of 8.5 m<sup>3</sup>/h (35 kg/h by raw material). One example of the unit was manufactured and put into operation at the Argonne National laboratory, Chicago, USA (Fig. 1);
- autonomous automatic unit of a local destination with capacity of 1-2 m<sup>3</sup>/h (5 kg/h by raw material (Fig. 2);
- TEG autonomous knapsack generator with a capacity of 0.8 m<sup>3</sup>/h (3 kg/h by raw material) (Fig. 3) [5];



**Fig. 1.** Pilot unit for TEG generation with a capacity of 8.5 m<sup>3</sup>/h Simulation (left). In metal (right)

The last three types of installations can work offline and used in liquidation of oil spills in difficult to access places. As well as the autonomous car based unit was designed (Fig.4)

Significant technical obstacle when using oil-absorbing sorbent on the basis of expanded graphite is its extremely low bulk density, resulting in low profitability of the technology as a whole with TEG delivery to the place of emergency spill. Spreading of the sorbent in the form of a dry powder to the contaminated surface is also associated with its entrainment (losses), which causes an increase in specific consumption of sorbent and contamination of the surrounding area. In the Gas

Institute of NAS of Ukraine various methods of preliminary TEG treatment have been investigated and tested on a pilot scale. Different modifications of the sorbent have been elaborated. They are:

- granulation by mechanical method with some binder (Fig. 5) [6, 7];
- pressing of TEG to obtain the sorption elements using a binder and without them, as well as using reinforcing interlaying and without them, followed by applying mechanical methods (Fig. 6) [8-10];
- preparation of the water-graphite suspension with subsequent application by means of a centrifugal pump (Fig. 7) [11, 12];
- preparation of the water-graphite foam suspense followed by the application of air-foam jetting [13].



**Fig. 2.** Autonomous automatic aggregate of a local destination with capacity of 1-2 m<sup>3</sup>/h by TEG



**Fig. 3.** TEG autonomous knapsack generator with a capacity of 0.8 m<sup>3</sup>/h (3 kg/h by raw material).



**Fig. 4.** Mobile unit in a container mounted on a wheeled chassis (truck GAZ-66-02).

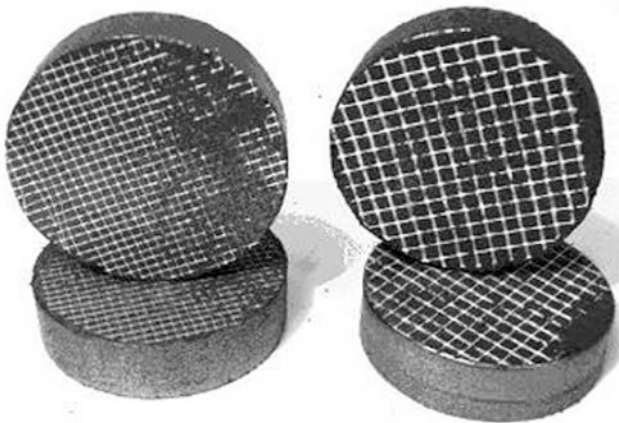


a)



b)

**Fig. 5.** The granular adsorbent of expanded graphite obtained by extrusion (a) and clumping (b)



**Fig. 6.** Extruded sorption elements, reinforced by polymer mesh

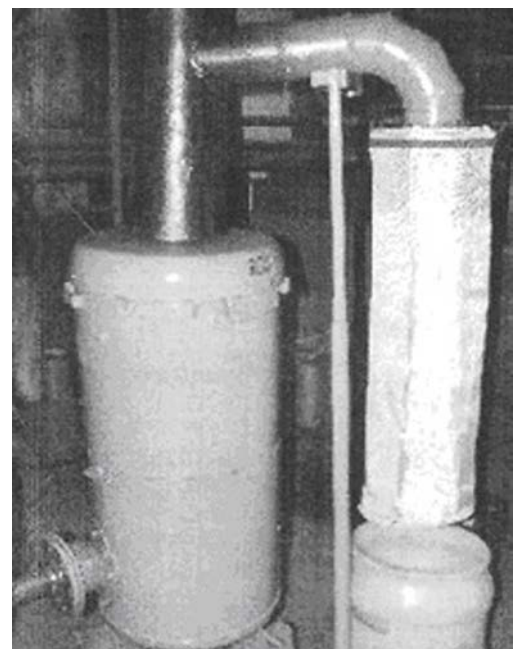


**Fig. 7.** Experimental unit for the preparation and application of a graphite-aqueous suspension

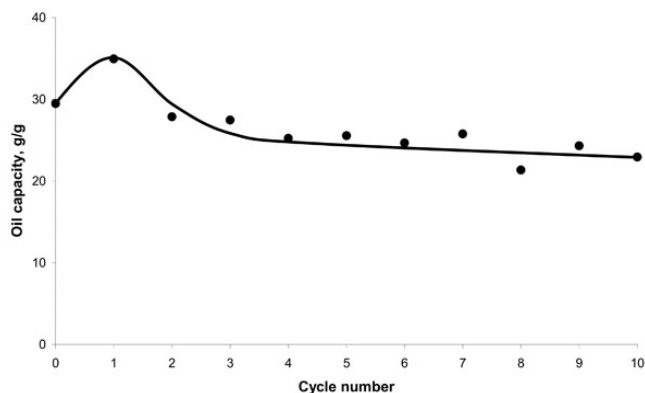
Choosing the method of sorbent preparation on the basis of TEG is accomplished taking into account a specificity of an emergency spill, properties of adsorbed liquid, the nature of the polluted surface and surrounding area conditions (e.g., availability of water sources for the preparation of water-graphite suspension).

It should be noted that the sorption capacity of any sorbent modification obtained after preprocessing of the original TEG is lower than sorption capacity of dry powder due to

increasing of its density. For example, at granulation of TEG powder with the use as a binder 2.5% solution of the glue – “PVA”, sorption capacity of the pellets, sufficient for reliable manipulation strength ( $0.15 \text{ kg/cm}^2$ ) is  $23.9 \text{ g/g}$  for diesel fuel, i.e., 40% lower than the original TEG. Sorption capacity of pressed sorption elements with density of  $12.5 \text{ kg/cm}^3$  is 12-14 g/g, i.e. three times less than that of the original TEG. However, considering the high degree of adaptability of cleaning operation of contaminated area on the whole a significant reduction of costs for sorbent delivery to the place of an accidental spillage – the economic feasibility of pre-treatment and preparation of initial TEG is justified. A little decrease in sorption capacity compared to original sorption capacity of TEG – 8.5-20% is observed when oil-absorbing sorbent from the TEG in the form of water-graphite and foam-graphite suspension is used. Thus, a high degree of cleaning of water surface and coastal sands is provided. Also, pollution of an environment by sorbent is prevented. In addition, this technology is characterized by relative simplicity and does not require the development of special technological equipment. Regardless of the type of pre-processing the original TEG and the method of its application on contaminated surface collecting the saturated sorbent is produced by any known and proven in practice methods: a perforated material or grid with a mesh size of up to 12 mm [14, 15] or vacuuming [1]. When emergency spillage is small collecting of saturated sorbent can be effected by any suitable means at hand. As noted above, a significant advantage of oil-absorbing sorbent compared to known is the possibility of desorption of absorbed liquid and regeneration of a "pressed" sorbent for reuse [4]. Up to 85% of absorbed oil is separated when desorption occurs by centrifugation. After appropriate treatment this product can be used for its intended purpose. Developed at the Gas Institute of NAS of Ukraine the technology of thermochemical regeneration of the spent sorbent provides for a high-temperature treatment of the waste and subjected to a desorption of a sorbent in the furnace of the cyclone type (Fig. 8) [16]. Wherein the content of residual oil in the pressed sorbent allows accomplish a thermo-chemical regeneration in the autothermal regime [17]. Experimentally it was proven a principle possibility of 10 regeneration cycles with maintaining an acceptable sorption capacity of the regenerated sorbent (Fig. 9).



**Fig.8.** External view of the experimental unit for the regeneration of a spent sorbent in a furnace of “cyclone” type



**Fig. 9.** Dynamics of changes in the sorption capacity of the regenerated sorbent depending of regeneration cycle's number

### 3. Conclusion

Proven technologies and technical solutions can be used as a basis for the creation of technical units in ministries and departments, responsible for the effective and rapid elimination of consequences of emergency spills of oil and oil products on water surface and sand beaches.

### 4. Literature

1. Kormak D. Struggle against pollution of the sea by oil and chemical substances / Dmitriy Kormak; - M., Transport, 1989 – 365 s.
2. E.V. Strativnov., A.P. Kozhan., V.M. Dmitriev., A.A. Sergienko., A.S. Vavrish., "A study of regeneration process of thermal expanded graphite" // *Energotehnologii i resursozberezhennie*. - 2012.-№1.- p. 47-52
3. Pat. 104098 Ukr., IASC (2012) B09C1/00. Method of cleaning water and soil from oil and oil products by graphite sorbent. / Dmitriev V.M., Kozhan A.P., Ryabchuk V.S., Strativnov E.V., Bondarenko O.B., – Publ. 12.08.2013.
4. Pat. 79769 Ukr., IASC (2012) B09C1/00. Method of cleaning water and soil from oil and oil products oil-absorbing by sorbent based on expanded graphite. / Dmitriev V. M., Kozhan A. P., Bondarenko O. B., Strativnov E.V., Ryabchuk V.S., Pisarenko A.I. Publ. 25.04.2013.
5. Pat. 85362 Ukraini, MPK<sup>7</sup> B 01 J 20/00. Portable autonomous apparatus in order to receive and application of sorbent / Bondarenko B.I., Kozhan O.P., Dmitriev V.M., Raybchuk V.S., Sergienko O.A. – Opubl. 12.10.2009, Byul. № 1.
6. Method of granulation of carbon sorbent: Pat. 23972 Ukraini, MPK<sup>7</sup> B 01 J 20 / 00, B 09 J 20 / 20 / Bondarenko B.I., Kozhan O.P., Dmitriev V.M., Sergienko O.A., Moskalik L.D. (Ukraini) – Zaaivnik i vlasnik: Institut gazu NAN Ukraini. - № u200701849; zayavl. 22.02.2007; opubl. 11.06.07, Byul. № 8. – 8 s.
7. Method of granulation of oil absorbing sorbent on the basis thermoexpanded graphite: Pat. 31784 Ukraini, MIIK7 B 01 J 20 / 00, B 09 J 20 / 20 / Bondarenko B.I., Kozhan O.P., Dmitriev V.M., Hohulay I.M., Raybchuk V.S. (Ukraini) – Zayavnik i vlasnik: Institut gazu NAN Ukraini. - № u200713038; zaaivl. 26.11.2007; opubl. 25.04.08, Byul.№ 8. – 7c.
8. A.P. Kozhan, V.M. Dmitriev, E.V. Strativnov, V.S. Ryabchuk, O.B. Bondarenko. "Cleaning surface of water basins and soil at oil outflow with using a sorbent on thermoexpanded graphite basis" // *Ecologiya i promishlennost* 2012, no. 4, pp. 33-42.
9. Method of water cleaning from oil and oil products with the help of carbon sorbent: Pat. 31783 Ukraini, MIIK7 E 02 B 15 / 04, C 02 F 1 / 28 / Bondarenko B.I., Kozhan O.P., Dmitriev V.M., Hohulay I.M., Aleksandrov V.V. (Ukraini) – Zayavnik i vlasnik: Institut gazu NAN Ukraini. -№ u200713037; zaaivl. 26.11.2007; opubl. 25.04.08, Byul. № 8. – 7c.
10. Cleaning method of water surface from hydrophobic pollution: Pat. 82819 Ukraini, MIIK7 E 02 B 15 / 04, C 02 F 1 / 28 / Bondarenko B.I., Kozhan O.P., Dmitriev V.M., Hohulay

I.M., Aleksandrov V.V. (Ukraini) – Zayavnik i vlasnik: Institut gazu NAN Ukraini. -№ u200713037; zayavl. 26.11.2007; opubl. 25.04.08, Byul.№ 8. – 7c.

11. A.P. Kozhan, V.M. Dmitriev, E.V. Strativnov, V. S. Ryabchuk, O. B. Bondarenko. "Purification of water surface and soil from accidental spills of oil and oil products by sorbent based on thermally expanded graphite", in: "Innovative solutions of actual problems of basic industries, environment, energy and resources": proceedings of the international scientific-practical conference / Kazantip – ECO – 2012/ June 4-8, 2012, ShChelkino, Crimea/ Ukrgt "Energostal": in 3 volumes - Kharkov: NTMT, 2012. – volume 3.p. 73-84.

12. A.P. Kozhan, V.M. Dmitriev, E.V. Strativnov, V.S. Ryabchuk, O.B. Bondarenko/ "Oil-absorbing sorbent based on nano-layered thin films of graphite", in: "III international scientific conference "NANOSTRUCTURED MATERIALS 2012: RUSSIA – UKRAINE – BELARUS": proceedings of the international scientific-practical conference / NANO – 2012/ 19-22 November 2012, Saint-Petersburg, Russia Scientific center of Russian Academy of Sciences (spbsc RAS), Institute of silicate chemistry of the. I. V. Grebenshchikov: p. 274.

13. Method of cleaning of soil and coastal strip from hydrophobic pollution: Pat. 83181 Ukraini, MIIK7 B 09 C 1 / 00 , B 01 J 20 / 20 /Bondarenko B.I., Kozhan O.P., Dmitriev V.M., Raybchuk V.S., Komisarenko A.A. (Ukraini) – Zayavnik i vlasnik: Institut gazu NAN Ukraini. -№ u200701852; zaaivl. 22.02.2007; opubl. 25.06.08, Byul.№ 12. – 6c.

14. Cleaning method of water surface from oil and hydrophobic liquid: Pat. 92000506 Rossii, MIIK7 C 01 B 31 / 04 Smirnov A.V. (Rossia) – Zayavitel i sobstvennik Smirnov A.V. - № 93000506/26; zayavl 15.10.1993; opubl.. 27.06.96, Byul. № 11. – 5 c.

15. Cleaning method of water surface from oil and oil products: Pat. 2140488 Rossii, MIIK7 Э 02 B 15 / 04 / Samosadnii V.P. (Rossiya) – Zayavitel i sobstvennik: OOO Nauchno proizvodstvennoe obединenie “Texnoprom” - № 98001306/32; zayavl 21.12.1998; opubl.27.10.99, Byul.. № 7. – 6c.

16. Cleaning method of soil from oil and oil products by graphite sorbent: Pat. 48026 Ukraini, MIIK9 Y 09 3 1 / 00 /Bondarenko B.I., Kozhan O.P., Dmitriev V.M., Raybchuk V.S., Sergienko O.A., (Ukraini) – Zayavnik i vlasnik: Institut gazu NAN Ukraini. -№ u200811085; zaaivl12.09.2008.; opubl. 10.03.10, Byul.№ 5. – 6c.

17. Cleaning method of soil from oil products sorbent graphite: Pat. 83180 Ukraini, MIIK7 B 09 C 1 / 00 , C 02 F 1 / 28 / Bondarenko B.I., Kozhan O.P., Dmitriev V.M., Raybchuk V.S., Sergienko O.A., (Ukraini) – Zayavnik i vlasnik: Institut gazu NAN Ukraini. -№ u200701850; zayavl 22.02.2007.; opubl. 25.06.08, Byul.№ 12. – 9c.



# SIMULTANEOUS RESONANCE CASES IN A PITCH – ROLL SHIP MODEL. PART 1: FIRST – ORDER APPROXIMATE SOLUTIONS

Assoc. Prof. Dr. Deleanu D.  
Faculty of Naval Electro mechanics - Maritime University of Constanta, Romania  
dumitrudeleanu@yahoo.com

**Abstract:** In the paper, a two-degrees-of-freedom ship model with quadratic coupled pitch and roll modes under sinusoidal harmonic excitation is considered. The Multiple Scales perturbation technique is applied to yield the first-order expansions for the special internal resonant case where the pitch frequency is twice the roll frequency. Increasing the wave frequency from zero to infinity, five resonant situations are detected. For each case, the governing equations for the transition towards the steady-state solutions, the first-order approximations for these solutions and the frequency-amplitude relationships are presented. A detailed analysis is performed only for the case where the excitation frequency is half of the roll frequency. The reliability of the analytical results derived in the paper is checked in a companion contribution by comparison with numerical solutions.

**Keywords:** SHIP ROLLING AND PITCHING, MULTIPLE SCALES, INTERNAL AND EXTERNAL RESONANCES

## 1. Introduction

A ship in waves, seen as a floating rigid body, has six degrees of freedom (called surge, sway, heave, roll, yaw and pitch), so its motion is extremely complicated and difficult to predict. Accurate calculation of ship – wave hydrodynamic interactions leads to strongly non – linear models, whose analysis is almost very cumbersome and has a computational cost remarkably high.

Between the six oscillatory motions of the ship, the most obvious are rolling and pitching. Roll is of maximum interest because with a typical hull-form, it is the least damped of the motions, hence the roll angle amplitude can be large enough to affect the ship's stability and even to capsize it. Pitch is also important because in heavy sea conditions it can cause the bow to come out of the water, then slam it hard in the water, and introducing enormous efforts in the ship structure. The other motions are typically heavily damped [1].

Various models with two or three degrees of freedom, including rolling and pitching, have been proposed by different authors. Thus, Ghadimi *et al.* have developed a model for the analysis of simultaneous heave, pitch and roll motions of planning vessels in regular waves [2]. Haddara and Xu have investigated the free response of a heaving and pitching ship from its stationary response to random waves [3]. Eissa *et al.* have modeled the interaction of heave and roll by a mass-spring-pendulum system where the effect of waves was included by a periodic forcing term [4]. Pan and co-workers have studied non-stationary responses of a ship model with nonlinearity coupled pitch and roll under modulated excitation. In their model, the differential equations of motion for a ship restrained to pitch and roll modes are as follows

$$\begin{aligned} \ddot{x}_1 + 2\varepsilon\mu_1\dot{x}_1 + \omega_1^2 x_1 + \varepsilon\alpha_1 x_1 x_2 &= F_1 \cos\Omega t \\ \ddot{x}_2 + 2\varepsilon\mu_2\dot{x}_2 + \omega_2^2 x_2 + \varepsilon\alpha_2 x_1^2 &= F_2 \cos\Omega t \end{aligned} \quad (1)$$

where  $x_1$  and  $x_2$  are the roll and pitch modal amplitudes,  $\mu_1$  and  $\mu_2$  the modal damping coefficients,  $\omega_1$  and  $\omega_2$  the natural angular frequencies,  $\Omega$  the excitation (wave) frequency,  $F_1$  and  $F_2$  the excitation force amplitudes,  $\alpha_1$  and  $\alpha_2$  the coefficients of nonlinear terms, and  $\varepsilon$  a small parameter [5, 6]. Finally, the dots stand for the differentiation with respect to time  $t$  and all the coefficients in (1) depend on fluid parameters, ship's characteristics, etc. Kamel has applied the multiple scales method for finding the approximate response of system (1) in the special case of internal resonance  $\omega_2 \approx 2\omega_1$  associated with the combined external resonance  $\omega_1 + \omega_2 = \Omega$  [7]. Continuing the work of Kamel for giving a picture of the various possible cases, Deleanu has investigated the primary resonance  $\omega_1 \approx \Omega$  [8].

In the paper we retain the condition that the pitch frequency is twice the roll frequency and make a complete analysis of the

different scenarios to appear when the excitation frequency is increased from zero to infinity. We describe in some detail the solution for the secondary resonance  $\Omega \approx \omega_1/2$  and present the first – order approximations for the other cases of interest, namely  $\Omega \approx 0$ ,  $\Omega \approx \omega_1$ ,  $\Omega \approx \omega_2$ ,  $\Omega \approx \omega_1 + \omega_2$  and  $\Omega$  far from the mentioned values. In a companion contribution, we verify the accuracy of the analytical approximations derived in the paper by contrasting them with the numerical solutions [9].

## 2. First – order uniform expansions with Multiple Scales method

Because the governing system (1) is weakly nonlinear, we employ the Multiple Scales method to determine its approximate solutions. Thus, we consider two time scales, namely the fast time  $T_0 = t$  and the slow time  $T_1 = \varepsilon t$ , and expand the dependent variables  $x_1$ ,  $x_2$  and their derivatives in power series in the small parameter  $\varepsilon$

$$\begin{aligned} x_1 &= x_{10}(T_0, T_1) + \varepsilon x_{11}(T_0, T_1) + \dots \\ x_2 &= x_{20}(T_0, T_1) + \varepsilon x_{21}(T_0, T_1) + \dots \\ \frac{d}{dt} &= D_0 + \varepsilon D_1 + \dots, \quad \frac{d^2}{dt^2} = D_0^2 + 2\varepsilon D_0 D_1 + \dots \end{aligned} \quad (2)$$

where  $D_i = \frac{\partial}{\partial T_i}$ ,  $D_i^2 = \frac{\partial^2}{\partial T_i^2}$ , and  $D_i D_j = \frac{\partial^2}{\partial T_i \partial T_j}$ ,  $i, j \in \{1, 2\}$ .

In what follows, we treat separately the six mentioned situations beginning with the external resonant cases, and closing with the non-resonant one. For the sake of space, an extended solution of the problem is presented only for the first analyzed case.

### The case $\Omega \approx \omega_1/2$

This case corresponds to a secondary resonance because a small - divisor term appears in the second order term,  $x_{11}$  [8]. Substituting (2) into (1) and equating coefficients of similar powers of  $\varepsilon$ , one obtains the following set of linear partial differential equations which can be solved successively

$$\varepsilon^0 \begin{cases} D_0^2 x_{10} + \omega_1^2 x_{10} = F_1 \cos\Omega T_0 \\ D_0^2 x_{20} + \omega_2^2 x_{20} = F_2 \cos\Omega T_0 \end{cases} \quad (3)$$

$$\varepsilon^1 \begin{cases} D_0^2 x_{11} + \omega_1^2 x_{11} = -2D_0 D_1 x_{10} - 2\mu_1 D_0 x_{10} - \alpha_1 x_{10} x_{20} \\ D_0^2 x_{21} + \omega_2^2 x_{21} = -2D_0 D_1 x_{20} - 2\mu_2 D_0 x_{20} - \alpha_2 x_{10}^2 \end{cases} \quad (4)$$

The first order solutions of (3) have the form

$$x_{10} = A_{10}(T_1)\exp(i\omega_1 T_0) + \frac{\Lambda_1}{2}\exp(i\Omega T_0) + cc \quad (5)$$

$$x_{20} = A_{20}(T_1)\exp(i\omega_2 T_0) + \frac{\Lambda_2}{2}\exp(i\Omega T_0) + cc$$

where  $cc$  stand for the complex conjugates of the preceding terms and  $\Lambda_n = F_n / (\omega_n^2 - \Omega^2)$ ,  $n=1,2$ . To express the closeness of  $\Omega$  to  $\omega_1/2$  and of  $\omega_2$  to  $2\omega_1$  we introduce the detuning parameters  $\sigma_1$  and  $\sigma_2$  as follows

$$2\Omega = \omega_1 + \varepsilon\sigma_1, \omega_2 = 2\omega_1 + \varepsilon\sigma_2 \quad (6)$$

Introducing (5) and (6) into (4), one obtains

$$\begin{aligned} (D_0^2 + \omega_1^2)x_{11} = & \left[ -2i\omega_1(D_1 A_{10} + \mu_1 A_{10}) - \frac{\alpha_1 \Lambda_1 \Lambda_2}{2} \exp(i\sigma_1 T_1) - \right. \\ & \left. - \alpha_1 \bar{A}_{10} A_{20} \exp(i\sigma_2 T_1) \right] \exp(i\omega_1 T_0) + NST_1 \quad (7) \\ (D_0^2 + \omega_2^2)x_{21} = & \left[ -2i\omega_2(D_1 A_{20} + \mu_2 A_{20}) - \alpha_2 A_{10}^2 \exp(-i\sigma_2 T_1) \right] \\ & \cdot \exp(i\omega_2 T_0) + NST_2 \end{aligned}$$

where  $NST_{1,2}$  stand for the terms which do not produce secular terms. The later, in (7), will vanish if and only if the coefficients of  $\exp(i\omega_n T_0)$ ,  $n=1,2$ , are equal to zero

$$\begin{aligned} -2i\omega_1(D_1 A_{10} + \mu_1 A_{10}) - \alpha_1 \bar{A}_{10} A_{20} e^{i\sigma_2 T_1} - \frac{\alpha_1 \Lambda_1 \Lambda_2}{2} e^{i\sigma_1 T_1} &= 0 \\ -2i\omega_2(D_1 A_{20} + \mu_2 A_{20}) - \alpha_2 A_{10}^2 \exp(-i\sigma_2 T_1) &= 0 \quad (8) \end{aligned}$$

We consider now the polar forms of the functions  $A_{n0}$ ,  $n=1,2$

$$A_{n0}(T_1) = \frac{1}{2} a_n(T_1) \exp(i\eta_n(T_1)), \quad n=1,2 \quad (9)$$

Inserting (9) into (8) and separating real and imaginary parts gives the following first order differential system of equations

$$\begin{aligned} a_1' &= -\mu_1 a_1 - \frac{\alpha_1 a_1 a_2}{4\omega_1} \sin \varphi_2 - \frac{\alpha_1 \Lambda_1 \Lambda_2}{4\omega_1} \sin \varphi_1 \\ a_1 \eta_1' &= \frac{\alpha_1 a_1 a_2}{4\omega_1} \cos \varphi_2 + \frac{\alpha_1 \Lambda_1 \Lambda_2}{4\omega_1} \cos \varphi_1 \\ a_2' &= -\mu_2 a_2 + \frac{\alpha_2 a_1^2}{4\omega_2} \sin \varphi_2 \\ a_2 \eta_2' &= \frac{\alpha_2 a_1^2}{4\omega_2} \cos \varphi_2 \quad (10) \end{aligned}$$

where  $\varphi_1 = \sigma_1 T_1 - \eta_1$ ,  $\varphi_2 = \sigma_2 T_1 + \eta_2 - 2\eta_1$ , and primes denote the differentiation with respect to slow time  $T_1$ .

Observing that  $\varphi_1' = \sigma_1 - \eta_1'$ ,  $\varphi_2' = \sigma_2 + \eta_2' - 2\eta_1'$ , the second and the fourth equations (10) may be rewritten as

$$\begin{aligned} a_1 \varphi_1' &= a_1 \sigma_1 - \frac{\alpha_1 \Lambda_1 \Lambda_2}{4\omega_1} \cos \varphi_1 - \frac{\alpha_1 a_1 a_2}{4\omega_1} \cos \varphi_2 \\ a_2 \varphi_2' &= a_2 \sigma_2 - \frac{\alpha_2 a_1^2}{2\omega_2} \cos \varphi_2 + \left( \frac{\alpha_2 a_1^2}{4\omega_2} - \frac{\alpha_1 a_2^2}{2\omega_1} \right) \cos \varphi_2 \quad (11) \end{aligned}$$

Thus, the first – order approximate solution for the system (1) is as follows

$$\begin{aligned} x_1 &= a_1 \cos(\omega_1 T_0 + \eta_1) + \Lambda_1 \cos \Omega T_0 = \\ &= a_1 \cos(2\Omega t - \varphi_1) + \Lambda_1 \cos \Omega t \\ x_2 &= a_2 \cos(\omega_2 T_0 + \eta_2) + \Lambda_2 \cos \Omega T_0 = \\ &= a_2 \cos(4\Omega t + \varphi_2 - 2\varphi_1) + \Lambda_2 \cos \Omega t \quad (12) \end{aligned}$$

where the amplitudes  $a_n$ ,  $n=1,2$ , and phases  $\varphi_n$ ,  $n=1,2$ , are given by (10) and (11) after returning to the normal time  $t$ . The

functions  $a_n, \varphi_n$ ,  $n=1,2$  tend to constant values as time  $t$  is large enough [10-12]. If we insert these values into (12), we obtain the so - called *steady – state solutions*, which are periodic with frequencies  $2\Omega$  and  $4\Omega$ . To obtain the steady-state solutions we have two choices. First, we can integrate for a large enough period of time. Second, we can use the fact that  $\dot{a}_n, \dot{\varphi}_n$ ,  $n=1,2$ , are constants, set  $\dot{a}_n = \dot{\varphi}_n = 0$ ,  $n=1,2$ , in (11) and solve for  $\sin \varphi_n$  and  $\cos \varphi_n$ . But  $\sin^2 \varphi_n + \cos^2 \varphi_n = 1$ , so we get a system of equations in the amplitudes  $a_n$ ,  $n=1,2$ , called *frequency – response equations*

$$\mu_2^2 + (2\sigma_1 - \sigma_2)^2 = \left( \frac{\alpha_1 a_1^2}{4\omega_2 a_2} \right)^2 \quad (13)$$

$$\left( \mu_1 + \mu_2 \frac{\alpha_1 \omega_2 a_2^2}{\alpha_2 \omega_1 a_1^2} \right)^2 + \left( \sigma_1 + (\sigma_2 - 2\sigma_1) \frac{\alpha_1 \omega_2 a_2^2}{\alpha_2 \omega_1 a_1^2} \right)^2 = \left( \frac{\alpha_1 \Lambda_1 \Lambda_2}{4\omega_1 a_1} \right)^2$$

Substituting  $a_2^2/a_1^2$  from the first equation (13) and inserting into the second, yields a cubic equation in  $a_1^2$

$$\begin{aligned} \frac{\alpha_1^2 \alpha_2^2}{256 \omega_1^2 \omega_2^2 (\mu_2^2 + (\sigma_2 - 2\sigma_1)^2)} a_1^6 + \frac{\alpha_1 \alpha_2 (\mu_1 \mu_2 + \sigma_1 (\sigma_2 - 2\sigma_1))}{8 \omega_1 \omega_2 (\mu_2^2 + (\sigma_2 - 2\sigma_1)^2)} a_1^4 + \\ + (\mu_1^2 + \sigma_1^2) a_1^2 - \left( \frac{\alpha_1 \Lambda_1 \Lambda_2}{4\omega_1} \right)^2 = 0 \quad (14) \end{aligned}$$

Generally, it has only one acceptable solution  $a_1$  which increases almost linearly with  $f_1$ .

#### The case $\Omega \approx 0$

The smallness of external frequency may be explicitly introduced in the equations by means of a detuning parameter,  $\sigma$ , so that  $\Omega = \varepsilon\sigma$ . But now  $\cos \Omega t = \cos \sigma T_1$ , such that the solution of (3) is

$$\begin{aligned} x_{10} &= A_{10}(T_1)\exp(i\omega_1 T_0) + \frac{F_1}{2\omega_1^2} \exp(i\sigma T_1) + cc \\ x_{20} &= A_{20}(T_1)\exp(i\omega_2 T_0) + \frac{F_2}{2\omega_2^2} \exp(i\sigma T_1) + cc \quad (15) \end{aligned}$$

Inserting it in (4) and preventing the secular terms, one gets the system describing the motion in the transient stage

$$\begin{aligned} a_1' &= -\mu_1 a_1 - \frac{\alpha_1 a_1 a_2}{4\omega_1} \sin \varphi_2 \\ a_1 \varphi_1' &= \frac{\alpha_1 a_1 a_2}{4\omega_1} \cos \varphi_2 + \frac{\alpha_1 a_1 F_2}{2\omega_1 \omega_2^2} \cos \sigma T_1 \\ a_2' &= -\mu_2 a_2 + \frac{\alpha_2 a_1^2}{4\omega_2} \sin \varphi_2 \\ a_2 \varphi_2' &= a_2 \sigma_2 + \left( \frac{\alpha_2 a_1^2}{4\omega_2} - \frac{\alpha_1 a_2^2}{2\omega_1} \right) \cos \varphi_2 - \frac{\alpha_1 a_2 F_2}{\omega_1 \omega_2^2} \cos \sigma T_1 \quad (16) \end{aligned}$$

Comparing the first and the third equation, we easily observe that the only steady-state solution is  $a_1 = a_2 = 0$ . Thus, the long-term behavior is described by the laws

$$x_1 = \frac{F_1}{\omega_1^2} \cos \Omega t, \quad x_2 = \frac{F_2}{\omega_2^2} \cos \Omega t \quad (17)$$

#### The case $\Omega \approx \omega_1$

This time we face with a primary resonance because the small-divisor terms appear firstly in the term  $x_{10}$ . The case was discussed

extensively in [8] so we reproduce here only the main results. Thus, the first-order approximation for the solution of (1) is written as

$$x_1 = a_1 \cos(\Omega t - \varphi_1), x_2 = a_2 \cos(2\Omega t + \varphi_2 - 2\varphi_1) + \Lambda_2 \cos \Omega t \quad (18)$$

where the amplitudes  $a_n, n=1,2$ , and phases  $\varphi_n, n=1,2$  are the steady-state solutions of the following system

$$\begin{aligned} \dot{a}_1 &= -\varepsilon \mu_1 a_1 - \frac{\varepsilon \alpha_1 a_1 a_2}{4\omega_1} \sin \varphi_2 + \frac{F_1}{2\omega_1} \sin \varphi_1 \\ a_1 \dot{\varphi}_1 &= a_1 (\Omega - \omega_1) + \frac{F_1}{2\omega_1} \cos \varphi_1 - \frac{\varepsilon \alpha_1 a_1 a_2}{4\omega_1} \cos \varphi_2 \\ \dot{a}_2 &= -\varepsilon \mu_2 a_2 + \frac{\varepsilon \alpha_2 a_1^2}{4\omega_1} \sin \varphi_2 \\ a_2 \dot{\varphi}_2 &= a_2 (\omega_2 - 2\omega_1) + \frac{a_2 F_1}{a_1 \omega_1} \cos \varphi_1 + \left( \frac{\varepsilon \alpha_2 a_1^2}{4\omega_2} - \frac{\varepsilon \alpha_1 a_2^2}{2\omega_1} \right) \cos \varphi_2 \end{aligned} \quad (19)$$

It is almost identical to (10), the only difference being the replacement of  $F_1$  with  $-\frac{\varepsilon \alpha_1 \Lambda_1 \Lambda_2}{2}$ . The same change is necessary in frequency-response equations' writing.

#### The case $\Omega \approx \omega_2$

In the case of this primary resonance, the system (1) evolves according to the laws

$$x_1 = a_1 \cos\left(\frac{\Omega t - \varphi_1 - \varphi_2}{2}\right) + \Lambda_1 \cos \Omega t, x_2 = a_2 \cos(\Omega t - \varphi_1) \quad (20)$$

The transient towards the steady-state is governed by the differential equations

$$\begin{aligned} \dot{a}_1 &= -\varepsilon \mu_1 a_1 - \frac{\varepsilon \alpha_1 a_1 a_2}{4\omega_1} \sin \varphi_2 \\ a_1 \dot{\varphi}_1 &= a_1 (\Omega - \omega_2) + \frac{F_2 a_1}{2\omega_2 a_2} \cos \varphi_1 - \frac{\varepsilon \alpha_2 a_1^3}{4\omega_2 a_2} \cos \varphi_2 \\ \dot{a}_2 &= -\varepsilon \mu_2 a_2 + \frac{F_2}{2\omega_2} \sin \varphi_1 + \frac{\varepsilon \alpha_2 a_1^2}{4\omega_2} \sin \varphi_2 \\ a_2 \dot{\varphi}_2 &= a_2 (\omega_2 - 2\omega_1) - \frac{F_2}{2\omega_2} \cos \varphi_1 + \left( \frac{\varepsilon \alpha_2 a_1^2}{4\omega_2} - \frac{\varepsilon \alpha_1 a_2^2}{2\omega_1} \right) \cos \varphi_2 \end{aligned} \quad (21)$$

A careful inspection of (21) reveals an interesting behavior, suggested by Nayfeh and co-workers [11]. If the excitation amplitude  $F_2$  is smaller than the critical value

$$F_{2,cr} = \frac{8\omega_1 \omega_2}{\alpha_1} \sqrt{\mu_1^2 + \left(\frac{\Omega - 2\omega_1}{2\varepsilon}\right)^2} \sqrt{\varepsilon^2 \mu_2^2 + (\omega_2 - \Omega)^2} \quad (22)$$

the roll amplitude  $a_1$  is null, while  $a_2$  increases directly proportional with  $F_2$ ,

$$a_2 = \frac{F_2}{2\omega_2 \sqrt{\varepsilon^2 \mu_2^2 + (\omega_2 - \Omega)^2}} \quad (23)$$

As  $F_2$  increases over  $F_{2,cr}$ , the pitch mode is saturated (amplitude  $a_2$  remains constant), and the extra energy introduced in system contributes to the roll mode. For this second stage, the frequency - response equations have the form

$$\mu_1^2 + \left(\frac{\sigma_1 + \sigma_2}{2}\right)^2 = \left(\frac{\alpha_1 a_2}{4\omega_1}\right)^2 \quad (24)$$

$$\left(\mu_1 + \mu_2 \frac{\alpha_1 \omega_2 a_2^2}{\alpha_2 \omega_1 a_1^2}\right)^2 + \left(\frac{\sigma_1 + \sigma_2}{2} - \sigma_1 \frac{\alpha_1 \omega_2 a_2^2}{\alpha_2 \omega_1 a_1^2}\right)^2 = \left(\frac{\alpha_1 a_2 f_2}{2\alpha_2 \omega_1 a_1^2}\right)^2$$

#### The case $\Omega \approx \omega_1 + \omega_2$

For this compound secondary resonance, Kamel [7] found the first-order solution

$$\begin{aligned} x_1 &= a_1 \cos\left(\frac{\Omega t - \varphi_1 - \varphi_2}{3}\right) + \Lambda_1 \cos \Omega t \\ x_2 &= a_2 \cos\left(\frac{2\Omega t + \varphi_1 - \varphi_2}{3}\right) + \Lambda_2 \cos \Omega t \end{aligned} \quad (25)$$

with amplitudes and phases given by

$$\begin{aligned} \dot{a}_1 &= -\varepsilon \mu_1 a_1 - \frac{\varepsilon \alpha_1 a_1 a_2}{4\omega_1} \sin \varphi_1 - \frac{\varepsilon \alpha_1 a_2 \Lambda_1}{4\omega_1} \sin \varphi_2 \\ a_1 \dot{\varphi}_1 &= a_1 (\omega_2 - 2\omega_1) + \left( \frac{\varepsilon \alpha_2 a_1^3}{4\omega_2 a_2} - \frac{\varepsilon \alpha_1 a_1 a_2}{2\omega_1} \right) \cos \varphi_1 - \\ &\quad - \left( \frac{\varepsilon \alpha_2 a_1^2 \Lambda_1}{2\omega_1 a_2} + \frac{\varepsilon \alpha_1 a_2 \Lambda_1}{2\omega_1} \right) \cos \varphi_2 \\ \dot{a}_2 &= -\varepsilon \mu_2 a_2 + \frac{\varepsilon \alpha_2 a_1^2}{4\omega_2} \sin \varphi_1 - \frac{\varepsilon \alpha_2 a_1 \Lambda_1}{2\omega_2} \sin \varphi_2 \\ a_2 \dot{\varphi}_2 &= a_2 (\Omega - \omega_1 - \omega_2) - \left( \frac{\varepsilon \alpha_2 a_1^2}{4\omega_2} + \frac{\varepsilon \alpha_1 a_2^2}{4\omega_1} \right) \cos \varphi_1 - \\ &\quad - \left( \frac{\varepsilon \alpha_2 a_1 \Lambda_1}{2\omega_2} + \frac{\varepsilon \alpha_1 a_2^2 \Lambda_1}{4\omega_1 a_1} \right) \cos \varphi_2. \end{aligned} \quad (26)$$

The frequency-response equations are written as

$$\begin{aligned} 9\mu_1^2 + (\sigma_1 + \sigma_2)^2 &= (a_1 + \Lambda_1)^2 \left( \frac{3\alpha_1 a_2}{4\omega_1 a_1} \right)^2 \\ 9\mu_2^2 + (2\sigma_1 - \sigma_2)^2 &= (a_1 + 2\Lambda_2)^2 \left( \frac{3\alpha_2 a_1}{4\omega_2 a_2} \right)^2 \end{aligned} \quad (27)$$

where  $2\Omega = \omega_1 + \omega_2 + \varepsilon \sigma_1, \omega_2 = 2\omega_1 + \varepsilon \sigma_2$ .

#### The case $\Omega$ far from $0, \omega_1/2, \omega_1, \omega_2$ and $\omega_1 + \omega_2$

The first - order approximations of the solution of (1) are written as

$$\begin{aligned} x_1 &= a_1 \cos(\omega_1 t + \varphi_1) + \Lambda_1 \cos \Omega t \\ x_2 &= a_2 \cos(2\omega_1 t + \varphi_2 + 2\varphi_1) + \Lambda_2 \cos \Omega t \end{aligned} \quad (28)$$

where the amplitudes  $a_n, n=1,2$ , and phases  $\varphi_n, n=1,2$ , are obtained from

$$\begin{aligned} \dot{a}_1 &= -\varepsilon \mu_1 a_1 - \frac{\varepsilon \alpha_1 a_1 a_2}{4\omega_1} \sin \varphi_2, a_1 \dot{\varphi}_1 = \frac{\varepsilon \alpha_1 a_1 a_2}{4\omega_1} \cos \varphi_2 \\ \dot{a}_2 &= -\varepsilon \mu_2 a_2 + \frac{\varepsilon \alpha_2 a_1^2}{4\omega_2} \sin \varphi_2 \\ a_2 \dot{\varphi}_2 &= a_2 (\omega_2 - 2\omega_1) + \left( \frac{\varepsilon \alpha_2 a_1^2}{4\omega_2} - \frac{\varepsilon \alpha_1 a_2^2}{2\omega_1} \right) \cos \varphi_2 \end{aligned} \quad (29)$$

The only steady-state solution is characterized by  $a_1 = a_2 = 0$ , so the system (1) oscillates in accordance with the laws

$$x_1 = \Lambda_1 \cos \Omega t, x_2 = \Lambda_2 \cos \Omega t \quad (30)$$

*Remark:* We should observe that the solution (30) is the same as that achieved in the case  $\Omega \approx 0$ .

### 3. Conclusions

In the present paper, a mathematical model for the analysis of simultaneous pitch and roll motions of a ship is considered. The coupling between the two modes of oscillation is realized by quadratic terms and the external excitation is of harmonically type. The ratio between pitch and roll frequencies is taken to be two to one. The governing system of differential equations is weakly nonlinear, thus the multiple scales method is applied to yield first-order approximations both for the transient behavior and for the steady state solutions. Five resonant cases and a non-resonant one are presented, part of them already discussed in the available published work and the other part analyzed in some detail by the author. The accuracy of the analytical solutions derived in the paper is checked in a companion paper and a good agreement with the numerical solution is observed.

### References

- [1] Fan, S., Xia, J., *Simulation of ship motions – coupled heave, pitch and roll*, Centre for Marine Science and Technology, Technical Report no. 35, 2002.
- [2] Ghadimi, P., Dashtimanesh, A., Djeddi, S.R., Maghrebi, Y.F., *Development of a mathematical model for simultaneous heave, pitch and roll motions of planning vessel in regular waves*, International Journal of Scientific World, 1(2), p. 44 – 56, 2013.
- [3] Haddara, M.R., Xu, J., *On the identification of the ship coupled heave – pitch motions using neural networks*, Ocean Engineering, 26, p. 381 – 400, 1999.
- [4] Eissa, M., El-Sera, S., El-Sheikh, M., Sayeda, M., *Stability and primary simultaneous resonance of harmonically excited nonlinear spring pendulum system*, Appl. Math. And Computation, 145, p. 421 – 444, 2003.
- [5] Pan, R., Davies, H.G., *Non-stationary response of a nonlinear coupled pitch-roll ship model under modulated excitation*, J. of Sound and Vibration, 192, p. 669 – 699, 1996.
- [6] Pan, R., Davies, H.G., *Response of a nonlinearly coupled pitch – roll ship model under harmonic excitation*, Journal of Nonlinear Dynamics, 2, p. 211-219, 1994.
- [7] Kamel, M.M., *Bifurcation analysis of a nonlinear coupled pitch – roll ship*, Mathematics and Computers in Simulation, 73, p. 300 – 308, 2007.
- [8] Deleanu, D., *Analysis of a combined case of internal and external resonances for a quadratic coupled pitch – roll ship*, The XXIV International Scientific Technical Conference TRANS'16 MOTAUTO, Burgas, Bulgaria, June 2016.
- [9] Deleanu, D., *Simultaneous resonance cases in a pitch-roll ship model. Part 2: Numerical analysis*, Fourth International Scientific Conference “Engineering, Technology, Education, Security”, Veliko Tarnovo, Bulgaria, 01-03.06 2016.
- [10] Dumitrache, C.L., Calimanesu, I., Comandar, C., *Naval standard and safety valve design using CAD solutions*, Int. Conference “Advanced Concepts in Mechanical Engineering” ACME 2014, Iasi, Romania, 12-15.10. 2014.
- [11] Nayfeh, A.H., Mook, D.T., Marshall, L.R., *Nonlinear coupling of pitch and roll modes in ship motions*, Journal of Hydronautics, 7(4), p. 145-152, 1973.
- [12] Nayfeh, A.H., *Introduction to perturbation techniques*, John Wiley and Sons, New York, 1992.

# SIMULTANEOUS RESONANCE CASES IN A PITCH – ROLL SHIP MODEL. PART 2: NUMERICAL ANALYSIS

Assoc. Prof. Dr. Deleanu D.  
Faculty of Naval Electro mechanics - Maritime University of Constanta, Romania  
dumitrudeleanu@yahoo.com

**Abstract:** In a companion paper, the response of a two-degrees-of-freedom ship model with nonlinear coupled pitch and roll modes under sinusoidal harmonic excitation was studied analytically by means of the Multiple Scales method for the case where the pitch frequency is twice the roll frequency. Five resonant cases were analysed and the governing equations for the transition towards the steady-state solutions, the first-order approximations for these solutions and the frequency-amplitude relationships were derived. The present contribution aimed to verify the accuracy of the analytical results by contrasting them with the numerical results provided by direct integration of the equations of motion. The two sets of results were found to be in excellent or, at least, in decent agreement every time the system parameters were selected without a flagrant violation of the order's magnitude.

**Keywords:** SHIP ROLLING AND PITCHING, NUMERICAL ANALYSIS, INTERNAL AND EXTERNAL RESONANCES

## 1. Introduction

Although considerable experimental and theoretical research has been realized, the development of a full satisfactory mathematical model for estimation the ship motion in waves remains an open problem. Models with one to six degrees of freedom have been developed and studied [1 – 4].

In the present paper, the model proposed by Pan and Davies for the nonlinear coupled pitch and roll modes under harmonic excitation is considered [5]. The equations of motion, which are weakly nonlinear and coupled by quadratic terms, are as follows

$$\begin{aligned} \ddot{x}_1 + 2\varepsilon\mu_1\dot{x}_1 + \omega_1^2 x_1 + \varepsilon\alpha_1 x_1 x_2 &= F_1 \cos \Omega t \\ \ddot{x}_2 + 2\varepsilon\mu_2\dot{x}_2 + \omega_2^2 x_2 + \varepsilon\alpha_2 x_1^2 &= F_2 \cos \Omega t \end{aligned} \quad (1)$$

where  $x_1$  and  $x_2$  are the roll and pitch modal amplitudes,  $\mu_1$  and  $\mu_2$  the modal damping coefficients,  $\omega_1$  and  $\omega_2$  the natural angular frequencies,  $\Omega$  the excitation (wave) frequency,  $F_1$  and  $F_2$  the excitation force amplitudes,  $\alpha_1$  and  $\alpha_2$  the coefficients of nonlinear terms, and  $\varepsilon$  a small parameter. The dots, as always, stand for the differentiation with respect to time  $t$  and all the coefficients in (1) depend on fluid parameters, ship's characteristics, etc. Deleanu has considered a straightforward expansion for the solution of system (1) and has obtained five resonant values of external excitation frequency and one internal resonance [6]. Kamel has applied the multiple scales method for finding the approximate response of system (1) in the special case of internal resonance  $\omega_2 \approx 2\omega_1$  associated with the combined external resonance  $\omega_1 + \omega_2 = \Omega$  [7]. In a companion paper, Deleanu has derived or just presented the governing equations for the transition towards the steady-state solutions, the first-order approximations for these solutions and the frequency-amplitude relationships for all the resonant cases, namely  $\Omega \approx 0$ ,  $\Omega \approx \omega_1/2$ ,  $\Omega \approx \omega_1$ ,  $\Omega \approx \omega_2$ , and  $\Omega \approx \omega_1 + \omega_2$  [8].

The goal of this paper is to check the accuracy of the analytical approximations derived in [7] and [8] by comparing them with the numerical solutions provided by direct integration of the equations of motion.

## 2. Analytical versus numerical results

In this section, we treat separately the five mentioned situations beginning with the non-resonant case, and continuing with the external resonant ones. For a better understanding of the topic, we include in each analyzed case the first-order approximate solution describing the long term behavior of system (1), as well as the governing differential equations for the transition period (see [8]).

### 2.1. The case $\Omega$ far from $0, \omega_1/2, \omega_1, \omega_2$ and $\omega_1 + \omega_2$

The first – order approximations for the solution of (1) in the transition period are written as

$$\begin{aligned} x_1 &= a_1 \cos(\omega_1 t + \varphi_1) + \Lambda_1 \cos \Omega t \\ x_2 &= a_2 \cos(2\omega_1 t + \varphi_2 + 2\varphi_1) + \Lambda_2 \cos \Omega t \end{aligned} \quad (2)$$

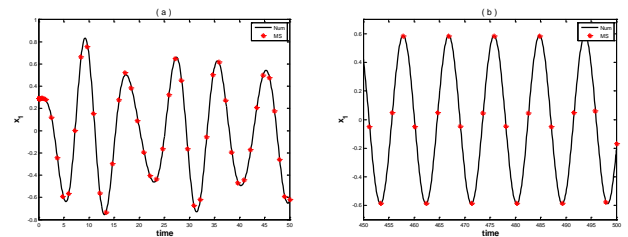
where the amplitudes  $a_n, n=1,2$ , and phases  $\varphi_n, n=1,2$ , are obtained from

$$\begin{aligned} \dot{a}_1 &= -\varepsilon\mu_1 a_1 - \frac{\varepsilon\alpha_1 a_1 a_2}{4\omega_1} \sin \varphi_2, \quad \dot{a}_1 \varphi_1 = \frac{\varepsilon\alpha_1 a_1 a_2}{4\omega_1} \cos \varphi_2 \\ \dot{a}_2 &= -\varepsilon\mu_2 a_2 + \frac{\varepsilon\alpha_2 a_1^2}{4\omega_2} \sin \varphi_2 \end{aligned} \quad (3)$$

$$\dot{a}_2 \varphi_2 = a_2 (\omega_2 - 2\omega_1) + \left( \frac{\varepsilon\alpha_2 a_1^2}{4\omega_2} - \frac{\varepsilon\alpha_1 a_2^2}{2\omega_1} \right) \cos \varphi_2$$

and  $\Lambda_n = F_n / (\omega_n^2 - \Omega^2), n=1,2$ .

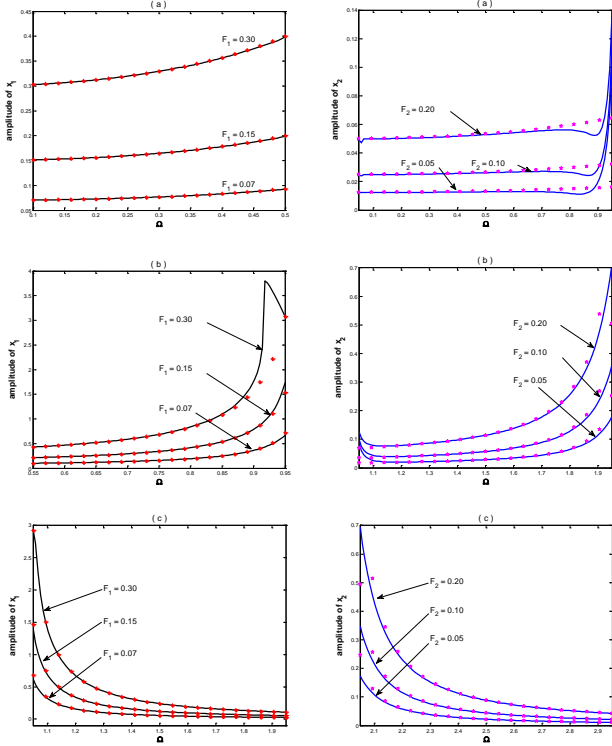
The steady – states solutions are characterized by  $\dot{a}_1 = \dot{a}_2 = 0$ . Fig. 1 illustrates a typical time series for the  $x_1$  component, both for transient and stationary stages. Throughout the paper, the continuous lines are used for numerical solution and the stars for analytical results provided by multiple scales method.



**Fig. 1** Time history for component  $x_1$  and parameters values  $\varepsilon = 0.1$ ,  $\alpha_1 = 1$ ,  $\alpha_2 = 2$ ,  $\mu_1 = 0.25$ ,  $\mu_2 = 0.5$ ,  $\omega_1 = 1$ ,  $\omega_2 = 2.03$ ,  $\Omega = 0.7$ ,  $F_1 = 0.3$  and  $F_2 = 0.1$  : a) transition period; b) steady – state solution.

Using roll and pitch amplitudes given by  $|\Lambda_n|$  or by numerical integration of (1), after the transients die out, one can construct the frequency - response curves shown in fig. 2. The important fixed parameters  $\omega_1 = 1$  and  $\omega_2 = 2.03$  were utilized. The external frequency  $\Omega$  was selected in the ranges  $[0.1, 0.5]$ ,  $[0.55, 0.95]$ ,  $[1.05, 1.95]$  and  $[2.05, 2.95]$ , meaning that it is relatively far from external resonances. It is obvious from fig. 2 that the approximate solution (2) with  $a_1 = a_2 = 0$  matches extremely well or, at least, pretty well with its numerical counterpart. Moreover, it is worth

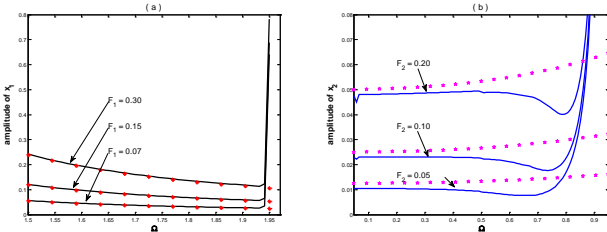
noting that this case represents more than 90% of all possible  $\Omega$  values.



**Fig. 2** Roll and pitch amplitudes as a function of external frequency for constant parameter values  $\varepsilon = 0.1$ ,  $\alpha_1 = 1$ ,  $\alpha_2 = 2$ ,  $\mu_1 = 0.25$ ,  $\mu_2 = 0.5$ ,  $\omega_1 = 1$ ,  $\omega_2 = 2.03$  and different forcing amplitudes .

**Left:** Roll amplitudes for  $F_1 \in \{0.07, 0.15, 0.3\}$  and  $F_2 = 0.05$  ;  
**Right:** Pitch amplitudes for  $F_1 = 0.07$  and  $F_2 \in \{0.05, 0.1, 0.2\}$ .

Some notable differences appear for large forcing and only in the nearness of external resonances (see fig. 3).



**Fig. 3** Roll and pitch amplitudes as a function of external frequency for constant parameter values  $\varepsilon = 0.1$ ,  $\alpha_1 = 1$ ,  $\alpha_2 = 2$ ,  $\mu_1 = 0.25$ ,  $\mu_2 = 0.5$ ,  $\omega_1 = 1$ ,  $\omega_2 = 2.03$  and different forcing amplitudes .

a)  $F_1 \in \{0.07, 0.15, 0.3\}$  and  $F_2 = 0.4$  ;  
b)  $F_1 = 0.2$  and  $F_2 \in \{0.05, 0.1, 0.2\}$ .

## 2.2. The case $\Omega \approx 0$

The long-term behavior is described by the laws

$$x_1 = \frac{F_1}{\omega_1^2} \cos \Omega t, \quad x_2 = \frac{F_2}{\omega_2^2} \cos \Omega t \quad (3)$$

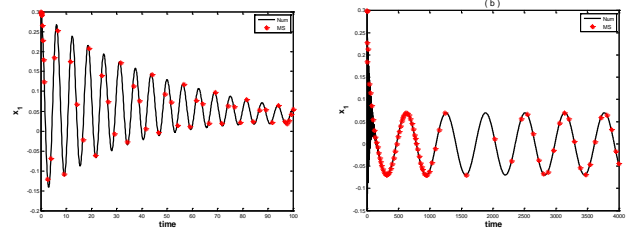
while the system describing the motion in the transient stage is written as

$$\begin{aligned} \dot{a}_1 &= -\varepsilon \mu_1 a_1 - \frac{\varepsilon \alpha_1 a_1 a_2}{4 \omega_1} \sin \varphi_2 \\ \dot{a}_1 \varphi_1 &= \frac{\varepsilon \alpha_1 a_1 a_2}{4 \omega_1} \cos \varphi_2 + \frac{\varepsilon \alpha_1 a_1 F_2}{2 \omega_1 \omega_2^2} \cos \Omega t \end{aligned} \quad (4)$$

$$\dot{a}_2 = -\varepsilon \mu_2 a_2 + \frac{\varepsilon \alpha_2 a_1^2}{4 \omega_2} \sin \varphi_2$$

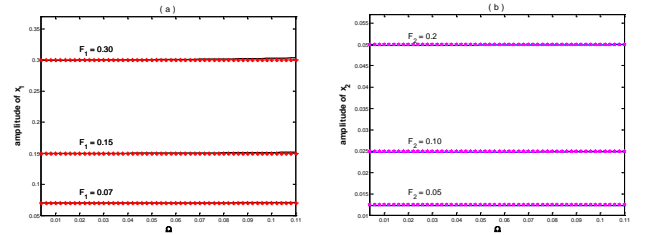
$$a_2 \dot{\varphi}_2 = a_2 (\omega_2 - 2 \omega_1) + \left( \frac{\varepsilon \alpha_2 a_1^2}{4 \omega_2} - \frac{\varepsilon \alpha_1 a_2^2}{2 \omega_1} \right) \cos \varphi_2 - \frac{\varepsilon \alpha_1 a_2 F_2}{\omega_1 \omega_2^2} \cos \Omega t$$

An example of time series associated to variable  $x_1$  is presented in fig. 4. Because the period  $T = 2\pi/\Omega$  of the stationary motions is much larger than in the previous case, we extended the integration time to 10000 u.t. instead 500 u.t.



**Fig. 4** Time history for component  $x_1$  and parameters values  $\varepsilon = 0.1$ ,  $\alpha_1 = 1$ ,  $\alpha_2 = 2$ ,  $\mu_1 = 0.25$ ,  $\mu_2 = 0.5$ ,  $\omega_1 = 1$ ,  $\omega_2 = 2.03$ ,  $\Omega = 0.01$   $F_1 = 0.07$  and  $F_2 = 0.05$  : a) transition period; b) steady - state solution.

From (3) we conclude that the roll and pitch modes amplitudes do not depend on  $\Omega$ . Indeed, fig. 5 shows that the long term behavior of system (1) is characterized by amplitudes almost independent on  $\Omega$  and proportional with  $F_1$  and  $F_2$ , respectively.



**Fig. 5** Roll and pitch amplitudes as a function of external frequency for constant parameter values  $\varepsilon = 0.1$ ,  $\alpha_1 = 1$ ,  $\alpha_2 = 2$ ,  $\mu_1 = 0.25$ ,  $\mu_2 = 0.5$ ,  $\omega_1 = 1$ ,  $\omega_2 = 2.03$  and different forcing amplitudes .

a)  $F_1 \in \{0.07, 0.15, 0.3\}$  and  $F_2 = 0.05$  ;  
b)  $F_1 = 0.07$  and  $F_2 \in \{0.05, 0.1, 0.2\}$ .

## 2.3. The case $\Omega \approx \omega_1 / 2$

According to [8], the first-order approximate solution for system (1) is as follows

$$x_1 = a_1 \cos(2\Omega t - \varphi_1) + \Lambda_1 \cos \Omega t \quad (5)$$

$$x_2 = a_2 \cos(4\Omega t + \varphi_2 - 2\varphi_1) + \Lambda_2 \cos \Omega t$$

with amplitudes and phases provided by the differential system of equations

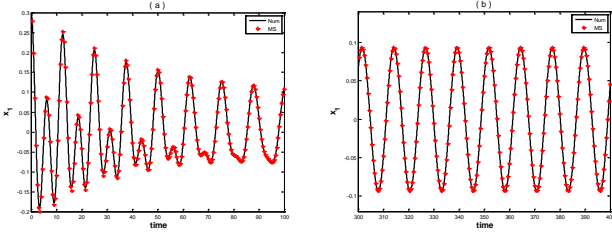
$$\dot{a}_1 = -\varepsilon \mu_1 a_1 - \frac{\varepsilon \alpha_1 a_1 a_2}{4 \omega_1} \sin \varphi_2 - \frac{\varepsilon \alpha_1 \Lambda_1 \Lambda_2}{4 \omega_1} \sin \varphi_1$$

$$a_1 \dot{\varphi}_1 = a_1 (2\Omega - \omega_1) - \frac{\varepsilon \alpha_1 \Lambda_1 \Lambda_2}{4 \omega_1} \cos \varphi_1 - \frac{\varepsilon \alpha_1 a_1 a_2}{4 \omega_1} \cos \varphi_2 \quad (6)$$

$$\dot{a}_2 = -\varepsilon \mu_2 a_2 + \frac{\varepsilon \alpha_2 a_1^2}{4 \omega_2} \sin \varphi_2$$

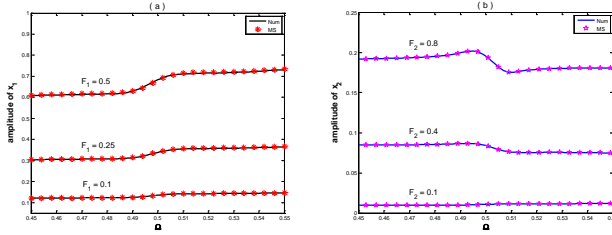
$$a_2 \dot{\varphi}_2 = a_2 (\omega_2 - 2\omega_1) - \frac{\varepsilon \alpha_1 a_2 \Lambda_1 \Lambda_2}{2 a_1 \omega_1} \cos \varphi_1 + \left( \frac{\varepsilon \alpha_2 a_1^2}{4 \omega_2} - \frac{\varepsilon \alpha_1 a_2^2}{2 \omega_1} \right) \cos \varphi_2$$

Fig. 6 contrasts the time series for rolling, given either by numerical integration of system (1) or by multiple scales method, for a set of parameters selected without order violations. As seen in the figure, the two solutions are again in excellent agreement.



**Fig. 6** Time history for component  $x_1$  and parameters values  $\varepsilon = 0.1$ ,  $\alpha_1 = 1$ ,  $\alpha_2 = 2$ ,  $\mu_1 = 0.25$ ,  $\mu_2 = 0.5$ ,  $\omega_1 = 1$ ,  $\omega_2 = 2.03$ ,  $\Omega = 0.5$   $F_1 = 0.07$  and  $F_2 = 0.05$ : a) transition period; b) steady – state solution.

As concerns the steady-state amplitudes for the two modes of oscillation, at low level of forcing none difference is observed when compared with non-resonant case. Some irrelevant jumps are registered around  $\Omega = 0.5$  for large forcing, as shown in fig. 7.



**Fig. 7** Roll and pitch amplitudes as a function of external frequency for constant parameter values  $\varepsilon = 0.1$ ,  $\alpha_1 = 1$ ,  $\alpha_2 = 2$ ,  $\mu_1 = 0.25$ ,  $\mu_2 = 0.5$ ,  $\omega_1 = 1$ ,  $\omega_2 = 2.03$  and different forcing amplitudes .  
a)  $F_1 \in \{0.1, 0.25, 0.5\}$  and  $F_2 = 0.4$  ;  
b)  $F_1 = 0.5$  and  $F_2 \in \{0.1, 0.4, 0.8\}$ .

#### 2.4. The case $\Omega \approx \omega_1$

The system (1) evolves according to the laws

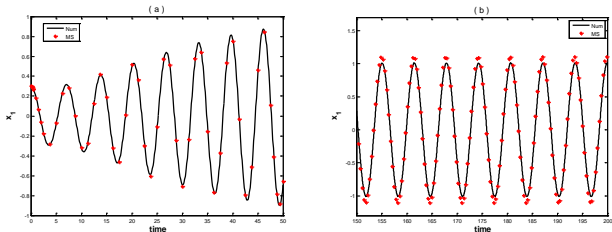
$$x_1 = a_1 \cos(\Omega t - \varphi_1), x_2 = a_2 \cos(2\Omega t + \varphi_2 - 2\varphi_1) + \Lambda_2 \cos \Omega t \quad (7)$$

where the amplitudes  $a_n, n = 1, 2$ , and phases  $\varphi_n, n = 1, 2$  are the steady-state solutions of the following system

$$\begin{aligned} \dot{a}_1 &= -\varepsilon \mu_1 a_1 - \frac{\varepsilon \alpha_1 a_1 a_2}{4\omega_1} \sin \varphi_2 + \frac{F_1}{2\omega_1} \sin \varphi_1 \\ \dot{a}_1 \varphi_1 &= a_1(\Omega - \omega_1) + \frac{F_1}{2\omega_1} \cos \varphi_1 - \frac{\varepsilon \alpha_1 a_1 a_2}{4\omega_1} \cos \varphi_2 \end{aligned} \quad (8)$$

$$\dot{a}_2 = -\varepsilon \mu_2 a_2 + \frac{\varepsilon \alpha_2 a_1^2}{4\omega_1} \sin \varphi_2$$

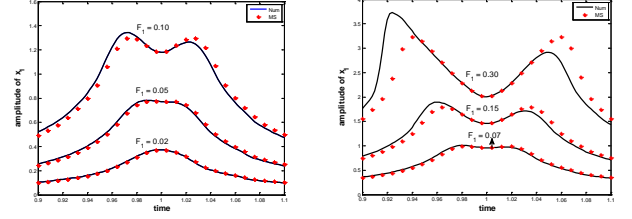
$$\dot{a}_2 \varphi_2 = a_2(\omega_2 - 2\omega_1) + \frac{a_2 F_1}{a_1 \omega_1} \cos \varphi_1 + \left( \frac{\varepsilon \alpha_2 a_1^2}{4\omega_2} - \frac{\varepsilon \alpha_1 a_2^2}{2\omega_1} \right) \cos \varphi_2$$



**Fig. 8** Time history for component  $x_1$  and parameters values  $\varepsilon = 0.1$ ,  $\alpha_1 = 1$ ,  $\alpha_2 = 2$ ,  $\mu_1 = 0.25$ ,  $\mu_2 = 0.5$ ,  $\omega_1 = 1$ ,  $\omega_2 = 2.03$ ,  $\Omega = 0.98$   $F_1 = 0.07$  and  $F_2 = 0.05$ : a) transition period; b) steady – state solution.

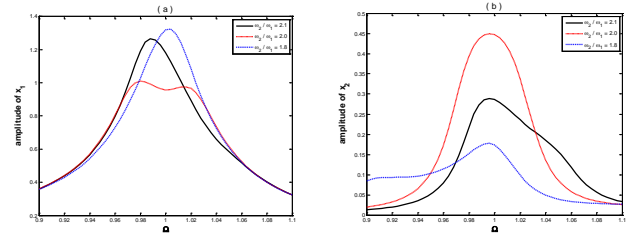
For the primary resonance  $\Omega \approx \omega_1$  even small forcing leads to high amplitudes of oscillation. Thus, fig. 8 illustrates this remark by

showing the time evolution of variable  $x_1$ . The transition period is characterized by a fast growth of rolling and pitching amplitudes and a good agreement between numerical and analytical solutions. On the other hand, a difference of about 5-20% between the two solutions is recorded in the long-term behavior, depending on the external forcing (see also fig.9).



**Fig. 9** Roll amplitudes as a function of external frequency for constant parameter values  $\varepsilon = 0.1$ ,  $\alpha_1 = 1$ ,  $\alpha_2 = 2$ ,  $\mu_1 = 0.25$ ,  $\mu_2 = 0.5$ ,  $\omega_1 = 1$ ,  $\omega_2 = 2.03$  and different forcing amplitudes .  
Left:  $F_1 \in \{0.02, 0.05, 0.1\}$  and  $F_2 = 0.25$  ;  
Right:  $F_1 \in \{0.07, 0.15, 0.3\}$  and  $F_2 = 0.5$  ;

In the analyzed case, the roll mode is less affected than the pitch one by small changes of the ratio  $\omega_2/\omega_1$ . Surprisingly, the roll amplitudes in the neighborhood of the external resonance  $\Omega \approx \omega_1$  are smaller for pure resonance  $\omega_2/\omega_1 = 2$  than for  $\omega_2/\omega_1 = 2.1$  or 1.8. However, in so far as the condition  $\omega_2/\omega_1 \approx 2$  is fulfilled the pitch amplitudes get higher. Some frequency – response curves showing these features are presented in fig. 10, where the numerical solution is plotted only.



**Fig. 10** Roll and pitch amplitudes as a function of external frequency for constant parameter values  $\varepsilon = 0.1$ ,  $\alpha_1 = 1$ ,  $\alpha_2 = 2$ ,  $\mu_1 = 0.25$ ,  $\mu_2 = 0.5$ ,  $\omega_1 = 1$ ,  $F_1 = 0.07$ ,  $F_2 = 0.05$  and different ratios  $\omega_2/\omega_1$  :  
a) roll mode; b) pitch mode.

#### The case $\Omega \approx \omega_2$

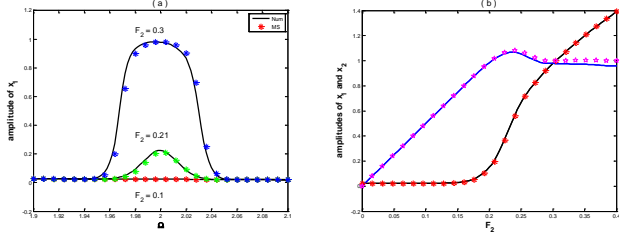
In the case of this primary resonance, the long-term behavior of system (1) is governed by the laws

$$x_1 = a_1 \cos\left(\frac{\Omega t - \varphi_1 - \varphi_2}{2}\right) + \Lambda_1 \cos \Omega t, x_2 = a_2 \cos(\Omega t - \varphi_1) \quad (9)$$

while the transient towards the steady-state is described by the differential equations

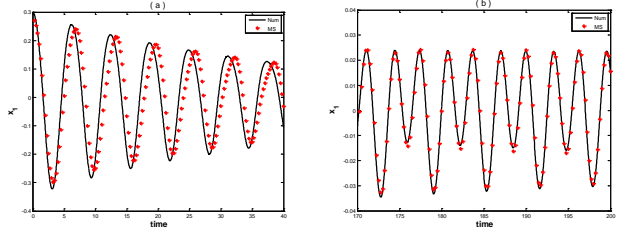
$$\begin{aligned} \dot{a}_1 &= -\varepsilon \mu_1 a_1 - \frac{\varepsilon \alpha_1 a_1 a_2}{4\omega_1} \sin \varphi_2 \\ \dot{a}_1 \varphi_1 &= a_1(\Omega - \omega_2) + \frac{F_2 a_1}{2\omega_2 a_2} \cos \varphi_1 - \frac{\varepsilon \alpha_2 a_1^3}{4\omega_2 a_2} \cos \varphi_2 \\ \dot{a}_2 &= -\varepsilon \mu_2 a_2 + \frac{F_2}{2\omega_2} \sin \varphi_1 + \frac{\varepsilon \alpha_2 a_1^2}{4\omega_2} \sin \varphi_2 \\ \dot{a}_2 \varphi_2 &= a_2(\omega_2 - 2\omega_1) - \frac{F_2}{2\omega_2} \cos \varphi_1 + \left( \frac{\varepsilon \alpha_2 a_1^2}{4\omega_2} - \frac{\varepsilon \alpha_1 a_2^2}{2\omega_1} \right) \cos \varphi_2 \end{aligned} \quad (10)$$

As is it pointed out in [8], for small forcing amplitudes  $F_2$  and arbitrary  $F_1$  the roll mode is not excited at all, while the pitch amplitudes are monotonic increasing quantities in  $F_2$ . After the forcing  $F_2$  reaches a critical value, the pitch amplitudes remain almost constant and the supplementary energy introduced in the system is directed towards the roll mode and produces a fast growth of amplitude  $a_1$  (see fig. 11a). This transfer of energy is realized only if the condition  $\Omega \approx \omega_2$  is satisfied (see fig. 11a).



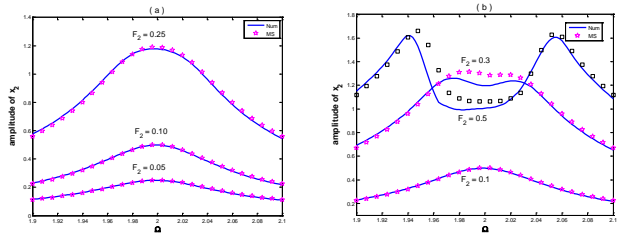
**Fig. 11** a) Roll amplitudes as a function of external frequency for constant parameter values  $\varepsilon = 0.1$ ,  $\alpha_1 = 1$ ,  $\alpha_2 = 2$ ,  $\mu_1 = 0.25$ ,  $\mu_2 = 0.5$ ,  $\omega_1 = 1$ ,  $\omega_2 = 2$ ,  $F_1 = 0.07$  and different forcing  $F_2$  ;  
b) roll and pitch amplitudes versus  $F_2$  for  $\Omega = 2$  .

A typical time series for the  $x_1$  component, both for transient and stationary periods, is reported in fig. 12. This time, some disagreement between the numerical and analytical solutions is observed in the transition stage.



**Fig. 12** Time history for component  $x_1$  and parameters values  $\varepsilon = 0.1$ ,  $\alpha_1 = 1$ ,  $\alpha_2 = 2$ ,  $\mu_1 = 0.25$ ,  $\mu_2 = 0.5$ ,  $\omega_1 = 1$ ,  $\omega_2 = 2$ ,  $\Omega = 2$ ,  $F_1 = 0.07$  and  $F_2 = 0.2$  : a) transition period; b) steady – state solution.

The steady-state amplitudes provided by the two methods match extremely or , at least, pretty well even for large forcing, as shown in fig. 13.



**Fig. 13** Pitch amplitudes as a function of external frequency for constant parameter values  $\varepsilon = 0.1$ ,  $\alpha_1 = 1$ ,  $\alpha_2 = 2$ ,  $\mu_1 = 0.25$ ,  $\mu_2 = 0.5$ ,  $\omega_1 = 1$ ,  $\omega_2 = 2$  and different forcing amplitudes .  
a)  $F_2 \in \{0.05, 0.10, 0.25\}$  and  $F_1 = 0.07$  ;  
b)  $F_2 \in \{0.1, 0.3, 0.5\}$  and  $F_1 = 0.3$  .

The case  $\Omega \approx \omega_1 + \omega_2$  is treated in detail in [7], such that its analysis is omitted here. The results are somewhat similar to those in the case  $\Omega \approx \omega_1 / 2$  .

### 3. Conclusions

In the paper, the nonlinear responses of a two-degrees-of-freedom model for pitch and roll ship motions have been studied numerically for the particular case in which the pitch frequency is almost twice the roll frequency. Four resonant cases and a non-resonant one have been analyzed and the obtained numerical solution was compared with its analytical counterpart derived in a companion paper. Using time series plots and frequency-amplitude curves, we have proved that the two solutions match well if the system's parameters were selected without order violations, both for transition and steady-state periods. The presented results are in good agreement with the available published studies on the same topic.

### References

- [1] Fan, S., Xia, J., *Simulation of ship motions – coupled heave, pitch and roll*, Centre for Marine Science and Technology, Technical Report no. 35, 2002.
- [2] Ghadimi, P., Dashtimanesh, A., Djeddi, S.R., Maghrebi, Y.F., *Development of a mathematical model for simultaneous heave, pitch and roll motions of planning vessel in regular waves*, International Journal of Scientific World, 1(2), p. 44 – 56, 2013.
- [3] Deleanu, D., *A numerical investigation into the capsizing phenomenon of a vessel*, International Journal of Modern Manufacturing Technologies, 7, p. 12 – 17, 2015.
- [4] Eissa, M., El-Sera, S., El-Sheikh, M., Sayeda, M., *Stability and primary simultaneous resonance of harmonically excited nonlinear spring pendulum system*, Appl. Math. And Computation, 145, p. 421 – 444, 2003.
- [5] Pan, R., Davies, H.G., *Non-stationary response of a nonlinear coupled pitch-roll ship model under modulated excitation*, J. of Sound and Vibration, 192, p. 669 – 699, 1996.
- [6] Deleanu, D., *Analysis of a combined case of internal and external resonances for a quadratic coupled pitch – roll ship*, The XXIV International Scientific Technical Conference TRANS'16 MOTAUTO, Burgas, Bulgaria, June 2016.
- [7] Kamel, M.M., *Bifurcation analysis of a nonlinear coupled pitch – roll ship*, Mathematics and Computers in Simulation, 73, p. 300 – 308, 2007.
- [8] Deleanu, D., *Simultaneous resonance cases in a pitch-roll ship model. Part 1: First-order approximate solutions*, Fourth International Scientific Conference “Engineering, Technology, Education, Security”, Veliko Tarnovo, Bulgaria, 01-03.06 2016.



# POSSIBLE WAYS FOR ECOLOGIC PROBLEMS LIMITING CONCERNING THE PRODUCTION AND USAGE OF PETROLEUM FUELS

## ВЪЗМОЖНОСТИ ЗА ОГРАНИЧАВАНЕ НА ЕКОЛОГИЧНИТЕ ПРОБЛЕМИ ПРИ ПРОИЗВОДСТВО И УПОТРЕБА НА НЕФТЕНИ ГОРИВА

Stoyanka Petkova – Georgieva – associate professor, PhD  
University “Prof. Dr. Asen Zlatarov”, Burgas, Bulgaria  
s.p.petkova@gmail.com

**Abstract:** *Most of the modernity ecological problems are as a result of the production and usage of petroleum fuels. The tendency of global warming and the accumulating of noxious atmosphere emissions are harmful for the human society, which makes the task for taking decisions of how to adjust the ecological balance on Earth very vital. In the article there are given guidelines for fulfilling the problem how to settle to minimum the quantity of toxic substances which the automobile engines and the different equipments that are using petroleum fuel are throwing out. There are many historical evidences for considering this effort as a very slow process because of the different approaches for solving this problem between the petrol refinery industry and the automobile industry. Also there are still negotiations for the importance of taking effective restrictions for keeping the purity of the environment by the automobile industry. In the world there are taken legislative steps for contemporary production dismiss of ethyl gasoline and for making high requirements for the diesel fuel production.*

**KEYWORDS:** PETROLEUM FUELS, ECOLOGIC PROBLEMS, PETROL REFINERY INDUSTRY

### 1. Увод

Голяма част от екологичните проблеми в нашето съвремие са в резултат на производството и употребата на нефтени горива. Глобалното затопляне и натрупването на вредни емисии в атмосферата, налагат Човечеството да разработи незабавно мерки, с които да коригира екологичното равновесие на Земята. В статията се дават конкретни насоки за разрешаване на проблема как да се намалят до минимум количеството на токсичните вещества, които се отделят в атмосферата заедно с отработените газове от двигателите с вътрешно горене, както и от различните апаратури, в които се изгарят нефтените горива. В исторически план се оказва, че този процес е сложен и бавен, защото възникват сериозни разногласия между участниците в нефтопреработвателната промишленост и автомобилната индустрия. Водят се преговори относно признаване на важността от въвеждането на ефективни мерки по отношение запазване чистотата на околната среда, с които да се съобразява автомобилната индустрия. В света се налагат и важни законодателни мерки за постепенно прекратяване на производството и употребата на етилирани бензини и повишаване на изискванията към дизеловите горива.

### 2. Предпоставки и начини за разрешаване на проблема

Глобалното затопляне и натрупването на вредни емисии в атмосферата, налагат Човечеството да разработи незабавно мерки, с които да коригира екологичното равновесие на Земята. Проучванията показва, че основни замърсители на земната атмосфера са нефтените горива и продуктите, които се получават при тяхното изгаряне. Вредното въздействие на горивата върху околната среда се проявява в три основни направления [1]. Най-силно е токсичното въздействие върху живите организми при непосредствен контакт с нефтените горива и замърсяването на атмосферата с вредни вещества, които се съдържат в отработените газове при експлоатацията им. Лесната запалимост на горивата е причина за нанасяне на големи поражения върху земната атмосфера и околната среда при възникване на пожари. Задължително е при работа с такива продукти да се спазват съответните нормативни документи, с което законодателно се регулира ограничаване на токсичното им влияние. Независимо от това, автомобилният транспорт масаво навлиза във всекидневния бит на човека и е основна причина за замърсяване най-вече на градската среда. Търсят се решения на проблема как да се намалят до минимум количеството на токсичните вещества, които се отделят в атмосферата заедно с отработените газове от двигателите с вътрешно горене, както и от различните апаратури, в които се изгарят нефтените горива. Постоянно се правят нови

технологични изследвания относно усъвършенстване конструкцията на горивните системи. Дават се и нови препоръки за производството и правилния подбор, качество и свойства на различните нефтени продукти [2]. Статистиката показва, че всеки съвременен автомобил отделя годишно в околното пространство средно 800кг въглеродни оксиди, 115кг въглеводороди и 38кг азотни оксиди.

Заедно с развитието на нефтопреработвателната промишленост в края на миналия век се забелязва тенденция за постоянно допълване на законодателните изисквания за спазване нормите за чистота на околната среда. Този процес се оказва сложен и бавен, защото възникват сериозни разногласия между участниците в нефтопреработвателната промишленост и автомобилната индустрия. Водят се преговори относно признаване на важността от въвеждането на ефективни мерки по отношение запазване чистотата на околната среда, с които да се съобразява автомобилната индустрия. Компромис в това отношение е постигнато като автомобилостроенето се насочва към разработване на нови технологии за усъвършенстване на двигателите и въвеждане на компютърно отрегулирането на системите за впръскване на горивото, в зависимост от релефа на местността, скоростта и условията на движение, използване на каталитични системи за доизгаряне на горивата в изпускателната система и др. Всички тези дейности са насочени към снижаване вредните емисии в изгорелите газове, независимо от качествата на горивата. От своя страна, нефтопроизводителите въвеждат мероприятия по отношение запазване чистотата на околната среда, които се свеждат до внедряване на екологосъобразни технологии при преработването на нефтената суровина. Обща цел става подобряването на качествата на произвежданите горива, които да гарантират по-висока екологична безопасност. В света се налагат и важни законодателни мерки за постепенно прекратяване на производството и употребата на етилирани бензини и повишаване на изискванията към дизеловите горива.

Независимо от стремежа на всички автомобилни инженери и конструктори горивният процес да протича до пълно изгаряне на горивата, на практика се оказва, че е много трудно да се постигне оптимален ефект. Основните фактори, които нарушават този процес на горене са следните: процесът на изгаряне протича в горивния цикъл на двигателите за много кратко време; горивната камера е обикновено с много малък обем, поради което значително количество от топлината на изгаряне се губи в стените на камерата; влияние на хладния пристънчен слой, който оказва силно въздействие върху протичане на горивните реакции; физическа и химическа нееднородност на горивната смес и променливо налягане и температура в различните условия на изгарянето. При изгарянето на нефтените горива най-голямо е количеството на

получения въглероден оксид, който е продукт от непълното окисление на въглерода. Образува се при недостатъчно количество въздух в горивната камера, но може да се образува и при излишък на въздуха, поради дисоциация на молекулите от въглероден диоксид при високи температури. Този процес може да протече и при ниски температури, които да са достатъчни за окисление на въглерода до въглероден оксид, но недостатъчни да се окисли образувания оксид до диоксид [2]. Такива условия се наблюдават при изгаряне на силно обеднени смеси или на горивни слоеве, близки до студените стени на горивната камера. При дизеловите двигатели, които обикновено работят при голям излишък на въздуха, съдържанието на въглероден оксид в изгорелите газове е сравнително малко и не надвишава 0,3%.

Проучванията показват, че съдържащите се в отработените газове въглеродороди са смеси от много химически съединения. Основна причина за тяхното наличие в отработените газове е затрудненото развитие на процесите на дехидрогенизация, които протичат в целия обем на горивната камера, но са най-силно изразени в пристенния слой. Наличието на въглеродороди свидетелства за нарушаване на процесите на смесообразуване и на горене, както и на недостатъчно количество въздух в горивната камера. Практиката показва, че значителни количества на въглеродороди в изгорелите газове се наблюдава при работа на студени двигатели, при наличие на много бедна и много богата горивна смес и при неефективна работа на запалителната система [3].

Особено значение се обръща на намиращите се в изгорелите газове въглеродороди с канцерогенно действие. Към тези вещества се отнасят всичките полициклически ароматни въглеродороди, сред които най-силно биологично действие има бензспирените. Това вещество се образува в резултат на разлагане и полимеризация на тежки фракции от горивата и маслата в условия на недостатъчно количество въздух. При температури над 1250 K се разлага. Поради високите температури на топене /452K/ и на кипене /583 K/ бензспирените в чист вид практически не са опасни замърсители на въздуха. Но тези вещества се адсорбират върху сажените частици, които се изхвърлят в атмосферата с отработените газове, могат в това състояние да се разнасят във въздушната среда и да попаднат в дихателната система на живите организми.

Саждата се получава при високотемпературния пиролиз на горивата протичащ при недостатъчно количество въздух в горивната камера на двигателите. Такива условия най-често се създават в дизеловите двигатели, където се получават зони, в които има излишък на гориво и се образуват саждени частици. Основната част от тези частици изгарят в двигателя, но една част около 1 % от тях се изхвърлят с изгорелите газове. Това количество зависи в много голяма степен от начина на образуването на горивната смес. Количеството на саждите в изходящите газове зависи и от начина на смесообразуването на горивовъздушната смес в горивната камера на двигателя. Изследванията показват, че при еднакви експлоатационни условия, вихровите и предкамерните дизелови двигатели отделят по-малко дим, от двигателите с непосредствено впръскане на горивото в горивната камера. Основно, въздушната среда се замърсява от саждените частици, върху които се адсорбират особено токсичните вещества от вида на бензспирените. От страна на автомобилостроителите непрекъснато се работи за усъвършенстване на конструкцията на двигателите, системата на впръскане на гориво, компютърното регулиране на подаване на гориво в зависимост от релефа на местността, скоростта и условия на движение на превозното средство. Задължително всички автомобили се конструират с каталитични системи за доизгаряне на изходящите от тях газове. Основно вниманието на конструкторите в автомобилостроенето е насочено към мероприятия, които намаляват вредността на изгорелите газове независимо от качествата на използваните горива [4].

От страна на нефтепреработвателите изпълнението на изискванията по опазване на околната среда се свеждат в две основни направления. Едното от тях е стремеж към подобряване качествата на нефтените горива като им се придават свойства, които да гарантират по-сигурна екологична безопасност при тяхната експлоатация. Второто направление е свързано с предприемане на високи изисквания за опазване на природата при самото производство на моторни горива в съответните нефтепреработвателни предприятия. При търсене на начини да се съгласуват интересите на автомобилостроителите и нефтепреработвателите се възприе убеждението, че трябва да има постоянен технологичен обмен на научни нововъведения в т. нар. система „автомобилен парк – моторни горива“, който да обединява интересите на собствениците на автомобили и производителите на нефтепродукти. В тази схема трябва да се обединят усилията за опазване на околната среда при търговията с автомобили, с нефтепродукти и законодатели, които да разработват нови закони и перманентно да внасят поправки в тях и в стандартите. Това ще даде тласък в опазване на околната среда от вредното влияние на нефтените продукти и основните им консуматори. Особено, ако разработваните нови модели на превозни средства са съобразени с все по-високите изисквания на обновените стандарти. Същевременно това е необходимо да се реализира по възможност в най-кратки срокове и преди да са нанесени трайни поражения върху околната среда. Всяко подобрене в качествата на горивата, което е свързано с опазване на екологията изисква и законодателни мерки, за да се утвърждават съответните стандарти и е свързано с въвеждане в повечето случаи на технологични промени за тяхното регулярно производство. Това неминувемо води до повишаване цените на екологосъобразно произведеното гориво и верижно ще се отразява върху цените на много продукти, които са свързани с увеличените транспортни разходи. Тези разходи същевременно оказват съществено влияние върху цялостната икономика на дадена страна [5].

За да се решават проблемите с производството на екологично чист бензин, от технологична гледна точка трябва да се внедряват и употребяват само безоловни бензини, да се измени традиционния състав на бензина, като в него се включат високооктанови компоненти от специализирани за тази цел производства и да се добавят алтернативни компоненти като алкохоли, втечен съпътстващ нефта газ и метил третичен бутилов етер. Въвежда се и по-високи изисквания в качествата на автомобилните бензини по отношение съдържанието на ароматни въглеродороди, бензен и сярна.

По отношение на дизеловите горива се ограничи почти до отсъствие съдържанието на сярна от 350 до 50 ppm. Проучванията показват, че употребата на дизеловото гориво в страните от ЕС с всяка година нараства с по-висок процент от употребата на бензин. Статистиката показва, че употребата на бензин в страните от Северозападна Европа годишно намалява с 0,4%, употребата на дизелово гориво нараства с 1,5% [6]. Това се дължи на увеличеният парк от дизелови автомобили до 2015г с 24% в западноевропейските страни, каквато тенденция се наблюдава и у нас.

### 3. Заключение

В заключение, по гореизложените причини се наложи в страните на Европейския съюз и в Европейския парламент да се приемат нови изисквания към експлоатационните характеристики на нефтените горива. Промениха се и изискванията в спецификациите за допустими норми на вредни компоненти в изгорелите газове от автомобилите [6]. В света се регламентираха нови условия, които да се спазват от автомобилната и нефтепреработвателната индустрия. Съгласно възприетите Европейски норми съдържанието на ароматни въглеродороди в бензините се намали от 45% об. до 35% об., а съдържанието на сярна от 150ppm до 50ppm. Непрекъснато се създават и прогнозни изчислителни методи за определяне на

летливите органични съединения, азотните оксиди и други токсични съединения, въз основата на физикохимичните свойства на стоквите нефтопродукти. Това дава възможност за предварителен подбор на продуктите, от които ще се получават смесите от нефтените горива, съобразени с редица икономически и производствени фактори. Крайната цел е да се спазват екологичните изисквания по отношение на околната среда. На пример, през 1990г. в САЩ са въведени антидъпигови мерки, които да не позволяват влошаване на качествата на горивата в резултат на внасянето в състава им на алтернативни компоненти. Много от нефтопреработвателните компании вложиха значителни средства в производството на метил третичен бутилов етер и етил третичен бутилов етер от групата на т.нар. оксигенати. Развиха се и производства на високооктанови компоненти. Разшириха се производствата на „риформинг” процесите, каталитичен крекинг и хидрокрекинг. Това, от своя страна, увеличава значително крайната цена на нефтените горива, но същевременно дава възможност да се актуализират стандартите за качествата на нефтените горива, както и пределните допустими норми на токсични вещества в отработените газове [6]. Световна обединителна крайна цел е нефтените горива да станат безопасни по отношение съхраняването на здравето на хората и на околната среда.

Внедряването в масова употреба на екологосъобразени в конструктивно отношение автомобили е непосредствено свързано с масовото използване на сравнително чисти нефтопродукти. Това задължава нефтопреработвателните предприятия да оптимизират композиционните съставки на продуктите, така че да отговарят на високите изисквания по отношение на стандартните документи за опазване здравето на човека и околната среда.

### *Литература:*

- [1] Обелицкий А.М., Топливо и смазочные материалы, Высшая школа, 2003г., стр. 207
- [2] Петков П., Сл. Иванов, Д. Минков, Химмотология на нефтените горива, Булсайтком, София, 1990г., стр. 320
- [3] Брагинский О.Б., Э. Шлихтер, Мировая нефтепереработка, РАН, Москва, 2012г., стр. 256
- [4] Crow P., Sulphur despite, Oil and Gas Journal, 1998, v.96, p.35-46
- [5] Rhodes A.K., World crude capacity stays flat while conversion capability raises again, Oil and Gas Journal, 2013, v.94, p.27-54
- [6] Брагинский О.Б., Мировая нефтехимическая промышленность, Наука, 2010, стр.578

# CERTIFICATION AND QUALIFICATION OF TOOLS FOR CODE GENERATION IN AUTOMOTIVE INDUSTRY

## СЕРТИФИЦИРАНост И КВАЛИФИЦИРАНост НА ПОМОЩНИ ПРОГРАМИ ЗА ГЕНЕРИРАНЕ НА КОД ЗА АВТОМОБИЛНАТА ИНДУСТРИЯ

Dipl. Eng. Nikolay Petev Brayanov  
Mag. Инж. Николай Петев Браянов

Department of Microelectronics - Technical University of Sofia

Катедра Микроелектроника – Технически университет София

npb@ecad.tu-sofia.bg

**Abstract:** After ISO 26262 was developed as a derivative of IEC 61508 used specially for automotive industry, all software tools used in automotive industry were required to be certified and qualified to assure their compatibility with this safety relevant standard. However the standard does not specify a particular method for tools assessment. It gives a rough frame which allows the each provider of tools to develop custom specification when implementing his solution. This paper identifies approaches, used by different tool suppliers to assure ISO 26262 requirements.

The paper goes in deep in automotive safety standards, searching for milestones relevant to tools' certification. It describes basic requirement that tools should fulfil and the way it should be implemented and assured. Then behaviours of tools, that is not assessed by ISO 26262, but is part of overall software safety assessment is investigated. Finally the research review how it is implemented in some of the most distinguishable tools' providers – MatLab and IBM.

In conclusion, publication assess how commercial tools correspond to the needs of safety relevant industries and automotive in particular. It gives an answer of the question "Is using of certified and qualified tool enough to assure compliance with safety requirements?". It allocates the issues that are still opened.

**Keywords:** AUTOMOTIVE, SAFETY, CERTIFIED CODE GENERATION, TOOLS CERTIFICATION

### 1. Увод

Делът на софтуера в съвременната автомобилна индустрия постоянно нараства. Паралелно с повишения брой на изискванията към софтуера, нараства и желанието за намаляване на времето от начало на разработката до нейното плащане на пазара и общите разходи. Един от подходите, предложен като отговор на тези нови нужди е автоматизираното генериране на код, а ползите от него са многобройни:

- Проследимост на изискванията в кода
- Консистентност и високо качество на генерирания код, съобразно правилата за безопасност на автомобилна индустрия
- Възможност за повторно използване
- Оптимизиране на цената
- Възможност за симулиране и често прототипиране

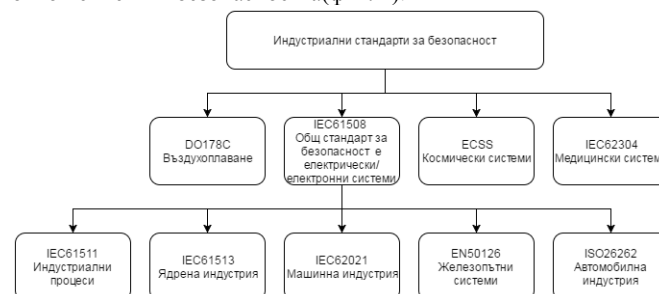
Основният проблем при разработки, в контекста на автомобилостроенето, е безопасността. Много нови функционалности - асистенция на водача, подпомагане на спирачната система, динамичен контрол на автомобила, въздушни възглавници и други активни и пасивни системи за сигурност са все по-обвързани с безопасността на автомобила. Разработването и интегрирането им води до нарастваща нужда от сигурен процес на системната разработка и необходимост от представяне на доказателства за изпълнението на целите за безопасност на системата. Това се постига чрез множество измервания, имплементирани в различни технологии и изпълнявани в различни етапи на разработката. В тази връзка възниква нуждата от квалифициране и сертифициране на помощните програми, използвани в индустриите с изисквания за безопасност.

В настоящия труд се разглеждат стандарта DO-178C използван във въздухоплаването, IEC61508 – главен стандарт за електрически и електронни системи и ISO26262, изработен на база IEC61508 и ориентиран към нуждите на автомобилостроенето. Разглежда се приложението на описаната методология, според практиката на два от най-големите доставчици на помощни програми за автомобилната индустрия, отчитайки преимуществата и недостатъците на методите и на приложението им съобразно стандарта. Разглеждат се алтернативни варианти за квалификация на

вериги от помощни програми. В резултат се дава отговор на поставения въпрос и са анализирани преимуществата и недостатъците на стандарта от гледна точка сертификация и квалификация на помощни програми, както и възможностите за подобряването му.

### 2. Предпоставки и начини за разрешаване на проблема

Създадени са стандарти, описващи методите за разработване и оценка безопасността за индустриите, имащи отношение към безопасността (фиг. 1).



Фиг. 1 Стандарти за индустриите с изисквания за безопасност

Всеки стандарт за безопасност поставя различни критерии за квалификация и сертификация на помощните програми.

DO-178C ясно дефинира методите за квалифициране на помощни програми [1]. Стандартът разглежда квалифицирането като процес, необходим за достигане на нужното ниво на сертифициране на дадена помощна програма в контекста на конкретно въздухоплавателна система. DO-178C разделя помощните програми на такива за разработване и такива за проверка. Разликата между тях е отговора на въпроса „Резултата от изпълнението на помощната програма част ли е от въздухоплавателния софтуер?“. Ако отговора на въпроса е да, помощната програма следва да бъде сертифицирана като такава за разработване. В противен случай тя се класифицира като програма за проверка, което значително улеснява сертификацията и. Според стандарта, когато помощната програма се използва за разработване, процесът при които е разработена тя трябва да удовлетворява процеса, нужен за текущата разработка на софтуер за въздухоплаването. Нивото на безопасност на продуктовия код е еквивалентно на това на използваната помощна програма. Стандартът дава възможност

за доказване на по-високо ниво на надеждност, чрез прилагане на допълнителни проверки. При квалифицирането на помощна програма за проверка, нещата са доста опростени. Необходимо е да бъде доказано че помощната програма работи коректно в контекста на употребата и. На практика това може да бъде постигнато чрез документиране на методите и ограниченията на работа.

IEC61508 дава концепция за сертифицирана помощна програма и препоръчва употребата им при изработване на проекти с изисквания за гарантирано ниво на безопасност [2]. Предлага се помощните програми да бъдат сертифицирани чрез продължителни тестове и проверка на резултатите или, алтернативно, чрез нарастване на доверието в следствие на продължителна употреба. На практика, на процеса на сертифициране се гледа като на измерване, необходимо в случаите когато не може да бъде доказано голямо доверие породено от употреба. Поради тази причина формалното сертифициране се счита за ненужно и утежняващо. Стандарта препоръчва да се сертифицират вериги от помощни приложения.

IEC61508 разделя помощните програми на онлайн и офлайн. Като онлайн се определят помощни програми, които могат да укажат пряко влияние на вградените системи с изисквания за безопасност, докато офлайн помощните програми не могат. Офлайн програмите са типизирани:

- резултатите от тип T1 не участват по никакъв начин в изпълнимия код
- тип T2 са отговорни за проверката на дизайна или изпълнимия код(в такива случаи в резултат от изпълнението не може да бъде променена работата на изпълнимия софтуер, но е възможно да не бъдат открити грешки)
- резултатите от тип T3 могат директно или индиректно да участват в изпълнимия код на система с изисквания за ниво на безопасност.

На база тази класификация, автоматизираното генериране на код е тип T3 на офлайн помощните програми. Сертификацията на програма от тази категория, изисква доказателства че тя отговаря на спецификацията си и инструкциите за употреба.

Въпреки че ISO26262 се базира на IEC61508, те имат доста различни подходи към квалификацията на помощни програми. Според стандарта, за всяка използвана помощна програма следва да бъдат анализирани и документираны случаите на употреба[3]. Анализа следва да удостовери, дали грешка при изпълнението на помощната програма или случайно генериран резултат, би довел до нарушение на изискванията за безопасност. Въздействието на помощната програма(TI – tool impact), има две стойности: TI1 – грешката не оказва въздействие; TI2 – грешката въздейства. В допълнение следва да бъде оценена вероятността такъв тип грешки да бъдат открити и премахнати. На база на този анализ се установява нужното ниво на доверие на помощната програма(tool confidence level (TCL), Таблица 1).

Таблица 1: Установява нужното ниво на доверие към помощната програма

		Вероятност за откриване на грешките на помощната програма		
		TD1 голяма	TD2 средна	TD3 други
Въздействие на помощната програма	TI1	TCL1	TCL1	TCL1
	TI2	TCL1	TCL2	TCL3

На база пресметнатия TCL и нивото на осигурена безопасност(Automotive Safety Integrity Level (ASIL)) се избира

нужния метод са квалифициране на помощната програма(таблица 2).

Таблица 2: Избор на методи за квалификация на помощна програма

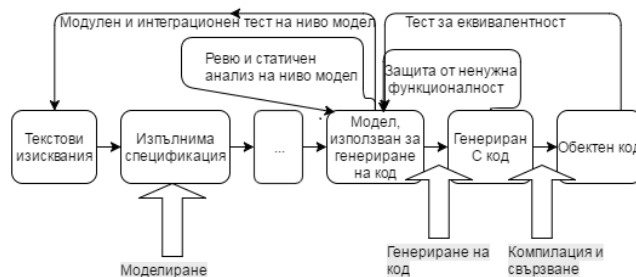
Методи	Препоръчани методи	
	за TCL2	за TCL3
1. Доверие, придобита от употреба	ASIL A, B и C	ASIL A и B
2. Проверка на процеса на разработване на помощната програма	ASIL A, B и C	ASIL A и B
3. Валидация на софтуера на помощната програма	ASIL D	ASIL C и D
4. Разработване на помощната програма според стандартите за безопасност за които се прилага	ASIL D	ASIL C и D

Метода „Доверие, придобито от употреба“ се възприема и от този стандарт. Както се вижда обаче, при по-голяма вероятност от неоткриваема грешка, той не е достатъчен.

### 3. Решение на проучения проблем

Публикацията [4] описва подхода, използван от MathWorks за квалифициране и сертифициране, чрез орган със сериозна акредитация в областта сертифициране/квалифициране на помощни програми - TÜV SÜD Automotive GmbH. За целта те използват вече създадените за IEC 61508 сертифициращи пакети и квалифициращите функционалности за DO-178C, които са били налични към този момент, както и подходите им за сертификация/квалификация.

Следващата фигура демонстрира процеса на проверка и валидация на модели и генериран код, създадени чрез „Simulink“ среда за моделиране и „Real-Time Workshop Embedded Coder“ генератор на C код.



Фиг.2: Последователност на проверка и валидация реализирани за квалифициране на Simulink“ и „Real-Time Workshop Embedded Coder“

Описаните проверки и валидация целят да откриват или предпазват резултата от грешки при изпълнение на помощните програми или други спонтанни такива. Според доклада за сертификация, прилагането на описания процес води до висока вероятност потенциалните грешни резултати на код генератора могат да бъдат открити или премахнати, т.е. TD1, което води до ниво на доверие към помощната програма TCL1. Според тази оценка генератора на код, приложен чрез този процес, е квалифициран и няма нужда от допълнителна квалификация и проверка.

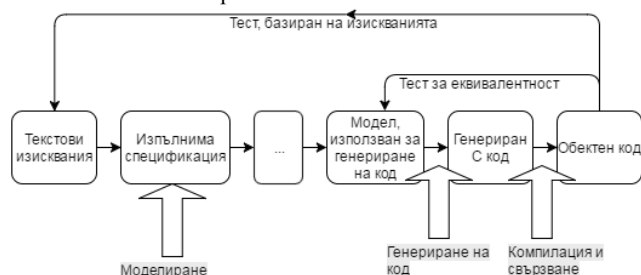
За да направят помощната програма гъвкава и приложима в нестандартни вериги от помощни програми, разработката предвижда и случаи в които вероятността за откриване на грешка е средна(TD2) и съответно е необходима ниво на доверие към помощната програма TCL2. В този случай е необходима допълнителна сертификация на база таблица 2. Помощната програма за проверка на C/C++ код „PolySpace“ също е класифицирана на ниво TCL2.

Приложени са методи за квалификация 2 и 3, с което се покриват всички нива на безопасност от ASIL A до ASIL D.

В допълнение се предлага „Пакет за Квалифициране на Помощни Програми“, който предоставя подход и бланки за квалифициране на вериги от помощни програми базирани на ISO/DIS 26262-8, както и независимата оценка на TÜV SÜD.

Описаният метод се опитва да предложи гъвкавост. Резултат от това е обемен и съответно бавен и скъп процес. Приложението му в малки проекти би било трудно, поради статичността му и нуждата от закупуване на допълнителен пакет за сертифициране.

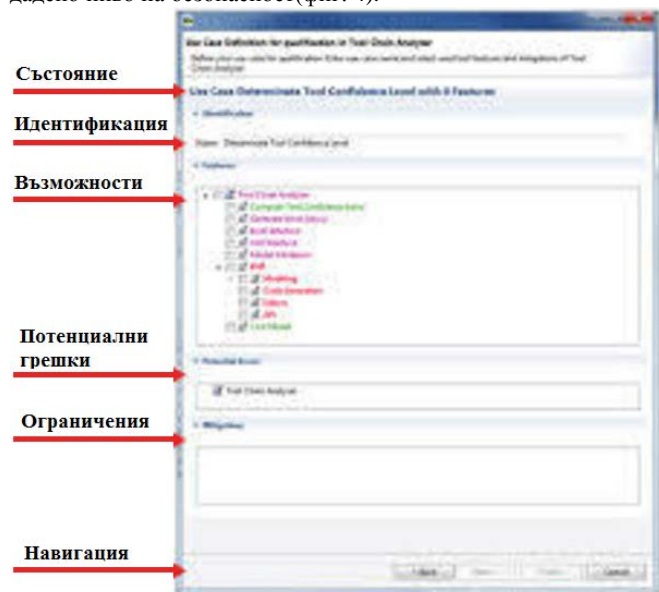
В публикация [5] се предлага сертифицирана и оптимизирана верига от помощни програми. Подобрението спрямо предходния метод е, че няма нарочна проверка на модела (фиг. 3). Според авторите, въпреки липсата на тази проверка в процеса, тя все пак се извършва косвено чрез проверка на резултата от автоматичната генерация на код, изпълнявайки тестове, базирани на изискванията. Недостатък на този тип проверка на ниво код е факта че в случай на грешка, анализа и трябва да бъде извършен на ниво код, а не на моделно ниво. След като проблема бъде идентифициран на ниво код, следва да бъдат направени релевантните промени на ниво модел, което евентуално ще коригира проблемите на ниво код. Един такъв подход не е никак рутинен, а и понякога отнема значително време.



Фиг. 3: Последователност на проверка и валидация реализирани за квалифициране на IBM помощна програма, оптимизирана чрез премахване на проверките за модела

В този случай опита на доставчиците за оптимизиране на процеса води до едно усложняване и необходимост от специфични умения. Все пак този метод е приемлив и може да бъде използван, макар и с не еднозначен резултат.

Други доставчици предлагат възможността потребителя сам да избере веригата от помощни програми, както и специфичните функционалности, които да използва [6]. В резултат от автоматичен анализ на риска, на потребите се предоставят избор от допълнителни тестове, които следва да бъдат извършени, за квалификацията на веригата спрямо дадено ниво на безопасност (фиг. 4).



Фиг.4: TI предлага готова конфигурация за да улеснят клиентите си

Решението е доста гъвкаво, просто и олекотяващо процеса. Като недостатък може да се посочи че такъв тип софтуери дават възможност за създаване на вериги, използвайки само един доставчик. Това ограничава избора, както поради причината че не дава възможност да се използва най-доброто предложение за всеки тип операции, така и заради потушаването на конкуренцията.

Алтернативата публикувана в [7] предлага моделно базирана помощна програма „Tool Chain Analyzer“, която може да оценява нестандартно изградени вериги от помощни програми. Недостатък в съчетаването на различни помощни програми е, че те трудно се синхронизират, защото имат различни интерфейси, а понякога се налага и добавяне на допълнителни проверки, което води до утежняване на процеса и допълнителна нужда от квалификация.

За последния проблем има решение в тази публикация [8]. Авторите предлагат метод за оптимизиране на броя на необходимите проверки. Според статията, приложението на метода успява да намали нужните помощните приложения, квалифицирани на ниво TCL3 от 7 до 0 и TCL2 от 4 на 1. В резултат от това те намаляват времето, необходимо за квалифициране на нужната верига от помощни програми с 50%, от 120 дни на 60. Резултатите са доста добри. За прилагане на метода обаче, се изискват някои специфични знания и умения.

#### 4. Резултати и дискусия;

ISO26262 е един от най-добре дефинираните стандарти за безопасност. Той дава методология за оценка на помощните програми, използвани в автомобилната индустрия. Добре описани са подходите чрез които те могат да бъдат квалифицирани и сертифицирани. За разлика от други стандарти ISO26262 дефинира еднакви изисквания за квалификация за програмите за разработване и тези за валидация. Мнението ми е, че това е гаранция за процес, гарантиращ константно ниво на безопасност. Реално, статистически винаги има вероятност за допускане на грешка и много важно е проверката да се извършва с реципрочното ниво на достоверност. Изследването доказа, че е достатъчно да бъдат използвани сертифицирани и квалифицирани помощни програми за осигуряване на съвместимост с нормите на безопасност.

Този факт не е достатъчен за да убеди индустрията в смисъла от използването на автоматизирани методи за създаване на софтуерни приложения и конкретно автоматично генериране на код. Целта на всеки бизнес е да оптимизира процесите си с цел редуциране на разходите и осигуряване на нужното качество и безопасност на продукта. В този смисъл, и в контекста на съвременния текст на стандарта, използването на автоматизираните системи за генериране на код е спорно.

Основен недостатък е, че квалифицирането и сертифицирането на вериги от помощни програми са бавни, специфични и не на последно място скъпи процедури. Това ги прави нерентабилни за малки проекти и фирми. На база опита, мнението ми е, че това е голяма пречка за широкото разпространение на автоматизираните методи за генерация на код, което води до по-бърз, евтин, качествен и безопасен резултат. Изхождайки от позицията че този тип помощни програми са нужният инструмент за оптимизиране на разработките, считам, че е нужна оптимизацията на стандартите за безопасност, както следва:

- Квалификацията и сертификацията да бъдат извършвани върху веригите от помощни програми. Оптимално е квалификацията на помощни програми да бъде извършвана за всяка отделна верига, минимизирайки нужните проверки, според необходимото ниво на безопасност. Проучването установи, че квалифицирането на помощни програми в частност, е излишен процес, тъй като сертификацията на помощната програма сама по себе си не носи облекчения на процеса на сертифициране на веригата, който е задължителен. Следва да се извършват

промени в стандарта за безопасност в частта си за квалификация и сертификация на помощни програми, с цел премахване на сертифицирането на единични помощни програми и подробно дефиниране и улесняване на квалифицирането на вериги.

- Хармонизиране на подходите за оценка и квалификация, дефинирани в различните стандарти. Това ще доведе до концентриране на ресурси и обединена работа на доставчиците на помощни програми, работещи в различни индустрии с изисквания за безопасност.

В допълнение, в стандарта липсва обосновка на добри практики, които да бъдат използвани по време на оценката на нивото на доверие към помощната програма. При следваща редакция, е препоръчително да бъдат добавени такива, осигурявайки еднозначното тълкуване по време на процеса на оценка.

## 5. Заключение

В настоящия труд бяха разгледани стандартите за безопасност и методите по които те квалифицират и/или сертифицират помощни програми, и в частност тези за генериране на кода за вградени системи в автомобилната индустрия. Спряхме се подробно на ISO26262, който е един от най-добре дефинираните стандарти в това отношение. Той се отнася до системи с изисквания за безопасност в автомобилната индустрия и описва процеса при оценката на ниво на доверие към помощната програма (TCL), както и следващите стъпки за квалификация на помощната програма във връзка с нивото на осигурена безопасност (ASIL) необходимо на изгражданата система.

Разгледахме решенията на този проблем, предложени от два от най-големите доставчици на помощни програми MathWorks и IBM, анализирайки преимуществата и недостатъците им. Анализа показва, че подходите им са оптимални и отговарят на стандарта. Недостатък беше посочен в невъзможността за квалифицирано ползване на част от веригата.

Конкуренцията, в лицето на TI, предлага подход за динамично квалифициране, в които потребителя може да избере кои функционалности да използва, след което полуавтоматично да квалифицира така създадената верига. В този случай, обаче, е невъзможно създаването на верига от помощни програми, използвайки конкурентни доставчици.

Бяха разгледани и решения за квалифициране на верига, съставена от различни помощни програми, както и оптимизиране на такъв тип вериги, заявяващи доста добри резултати. Многогранната работа върху този проблем е доказателство за неговата важност и за това че все още той е неразрешен.

Обобщават се и се обсъждат резултатите, изхождайки от позицията, че помощните програми за автоматично генериране на код са част от решението за повишения брой на изискванията към софтуера, съвместно с нуждата от намаляване на времето от начало на разработката до нейното пласиране на пазара и общите разходи. В резултат от проучването, се обоснова извода, че използването на сертифицирана и квалифицирана помощна програма е достатъчно условие за осигуряване на съвместимост с нормите на безопасност. В допълнение беше достигнат извода, че стандартите, в текущата им форма, значително усложняват процеса на разработката. Възможен подход за справяне с този проблем е стандартите за безопасност да бъдат хомогенизирани, обединявайки доставчиците от различните индустрии с цел безопасност на продуктите им. От друга страна основен недостатък на стандарта е, че предлага подход насочен към квалифициране на помощните програми, а не към веригите. Опитът показва че квалифицирането на помощни

програми сами по себе си е ненужно. Поради тази причина се предлага промяна на стандарта, улесняване и задаване на насоки за квалифициране на вериги от помощни програми.

Изследването е извършено с финансовата подкрепа на НИС при ТУ - София по проект №162ПД0022-03 на тема "Изследване на възможностите за моделно базирана разработка на вграден код съгласно изискванията в автомобилната индустрия"

## 6. Литература.

[1] Software Considerations in Airborne Systems and Equipment Certification, DO-178C, RTCA Inc./EUROCAE, 2011

[2] Functional safety of E/E/PE safety-related systems, IEC 61508:2010, IEC.

[3] Road Vehicles – Functional safety– ISO26262:2011.

[4] Mirko Conrad, Patrick Munier, Frank Rauch Qualifying Software Tools According to ISO 26262

[5] IBM Rational Rhapsody Reference Workflow Guide Version 1.9

[6] Dr. Oscar Slotosch, Dr. Marcel Beemster Model-Based Tool Qualification of the TI C/C++ ARM® Compiler

[7] Oscar Slotosch Model-Based Tool Qualification The Roadmap of Eclipse towards Tool Qualification

[8] Oscar Slotosch, Martin Wildmoser, Jan Philipps, Reinhard Jeschull, Rafael Zalman ISO 26262 - Tool Chain Analysis Reduces Tool Qualification Costs

# EFFECT OF ADDITIVES IN PHASE COMPOSITION OF CARBON CATALYSTS OTHER THAN ASC WHETLERITE TYPE CARBONS ON THEIR REMOVAL EFFICIENCY AGAINST HYDROGEN CYANIDE VAPORS IN THE AIR

ЕФЕКТ НА ДОБАВКИТЕ ВЪВ ФАЗОВИЯ СЪСТАВ НА ВЪГЛЕН КАТАЛИЗАТОРИ РАЗЛИЧНИ ОТ ASC WHETLERITE ТИП ВЪГЛЕНИТЕ ВЪРХУ ТЯХНАТА ЕФЕКТИВНОСТ В ОЧИСТВАНЕТО НА ПАРИТЕ НА ЦИАНОВОДОРОДА ОТ ВЪЗДУХА

Mag.-Eng. Manoilova L.<sup>1</sup>, Mag.-Eng. Chatzis A.<sup>1</sup>, Assist. Prof. Dr. Eng. Vladov D.<sup>1</sup>

Ass. Prof. Dr. Eng. Spassova Iv.<sup>2</sup>, Ass. Prof. Dr. Eng. Nickolov R.<sup>1</sup>

University of Chemical technology and Metallurgy-Sofia<sup>1</sup>, Institute of General and Inorganic Chemistry - BAS<sup>2</sup>

E-mail: lili\_manoilova@abv.bg, at.xatz@gmail.com, dchvladov@gmail.com, ispasova@svr.igic.bas.bg, r\_nickolov@uctm.edu

**ABSTRACT:** Canisters for present-day gas masks are usually filled with impregnated ASC Whetlerite activated carbons. To solve the inherent problems of the carbon catalysts new types of Cu/Zn-based impregnated carbons with complete substitution of Cr with Mo and by addition in the impregnating solution of alkaline  $K_2CO_3$  and TEDA in some cases were prepared. The removal efficiency of these samples against HCN vapours in air tested under standard conditions demonstrated that the content of  $K_2CO_3$  to ~ 4% in Cu/Zn samples extends the protection effect to practically equal to the same parameter for the ASC Whetlerite. The inclusion of TEDA in the phase composition of the catalysts does not impair the protection properties towards HCN of the carbon catalysts.

**KEY WORDS:** GAS MASK'S CANISTERS, IMPREGNATED ACTIVATED CARBON, ASC WHETLERITE TYPE CARBON, Cu/Zn-BASED IMPREGNATED CARBONS, ADDITIVES IN PHASE COMPOSITION,

## 1. Introduction

HCN is widely used, strongly toxic precursor for many laboratory and industrial syntheses, whose world production exceeds 0.5 million tons per year, besides, HCN is formed in the ignition of a series of materials of domestic use. Historically, HCN is used as chemical warfare agent during the World War I. Despite the restricted opportunity to use HCN by the modern armies as a CWA, it represents a highly effective potential terroristic poisonous substance.

An optimal protection of the respiratory organs of the armed forces staff and the population in case of terroristic actions and the occurrence of centers of chemical contamination, they provide for the filtering breathing masks, founding their effect in terms of most of the known toxic substances on physical adsorption of activated carbon materials in the breathers or the filtering adsorbing elements.

Since the physical adsorption of highly volatile non-persistent chemical warfare agents such as hydrogen cyanide, cyanogen chloride, phosgene, arsine and phosphin of the non-impregnated activated carbons is weak and hence, reversible at room temperature, the breathers of the modern breathing masks and filter-absorbent of the collective means for protection, are equipped with impregnated activated carbons. As of the moment, to remove the vapours of HCN, ClCN,  $COCl_2$ ,  $AsH_3$  and  $PH_3$  from the air by the breathers of gas masks and filter absorbents, the activated carbons have found the widest application, impregnated with Cu and Cr salts, known as ASCWhetlerite carbons.

Despite of their proven high efficiency in terms of the protection from the vapors of the highly volatile non-persistent chemical warfare agents, the impregnated carbons containing  $Cr^{6+}$  are considered as non-perspective by the specialists, such as the ones of the US Environmental Protection Agency [1] due to:

- risk of cancer-producing effect of some of the forms of  $Cr^{6+}$  [9] for the production personnel and the army staff, using the relevant gas masks and collective means of protection [2];
- a problem with annihilation of this type of impregnated carbon, after the expiration of the term of use defined by the manufacturer;
- the irreversible deactivation that this type of impregnated carbons are easily susceptible to as a result of the increased temperature [3] and/or enhanced humidity [4-6].

A solution of the problems referred is the creation of a generally new types of impregnation compositions on a basis other than the one of Cu/Cr compositions. Such impregnated carbons are the ones on a Cu/Znbase, alike the American impregnated carbon of new generation, ASZM-T, developed by Calgon Corp. [7].

Due to the complex nature of the removal of vapours of HCN by the impregnated carbons and the existence of a relation between the reaction capability of vapours and other highly volatile non-persistent chemical warfare, it was decided that the studies of the impregnated carbons on Cu/Znbase start namely with the vapours of HCN.

The absence of  $Cr^{6+}$  in the impregnation compositions, on the other hand, leads to the forming as a by-product of  $(CN)_2$  as a result of the decomposing of the chemically unstable  $Cu(CN)_2$ , a product of the removal of HCN. To solve this problem, we have received and studied a new type of impregnated carbon on Cu/Znbase, with addition of insignificant amounts of Agard Cr (< 0.6%). This type of impregnated carbon, signified with VSZC, is characterized with protection effect against the vapours of HCN, practically equal to the same parameter for the ASC Whetlaritetype of impregnated activated carbons however with impaired parameter in terms of the forming of  $(CN)_2$  compared to them.

The last can be corrected via the increase of the content of  $Cr^{6+}$ , which is however inadmissible due to its cancerogenity, via overall replacement of Cr, with Mo or via the introduction in the impregnation composition of VSZC of an alkaline additive – for instance  $K_2CO_3$ . In the presence of  $K_2CO_3$  in the active phase, the removal of HCN runs on a two-grade mechanism whereat the instable cupricyanide reacts with KCN in alkaline medium, forming  $K_2[Cu(CN)_4]$ .

It is a practical interest to study the impact on the protection effect against the vapours of HCN and on the forming as a by-product of  $(CN)_2$  in the impregnated carbons on Cu/Znbase of the complete replacement of Cr, with Mo or the introduction in the impregnation composition of VSZC of an alkaline additive –  $K_2CO_3$ .

Therefore the objective of this work is to study the effect of Mo and of the alkaline ingredient ( $K_2CO_3$ ) in the composition of the active phase of the impregnated carbons on Cu/Znbase, in terms of efficiency of defusing HCN vapours from the air, compared to the same in the ASC Whetlerite type of carbons.

## 2. Experimental part

### 2.1. Samples

The activated carbon used in the studies is a commercial product obtained from apricot shells with particle size 1.0 – 1.5 mm, signified as ACVM.

The textural parameters of the starting and the impregnated activated carbons as well as the impregnation compositions of the latter are presented in Table 1.



The samples were obtained via standard impregnation procedure of the activated carbon. The following salts (individually or in suitable combinations) were used to prepare the impregnation solutions: basic copper carbonate, zinc oxide, chrome oxide, molybdenum oxide and silver nitrate. The indicated compounds were dissolved in a solution of ammonia carbonate, water and ammonium hydroxide (25 %). In some of the cases, the impregnation solution was added up with TEDA.

Each of the samples was obtained via slow spraying of the relevant impregnation solution on the activated carbon in a rotating flask on a modified rotary evaporator.

The samples prepared in this way were signified as follows:

VSZ – activated carbon, impregnated with mixed ammoniacal copper zinc + silver nitrate solution.

VSZ-A2 - activated carbon, impregnated with mixed ammoniacal copper zinc + silver nitrate solution, containing 2 mass %  $K_2CO_3$ .

VSZC - activated carbon, impregnated with mixed ammoniacal copper zinc + chromic acid solution.

VSZC-T - activated carbon, impregnated with mixed ammoniacal copper zinc + chromic acid solution, containing TEDA.

VSZC-A2 - activated carbon, impregnated with mixed ammoniacal copper zinc + chromic acid solution, containing 2 mass %  $K_2CO_3$ .

VSZC-A4 - activated carbon, impregnated with mixed ammoniacal copper zinc + chromic acid solution, containing 4 mass %  $K_2CO_3$ .

VSZC-A6 - activated carbon, impregnated with mixed ammoniacal copper zinc + chromic acid solution, containing 6 mass %  $K_2CO_3$ .

VSZC-A8 - activated carbon, impregnated with mixed ammoniacal copper zinc + chromic acid solution, containing 8 mass %  $K_2CO_3$ .

VSZM - activated carbon, impregnated with mixed copper ammoniacal zinc molybdate + silver nitrate solution.

VSZM-T - activated carbon, impregnated with mixed ammoniacal copper zinc molybdate + silver nitrate solution, containing TEDA.

VC5W - ASC Whetlerite type of carbon, obtained as per standard procedure („whetlerization process”).

After each application of the precursors, the samples were allowed to stand in a controlled closed volume at room temperature for 2 hours.

The samples prepared in this way were heated at not higher than 423 K in a draft oven (under pressure), as in the case of the VSZC-T and VSZM-T samples, the heating temperature was maintained to preserve the main part of the pyridine.

## 2.2. Test methods

The characterization of the specific surfaces and porous texture of the initial activated carbon (ACVM) and the impregnated samples was carried out via low temperature adsorption of nitrogen (77.4 K) using Quantachrome Instruments NOVA 1200e (USA) apparatus.

Based on the adsorption – desorption nitrogen isotherms, via the specialized software set in the equipment, the following texture parameters were calculated: specific surface area ( $A_{BET}$ ) according to the Brunauer–Emmett–Teller (BET) equation, for the interval  $P/P_0 = 0.05 - 0.35$  (adsorptive  $N_2$ , 77.4 K); total pore volume ( $V_t$ ) as per the Gurvich-rule for  $P/P_0 = 0.95$  (adsorptive  $N_2$ , 77.4 K); micropore volume ( $V_{MI}$ ) using the density functionale theory (DFT) (adsorptive  $N_2$ , 77.4 K); volume of the mesopores ( $V_{MES}$ ) as a difference between the total volume and the micropore volume (adsorptive  $N_2$ , 77.4 K); average radius of the pores ( $R_p$ ) as a ratio of the double  $V_t$  and  $A_{BET}$  (adsorptive  $N_2$ , 77.4 K); the half-width ( $x_0$ ) of the micropores (as per the flat parallel model) for the maximum of the distribution curve as per the simplified equation [8,9].

The textural parameters of the samples calculated by the methods referred are presented in Table 1.

The copper, zinc, chrome, molybdenum and silver were determined by atomic absorption using a Pye Unicam SP 90B spectrometer.

The photoelectrons and Auger specters of the samples were registered using an ESCALAB MkII (VG Scientific) XR photoelectron spectrometer with  $AlK_{\alpha}$  (1486.6 eV) source. The C 1s peak at 284.6 eV, was used as an internal standard for calibration of the connecting energies. The samples surface composition according to XPS, was determined based on the photoelectron intensities estimated by the corresponding Scofield cross sections.

## 2.3. Adsorption –dynamic studies

The experimental dynamic equipment and the procedures for study of the sorption, resp. protective properties of the impregnated carbons against HCN, are analogous to the ones described in [4].

The predried (378 K, 2 hours) impregnated carbons were reproducibly packed in glass dynamic tubes and air (HCN)- vapor flow was passed through the samples, following the parameters set:

- sample bed depth	3.0 cm
- sample bed diameter	2.0 cm
- volume flow rate	1.57 l/min
- relative humidity	50%
- temperature	293 + 3K
- HCN challenge concentration	3± 0.3 mg/l
- HCN breakthrough concentration	10 ml/m <sup>3</sup>
- (CN) <sub>2</sub> breakthrough concentration	5 ml/m <sup>3</sup>

The removal efficiency of the impregnated carbons was evaluated indirectly, during the ( $t_B$ ) removal action, against HCN and (CN)<sub>2</sub> (in the cases when free dicyan is formed), as the resolution of HCN and (CN)<sub>2</sub> is based on the difference in the interaction of the two substances with  $AgNO_3$  solution.

The registration of the relevant breakthrough concentrations was carried out by:

- reaction between HCN and aqueous solution containing benzidine, copper acetate and acetic acid;
- reaction between (CN)<sub>2</sub> and aqueous solution of KCN, containing 8-hydroxyquinoline.

## 3. Discussion of the experimental results

### 3.1. Adsorption-textural characterization

Via comparing the adsorption textural parameters of the impregnated samples with the ones of the initial activated carbon (Table 1), it was estimated that the impregnation process concerns more the microporous than their mesoporous textures, respectively their specific surfaces.

The reduction of the micropore volumes is most likely due to blocking parts of the micropore space of the samples or to blocking the access to the micropores.

The increase of the microporous heterogeneity of the samples (characterized via the alterations of the values of  $x_0$ ), best expressed in the impregnated samples VC5W, VSZ-A2, VSZC-T, is related to the distribution of the micropores of the initial carbon by size [10], with the stage of heating and attending migration of the active phases and the metal ions nature.

Despite of the fact that as a result of the impregnation and following heating, the parameters of the porous texture and all sample specific surfaces change, Table 1 displays that the biggest changes occur in the samples including in their phases  $K_2CO_3$  and TEDA.

In this sense, the change is bigger of the parameters referred in the samples including TEDA (VSZC-T and VSZM-T) compared to the single type VSZC and VSZM, than the samples containing various quantities of  $K_2CO_3$ .

It must be noted that, with the increase of the content of  $K_2CO_3$  (> 2%), the specific surfaces decrease and the average radiuses of the sample pores increase in synchrony (Table 1), which is an evidence for the simultaneous change of the external and internal surfaces of the impregnated carbons.

Table 1 Elemental phase composition and main texture parameters of the initial activated carbon and of impregnated samples

Samples	Content (mass %)				$A_{\text{BET}}$ ( $\text{m}^2/\text{g}$ )	$V_t$ ( $\text{cm}^3/\text{g}$ )	$V_{\text{mi}}$ ( $\text{cm}^3/\text{g}$ )	$V_{\text{mes}}$ ( $\text{cm}^3/\text{g}$ )	$x_o$ (nm)	$\Gamma_{\text{Pmes}}$ (Å)
	Cu	Zn	Cr	Mo						
ACVM	-	-	-	-	1060	0.930	0.396	0.534	0.68	17.5
VC5W <sup>(a)</sup>	7.1	-	2.07	-	892	0.861	0.352	0.509	0.93	19.3
VSZ <sup>(a)</sup>	6.3	5.6	-	-	882	0.830	0.327	0.503	0.87	18.8
VSZ-A2 <sup>(a),(b)</sup>	6.2	5.6	-	-	851	0.829	0.324	0.505	0.99	19.5
VSZC <sup>(a)</sup>	5.8	5.4	0.63	-	872	0.820	0.312	0.508	0.82	18.8
VSZC-T <sup>(c)</sup>	5.7	5.3	0.60	-	823	0.816	0.292	0.524	0.90	19.8
VSZC-A2 <sup>(a),(b)</sup>	5.6	5.3	0.62	-	846	0.813	0.300	0.513	0.85	19.2
VSZC-A4 <sup>(a),(b)</sup>	5.5	5.2	0.61	-	829	0.814	0.284	0.530	0.85	19.6
VSZC-A6 <sup>(a),(b)</sup>	5.7	5.4	0.61	-	817	0.812	0.263	0.549	0.75	19.9
VSZC-A8 <sup>(a),(b)</sup>	5.7	5.3	0.59	-	776	0.808	0.272	0.536	0.86	20.8
VSZM <sup>(a)</sup>	5.5	5.2	-	1.9	827	0.807	0.309	0.498	0.87	19.5
VSZM-T <sup>(a),(c)</sup>	5.6	5.3	-	1.8	783	0.788	0.252	0.536	0.77	20.1

(a) - Sample contains about 0.05 mass % Ag

(b) - Sample contains  $\text{K}_2\text{CO}_3$ , in a quantity (mass %) indicated after "A"

(c) - Sample contains about 3 mass % TEDA

### 3.2. Chemical analysis and sample surface analysis

The content of Cu, Zn, Cr and Mo in the studied samples was determined via atomic absorption. The results are presented in Table 1.

The determination of the oxidative state of the studied elements in the impregnants, element composition of the sample surface as well as the location of the impregnants on the surface or in the sample volume, was carried out via XPS.

Due to the higher sensitivity of the Auger signal towards Cu (1+), as well as the relative invariance with respect to the oxidation state of Zn in the values of the Zn 2p photoelectron peak, Auger spectroscopy was also used to characterize the copper and zinc phase. The photoelectron specters obtained for the Cu 2p photoelectron area, in all copper containing samples, demonstrate binding energies for Cu (2+) oxidation state of the Cu 2p<sub>3/2</sub> peaks, whose shoulders to the higher binding energies on their turn demonstrate the presence of incompletely decomposed  $\text{CuCO}_3$  and  $\text{Cu(OH)}_2$  phases. Via studies using Cu L<sub>3</sub>M<sub>4,5</sub>M<sub>4,5</sub> Auger specters, presence of Cu (1+) was not found in the samples of Table 1.

In the case of the samples containing zinc (VSZ, VSZ-A2, VSZC, VSZC-T, VSZC-A2, VSZC-A4, VSZC-A6, VSZC-A8, VSZM, VSZM-T), the oxidation state of Zn was determined by the Zn L<sub>3</sub>M<sub>4,5</sub>M<sub>4,5</sub> Auger line. The data obtained are likely to demonstrate the presence in our samples, except of a main component of the zinc phase,  $\text{ZnCO}_3$  and of hydroxycarbonate, with approximate composition  $2\text{ZnCO}_3 \cdot 3\text{Zn(OH)}_2$  (k.e. 988.0 eV), whose composition is not permanent and depends on the conditions of receipt and thermal treatment.

In the case of the samples VSZC, VSZC-T, VSZC-A2, VSZC-A4, VSZC-A6, VSZC-A8, the content of Cr is relatively low (approximately 0.61 mass.%, Table 1), which is a reason for the lack of adequate reliability in the results regarding its valent state. Nevertheless, by analogy with VC5W [11], it can be assumed that Cr (6+) appears under the form of  $\text{CuOH} \cdot \text{NH}_4 \cdot \text{CrO}_6$  [22]). The latter is close to the adopted composition  $\text{CuCrO}_4 \cdot \text{NH}_3 \cdot \text{H}_2\text{O}$ , according to the references cited by Nikolov [4].

It is an obscure picture of the type and nature of the Mo-phase in the case of VSZM and VSZM-T. Various authors assume that in the case of this type of carbon, Mo exists under various forms (above all as a fine dispersed phase, distributed predominantly in the volume of VSZM [12]). However, the one responsible for the removal of the forming  $(\text{CN})_2$  is  $\text{Mo}^{6+}$  [13]. Our

photoelectron specters for the Mo 3d<sub>2/5</sub> photoelectron area provide for ground in the Mo-phase of VSZM (VSZM-T) to distinguish  $\text{MoO}_3$  (b.e. 231.7 eV),  $(\text{NH}_4)_2\text{MoO}_4$  (b.e. 232.1 eV) and  $(\text{NH}_4)_2[\text{Mo}_2\text{O}_7]$  (b.e. 232.5 eV).

The inclusion of TEDA to Cu- and Zn-phase (regardless of the presence of Cr (VSZC-T) or Mo (VSZM-T) (VSZM-T) affects the copper phase as its content in the volume of the samples referred to increase with about 10% compared to VSZC and VSZM, accordingly, as in parallel, the content of Zn on our surface also increases. On the opposite, the inclusion of  $\text{K}_2\text{CO}_3$  to the composition of the impregnants (in the case of samples VSZC-A2, VSZC-A4, VSZC-A6, VSZC-A8) results in the re-distribution compared to VSZC, of the Cu- and Zn-phase between their volume and external surface. Thus, depending on the quantity of  $\text{K}_2\text{CO}_3$ , the content of the Cu-phase decreases in the volume, whereas, otherwise, the content of the Zn-phase on the external surface increases.

### 3.3. Breakthrough time of the samples

In the case of gas-mask equipment, the service time ( $t_B$ ) is defined as time during which the concentration of PS in the air vapor flow, after the sorbent bed, reaches a preset value for the relevant experimental conditions.

Table 2 present  $t_B$  against HCN and  $(\text{CN})_2$  of the studied impregnated carbons and for reference, the ones of the initial activated carbon (ACVM).

As it can be expected, ACVM practically does not remove the vapors of HCN. Table 2 displays that the studied samples (except VSZ, VSZ-A2, VSZC-T) are characterized with  $t_B$  against the vapors of HCN > 50 min.

The sample VSZ (appearing to be basic with its Cu/Zn active phase) is characterized simultaneously with the lowest  $t_B$  among the rest of the samples both against the vapors of HCN, and against  $(\text{CN})_2$ . Nevertheless, Table 2 displays that  $t_B$  against the vapors of HCN in the case of VSZ is practically the same as of the sample VSZC containing Cr, accordingly less against the vapors of  $(\text{CN})_2$  and significantly less regarding this parameter compared to the sample VSZM containing Mo.

Table 2. Breakthrough times for initial and impregnated carbon samples

Образци	$t_B$ (min)	
	HCN	(CN) <sub>2</sub>
ACVM	2.5-3.0	(a)
VC5W	53.0	(b)
VSZ	49.0	29.0
VSZ-A2	49.0	31.0
VSZC	51.0	32.0
VSZC-T	49.0	33.0
VSZG-A2	51.0	33.0
VSZG-A4	53.0	40.0
VSZG-A6	51.0	38.0
VSZG-A8	51.0	37.0
VSZM	52.0	47.0
VSZM-T	53.0	48.0

(a) - Not determined experimentally. According to literature data it is close to breakthrough time against HCN.

(b) - breakthrough concentration of (CN)<sub>2</sub> not reached.

In the case of VSZC, after the exhausting of Zn-phase (as a result of the chemisorption of HCN) the function of the direct destruction of (CN)<sub>2</sub> is taken by Cr<sup>6+</sup>. The presence of Cr<sup>6+</sup> in the composition of the impregnants of VSZC practically does not change  $t_B$  by the HCN of the sample compared to the one of VSZ. On the opposite,  $t_B$  by (CN)<sub>2</sub> increases with about 10% against the same for VSZ, however remains lower than the same parameter for the other sample containing Cr<sup>6+</sup> (about 2 %) - VC5W (Table 2).

The sample VSZM proves the positive impact of Mo in the composition of Cu/Zn active phase, appearing an alternative variant of the sample with best parameters in the study VC5W. In its case,  $t_B$  by HCN is practically the same as of the sample VC5W, and the forming of (CN)<sub>2</sub>, starts upon spending its time for removal of HCN. The mechanism of effect of the impregnants against HCN, in this type of impregnated carbons is not entirely clear. Our studies demonstrate that there is an analogy in the functioning of Zn- and the Cu-phase in the samples VSZM and VSZC, as, after spending the Zn-phase in VSZM (as a result of the chemisorption of HCN), the (CN)<sub>2</sub> being formed reacts with the Mo-phase to tightly bound with the carbon surface, non-toxic product (likely oxamide).

The most likely explanation of the difference (although insignificant) in the values in  $t_B$  by HCN and by (CN)<sub>2</sub> between VC5W and VSZM are: the less content of the Mo-phase than needed (Table 1) or of some of the Mo-forms, and also increase of the content of the Cu-phase on the external surface, at the expense of the same in the volume in the case of VSZM [M!].

The samples of the type VSZ and VSZC (VSZ-A2, VSZC-A2, VSZC-A4, VSZC-A6 and VSZC-A8) are interesting, containing in the composition of their impregnants K<sub>2</sub>CO<sub>3</sub> (between 2 and 8 mass. %), which, upon removal of HCN impedes or even disables the formation of (CN)<sub>2</sub>.

Based on the results in Table 2, it can be concluded that the inclusion of K<sub>2</sub>CO<sub>3</sub> in the composition of the impregnants (except the sample VSZC-A4, containing 4 mass. %) does not result in the increase of  $t_B$  against the vapors of HCN. The impact of K<sub>2</sub>CO<sub>3</sub> is much more significant regarding  $t_B$  against (CN)<sub>2</sub>. In this case, there is dependence even between  $t_B$  and the content of K<sub>2</sub>CO<sub>3</sub>, which passes through maximum with the content of K<sub>2</sub>CO<sub>3</sub> about 4 mass. %. Probably in case of content of K<sub>2</sub>CO<sub>3</sub> above the determined, exhausting of the Cu-phase appears via the binding to K<sub>2</sub>[Cu(CN)<sub>4</sub>] and the exclusion of it from the general process of removal of HCN.

The inclusion of TEDA in the composition of the phase of the samples VSZC and VSZM, i.e. the samples VSZC-T and VSZM-T, increases insignificantly  $t_B$  by (CN)<sub>2</sub> compared to VSZC and VSZM. Analogically,  $t_B$  against the vapors of the HCN in the case of the two samples changes within the limits of 2-4 %. Most likely the effect of TEDA in the phase composition of the impregnants can be related to the fact that TEDA to a very slight extent affects the Cu-phase as this is more likely to manifest in the

stronger expressed positioning of the Cu-phase in the mesoporous space of the VSZM-T, compared to the same for the sample VSZC-T. TEDA does not affect the Zn-phase. Generally, it can be concluded that TEDA practically does not affect the chemisorption of HCN.

#### 4. Conclusion

A study has been carried out of the effect of additives to the phase composition of the carbon catalysts on Cu- Zn base in terms of their effectiveness for the elimination of the HCN vapours in the air. It was found that the inclusion in Cu- Zn phase of the samples of Mo, Cr<sup>6+</sup> (~ 0.60 mass. %), K<sub>2</sub>CO<sub>3</sub> or TEDA results in their commensurable effectiveness in terms of the removal of the HCN vapours in the air (determined as a breakthrough time) with the one of the standard ASC Whetlerite type of carbon.

Despite of the fact that the inclusion of the additives referred in the Cu-Zn phase composition results in the increase of  $t_B$  of the samples against the vapours of (CN)<sub>2</sub>, by this parameter, they stay behind the ASC Whetlerite type of carbon.

Regardless of the fact that the sample containing Mo in their phase composition is closest to the  $t_B$  against the vapours of (CN)<sub>2</sub> of the ASC Whetlerite type of carbon, as the same parameter in its case remains smaller, probably due to the smaller amount of the Mo-phase than the needed or of any of the Mo-forms.

The inclusion to the phase composition of the carbon catalysts on Cu- Zn base (containing or not Cr<sup>6+</sup>) K<sub>2</sub>CO<sub>3</sub>, does not result in the increase of  $t_B$  against the vapours of HCN (except the sample VSZC-A4, containing 4 mass. %). The impact of K<sub>2</sub>CO<sub>3</sub> however is much more significant in terms of  $t_B$  against (CN)<sub>2</sub>. In this case, there is even dependence between  $t_B$  and the content of K<sub>2</sub>CO<sub>3</sub>, which passes through a maximum in the event of content of K<sub>2</sub>CO<sub>3</sub> about 4 mass. %.

The inclusion of TEDA in the composition of the phase of samples VSZC and VSZM practically does not affect their effectiveness for the removal of the HCN vapours, but in all cases, it provides further protection also from the ClCN vapours.

#### 5. References

- Rossin, J., R. Morrison, Spectroscopic analysis and performance of an experimental copper/zinc impregnated, activated carbon, Carbon 29, 1991, 887-892.
- Николов, Р., Д. Механджиев, Структура и състав на фазата на перспективен медно-цинков въглен катализатор, предназначен за защита от парите на токсични вещества, ВНИИ, Научна сесия „Въоръжение и военна техника на 2000<sup>та</sup> година”, Химия и ядрена физика 8, 1995, 77-82.
- Vas, N., J. Hammarstrom, A. Sacco, Jr., Thermal decomposition studies on copper-chromium-silver impregnated activated charcoal, Carbon 25, 1987, 545-549.
- Николов, Р. *Дисертация*, София, ВНИИ, 1988.
- Rossin, J., E. Petersen, R. Lamontagne, L. Isaacson, Effect of environmental weathering on the properties of ASC-Whetlerite, Carbon 29, 1991, 197-205.
- Zhiqiang, L., Z. Mingrong, C. Kuixue, The investigation for the deactivation mechanism of Cu-Cr impregnated carbon by XPS, Carbon 31, 1993, 1179-1184.
- Doughty, D. *Development of a chromium-free impregnated carbon for adsorption of toxic agents*, Pittsburgh, PA: Calgon Carbon Corporation, 1991.
- Nickolov, R., D. Mehandjiev, Adsorption studies on the changes in microporous texture of an ASC Whetlerite type carbon catalyst modified with Co in an organic medium, Ann. Univ. Sofia “St. Kl. Ohridski” 89, 1997, 229-236.
- Mehandjiev, D., E. Bekyarova, R. Nickolov, Micropore Size Distribution by a Simplified Equation, Carbon 32, 1994, 372-374.
- Molina-Sabio, M., V. Perez, F. Rodriguez-Reinoso, Impregnation of activated carbon with chromium and copper salts: effect of porosity and metal content, Carbon 32, 1994, 1259-1265.
- Nickolov, R., D. Mehandjiev, Comparative study on removal efficiency of impregnated carbons for hydrogen cyanide vapors in

air depending on their phase composition and porous texture, *J. Colloid Interface Sci.* 273, 2004, 87-94.

12. Park, S., S. McClain, S. Tian, S. Suib, C. Karwacki, Surface and bulk measurements of metals deposited on activated carbon, *Chem. Mater.* 9, 1997, 176-183.

13. Rossin, J., R. Morrison, The effect of molybdenum on stabilizing the performance of an experimental copper / zinc impregnated, activated carbon, *Carbon* 31, 1993, 657-659.

# MODIFIED ACTIVATED CARBONS AS MATERIALS FOR A DECONTAMINATION OF Tl POISONED WATER

## МОДИФИЦИРАНИ АКТИВНИ ВЪГЛЕНИ КАТО МАТЕРИАЛИ ЗА ОЧИСТВАНЕ НА ВОДИ ЗАРАЗЕНИ С Тl

Mag.-Eng. Chatzis A.<sup>1</sup>, Assist. Prof. Dr. Eng. Tzvetkova P.<sup>2</sup>, Mag.-Eng. Manoilova L.<sup>1</sup>,  
Assist. Prof. Dr. Eng. Gentsheva G.<sup>2</sup>, Ass. Prof. Dr. Eng. Nickolov R.<sup>1</sup>  
University of Chemical technology and Metallurgy-Sofia<sup>1</sup>, Institute of General and Inorganic Chemistry - BAS<sup>2</sup>  
E-mail: at.xatz@gmail.com, ptzvetkova@svr.igic.bas.bg, lili\_manoilova@abv.bg, gentg@svr.igic.bas.bg,  
r\_nickolov@uctm.edu

**ABSTRACT:** Removal of large monovalent cations, as highly toxic thallium (Tl), from the waters is a subject of significant interest due to the hazards its pose. Active materials on the basis of activated carbons intended for removal of Tl ions from drinking water was synthesized and characterized in two stages. During the first, deposition and stabilization of the Fe (3+) phase in the internal surface of activated carbon samples (AC/Fe (3+)) was carry out. During the second, deposition on the AC/Fe (3+) of  $K_4[Fe(CN)_6]$  phase and subsequent chemical reaction were realized. The removal performance of the samples prepared for Tl ions in aqueous solution was investigated by adsorption process. Increased sorption possibilities were observed toward Tl ions as compare to initial carbons.

**KEY WORDS:** Tl COMPOUNDS AS TERRORISTIC POISONOUS AGENTS, Tl COMPOUNDS AS SOURCE OF WATER CONTAMINATION, ACTIVE MATERIALS INTENDED FOR REMOVAL OF Tl IONS FROM DRINKING WATER, COMPLEX COMPOUND  $Fe_4^{3+}[Fe^{2+}(CN)_6]_3$  ("PRUSSIAN BLUE")

### 1. Introduction

It is known that the thallium compounds appear to be extremely strong poisons [1,2] to man and animals.

The main source of thallium compounds in water, including underground waters are various mines, mostly for gold yielding but also coal mining, enriching factories and facilities of the color metallurgy. Another source of thallium in waters is the cement factories, the manufacturers of electronic elements, of art glass articles[2,3,4].

A likely source of water contamination (above all potable) with thallium could be the domestic crimes and terroristic actions.

The first ones are made possible by deratization agents (rodenticides) available in the population of a series of countries on a thallium base.

In terms of the use of thallium compounds by terrorists in the quality of poisonous agents for contamination of potable waters, precedents exist which provide for a ground for the priority inclusion of the thallium in the group of terroristic – diversion means [5,6,7,10], etc.

The decontamination of the industrial (the mines in particular) waters from the thallium compounds represents a subject of a series of studies.

For this purpose, various methods have been studied such as reverse osmosis, biological treatment, sulfide sedimentation, etc. [3].

Trials proved that the only generally effective method for decontamination of the industrial and potable waters is the adsorption method.

Due to the nature of the antiterrorist problematic, the literature is lacking data for the decontamination of potable waters contaminated with thallium compounds, but it is absolutely sure that the sorbents used for this purpose are different for the industrial and potable waters.

In this sense, the natural and most of the synthetic zeoliths used (NaY, NaA), incl. modified, cannot provide for decontamination to the required minimal contents of thallium in potable waters, which is 5-7 times lower than the admissible for the decontaminated industrial waters.

A very important reason for this can be the fact that the sorption of thallium ions of industrial waters is realized under controlled pH, whereas in the case of potable water, the pH of water cannot vary but an optimal ratio must be sought: physisorption / chemisorptions, whereas the chemisorbing phases are characterized with high efficiency.

In this sense, the best variant is the use as a chemisorbent, of the complex compound  $Fe_4^{3+}[Fe^{2+}(CN)_6]_3$  ("Prussian blue") [8].

The "Prussian blue" according to the American specialists is the active substance of the only antidote used as of the moment against intoxications with thallium compounds[9].

The selection of suitable sorbents for purification of thallium compounds of potable waters is based on the presence in them of suitable texture parameters which are advantageous for the introduction of the chemisorptions phase in the porous texture of the sorbents. Only in this case, the processes of physical adsorption (physisorption) and chemisorptions can be realized optimally and simultaneously in the process of water decontamination from the thallium compounds.

The synthesis of complex compounds in the porous texture of the sorbents however is complicated by the fact that the active phase which provides the chemisorptions of thallium ions should not impede the physical adsorption, respectively to reduce the specific surface and volume of sorbing pores.

As per the literature data, for the synthesis if the metal ferrocyanides in single pore systems, the Kurim method is most suitable [11]. It is a serious problem that this method has not been applied for micro-mesoporous materials such as for instance the activated carbons, sorbents, suitable for sorption of various water compounds.

The activated carbons are characterized with high specific surface and strongly developed porous structure which makes them suitable both with their adsorption function and as carriers of active phases in various processes for water decontamination.

A problem in the case of the activated carbons would be the synthesis in their porous texture of the relatively large molecules of  $Fe_4^{3+}[Fe^{2+}(CN)_6]_3$ , without significantly reducing the volumes of the sorbing pores and of the admissionporesto the chemisorbing phase.

The last necessitates some variation (modification) by the Kurim method for synthesis in the pores as per the specificities of the compound (micro-mesoporous textures) such as the activated carbons'.

Besides, considering the dependence of the sorption of metal ions in water media of pH of the latter, it is very important to establish the interval of pH, in which the activated carbons with iron hexaferratic complex в sorbe effectively  $Tl^{1+}$  ions and its conformity to pH specific to the most frequent potable waters.

As a result of all stated above, the objective of the study is to obtain activated materials based on activated carbon through a synthesis in their porous texture by the modified method of Kurim of iron (3+) hexacyanoferratic (2+) complex, which active materials should be studied in their quality of sorbents for purification of potable waters contaminated with thallium compounds, as per pH of these waters.

## 2. Experimental part

### 2.1. Samples

Since no requirements have been formulated for the basic activated carbons intended for the synthesis of the active materials in the conditions of technological difficulties for the performance of the Kurim synthesis in micro-mesoporous systems, we have adopted the empirical approach for selection. For the purpose, the selected activated carbons were predetermined using the low-temperature (77 K) adsorption of nitrogen some of their texture parameters. On the other hand, the chemical nature of the carbon

surface was characterized through the determination of the IEP of these.

For the purposes of study, three types of activated carbons were selected (commercial products) on wooden basis (signified BAC), based on apricot shells (signified AAC) and based on coconut shells (signified CNAC), differing by the values of the specific surfaces and of the rest of the texture parameters. The three activated carbons have been obtained through gas-vapor activation. Their main adsorption – texture parameters and values of the IEP are given in Table 1.

Table 1 Main parameters of the porous texture and values of IEP of the studied activated carbons

Samples	$A_{BET}, m^2/g$	$V_t, cm^3/g$	$V_{MI}, cm^3/g$	$V_{MES}, cm^3/g$	$R_p, \text{Å}$	IEP
BAC	658	0.38	0.20	0.18	11.6	6.1
AAC	895	0.50	0.29	0.21	11.2	7.6
CNAC	1019	0.61	0.33	0.28	12.0	6.8

$A_{BET}$  – specific surface;  $V_t$  – total pore volume;  $V_{MI}$  – volume of the micropores;  $V_{MES}$  – volume of the mesopores,  $R_p$  – average radius of the pores; IEP – isoelectric point.

### 2.2. Synthesis of $Fe_4^{3+}[Fe^{2+}(CN)_6]_3$ in the porous texture of the activated carbons

The synthesis by the Kurim method, in the porous texture of the activated carbons of  $Fe_4^{3+}[Fe^{2+}(CN)_6]_3$  represents a practical problem.

The main reason is reduced to the need of preparative provision of uniform distribution on the internal surface of the samples of  $FeCl_3 \cdot 3H_2O$ , maximally preserving the contact surface considering the follow up interaction with  $K_4[Fe(CN)_6] \cdot H_2O$ , as well as to the iron (3+) hexacyanoferrate (2-) complex of the thalium ions of the water solutions.

The opportunities for introduction of the ferric chloride from aqueous and non-aqueous (methanol) solutions were studied. Based on a comparison of the adsorption-texture parameters (determined via low-temperature adsorption of nitrogen) of samples of activated carbons with introduced  $FeCl_3 \cdot 3H_2O$  from water and methanol media, it was found that in the case of use of the aqueous solution, probably as a result of blocking parts of the porous texture, the specific surfaces, total and mesoporous volumes decrease with the average of about 20-23% for the three carbons.

On the opposite, in the case of the methanol solutions, such effect was not observed. This determined the use of methanol solutions of  $FeCl_3 \cdot 3H_2O$  for the introduction in the porous texture of the activated carbons.

The introduction of  $K_4[Fe(CN)_6] \cdot H_2O$  was carried out from aqueous solutions, after vacuum drying of the samples with ferric chloride at room temperature.

The samples with introduced ferric chloride and  $K_4[Fe(CN)_6] \cdot H_2O$  phases were left in a desiccant, at room temperature for 24 hours, during which it was assumed that the forming of the complex  $Fe_4[Fe(CN)_6]_3$  is complete.

The main adsorption – texture parameters of the synthesized activated materials (signified accordingly as Fe/BAC, Fe/AAC and Fe/CNAC), calculated based on their adsorption isotherms (77 K), are given in table 2.

Table 2 The summary assay of iron and main texture parameters of active materials

Active material samples	Summary content of Fe (mass %)	$A_{BET}, m^2/g$	$V_t, cm^3/g$	$V_{MI}, cm^3/g$	$V_{MES}, cm^3/g$	$R_p, \text{Å}$
Fe/BAC	12.6	547	0.31	0.18	0.15	11.3
Fe/AAC	12.3	743	0.39	0.23	0.16	10.5
Fe/CNAC	13.0	825	0.50	0.27	0.22	12.1

### 2.3. Methods of study

The activated carbons and synthesized activated materials on their base are characterized via the low temperature nitrogen adsorption (77.4 K) with Quantachrome Instruments NOVA 1200e (USA) apparatus.

Based on the adsorption-desorption nitrogen isotherms, via the specialized software set in the equipment, the following texture parameters were calculated:

- specific surface area ( $A_{BET}$ ) by the equation of Brunauer–Emmett–Teller, for the interval  $P/P_0 = 0.05 - 0.35$  (adsorptive  $N_2$ , 77.4 K);

- total volume of the pores ( $V_t$ ) as per the Gurvich rule for  $P/P_0 = 0.95$  (adsorptive  $N_2$ , 77.4 K);

- volume of the micropores ( $V_{MI}$ ) using the Density functional theory (DFT) (adsorptive  $N_2$ , 77.4 K);

- volume of the mesopores ( $V_{MES}$ ) as a difference between the total volume and the volume of the micropores (adsorptive  $N_2$ , 77.4 K);

- average radius of the pores ( $R_p$ ) as a relation of the double  $V_t$  and  $A_{BET}$  (adsorptive  $N_2$ , 77.4 K);

The texture parameters of the samples calculated by the methods referred are presented in Table 1 and 2.

The isoelectric points (IEP) of the carbons were determined by the method of NohSchwarz [12]. For the purpose, for each of the carbons, three different initial solutions were prepared with different pH (accordingly 3, 6 and 11), using  $HNO_3$  (0.1 M) and  $NaOH$  (0.1 M). Six flasks were filled each with 20 ml of the solutions and with different quantities of activated carbon (0.05, 0.50, 0.75, 1.00, 5.00 and 10.00g). The balance pH was determined after 24 hours. The curves of the dependences of pH on the carbon masses demonstrate plateau and the isoelectric point is defined as the value which turns the change of pH to zero.

The summary content of iron ( $\text{Fe}^{3+}$  and  $\text{Fe}^{2+}$ ) in the activated materials was determined via atomic absorption using a spectrometer type Pye Unicam SP 90B.

The study of the sorption of the thallium ions ( $\text{Tl}^{1+}$ ) in potable water of the initial activated carbons and the activated materials Fe/BAC, Fe/AAC and Fe/CNAC, obtained on their ground, was carried out by the method of the periodic adsorption (concentration 0,91 mg/l and pH in the interval 3-7.5, 293 K), as a difference of the concentrations before and after adsorption determined through atomic absorption analysis (spectrometer type Pye Unicam SP 90B).

The sorption effectiveness (S, %) of the initial activated carbons and the synthesized active materials on their ground in terms of the thallium ions ( $\text{Tl}^{1+}$ ) in potable water, depending on pH of water has been expressed in percentage against the initial concentration (100 %)

### 3. Discussion of the experimental results

Table 3 Sorption effectiveness of the initial activated carbons and the synthesized active materials in terms of the thallium ions, depending on the pH of water

pH	sorption effectiveness, %					
	BAC	AAC	CNAC	Fe/BAC	Fe/AAC	Fe/CNAC
3	15	19	16	57	54	50
4	23	27	20	71	63	59
5	25	28	22	58	66	74
6	28	20	21	84	73	90
7	21	18	21	77	72	92
7.5	20	17	19	75	70	86

The analysis of the results from Table 3 demonstrates the determining role of pH of water medium on the sorption activeness of the samples both for the initial activated carbons and the activated materials synthesized on their base.

Impression is made by the strongly dominating sorption capability of the activated materials compared to the initial activated carbons on the base of which these are obtained, and also that the maximal sorption of  $\text{Tl}^{1+}$  ions in the activated carbons was displaced compared to the activated materials in the field of the lower pH (pH about 4 - 5), and also that, regardless of the difference in the adsorption texture parameters, the sorption effectiveness in the studied activated carbons is very close. Most likely, a limiting factor in the sorption of the  $\text{Tl}^{1+}$  ions by the activated carbons happen to be their IEP.

Except that, the sorption activity of the activated materials in terms of the  $\text{Tl}^{1+}$  ions is significantly higher compared to the initial activated carbons, it is determined also by the pH of water. The three studied samples sorb best within the interval pH: 6 - 7, which is a very important interval since it corresponds to the pH of most of the potable water in our country.

In the field of the low values of pH (pH = 3 - 4), the sample Fe/BAC sorbs best the  $\text{Tl}^{1+}$  ions.

Based on the results of Table 2 and 3, it can be concluded that a direct dependence between the specific surfaces, total and mesoporous volumes of the pores of the activated materials (for practically identical amounts of  $\text{Fe}_4[\text{Fe}(\text{CN})_6]_3$  phase) on one hand, and their sorption capacities in terms of  $\text{Tl}^{1+}$  ions in the potable water, is lacking.

For the interval of values of pH (pH=5-7), characterizing with the highest sorption in the studied process, by its sorption activity against the thallium ions, the activated materials can be presented in the following downward row: Fe/CNAC > Fe/BAC > Fe/AAC.

### 4. Conclusion

Activated materials have been synthesized through modified method of Kurim based on activated carbon and the iron

The comparison of the adsorption texture parameters of the initial activated carbons (Table 1) and of the activated materials (Table 2) demonstrate that as a result of the synthesis in the pores of the activated carbons of the iron (3+) hexacyanoferric (2+) complex, all adsorption texture parameters practically change, however preserving the high values of the specific surfaces and the average radiuses of the pores, to levels facilitating the free access of the thallium ions to the phase introduced.

The data for the summary assay of iron ( $\text{Fe}^{3+}$  and  $\text{Fe}^{2+}$ ) in the activated materials (Table 2) demonstrates close values for the three samples. This provides us a ground to consider that the effectiveness of the iron hexacyanoferric phase in the samples is also close.

The results for the sorption effectiveness (S, %) of the initial active carbons and the synthesized active materials on their base in terms of the thallium ions ( $\text{Tl}^{1+}$ ) in potable water, depending on the pH of water, under the conditions of the experiments are presented in Table 3.

(3+) hexacyanoferric (2+) complex, intended for the decontamination of potable water poisoned with  $\text{Tl}^{1+}$  ions.

The active materials obtained possess significantly higher sorption activeness against the thallium ( $\text{Tl}^{1+}$ ) ions compared to the initial activated carbons.

Dependence has been established between pH of the water media and the sorption effectiveness in terms of the  $\text{Tl}^{1+}$  ions on behalf of the activated materials. The maximal sorption effectiveness is observed for the interval of pH (pH about 6-7) specific to most of the potable water in our country.

The results obtained provide us a ground to continue our studies on the synthesis of activated materials with introduced iron hexacyanoferric phase and other micro-porous carriers other than the activated carbons.

### 5. References

1. Cvjetko P, I. Cvjetko, M. Pavlica, Thallium Toxicity in Humans, Arh. Hig. Rada Toksikol. 61, 2010, 111-119.
2. Grudnik T., R. Koiaicz, Z. Dobrzacski, The Protective Effect of Aluminosilicates in Laying Hens Chronically Intoxicated with Thallium, Polish Journal of Environmental Studies 14, 2005, 739-742.
3. Reinsel M., S. Mason, Natural zeolites remove thallium from mining water, Environmental Science & Engineering Magazine, January 2013, 280-285.
4. Karski S., I. Witonska, Thallium as an additive modifying the selectivity of Pd/SiO<sub>2</sub> catalysts, Kinet. Catal. 45, 2004, 256-259
5. McGeorge H.J., Chemical and Biological Terrorism: Analyzing The Problem, The Applied Science and Analysis Newsletter, issue number 42, June 16, 1994.
6. Purver R., Chemical and Biological Terrorism: The Threat According to the Open Literature, Canadian Security Intelligence Service Publication, June 1995.
7. Franke S., Lehrbuch der Militärchemie, Berlin, Deutscher Militärverlag, vol. 1, 1967.
8. Altagracia-Martinez M. et al., Prussian blue as an antidote for radioactive thallium and cesium poisoning, Orphan Drugs: Research and Reviews June 2012, 13-20.

9. Guidance for Industry. Prussian Blue Drug Products— Submitting a New Drug Application, U.S. Department of Health and Human Services, Food and Drug Administration, Center for Drug Evaluation and Research (CDER), January 2003
10. Sangvanich T. et al., Selective capture of cesium and thallium from natural waters and simulated wastes with copper ferrocyanide functionalized mesoporous silica, *Journal of Hazardous Materials* 182, 2010, 225–231.
11. Kourim V., J. Rais, B. Million, Exchange properties of complex cyanides-I, Ion-exchange of caesium on ferrocyanides, *J. Inorg. Nucl. Chem.* 26, 1994, 1111-1115.
12. Noh, J., J. Schwarz, Effect of HNO<sub>3</sub> treatment on the surface acidity of activated carbons, *Carbon* 28, 1990, 675-682.



# ИЗБОР НА ВАРИАНТ ЗА ТРЕТИРАНЕ НА УТАЙКИТЕ ОТ ПРЕЧИСТВАТЕЛНА СТАНЦИЯ ЗА ОТПАДЪЧНИ ВОДИ – В. ТЪРНОВО

## CHOICE OF OPTION FOR TREATMENT OF SLUDGE OF THE WASTEWATER TREATMENT PLANT – VELIKO TARNOVO

доц. д-р инж. Пенчо Стойчев  
Технически университет – Габрово,  
катедра „Физика, химия и екология”

pstoychev@tugab.bg

**Abstract:** Directive 91/271 / EEC on the treatment of wastewater from towns and villages raises the question of wastewater treatment to a level that allows its discharge to natural water basins. By wastewater are separated sludge, whose treatment and recovery are the focus of this study.

**Keywords:** TREATMENT PLANT, WASTEWATER, WASTEWATER TREATMENT

### 1. Въведение

Строителството на съществуващата пречиствателна станция за отпадъчни води (ПСОВ) в гр. Велико Търново е започнало през 1974 г.

След дългогодишни промени в технологията и съоръженията към настоящия момент ПСОВ –В. Търново работи по следната технологична схема по пътя на водата:

1. Решетки - груби и фини – 3+3 броя;
2. Горизонтален аеруем пясъкомаслозадържател /двукоридорен/ - 1 бр.;
- 2а. Сграда с въздуходувки и класификатор за пясък;
3. Измерително устройство;
4. Разпределително устройство (РУ) към ПРУ;
5. Първични радиални утаители (ПРУ) с  $D = 25$  m – 3бр.;
6. Дъждопреливник – двустранен преди биобасейна;
7. Биобасейни с повърхностна аерация – 3 бр.;
8. РУ преди Вторичните радиални утаители  $D = 25$  m;
9. Вторични радиални утаители;  $D = 25$  m – 3бр.;
10. РУ преди Вторичните радиални утаители  $D = 26$  m;
11. Вторични радиални утаители;  $D = 26$  m – 2 бр.;
12. Контактни резервоари;  $D = 20$  m – 2 бр.;
13. Заустване в река Янтра;
14. ПС за калови, дренажни води и хлорни утайки.

### 2. Изложение

В резултат на задълбочено проучване се достигна до следните предложения за усъвършенстване в технологичната схема на Пречиствателната станция за отпадъчни води на гр. Велико Търново, в частта и за третиране на утайките:

- **Помпена станция за активна утайка – реконструкция**

Съществуващата помпена станция за активна утайка е с подземна част (черпателен резервоар и помпено помещение) и надземна (помещение за ел. табла и обслужващи пасарелки).

В ПС са инсталирани 4 бр. центробежни помпи за Рециркулираща активна утайка (РАУ) и 2 бр. помпи за Излишна активна утайка (ИАУ). Помпената станция трябва да се отремонтира и да се подмени оборудването. Една от помпите за РАУ ще е за резервна, две ще покриват основното натоварване, а четвъртата ще работи с честотен преобразовател и ще се контролира от входното измервателно устройство.

Помпите за РАУ транспортират активната утайка в канала пред биобасейна. Измервателното устройство ще се монтира на тласкателя.

Излишната активна утайка от продуцираната биомаса ще се препомпва до съществуващия утайкоуплътнител. Тези помпи работят на времеви интервали.

- **Утайкоуплътнител за първичната утайка – нов**

Предвижда се изграждане на нов обем за акумулиране и гравитачно уплътняване на първичната утайка (ПУ). Обема ще бъде за едnodневно количество. Т.е. оразмеряването трябва да е за обем на първичната утайка  $250$  m<sup>3</sup> дневно.

Оттук ще черпят зареждащите помпи към метантанка.

- **Утайкоуплътнител за ИАУ – реконструкция**

Съществуващият утайкоуплътнител е тип радиален с диаметър  $15$  m.;  $H_{\text{раб}} = 2.70$ .

Трябва да се подменят утайкочистача и металните части.

- **Помпена станция за уплътнена ИАУ – реконструкция**

Помпената станция (ПС) при утайкоуплътнителя е предназначена за препомпване на уплътнени излишни активни утайки от утайкоуплътнителя към черпателните резервоари на ПС при изгнивателите.

Предвижда се доставка на нови помпи, които да зареждат директно съгъстителите и да са съобразени с техния дебит. Напорните тръбопроводи след помпите ще са самостоятелни.

- **Помпена станция при метантанкове с МССЗ – реконструкция**

В основния проект ПС5 и ПС6 са проектирани да обслужват четирите метантанкове. В момента метантанковете работят като окрити изгниватели и съответното оборудване в помпената станция е съобразено с тази схема.

При реконструкцията ще се преоборудват метантанковете и съответно помпените станции към тях. В съществуващата сграда са предвидени механични ротационни съгъстителни за намаляване влажността, респективно обема на излишната активна утайка, тъй като ИАУ е с високо водно съдържание и не е подходяща за директно подаване в метантанка. За интензифициране на процеса в реактора пред съгъстителите се добавя полиелектролит -  $3.0$  kg/t сухо вещество (СВ). Съгъстената активна утайка с влажност  $94$  % се подава в метантанка за стабилизиране.

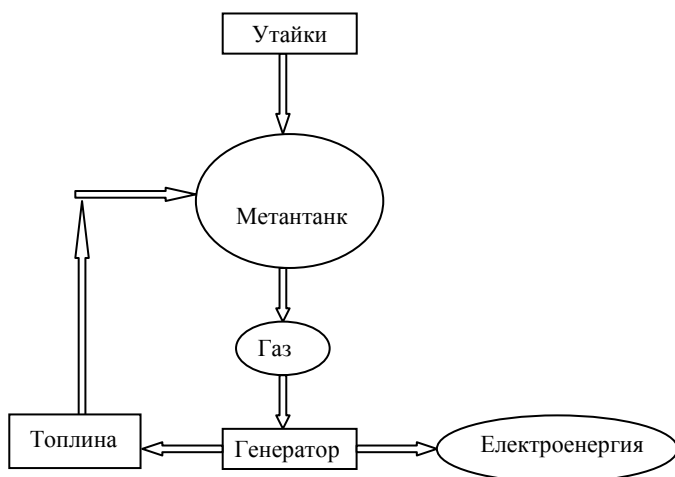
В тази сграда ще са разположени и рециркулиращите помпи към метантанка и топлообменниците. Тук също ще бъде разположен и местният диспечерски пункт за утайково стопанство.

- **Метантанкове – реконструкция**

Най-общо метантанковете представляват съоръжения, в които протича ускорено анаеробно стабилизиране на утайките при изкуствено създадени условия. Използват се предимно при големи и средни като капацитет пречиствателни станции за анаеробно третиране на отпадъчни води с висока концентрация на замърсителите.

Подаваните в метантанка пресни (първична и сгъстена излишна активна) утайки се смесват с изгнилите утайки за „подквасване“, като едновременно с това се подлагат на интензивно разбъркване и подгряване, с което се ускорява процесът. Полученият продукт е биологичен газ (биогаз), съдържащ предимно метан (CH<sub>4</sub>), който се отвежда до газхолдери с цел съхранение. Метанът би могъл да се използва за производство на топла вода, пара и ел. енергия за задоволяване нуждите на пречиствателната станция или за други стопански цели.

На фигура 1 е показана принципната схема за оползотворяването на получения газ.



Фиг.1. Оползотворяване на газ

Като конструкция метантанковете представляват цилиндрични стоманобетонни резервоари с конични дъна и куполни покривни конструкции. Техни основни елементи са: стоманобетонен корпус, помпена станция, посредством която се подават утайките, системи за подгряване и разбъркване, системи за отвеждане на утайковата вода и изгнилите утайки, както и система за отвеждане на получения газ. В повечето случаи, управлението за целия комплекс с автоматизирано.

В зависимост от температурата, при която протича процесът на гниене, метантанковете се разделят на два вида. Първият е т.нар. мезофилен метантанк, в който процесът протича при температури от порядъка на 32-35°C. Вторият вид метантанк е термофилният, при който температурите са от порядъка на 52-55°C.

При мезофилното гниене се постига стабилност на режима и положителен топлинен баланс. Сред основните му предимства са и по лесното обезводняване на изгнилите утайки, както и безпроблемната експлоатация и отсъствието на неприятна миризма и вредно влияние върху обкръжаващата среда.

Термофилното гниене, от своя страна, осигурява приблизително два пъти по-бързо протичане на процеса на стабилизиране на утайките, както и средно два пъти по-малък обем на метантанка, в сравнение с мезофилния режим. Съответно и количеството на отделения газ, за едно и също време на протичане, е по-голямо. Друго основно предимство на

термофилното гниене е постигането на пълна дехелминтизация на утайките и по-висок бактерициден ефект. Установено е, че в термофилни условия се унищожават около 50 до 80 % от яйцата на хелминтите.

Основни недостатъци на термофилния метод са свързани с отрицателния топлинен баланс, което е свързано с допълнително по-трудно обезводняване на изгнилите утайки, както и усложнената експлоатация.

Освен предимствата и недостатъците на процесите, при избора на режим на изгниване е препоръчително да се вземе предвид начина на последваща обработка на утайките, оползотворяването им, както и санитарните изисквания.

Тъй като в ПСОВ-В.Търново има механично обезводняване на утайките чрез лентова филтърпреса, най-удачно е да се избере мезофилен режим на изгниване.

В метантанка се извършва биологично анаеробно стабилизиране на първична и сгъстена излишна активна утайка в четири етапа:

- етап хидролиза – някои съставки на утайката като въглехидрати, мазнини и протеини ще бъдат хидролизирани, което означава, че ще се превърнат в разтворими частици;
- етап ацидификация – частиците се превръщат в органични киселини, алкохоли, алдехиди, CO<sub>2</sub> и H<sub>2</sub>;
- ацетатен етап – продуктите от разлагането на първия етап се превръщат от ацетонови бактерии в оцетна киселина;
- метанов етап – метанови бактерии превръщат преобладаващите оцетна киселина, CO<sub>2</sub> и H<sub>2</sub> в метан и въглероден диоксид;

- **Газхолдер – нов**

Газът, произведен при анаеробната стабилизация ще се съхранява в мембранен газов резервоар (газхолдер) с времепрестой над 5 часа (обем 500 m<sup>3</sup>).

Независимо от вида на съоръжението основно изискване към всички съоръжения за съхранение на биогаз е те да са херметични и да издържат на промени в налягането. В случаите, при които те са разположени на открито, е необходимо да са устойчиви спрямо въздействието на фактори от околната среда като ултравиолетова светлина, различни температури, климатични условия. Преди инсталацията да бъде пусната в експлоатация се препоръчва да се провери херметичността на газхолдерите. С оглед на съображенията за безопасност е добре те да бъдат оборудвани с изпускателни клапани (за подналягане и свръхналягане), за да се предотврати възможността от повреди и осигуряване на безопасността. Също така е необходимо предвиждането на аварийен факел. Изисква се газхолдерите да бъдат защитени от корозионно действие на въглената киселина. За да се предпази от замръзване през дните с отрицателни температури, водата в резервоара се затопля.

- **Факел за газ – нов**

Предвиден е факел за изгаряне на биогаза в случаите, когато газхолдера е пълен до максималното ниво. Управлението на газовия пламък и защитата ще бъдат автоматични, но ще бъде предвиден и ръчен режим на експлоатация. Местонахождението на факела трябва да се съобрази с нормите за безопасно отстояние от сгради и оборудване (Наредба 2 за противопожарните строително-технически норми).

- **Сграда с котелно – нова**

Необходимо е да се изгради допълнително помещение за инсталиране на котел, който ще работи с биогаза през зимата, когато нуждата от топлинна енергия за отопление на сградите (ПС към метантанк, обезводнителна сграда, хлораторна сграда и ПС за активна утайка) е по-голяма. Котелът ще работи заедно с единият ко-генератор. Като резервно гориво котелът ще използва дизелово гориво.

- **Ко-генератори (станция за оползотворяване на биогаза) – нови**

Станцията за оползотворяване на биогаза има за основна цел производството на електроенергия и топлоенергия. Предвиждат се два ко-генератора по 125 kW.

- **Силоз за стабилизирана утайка**

Стабилизираната утайка от метантанковете се подава помпено или под хидростатичен напор в силоза с работен обем 150 m<sup>3</sup>, а оттам към механично обезводняване.

Постъпващата в силоза утайка се прецежда през дъгообразна решетка с механично почистване. Отворите са 4 mm и задържат по-едрите вещества.

Монтираният миксер 120 – GFAU от Sigma не постига посочените параметри за хомогенизиране и ще бъде сменен с нов, който да отговаря на изискванията.

- **Сграда с обезводнителна инсталация**

Стабилизираните активна и първична утайки в метантанка ще се обезводняват на съществуващата лентова филтърпреса. Производителността и  $\square$  600 kg/h, което значи, че за краен етап натоварване ще работи по 10 h на ден. Нормално се постига влажност 78÷82% на кека (обезводнената утайка).

За да може от утайката да се освободи химически свързаната вода, при механичното обезводняване се изисква подготовка на утайките (кондициониране) със специален ограничен полиелектролит (флокулант). Флокулантите се доставят в прахообразен вид и на място се приготвят във вид на рядък разтвор, който се дозира към утайката на вход Лентова филтърпреса (ЛФП).

Крайната влажност на обезводената утайка (кек) се постига чрез регулиране дебита на утайката, дебита и концентрацията на полимера. Към момента филтърпресата работи с концентрация на флокулант – 4 kg/t сухо вещество (СВ).

Отделения от пресата кек чрез транспортна лента се подава в транспортно средство и се извозва до депо. Промивката на платната на пресата става автоматично с пречистена вода от контактните резервоари.

- **Депо за стабилизирана обезводнена утайка – реконструкция на 4 бр. изсушителни полета**

Получените утайки от ПСОВ –В. Търново се депонират на временно депо край с. Ресен. Удачно е за реконструкция да се предложи вариант с преустройство на 4 бр. изсушителни полета като временно депо за стабилизирана обезводнена утайка. Площта от 1000 m<sup>2</sup> е достатъчна за временно складиране на кек при възникнали проблеми с транспорта или основното депо.

- **Изсушителни полета – реконструкция**

Изсушителните полета за утайката по основния проект са 20 бр. Две от тях са отнети за изграждането на силоз, сграда за обезводнителна инсталация и площадка. Две ще бъдат отнети за изграждането на котелно и ко-генератори. Четири ще бъдат реконструирани за временно депо за кек. Оставащите 12 бр. ще се използват като резервни изсушителни полета.

- **ПС за битови води и филтрат – реконструкция**

Предназначението и  $\square$ ю основния проект е да препомпва каловата канализация на ПСОВ до канала пред биобасейна. С включването на филтрата от обезводнителната и сгъстителна инсталации е наложително да се предвидят помпи с достатъчен капацитет.

- **Обезмирисителни инсталации – нови**

Зоните, в които се предполага образуването на миризми и от които трябва да се отвежда въздуха са:

- Сграда решетки;
- Сграда с обезводнителна инсталация;
- ПС при метантанк;

Предвиждат се две обезмирисителни инсталации по 10000 m<sup>3</sup>/h, съответно по 100 m<sup>2</sup> филтрираща повърхност на контейнера при въздушен поток 100 m<sup>3</sup>/h.m<sup>2</sup> и височина на биомасата около 1.2 m.

Биологичните агенти на процеса елиминират молекулите, на които се дължи миризмата, благодарение на специфични метаболитни процеси.

Биофилтърът е съставен от основен вентилационен биофилтърен въздуховод, взривообезопасен вентилатор, въздухоувлажнителна камера и биофилтърен контейнер.

#### **Управление на утайките**

Съгласно Директива 86/278/ЕИО методите и технологиите за третиране на утайки от ПСОВ, следва да отговарят на изискванията за ефективно и ефикасно използване на природните ресурси. Изборът на конкретен модул за управление на утайките трябва да води до минимално отрицателно въздействие върху околната среда и здравето на хората и да дава предимство на употребата им като ресурс.

Понастоящем в света се използват няколко технологии за третиране на утайки, позволяващи да ги преобразуват в полезен ресурс. Такива са:

- анаеробно разграждане с производство на биогаз, което е част от технологичната схема в настоящата изследване за реконструкция на ПСОВ – В. Търново;
- аеробно компостиране;
- директно влагане в почвата за земеделски и рекултивационни цели;
- ко-генерация на биогаз с производство на електро- и топлоенергия;
- смесено изгаряне или моноизгаряне с цел оползотворяване на енергията (само в краен случай утайките от ПСОВ се използват, като източник за производство на енергия чрез изгаряне);

Съществуват и други, разпространени алтернативни методи, каквито са пиролизата, термична стабилизация, газификацията и процесите на окисление. При някои от споменатите методи за третиране, утайките се обеззаразяват, като практически се намалява броя на патогенните микроорганизми и се ограничава процеса на образуване на неприятно мирисещи вещества.

В изпълнение на Директива 2001/77/ЕС за производството на електроенергия от възобновяеми енергийни източници (ВЕИ) съществуват технологични решения за комбинирано производство на биогаз, електро и/или топлоенергия.

Като цяло предпочитените методи за третиране на утайки в страните от Общността са – компостиране, депониране и изгаряне. Следва да се отчете, че за всяка страна има специфични особености, които повлияват за избора на модел за управление на утайките. Например в Холандия процентът на изгаряните утайки е по-висок от тези използвани в земеделието, т.е. генерира повече утайки отколкото би могла да вложи в селското стопанство.

Депонирането на утайки е възможно най-неприемливия начин за тяхното третиране.

#### **Количествена и качествена характеристика на утайките**

На базата на прогнозните водни количества и замърсителни товари е направено примерно оразмеряване на утайковото стопанство към 2033 г. Количествена и качествена характеристика на получените в процеса на пречистване утайки от ПСОВ –В. Търново след реконструкция.

#### **Първична утайка**

Количество първична утайка на вход метантанкове:  
Ефект на пречистване по НВ в ПРУ = 65 %  
Първична утайка по СВ = 3450\*0.230\*0.65=5160 kg/d  
Концентрация = 40÷50 kg/m<sup>3</sup>  
Обем първична утайка вход метантанкове = 130–100 m<sup>3</sup>/d

### Излишна активна утайка

Количеството на излишната активна утайка се влияе от постъпващите органични вещества в биобасейните, степента на пречистване, отстраняването на фосфор с реагенти и др.

#### Количеството излишна утайка на вход метантанкове

- Излишна утайка по СВ = 9100 – 9950 kg/d
- Проектна излишна утайка по СВ = 9500 kg/d
- Концентрация на ИАУ от дъно ВРУ = 7 kg/m<sup>3</sup>
- Обем излишна утайка изход ВРУ = 1360 m<sup>3</sup>/d

#### Утайкоуплътнител за излишната утайка

- Концентрация след УУ = 22 kg/m<sup>3</sup>
- Обем излишна утайка изход УУ = 425 m<sup>3</sup>/d
- Концентрация след механични съгъстители = 50–60 kg/m<sup>3</sup>
- Обем утайка изход съгъстители = 190 - 158 m<sup>3</sup>/d

За оразмеряване на метантанковете е прието да се използват по-неблагоприятните стойности за двата вида сурови утайки:

- Съдържание на органика в ПУ = 68%
- Съдържание на органика в ИАУ = 65%
- Концентрация на ПУ след ПРУ = 4% (130 m<sup>3</sup>)
- Конц. на ИАУ след механично съгъстяване = 5% (190 m<sup>3</sup>)

#### Натоварване на вход метантанкове

Конц. на постъпващите утайки: 14660/320=45.8 kg/m<sup>3</sup>  
 Нови метантанкове - 2 бр.  
 Обем на всеки метантанк - 3000 m<sup>3</sup>  
 Общ изгнвателен обем - 6000 m<sup>3</sup>  
 Препоръчително време за изгнване в обема: T<sub>изгн</sub>=18-24 d;  
 Действителен времепрестой: T<sub>изгн</sub> = 6000/320 = 19 d

В Таблица 1 е показана характеристика на изгнвателния процес при максимално натоварване.

Таблица 1. Характеристика на изгнвателния процес

Параметри при максимално натоварване		
Количество уплътнена първична утайка по СВ	kg/d	5 160.00
СВ – начална концентрация-средна	kg/m <sup>3</sup>	40.00
Обем уплътнена първична утайка	m <sup>3</sup> /d	130.00
Съдържание на органични в-ва в ПУ	%	67.00
Количество органични в-ва в ПУ	kg/d	2 960.00
Количество съгъстена ИАУ по СВ	kg/d	9 500.00
СВ – начална концентрация	kg/m <sup>3</sup>	50.00
Обем съгъстена ИАУ	m <sup>3</sup> /d	190.00
Съдържание на органични в-ва в ИАУ	%	65.00
Количество органични в-ва в ИАУ	kg/d	5 525.00
Общо количество сухо в-во на вход в МТ	kg/d	14 660.00
Общо количество органични в-ва на вход в МТ	kg/d	8 485.00
Степен на разграждане на орг. в-ва в МТ	%	40.00
Разградени органични в-ва	kg/d	3 400.00
Съдържание на СВ в изгнилите утайки	kg/d	9 520.00
Обем изгнила утайка	m <sup>3</sup> /d	320.00
Концентрация на изгнилата утайка	kg/m <sup>3</sup>	34.00
Продукция на биогаз за 1kg входяща орг. материя	l/kg VDS	450.00
Продукция за биогаз изчислителна	m <sup>3</sup> /d	3 820.00

Продукция за биогаз проектна	m <sup>3</sup> /d	3 250.00
Допълнително разграждане в ОИ II-ра степен	%	10.00
Разградени органични в-ва в ОИ II-ра степен	kg/d	500.00
Натоварване на инсталацията за обезводняване на сухо в-во на вход	kg/d	9 000.00
Начална концентрация след ОИ II-ра степен	kg/m <sup>3</sup>	50.00
Обем на обезводняване	m <sup>3</sup> /d	180.00
Концентрация на обезводнена утайка	kg/m <sup>3</sup>	200.00
Обем обезводнена утайка (кек)	m <sup>3</sup> /d	45.00
Обем обезводнена утайка (кек)	m <sup>3</sup> /г	16 400.00

### 3. Заключение

При номинално натоварване на ПСОВ – В. Търново с 114 188 Е.Ж. към 2033 год. средно дневното количество постъпващи за разграждане органични вещества е 8485 kg/d.

Произведената ел. енергия ще покрива част от нуждите на ПСОВ –В. Търново. При работа на газовите двигатели, се рекуперира отделената топлинна енергия от охладителната риза на двигателя и от изгорелите при работата им газове. Произвежда се топла вода, която загрева утайките в тръбни противоточни топлонагреватели. По този начин се покриват нуждите от топлина за подгръването на утайките в метантанковете, а при възможност и на битовите нужди на част от сградите на площадката на ПСОВ.

Биогаза ще се утилизира с два газови ко-генератора. Предвижда се доставка и монтаж на ко-генератори оползотворяващи до 100% от проектния среден добив на биогаз (3250 m<sup>3</sup>/d).

Всеки от тях трябва да има електрически капацитет от 160 kW и топлинен капацитет 190 kW.

Консумацията на биогаз е 65 m<sup>3</sup>/h за един ко-генератор. Те ще работят средно 20-24 h/d.

Топлопленостната мрежа ще е заредена с антифриз или чиста питейна вода.

Разходът на биогаз и производство на ел. енергия ще се отчита. Генераторите ще бъдат свързани към вътрешната мрежа 400V. Работата им е напълно автоматизирана според наличието на газ, нуждата от топлина или аварийни нужди от електроенергия.

Изгнилата утайка от метантанковете преминава в съществуващите открити изгнватели. Тук тя се освобождава от водата получена при гниенето и се уплътнява до 50 kg/m<sup>3</sup> при дъната. Уплътнената утайка се изпомпва от дъното на откритите изгнватели в силос преди обезводняването.

По данни на РИОСВ – В. Търново, няма предприятия в града, формиращи отпадъчни води с високо съдържание на тежки метали и заустващи в градската канализационна мрежа.

В бъдеще при реализация на производства, които генерират отпадъчни води със съдържание на тежки метали или други вредни вещества трябва да се предвидят локални пречиствателни съоръжения, които да пречистват отпадъчните води до необходимите изисквания за заустване в градска канализация, респективно ПСОВ, като строгият контрол и управление и на технологичните процеси ще гарантира и качеството на формираните в ПСОВ –В. Търново утайки.

# ЭКОЛОГИЧЕСКАЯ БЕЗОПАСНОСТЬ ИСТОЧНИКОВ ВОДОСНАБЖЕНИЯ КЫРГЫЗСКОЙ РЕСПУБЛИКИ.

## ENVIRONMENTAL SAFETY OF SOURCES OF WATER SUPPLY OF THE KYRGYZ REPUBLIC

К.т.н., проф. Каримов Т.Х.<sup>1</sup>, доцент Байгазы кызы Н.<sup>2</sup>, преп. Канаев М.Дж.<sup>3</sup>,  
Институт экологии и энергосбережения<sup>1,2,3</sup> – Кыргызский Государственный Университет Строительства, Транспорта и  
Архитектуры им. Н.Исанова, Кыргызская Республика  
E-mail: tashmukhamied@mail.ru<sup>1</sup>, Kanaev-87@mail.ru<sup>3</sup>

**Abstract:** The sources of deterioration of ecological environment in Kyrgyzstan, related with technological wear system of drinking water supply and sewerage, and problems of radiation are highlighted in this article.

**KEYWORDS:** ENVIRONMENTAL SAFETY, WATER RESOURCES, WATER SOURCES, SEWERAGE, WATER PROTECTION ZONE, BACTERIAL CONTAMINATION

В современном мире актуальность экологической безопасности уже давно признана и активно исследуется, а окружающая среда как предмет безопасности стала выделяться в связи с ее повсеместной деградацией. Решение проблемы безопасности является центральной стратегической задачей любого государства.

Специфические природные и климатические особенности Кыргызстана (рис. 1), а так же непродуманная хозяйственная деятельность обусловили возникновение и нарастание экологических проблем. В районах, примыкающих к бывшим и действующим горно-металлургическим предприятиям отмечаются неблагоприятные демографические изменения, выражаемые в росте числа случаев заболеваний и нарушений генофонда, людей связанных с радиацией. Многие экологические проблемы связаны с загрязнением водных ресурсов Кыргызстана.

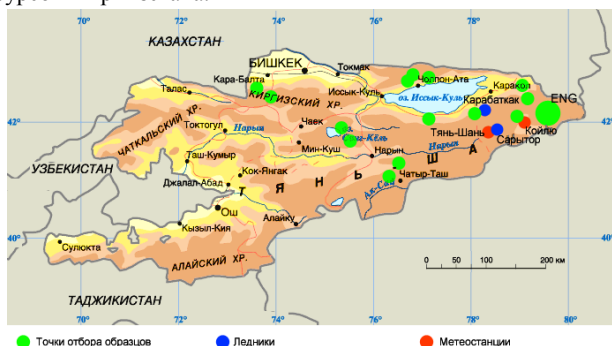


Рис.1 Карта Кыргызской Республики

Хотя большинство водных ресурсов Кыргызстана оцениваются как чистые, в последнее десятилетие наблюдается ухудшение качества воды из-за недостатка или неисправности существующих систем водоотведения и водораспределения, что, в конечном счете, влияет на экологическую безопасность государства.

На большей части территории страны, подавляющая часть малых рек в долинной части практически непригодна для питьевых целей. Большинство малых городов республики не имеют централизованных канализационных систем и очистных сооружений. Фильтрация с полей при орошении за счет растворения удобрений и пестицидов, неорганизованные сбросы с сельскохозяйственных объектов, сбросные воды с полей являются основными источниками загрязнения подземных вод и открытых водных объектов. [1]

В целом по республике из 350 сооружений по очистке сточных вод санитарным требованиям соответствуют лишь 105 (30%), совершенно не выполняют свои функции 140 (40%).

Более половины малых городов и областных центров не располагают централизованными системами водоотведения и станциями водоочистки, например, 35% населения города Кара-Балта, около 30% населения города Джалал-Абад, и только 13% населения в Нарыне. В отдаленных горных селах население употребляет воду для питья прямо из рек, не зная о степени их загрязнения.

Ежегодно в поверхностные водные объекты республики отводится 900-1150 млн. м<sup>3</sup> различных стоков, из них 301-635 млн. м<sup>3</sup> сточных вод проходит биологическую, физико-химическую или механическую очистку. Без очистки в год сбрасывается в открытые водоемы и водотоки 0.42-0.75 млн. м<sup>3</sup> опасно загрязненных сточных вод. Содержание в них вредных веществ в десятки раз превышает установленные нормативы. Наблюдения республиканской санитарно-эпидемиологической станции (СЭС) показали, что 14% проб воды не соответствуют бактериологическим нормам, а 34% - физико-химическим нормам. [4]

Поступление в водные объекты органических загрязнений, нефти и нефтепродуктов, фенолов и других вредных веществ, связано с неэффективной очисткой городских коммунальных стоков, стоков предприятий мясомолочной, пищевой промышленности, кожевенного и сельскохозяйственного производства, автотранспортных предприятий.

Еще одним фактором опасности экологической ситуации является то, что на территории Кыргызстана находится 92 объекта, в которых размещено свыше 250 миллионов м<sup>3</sup> тонн токсичных и радиоактивных отходов. Так как большинство из них расположено в конусах выноса и в поймах рек существует возможность их разрушения, что представляет угрозу окружающей среде. С активизацией в последнее время техногенных катастрофических явлений, оползневых, селевых, эрозионных процессов, угроза загрязнения ими поверхностных и подземных вод многократно возрастает. [4]

Существенным фактором, оказывающим негативное влияние на качество водных ресурсов, является неупорядоченная хозяйственная деятельность в водоохранных зонах и полосах поверхностных водных объектов, а также неудовлетворительное состояние зон санитарной охраны месторождений подземных вод.

В последние годы так же начали проявляться основные показатели регресса, связанные с изменением климата. Вследствие этого происходит рост необеспеченности питьевой водой, разрушение экосистемы и повышается угроза здоровью населения.

Уже сейчас около 70% населения имеет проблемы с доступом к чистой питьевой воде. Самый высокий уровень бактериологического загрязнения водопроводной воды по

республике наблюдается в Джалал-Абадской (28,3%), Чуйской (18,4%), Иссык-Кульской (19,3%) областях, а также в городах Ош (28,2%) и Каракол (33,8%). В Чуйской области наиболее высокий уровень бактериального загрязнения водопроводной воды отмечается в населенных пунктах Аламудунского (33%), Кеминского (20,2%) районов и города Токмок (13,2%) при среднем по республике – 9,8%. [2]

Результаты исследования АРИС, проведенного в 2013 году, показали, что только у 59,9 % сельского населения есть доступ к питьевой воде, так как из 1890 сельских поселений, 725 сел не имеют достаточного доступа к централизованному питьевому водоснабжению (в 267 селах водопроводы построены до 1960 года, в 458 селах - до 1980 года, в 396 селах водопроводы полностью отсутствуют).

Полный охват населения системой водопроводов отмечается только в городе Бишкек (81%), высокий, более 90 % — в Чуйской, Иссык-Кульской, Таласской областях, низкий — в Джалал-Абадской, Ошской, наиболее низкий – в Баткенской, недостаточное количество водопроводов отмечено в городе Ош, и Нарынской области.

Все дело в том, что водоносная инфраструктура, заложенная еще в середине прошлого века, значительно изношена, а в большинстве селений пришла в негодность. Доступ к чистой питьевой воде существенно ограничен в связи, с чем увеличивается число заболеваний среди населения.

Одной из наиболее остро стоящих угроз экологии являются бытовые отходы. Следует отметить, что уборка твердых бытовых отходов в крупных городах (Бишкек и Ош) не отвечает санитарным и экологическим требованиям, нет технологии их промышленной утилизации. Так, на Бишкекском свалочном полигоне (проектная мощность 3,3 млн. м<sup>3</sup>.) в настоящее время складировано 24 млн. м<sup>3</sup>. отходов, что создает риск загрязнения подземных вод, питающих город Бишкек.[3]

В последние годы большинство случаев возникновения заболеваний, связанных с качеством питьевой воды, было зарегистрировано в сельских районах Кыргызской Республики, особенно в Южных регионах страны (Баткенская, Ошская, Джалал-Абадская области) и южной части Иссык-Кульской области (Тон, Джети-Огуз, Ак-Суу).

Среднереспубликанский показатель заболеваемости инфекциями общей кишечной группы держится на стабильно высоком уровне, достигая в отдельные годы показателя от 332,4 на 100 тыс. населения до 490,2. Наиболее высокая заболеваемость зарегистрирована в Баткенской области (980 человек на 100 тыс. населения) и Джалал-Абадской (552,8), превысив показатель страны в целом в 1,8 раза.

Более уязвимыми слоями общества являются дети, пожилые и престарелые, больные люди. Ежегодно по республике официально регистрируется до 40 тысяч случаев заболевших кишечной инфекцией, из них более 80% заболевших это дети до 14 лет. Летальность составляет от 150 до 300 детей до 14 лет жизни. Наибольшая летальность отмечается в областях южного региона (Ошская, Джалал-Абадская, Баткенская), на которые приходится 80-90% всех летальных исходов в республике.[3]

Среди болезней, связанных с качеством питьевой воды, - брюшной тиф, вспышки которого происходят в течение ряда лет в городе Майлуу-Суу и Ноокенском районе Джалал-Абадской области. Это обусловлено, главным образом, недостаточным доступом к безопасной питьевой воде.

Все вышеназванные факторы, т.е. уменьшение природоемкости всех видов деятельности является угрозой экологической безопасности КР. При этом в настоящее время затраты, на охрану окружающей среды не превышают 0,03% от ВВП.

Безусловно, на современном этапе, когда Кыргызская Республика переживает кризисы в экономике и политике, экологическая безопасность может вызывать меньшую озабоченность, однако надо помнить что недостаток внимания к ним приводит к снижению качества среды обитания человека

и создает угрозы здоровью и безопасному развитию населения Кыргызстана, в конечном итоге — это экологическая безопасность государства в будущем.

## Литература

1. Состояние водных ресурсов Кыргызской Республики // Национальный институт стратегических исследований Кыргызской Республики - Бишкек 2014.
2. Ивашенко. Е. Питьевая вода как государственная проблема. Международное информационное агентство. // Фергана-2014.
3. Тайлакова А.А. Гендерный аспект доступа населения Кыргызской Республики к чистой питьевой воде. // Инновации в науке-2015-№9-(46)
4. Глобальная водная солидарность, Улучшение доступа к воде и санитарии посредством децентрализованного сотрудничества в Кыргызской Республике // Глобальная Инициатива ART по водной солидарности ПРООН-2014.

# ОПРЕДЕЛЯНЕ РАЗХОДА НА ГОРИВО ПРИ ИЗМЕНЕНИЕ МОМЕНТА НА ПОДАВАНЕТО НА ГОРИВО

## DETERMINATION OF FUEL CONSUMPTION AT THE TIME OF AMENDMENT FUEL SUPPLY

д-р инж. Иван Георгиев, д-р инж. Евгени Драголов, доц. д-р инж. Стоян Георгиев, доц. д-р инж. Илиан Лилев  
 Национален военен университет „Васил Левски“ – Велико Търново, България  
 Технически Университет - София-колеж- Сливен  
 ivan\_georgiev688@abv.bg, edragolov@yahoo.com, stoyan\_gg@abv.bg, inlilov@nvu.bg

**Abstract:** The paper has done experimental study to determine the impact of time of fuel in the cylinders by changing the angle of the overtaking of the fuel supply of diesel engine.

**Keywords:** DIESEL, FUEL, OUTLAY

### 1. Увод

В зависимост от моментното състояние на структурните параметри и тяхната динамика на изменение във времето, същите оказват различно влияние върху големината на контролируемите диагностични параметри, като разхода на гориво.

За измерване разхода на гориво се използват основно два метода. При единия метод се измерва обема, а при другия – масата на изразходваното гориво.

### 2. Изложение

Същността на метода, свързан с измерване на масовия разход на гориво с помощта на везна и времето на неговото изразходване.

Часовият разход се изчислява по зависимостта:

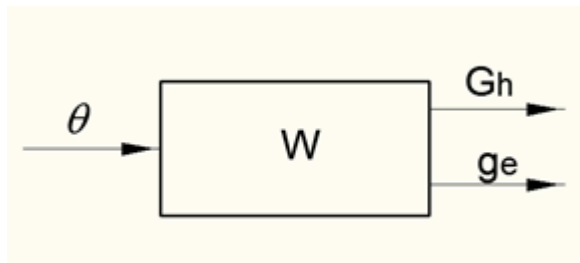
$$(1) \quad G_h = 3,6 \frac{G_{\text{опн}}}{t_{\text{опн}}}, \quad \frac{kg}{h}$$

където:  $G_{\text{опн}}$  е количеството гориво, измерено по време на опита,  $g$

$t_{\text{опн}}$  е продължителността на опита,  $s$

Количеството изразходвано гориво по обемния метод се определя като се измери обема на определена доза гориво и времето, за което то се изразходва.

На фиг. 1 е показан кибернетичен модел за определяне на часовия и специфичен разход на гориво при изменение на ъгъла на изпреварване на подаването на гориво.

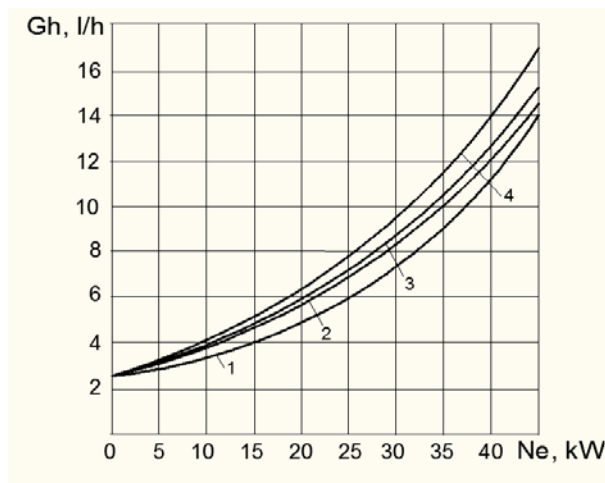


Фиг. 1. Кибернетичен модел

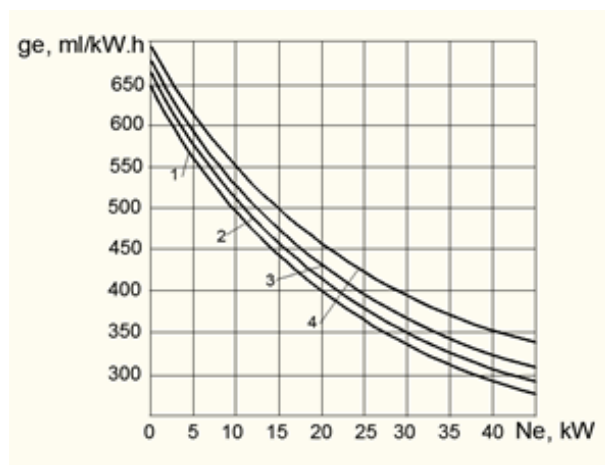
За определяне влиянието на момента на подаване на гориво в цилиндрите са проведени опити, съответстващи както на номиналния ъгъл  $\theta_1 = 23^\circ$ , така и при ъгли  $\theta_2 = 20^\circ$ ,  $\theta_3 = 17^\circ$  и  $\theta_4 = 14^\circ$ .

Получените резултати са показани съответно на фиг. 2 и фиг. 3.

За определяне на разхода на гориво в практиката се използват различни разходомери, които позволяват определянето големината на този параметър по обемния метод. Същите се подразделят на: с променливо налягане (диафрагмени); тахометрически; турбинни – с радиални и тангенциални турбинки; камерни – бутални; зъбни и лопаткови хидродвигатели; топлинни с електрическо нагряване – калориметрични с външно нагряване; ултразвукови и др.



Фиг. 2. Изменение на часовия разход на гориво в зависимост от мощността на двигателя при намаляване на ъгъла на изпреварване на подаването на гориво.  
 1 –  $23^\circ$ , 2 –  $20^\circ$ , 3 –  $17^\circ$ , 4 –  $14^\circ$



Фиг. 3. Изменение на специфичния ефективен разход на гориво в зависимост от мощността на двигателя при намаляване на ъгъла на изпреварване на подаването на гориво.  
 1 –  $23^\circ$ , 2 –  $20^\circ$ , 3 –  $17^\circ$ , 4 –  $14^\circ$

От приведените резултати се вижда, че момента на подаването на гориво оказва значително влияние върху степента на изменение както на часовия, така също и на специфичния ефективен разход на гориво. И в този случай, както и в предходните резултати, чувствително изменение на разхода на гориво се наблюдава след достигане на мощност 20 – 25 kW, като максималното изменение е при номинална мощност.

При номинална мощност и ъгъл на изпреварване на подаването на гориво от 20°, разхода на гориво спрямо номиналния се увеличава с 8%, а при ъгъл 17° и 14° съответно с 14% и 26% - фиг. 2.

Причините за увеличаване разход на гориво при по-малък ъгъл на изпреварване се дължи на факта, че работния процес се пренася в по-голямата си част след горно мъртво положение (ГМП) и се развива при увеличаващ се обем на горивната камера. Горивото се впръсква във въздушна среда, при която налягането и температурата са по-високи, отколкото при оптималния ъгъл.

Периода, свързан с продължителността на задържане на възпламеняването се намалява и се измества по посока на ГМП. Към момента на възпламеняване на горивната смес в цилиндриците постъпва по-малко количество гориво в резултат на по-малкия градиент на нарастване на налягането. Това е свързано от своя страна с намаляване ефективността на горенето, разширяването на газовете е след ГМП, което е и причина за понижаване на скоростта на топлоотделянето при горенето. В резултат на това се намалява ефективността на използване на отделящата се топлина, увеличават се загубите на тази топлина с отработилите газове, а така също се увеличава и тяхната температура (Tr). Протичането на тези процеси са причина за намаляване на индикаторния, механичния и ефективен коефициент на полезно действие (КПД) и като следствие се намаляват мощностните и икономични показатели на двигателя, респективно се увеличава специфичния ефективен разход на гориво, фиг. 3.

### **3. Изводи и заключение**

От получените резултати от изследването се вижда, че момента на подаване на гориво оказва значително влияние върху степента на изменение както на часовия, така и на специфичния ефективен разход на гориво. И в този случай, както и в предварителните изследвания е характерно, че чувствителните изменения на разхода на гориво се наблюдава след достигане на мощност от 20 до 25 kW, като максималното изменение е при максимална мощност.

### **4. Литература**

1.1. Бехчед Б., Т. Деликостов, Д. Бекана, Анализ на факторите, влияещи върху разхода на гориво. Научни трудове, РУ „А. Кънчев“ 2003, том 48, серия 1.1, стр. 137-141.

2. Драголов Е. Д., Повишаване трайността на възстановените детайли от земеделската и автотракторната техника чрез покрития от електролитни железни сплави. Дисертация за получаване на н.с. „доктор“, РУ „А. Кънчев“, 2013 г.



# ОПРЕДЕЛЯНЕ ФУНКЦИОНАЛНАТА ВРЪЗКА МЕЖДУ РАЗХОДА НА ГОРИВО И СЪСТАВА НА ОТРАБОТИЛИТЕ ГАЗОВЕ ПРИ ИЗПРАВЕН ДВИГАТЕЛ

## DETERMINATION FUNCTIONAL LINK BETWEEN FUEL CONSUMPTION AND EXHAUST CONSTITUENTS IN THE UPRIGHT ENGINE

д-р инж. Иван Георгиев, д-р инж. Евгени Драголов, доц. д-р инж. Стоян Георгиев, доц. д-р инж. Илиан Лилев  
Национален военен университет „Васил Левски“ – Велико Търново, България  
Технически Университет - София-колеж- Сливен  
ivan\_georgiev688@abv.bg, edragolov@yahoo.com, stoyan\_gg@abv.bg, inililov@nvu.bg

**Abstract:** The work received dependencies amending hourly fuel consumption and the main components constituting the exhaust gas with upright engine. They serve as a basis for determining the degree of influence of various structural parameters of resourcedefining subsystems on the intensity of climate-controlled forming and their ratio.

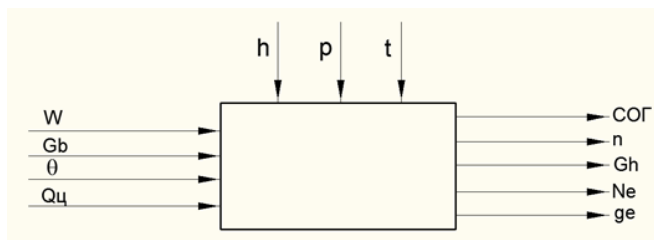
**Keywords:** FUEL, CONSUMPTION, EXHAUST

### 1. Увод

Въз основа на базата данни за мобилните машини, използвани в земеделието и транспорта и след анализ на конструктивните особености на съответните им двигатели, като обект на изследването е избран двигател Perkins PRIMA 65.

### 2. Изложение

На фиг. 1 е показан модела на двигателя като обект на управление.



Фиг. 1. Кибернетичен модел на изследване на техническото състояние на ДВГ

**Входни фактори:**  $W$  – степен на запълване на цилиндрите с прясно работно тяло;

$G_b$  – количество въздух по време на пълненето;

$Q_c$  – циклово количество гориво;

$\theta$  – ъгъл на изпреварване на впръскването на гориво.

**Изходни параметри:**  $COG$  – състав на отработилите газове;

$n$  – честота на въртене на колянния вал;

$G_h$  – часов разход на гориво;

$N_e$  – ефективна мощност на двигателя;

$g_e$  – специфичен ефективен разход на гориво.

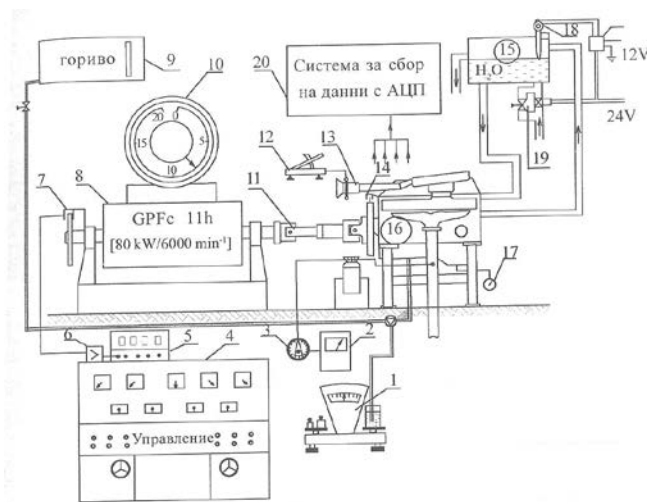
**Смущаващи фактори:**  $h$  – влажност на въздуха;

$p$  – атмосферно налягане;

$t$  – температура на околната среда.

За определяне влиянието на основните структурни параметри на подсистемите, оказващи влияние върху разхода на гориво и състава на отработилите газове (ОГ), предварително бяха проведени изпитвания с наличния двигател за определяне на техническото му състояние и установяване съответствието на основните му параметри с тези, заложи от производителя.

За целта са проведени лабораторни изследвания по схемата на фиг. 2.



Фиг. 2. Схема на стенд за изпитване на двигател Perkins PRIMA 65

Преди пристъпване към изпитване на двигателя за определяне на екологичните му характеристики, са извършени следните проверки и регулировки:

- Топлинната хлабина в газоразпределителния механизъм;

- Снемане на ГНП и изпитване на стенд за установяване на съответствието на основните й параметри;

- Измерване на налягането в края на процеса съгъстяване;

- Смяна на въздушния филтър, маслото и горивния филтър

Натоварването на двигателя се осъществява посредством пендел-генераторна електрическа спиратка с номинални данни 80 kW при 6000 min<sup>-1</sup>. (фиг. 2)

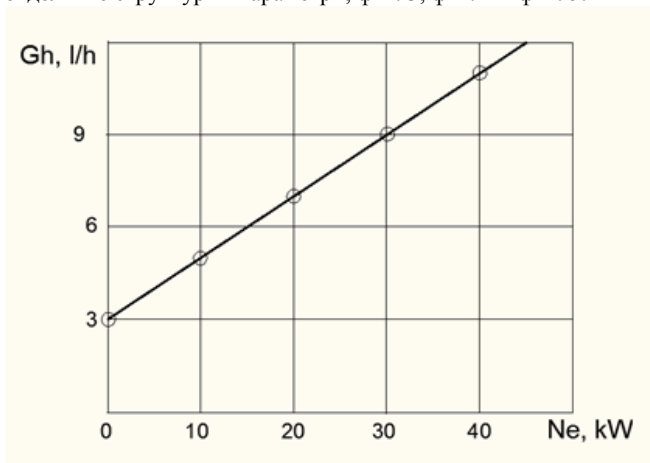
За снемане на характеристиките на двигателя изпитването е проведено при нормален температурен режим, постоянна честота на въртене на колянния вал и степенно изменение на натоварването посредством електрическата спиратка.

С увеличаването на съпротивителния момент (натоварването) на електрическата спиратка, честотата на въртене на колянния вал на двигателя намалява (при двурежимен механичен регулатор на ГНП). За поддържане на постоянна ъглова скорост се използва лоста за управление на ГНП в посока увеличаване на подаването на гориво.

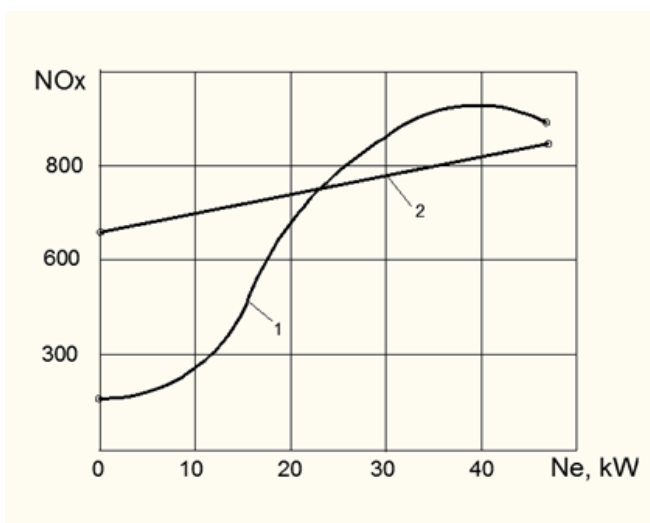
За регистриране на компонентите на състава на отработилите газове е използван многокомпонентен газоанализатор. Той позволява регистрирането на количеството на  $HC$ ,  $CO$ ,  $CO_2$ ,  $NO_x$  и  $\alpha$  в отработилите газове.

Построяването на графичните зависимости за изменение на часовия разход на гориво и състава на отработилите газове във функция от мощността (натоварването) при изправен двигател

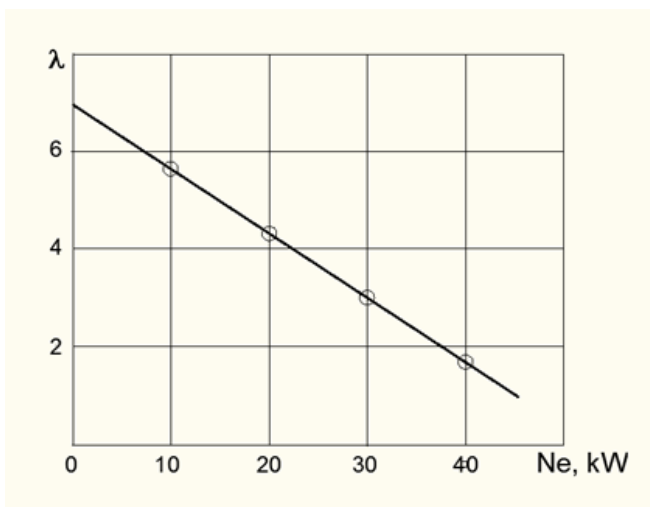
служат като база за определяне степента на влияние на отделните структурни параметри, фиг. 3, фиг. 4 и фиг. 5.



Фиг. 3. Изменение на часовия разход на гориво във функция от натоварването при изправен двигател



Фиг. 4. Изменение на количеството азотни окиси и въглеводороди в отработилите газове във функция от натоварването при изправен двигател  
1 – NOx; 2 – HC



Фиг. 5. Изменение на коефициента на излишък на въздух във функция от натоварването при изправен двигател

### 3. Изводи и заключение

Въз основа на прилагане на контролираните параметри се дава възможност за разработване на рационални алгоритми, свързани с определяне на необходимия брой елементарни проверки и тяхната последователност в процеса на диагностичния контрол.

### 4. Литература

1. Драголов Е. Д., Повишаване трайността на възстановените детайли от земеделската и автотракторната техника чрез покрития от електролитни железни сплави. Дисертация за получаване на н.с. „доктор“, РУ „А. Кънчев“, 2013 г.
2. Енчев Т. Е. „Мониторинг на техническото състояние на ДВГ от земеделската техника.“ Дисертация за получаване на н.с. „доктор“, РУ „А. Кънчев“, 2015 г.

# ПОДОБРЕНИЕ НА АНАЛИТИЧНИЯ МЕТОД ЗА РЕШАВАНЕ НА ТРАНСПОРТНА ЗАДАЧА ПО КРИТЕРИЙ ВРЕМЕ

## SOME IMPROVEMENTS OF ANALYTICAL METHOD FOR SOLVING OF TIME TRANSPORTATION TASK

доц. д-р инж. Лилов И. Н.  
Национален военен университет „Васил Левски“ бул. „България“ №76  
e-mail: inlilov@nvu.bg

**Abstract:** The following paper shows a formulation of time transportation task. Some specifications of function of the aim and method for task solving are presented, particularly in the part of additional procedures.

**Keywords:** FUNCTION OF THE AIM, FUNCTION OF THE CONSTRAINS, NUMBER OF IMPROVEMENT

### 1. Увод

Освен познатата постановка на транспортната и другите разпределителни задачи, при които целта е да се предложи организация на транспорта за минимално реализирани разходи, съществува и друга постановка, при която критерия за определяне на целевата функция е организация на транспорта за минимално възможно време. При така поставената задача, в транспортната таблица 1 вместо единични транспортни разходи  $c_{ij}$  за текущия маршрут в горния десен ъгъл се задава времето за съответния превоз –  $t_{ij}$ , в дименсия, която трябва да е еднаква за всички маршрути. В долния ляв ъгъл се намират неизвестните, които както в другите разпределителни задачи, имат смисъла на количеството ресурс който ще се транспортира по маршрута и се наричат още товар на клетките.

Таблица 1

A \ B	B <sub>1</sub>	B <sub>2</sub>		B <sub>m</sub>	a <sub>i</sub>
A <sub>1</sub>	$x_{11}$	$x_{12}$		$x_{1m}$	a <sub>1</sub>
A <sub>2</sub>	$x_{21}$	$x_{22}$		$x_{2m}$	a <sub>2</sub>
.....					....
A <sub>n</sub>	$x_{n1}$	$x_{n2}$		$x_{nm}$	a <sub>n</sub>
b <sub>j</sub>	b <sub>1</sub>	b <sub>2</sub>	b <sub>j</sub>	b <sub>m</sub>	$\Sigma b$

Така формулирана транспортна задача по критерий време се отличава от класическите разпределителни задачи, което налага уточнение в математическия ѝ модел и метода за решаването му. [1, 2, 4, 5]

**Целта на настоящия доклад е да се уточни целевата функция на задачата по критерий време и да се внесат няколко подобрения в метода за нейното решаване.**

### 2. Ограничителни условия

Ограничителните условия, възможностите за съставяне на първоначален опорен план и условията за балансиране на задачата, запазват познатия си характер:

$$\sum_{i=1}^n X_{ij} = a_i \text{ за } i=1,2,\dots,n \quad \sum_{j=1}^m X_{ij} = b_j \text{ за } j=1,2,\dots,m,$$

$$X_{ij} \geq 0$$

$$X_{ij} = \text{int} . (\text{ако е необходимо})$$

### 3. Целева функция

В таблици 2 и 3 са показани два от възможните опорни плановете на една и съща задача.

Общото време необходимо за осигуряване на транспортната схема за текущ опорен план се определя от пълната клетка с най-голямо време (измежду пълните клетки). Това е така защото транспорта по всички маршрути, посочени от пълните клетки, стартира едновременно. За итерацията в таблица 3.18 времето е 73 часа и се определя от клетка разрешаващата клетка (3,3) с време 73 часа.

Таблица 2

A \ B	B <sub>1</sub>	B <sub>2</sub>	B <sub>3</sub>	B <sub>4</sub>	a <sub>i</sub>
A <sub>1</sub>	20	30	12	32	50
A <sub>2</sub>	3	40	23	6	8
A <sub>3</sub>	43	10	32	73	24
A <sub>4</sub>	8	16	30	30	60
b <sub>j</sub>	20	80	40	30	170

Таблица 3

A \ B	B <sub>1</sub>	B <sub>2</sub>	B <sub>3</sub>	B <sub>4</sub>	a <sub>i</sub>
A <sub>1</sub>	3	5	20	30	50
A <sub>2</sub>	3	20	20	6	8
A <sub>3</sub>	43	20	32	73	24
A <sub>4</sub>	20	40	16	35	60
b <sub>j</sub>	20	80	40	30	170

За същия пример може да бъде съставен и друг опорен план (Таблица 3 по метода на североизточния ъгъл), който определя продължителност на превоза от 32 часа, съгласно клетките (3,2) и (1,4) и предлага организиране на транспортната схема за съществено по-кратко време от този в първия план.

Възможен е и трети вариант посочен в таблица 4.

Таблица 4

A \ B	B <sub>1</sub>	B <sub>2</sub>	B <sub>3</sub>	B <sub>4</sub>	a <sub>i</sub>
A <sub>1</sub>	3 20	5 30	12	32	50
A <sub>2</sub>	3	23	6 40	8	40
A <sub>3</sub>	43	32	73	24 20	20
A <sub>4</sub>	8	16 50	35	64 10	60
b <sub>j</sub>	20	80	40	30	170 170

При него транспорта по всички маршрути ще приключи за 64 часа, определени от клетка (4,4).

Да предположим, че задачата има  $k$  възможни опорни плана. Даден опорен план се задава със символа  $X_l$  ( $l = 1 \div k$ ) и на него отговаря време за приключване на транспорта –  $\max(t_{ij})_{x_l}$  – най-голямото време измежду пълните клетки

съставлящи плана. Оптимален от всички планове е този, за който продължителността на превоза е най-кратка. Тогава целевата функция се задава със следното логическо уравнение

$$Z[h] = \min \left\{ \max_{x_1}(t_{ij_1}), \max_{x_2}(t_{ij_2}), \dots, \max_{x_k}(t_{ij_k}) \right\}$$

$$\text{или } Z[h] = \min \left\{ \max_{x_l}(t_{ij_l}[h]) \right\} \text{ за } l=1,2,\dots,k.$$

Целевата функция в тази задача представлява логическо уравнение, при което:

- първо в  $l$  на брой редици числа се отделят най-големите измежду тях, за да се образува втора редица числа;

- от тази втора редица числа се определя най-малкото.

Това най-малко число от втората редица съответства на план който е оптимален за организация на транспорта за най-кратко време.

Така описана целевата функция на транспортната задача по критерий време е нелинейно уравнение. По тази причина задачата не може да се реши чрез симплекс метода или с помощта на *Microsoft-Excel-Solver*. За решаването ѝ е разработен конкретен метод на контурите, съобразен с нейната нелинейност и съчетава в себе си основни и допълнителни процедури.

#### 4. Метод за решение на транспортна задача по критерий време – основни процедури

Методът за решаване на транспортна задача по критерий време се заключава в последователно подобряване на първоначалния опорен план, чрез построяване на правоъгълни контури при спазване на правила, описани в следните последователни стъпки:[3]

**4.1.** Построява се първоначален опорен план. (За полесното разбиране на процедурите по-долу е решен примерна задача, към която се отправят препратки за онагледяване на отделните стъпки. В нея първоначалния опорен план е построен по метода на северозападния ъгъл и е представен с повдигнатите клетки (1,1), (1,2), (2,3), (2,4) и (3,4);

**4.2.** Определя се **разрешаващата клетка** по критерий „най-голямо време“ от всички пълни клетки от първоначалния план (в примера това е клетка (3,4) и е повдигната с червен цвят). Времето на разрешаващата клетка е и стойността на текущата целева функция;

**4.3.** Във всички празни клетки, с време по-голямо или равно на това на разрешаващата се поставя знак „X“. Тези клетки се наричат **забранени**. (В примерната задача в първата итерация такива клетки липсват, но се появяват при следващите);

**4.4.** Построява се правоъгълен контур с прекъснатата линия и начало разрешаващата клетка. За срещуположния ъгъл на контура се избира друга пълна клетка, наречена **срещуположна** (на примера е повдигната със зелен цвят). При избора на срещуположна клетка се съблюдават следните четири правила:

**4.4.1.** Това е друга пълна клетка;

**4.4.2.** която не трябва да лежи на реда или стълба на разрешаващата;

**4.4.3.** да притежава по-голям или равен товар от този на разрешаващата клетка (Това условие е гъвкаво и може да не се спазва при определена ситуация, описана като допълнителна процедура в 5.2.);

**4.4.4.** Четвъртото условие е в другите два ъгъла на контура да не попада забранена клетка.

**4.5.** Построеният контур обхваща четири клетки. Разрешаващата и срещуположната са в два срещуположни ъгъла на този контур. Участват и две клетки в другите два ъгъла на контура. Клетки, през които линията на контура преминава без да сключва 90° ъгъл, не са негови елементи. На клетките от контура последователно се поставят знаците „-“, „+“, „-“, „+“ като се започва от разрешаващата клетка;

**4.6.** Изчислява се число за подобрене – ЧП. Това е по-малкото число от товарите в разрешаващата и срещуположна клетки. В примерната задача при първата итерация  $ЧП_1 = \min(30,30)=30$ . Във втората –  $ЧП_2 = \min(70,20)=20$ .

**4.7.** Извършва се подобряване на текущия план. За тази цел числото за подобрене се събира или изважда от товарите в ъгловите клетки от контура според това какъв знак има в тях. При тази операция се променят товарите в тези четири клетки. Някой от пълни стават празни, други – обратното. Получава се нов подобрен план на задачата. (При някой ситуации плана може да не се подобри а да остане със същата стойност на целевата функция (но никога по-голяма!). Това са допълнителни процедури описани по-долу);

**4.8.** За така получения нов план се определя новата разрешаваща клетка, която показва как се е променила ЦФ на модела. Последователността по подобряване на плана се повтаря до тогава докато възможността за построяване на контур се изчерпи. Стойността за времето в последната разрешаваща клетка при последното подобряване определя и целта на задачата;

#### 5. Метод за решение – допълнителни процедури

**5.1.** Ако за срещуположна клетка може да се избере повече от една клетка, последователността за решение на задачата трябва да се разклони и да се получат повече от един оптимални планове (в примерната задача това е показано с Вариант 1 и Вариант 2);

**5.2.** Ако възможността за построяване на контур се изчерпи по горе описаните изисквания, но съществува срещуположна клетка с товар по-малък от този на разрешаващата и е възможно да е построи контур с нея без ъглови клетки с знак „x“ да попаднат в него, то опитите за подобрене на плана могат да продължат по този начин. Ако тези срещуположни клетки са повече за построяване на контур се избира тази клетка, която притежава най-голям товар. Ако и те са повече – задачата може да се разклони подобно на гореописаната последователност. При тази итерация (итерации) не се постига подобрене на плана, но се подготвя за евентуално подобрене в следващата итерация.

**5.3.** Ако при някоя от итерациите по подобряване на плана се окаже, че има повече от една разрешаващи клетки, т.е. няколко от пълните клетки притежават равно и най-голямо време за плана, тогава последователно трябва да се извършва подобрене с всяка една от тях. Най-добрият подход в такава ситуация е ако е възможно едната клетка да се избере за разрешаваща, а другата за срещуположна. Така с една итерация могат да се изключат и двете от плана.

5.4. Забраняването на празна клетка с време равно на разрешаващата не винаги е задължително. Ако при някоя от итерациите се окаже, че подобряването на плана не може да продължи, тъй като в обратния диагонал на контура попада клетка с време **равно** на разрешаващата и не е възможно да се намери друга срещуположна клетка с която да се извърши подобрене, то такава клетка (с време равно на това на разрешаващата) не се забранява и се построява контур в който тя участва. При тази итерация не се постига подобрене на плана, но се подготвя за евентуално подобрене в следваща итерация.

5.5. Съществува и друга освен описаната в 5.1. възможност за намиране на повече от един оптимален план след разкриване на най-краткото възможно време за организиране на транспорта. Ако в таблицата от последната итерация съществуват четири клетки, (включително и без разрешаващата да е една от тях) които могат да бъдат свързани в контур и да се извърши преразпределение на товари, то такава операция може да се извърши за намиране на друга възможност за организиране на транспортната схема за същото време.

Характерно за транспортната задача по критерий време е, че не се прави проверка за изроденост на плана, тъй като последователността за решаване не изисква пресмятане на потенциалите на отправните и приемните пунктове.

## 6. Примерна задача.

От три отправни пункта с наличности съответно 100, 50 и 30 относителни единици спасителна техника, необходима за действия при кризи, бедствия, аварии и катастрофи трябва да се организира транспорт за най-кратко време до четири приемателни пункта с нужди съответно 30, 70, 20 и 60 единици техника. Времето в часове за транспорта по всеки един маршрут е посочено в таблицата.

A \ B	B <sub>1</sub>	B <sub>2</sub>	B <sub>3</sub>	B <sub>4</sub>	a <sub>i</sub>
A <sub>1</sub>	3	8	6	5	100
A <sub>2</sub>	2	4	10	12	50
A <sub>3</sub>	6	3	2	4	30
b <sub>j</sub>	30	70	20	60	180

Вариант 1

A <sub>1</sub>	3	8	6	5	100
A <sub>2</sub>	2	4	10	12	50
A <sub>3</sub>	6	3	2	4	30
	30	70	20	60	180

Z1=12 h

A <sub>1</sub>	3	8	6	5	100
A <sub>2</sub>	2	4	10	12	50
A <sub>3</sub>	6	3	2	4	30
	30	70	20	60	180

Z2=10h

A <sub>1</sub>	3	8	6	5	100
A <sub>2</sub>	2	4	10	12	50
A <sub>3</sub>	6	3	2	4	30
	30	70	20	60	180

Z3=8h

A <sub>1</sub>	3	8	6	5	100
A <sub>2</sub>	2	4	10	12	50
A <sub>3</sub>	6	3	2	4	30
	30	70	20	60	180

Z4=8h

A <sub>1</sub>	3	8	6	5	100
A <sub>2</sub>	2	4	10	12	50
A <sub>3</sub>	6	3	2	4	30
	30	70	20	60	180

Z5=6h

Вариант 2

A <sub>1</sub>	3	8	6	5	100
A <sub>2</sub>	2	4	10	12	50
A <sub>3</sub>	6	3	2	4	30
	30	70	20	60	180

Z1=12 h

A <sub>1</sub>	3	8	6	5	100
A <sub>2</sub>	2	4	10	12	50
A <sub>3</sub>	6	3	2	4	30
	30	70	20	60	180

Z2=10h

A <sub>1</sub>	3	8	6	5	100
A <sub>2</sub>	2	4	10	12	50
A <sub>3</sub>	6	3	2	4	30
	30	70	20	60	180

Z3=8h

A <sub>1</sub>	3	8	6	5	100
A <sub>2</sub>	2	4	10	12	50
A <sub>3</sub>	6	3	2	4	30
	30	70	20	60	180

Z4=6h

## **7. Изводи**

7.1. Минималното възможно време за организиране на транспорта е 6 часа;

7.2. Първият пункт на който ще бъде изпълнена заявката е  $V_1$  – 3 часа; след това  $V_2$ - за 4 часа,  $V_4$ - за 5 часа и последен  $V_3$  – за 6 часа

Ако се приложат всички възможни подходи за решаване на задачата (всички възможности за подобряване на опорния план) се получават няколко различни решения (организации на транспорта) с равно минимално време за изпълнение. От всички тях може да се избере това решение, което е най-целесъобразно по други критерии (например транспортни разходи).

## **8. Литература:**

1. „Изследване на операциите”, ДВИ, София, 1975
2. Василев Н., Цанов Л. и др., Приложна математика, „ВИ”, София, 1985.
3. Лилов И., Количествени методи в логистиката, НВУ „Васил Левски”, В. Търново, 2013г.
4. Taha H. Operations research an introduction. Education, Ins, 2003.
5. Winston W. L. Operations research. Applications and algorithms, Duxbury press, 2003.

# INFLUENCE OF URANIUM MINES IN THE FORMATION OF NATURAL BACKGROUND RADIATION

## ВЛИЯНИЕТО НА УРАНОДОБИВНИТЕ МИНИ ПРИ ФОРМИРАНЕТО НА ЕСТЕСТВЕНИЯ РАДИАЦИОНЕН ФОН

Ass. eng. Dolchinkov N. T., Prof., Doctor of chemical sciences, eng. Haralampiev M. S.

National Military University „Vasil Levski“, Veliko Tarnovo, Bulgaria

n\_dolchinkov@abv.bg, mihail43@yahoo.com

**Abstract:** First began to draw uranium in Bulgaria the Germans - in 1938 in Buhovo. In the first year they draw 100 tons of metal. In 1939 they stopped. After the Second World War, uranium mining was renewed in secrecy, but this time by the Soviet-Bulgarian mining company. 48 mines have drawn uranium according to decree № 74 of the Council of Ministers in 1992, the government of Philip Dimitrov takes the decision to liquidate the uranium and another 30 were under investigation and trial operation. It is largely based in southern Bulgaria. Every year the world produces about 42,000 tons of uranium. One third of the yield is in Canada where deposits are 5 million tons. The control in the system of the Ministry of radiation status of the environment which is near former mines extracting uranium, includes field radiometric measurements and laboratory analyzes of soils, waste products in tailing ponds and landfills, sediments, groundwater and surface waters. A network of stations is built for monitoring of soil, groundwater and surface water and air, and produces agricultural products in the areas of uranium mining.

**Keywords** URANIUM MINES, URANIUM, CONTROL MONITORING, BUHOVO, RHODOPES, RADIATION CONTROL, RADIOLOGICAL RISK, LIQUIDATION, RADIONUCLIDES

### 1. Introduction

Many experts believe that the liquidation of uranium mining in the country in which they are finally exhausted, and even then there is extraction of uranium from old dumps. And no country liquidates its uranium production, if it has nuclear power plants. However, Bulgaria closed uranium mining in 1992 and threw over 50 million lev budget and a lot more under the PHARE 1991, was carried out hastily, with the result that in many areas are not realized complete technical solutions for this activity. Experience shows that no country in the world except Bulgaria, doesn't close its uranium deposits program for the eradication of mines and land reclamation.

First began to draw uranium in Bulgaria the Germans - in 1938 in Buhovo. In the first year they draw 100 tons of metal. In 1939 they stopped. After the Second World War, uranium mining was renewed in secrecy, but this time by the Soviet-Bulgarian mining company. It existed until 1956, when as a cap uranium grouping is formed "Rare Metals", which is referred to as a "state within a state." It had 13 000 people-workers. It controlled the geological measures, mining, processing and export of the obtained uranium concentrate. Under his hat were the others: "Buhovo", "Trakia" - Plovdiv and "Rise" - Smolyan.

48 mines have drawn uranium according to decree № 74 of the Council of Ministers in 1992, the government of Philip Dimitrov takes the decision to liquidate the uranium and another 30 were under investigation and trial operation. It is largely based in southern Bulgaria. The most famous are Eleshnitsa Sborishte, White Water, Dolna Banya. Near Buhovo are made mining developments, near Sofia there is uranium in Seslavtsi and Kremikovtzi ....

In the Rhodope mountain the areas are four: near Eleshnitsa / 15 km away from Bansko /, Dospat, Smolyan, Velinograd. In Thracian Valley - Stryama, Rakovski and around Plovdiv, Yambol Municipality. There is uranium in Montana, Simitli, Sliven and Stara Zagora, Burgas, Veliko Tarnovo, Gabrovo, Lovech and Pleven, Targovishte, Shumen, Ruse, Razgrad, Silistra, Dobrich and Varna. In 1974 the output reached 400 tons per year. Before the decision to liquidate the industry in 1992, uranium mining reached 645 tons per year. Throughout the time till 1989 the yield is secret, while production is strategic. Export is entirely to the Soviet Union.

The Bulgarian product is named "triuranievosmookis" (or oxide-zakis). The classical technology of digging uranium ore is on loss. This is an expensive process, but that is because of the

strategic production. The other scheme is geotechnological. It is clean and very cheap. Tailings have only two plants for processing uranium ore - "Eleshnitsa" and "Buhovo." Now technology enables the extraction of uranium from much poorer ores and tailings piles in both can still be extracted uranium. Yellow cake - commercial product uranium from 30% to 60% is obtained after processing at the plant in Eleshnitsa, and in Buhovo was firing extra and was received a concentrate containing uranium about 80%. From there it is transported in containers to the Soviet Union, where nuclear fuel was produced and was sent back to our Kozloduy NPP.

Every year the world produces about 42,000 tons of uranium. One third of the yield is in Canada where deposits are 5 million tons. The richest deposits of uranium are in Australia and in the top ten are still Kazakhstan which declared its intentions by 2012 to become the largest producer of uranium, and South Africa. In Bulgaria uranium reserves are estimated at 20,000 tons. From them suitable for exploitation by geotechnological method are 12,000 tons and in practice can be extracted 6500 tons. However, they could secure our nuclear power for at least 20 years. Geotechnology is applicable for deposits in Plovdiv, Yambol, and the valley of Struma. Experts in the industry believe that Bulgaria is fully capable of pulling 300 tonnes of uranium per year. Only a small mine with no more than 100 people staff gave 600 thousand dollars a year profit at all deductions for taxes, transport, food, prevention of the workers export and further processing of the metal to the commercial product.

Until 1992 most of the minimum prices on the London stock exchange. The threeuranium eightoxide costed \$ 42 per kilogram. In regular supply the price jumped nearly doubled - to \$ 70 per kilogram. Now the price is about \$ 140 per kilo, which would bring 42 million dollars annual profit of Bulgaria in the resumption of uranium. However, the trend is the product to reach a price of 200 dollars per kilogram. That's what dictates the interest of Canadian and Russian producers to the revival of uranium mining in Bulgaria. The control in the system of the Ministry of radiation status of the environment which is near former mines extracting uranium, includes field radiometric measurements and laboratory analyzes of soils, waste products in tailing ponds and landfills, sediments, groundwater and surface waters. Radiological parameters of soil, bottom sediments and waste materials are evaluated by analysis of samples from the network of the EEA for the control of potential pollutants. Water samples are analyzed radiochemically regarding to the targets set out in BS 2823 "Drinking water" - total beta radioactivity, uranium and radium.

## 2. Materials for Production of Prototype Parts

With the entry into Decree №74/27.03.1998 on eliminating the consequences of the extraction and processing of uranium ores is assigned to the "Ecoengineering -RM" Ltd. to organize and supervise technical liquidation activities, technical and biological reclamation of scrubbing results and conduct a comprehensive departmental monitoring of environmental components. Despite the existence of a legal basis, not all sites are built and operated monitoring networks as approved by the Chairman of the Energy Committee "Instruction on organization of monitoring system design, construction and operation of networks for environmental monitoring in the affected by uranium industry development ". The liquidation of every mine begins with closing the shafts and horizontal galleries. Blocking the entrances with concrete walls, parallel overhead bunkers and destroying buildings and then taking technical and biological reclamation of affected lands.

In the Phare project "Comprehensive Program for cleaning and monitoring areas affected by mining and processing of uranium in Buhovo" in March 1999 is built a local system for basic environmental monitoring in the area of Buhovo - Yana (LSBM). The system consists : two monitoring container located in Buhovo and in Yana, two reception centers - in "Rare Metals" Ltd Buhovo and EEA - MoEW and information board for continuous public information installed on the cultural center in Buhovo . The LBMS is intended to carry out continuous monitoring of indicators of environmental rehabilitation activities before, during and long after the completion of restoration works in the area. Monitoring containers are equipped with measure instruments for continuous monitoring of total dust, radiological parameters power of gamma radiation dose, concentration of radon in ground-air meteorological parameters: direction and wind speed, temperature and humidity on the ground air, atmospheric pressure and precipitation.

A network of stations is built for monitoring of soil, groundwater and surface water and air, and produces agricultural products in the areas of uranium mining. Measurements show that there is no risk for people, animals and plant life, because values for heavy and toxic elements and radionuclides are below the limit concentrations. In 2001, after the closure of sites for uranium, in reference to the "NRA" Sofia were carried out radiation measurements for researching the radiation status of this region. The results of the measurements of background radiation are given in Table 1. In Table 2. are given the specific activity of soil samples from the surface layer 0 -10 cm, from places which are expected to have a lot of dirt.

Measuring points	Coordinates altitude	Background radiation * Sv / h
1. Levels near "The breeding-pond"	N42 18 10.3 E24 54 39.5 204.0 m	0,23 - 0,28
2. Levels near the canal	N42 18 20.9 E24 54 08.2 204.2 m	0,18 - 0,20
3. Uranium mining site	N42 18 22.4 E24 53 55.1 183.7 m	0,24 - 0,31
4. Stock tubes "Rare metals"	N42 18 36.2 E24 53 44.3 182.1 m	0,22 - 0,23
5. Road to Padarsko village	N42 19 11.9 E24 53 36.4 219.1 m	0,21 - 0,22
6. Village	N42 18 34.3 E24	0,20 - 0,22

cemetery	53 32.6184.5 m	
7. "Cemetery" of "Rare metals"	N42 17 59.1 E24 53 01.6179.4 m	0,23 - 0,24

Table 1. Results of measures of natural background radiation in the vicinity of Momino village.

Place of samplers	U-238 [Bq/kg]	Th-232 [Bq/kg]
Momino village	90	67
"The cemetery"	72	83
"The breeding-pond"	37	44
To uranium mining site		
Rakovski city	73	68
Parvomay city	73	70

Table 2. Contents of radionuclides in soil samples, Momino village

The area, which has conducted uranium mining activities in the Rhodopes, starts not far from Asenovgrad and extends to the southern border. He is known as the center of tourism and recreation activities. Ongoing for decades uranium questioned the radiological purity, despite the talks of the liquidation events.

Receipt of uranium ore in these areas is done by digging pits / gallery /. For the transportation of ore are built roads and Mine excavated mass without industrial uranium forms a "mound" near the adit, which gradually overgrows. Open pits are walled, buried with earth and they are indistinguishable, but some of them are broken partitions. Given the radiological significance of the problem, the first studies were carried out in the upper stream of the Arda River in 1996 with a project funded by the MEST. Figure 1. shows the area of research and the points of samplers. Periodically conducted measurements showed that the level of background radiation does not exceed 0,28 Sv / h, v area. The content of radionuclides in the soil and water samples turned out to be within the average for the country [2].

The only point in which it was found to increase the background radiation (0,40 Sv / h) v audits area but close to dysfunctional ramp for loading the uranium ore. This provokes taking radiation measurements in uranium indoor areas, which was funded in three consecutive years of NRA Sofia [3, 5, 6]. Object of research were three divisions - Gerzovica and Kiselchovo, Smolyan, Narechenski ore yield area, Belocherkovski rid, Plovdiv.





Fig. 1. Location of sampling from the closed uranium mines.

On figure 1. are reflected the points where samplers were made. These are the places that were open to the adit of closed mines and there is expected aggravated radiation situation. After inspection by the responsible institutions they have identified the following deficiencies in the former uranium mines, which must be removed with funding from PMS №№ 3 / 15.01.2014g. For allocating the funds on programs for technical liquidation and conservation of objects from the mining sector for 2014.

MDP "Eleshnitsa" factory "Star" - Eleshnitsa village. Potential danger is the collector channel under the plant tailings and wastes dumping mining workings that are not reclaimed.

2.Object "Sunrise" (Dospat) - Barutin village. It is necessary to stop farming in the "Potato levels" until the completion of the reclamation activities. The measured specific activities of the uranium-238, radium-226, lead-210 and thorium-230 in the arable soil are in excess of 2 to 45 times the natural background levels for these radionuclides in the area of Barutin village. The waters of river Barutinska in the area are mainly contaminated by mine waste water. It is necessary to indicate the pitch and inform the population that the waters of self-discharge of shaft 3 and the river Barutinska are with increased content of natural radionuclides.

3.Object "Balkan" - Tserovo village.

Adit №№ 1 and 2 are left open, as the dumps are not reclaimed. Potential danger of radiation contamination is the embankment of Adit 1.

4.Object "Gabra" - Gabra village. Unfinished reclamation of embankment of Adit 2.

5.Object "Iskra" - Katina village. Reclamation is not complete and has not resolved the issue of treatment of mine water.

6.Object "Georesurs" - y-s "Brezhani" "Haying," "Igralishte." Mining waters from Adit 2 in "Brezhani" and gallery in "Igralishte" are available for animals to drink. The sorption column is not removed in "Haying" and the issue with the leaking contaminated water is not resolved. Due to erosion processes rock material from the dumps was pulled down in the valleys. It is necessary to prevent its further movement.

7.Object "White Water" - Ochusha village. After the commissioning of the treatment plant for purification of mine water a comprehensive assessment must be made of the radiation contamination along the river Ochushnitsa.

8.Object "Geostroycomplex" - Seslavtsi village. Particularly serious is the problem with mining water expire - channel under sorption "Chora" Adit 93, which is very near to the village Kremikovtzi, channel after tailings plant "Metallurg" and gallery 123.

The results and their comparison with the normative Documents warrant some general assessments and conclusions.

a / in settlements located near the surveyed former uranium mining areas and adjoining farmland concentration of natural

radionuclides in soil and the level of background radiation is not changed.

b / after the liquidation of the mining mines, access to some of them is not sufficiently restricted.

c / in places where radiation background was repeatedly increased in comparison with the natural, the access should be limited for the population, despite the slight radiation risk.

d / in loading ramp "Gerzovica" the liquidation procedures should be completed and the sould should be deactivated in restricted area station. Around the embankment of uranium ore "Revie fields" - Dobralak village a concrete wall should be built, precluding spillage or inappropriate use of the ore mass.

The results of the research are available for the relevant municipalities so the local community can be informed and the manifestations are limited of radiophobia or credulity on the side of people in those areas. Moreover, evaluations, more broadly, will help to conduct an adequate economic policy in the surveyed regions.

Even to resume uranium production in Bulgaria, now it would be very expensive and would require huge investments. All mines have been sealed for a long time. We'll have a new drilling at great depths, which is very expensive.

Of course, on the other side of the scales will stand usefulness of any resumption of uranium - thousands of new jobs, new technologies, fuel for both our nuclear power plants. But in this situation it will also need to build a new plant for processing uranium, which also means new risk of new contamination at still unliquidated old. But potential investors - canadians or russians in need of huge investments will probably want all the profits for themselves. Which will not be profitable for Bulgaria, unless Bulgaria does not produce bulgarian technologists and technical equipment, workers - specialists in uranium yield, that is how it will enter the era of technology and will save a lot of taxpayer money.

### 3. Conclusions:

1. Government documents have been accepted to solve the problems of the consequences of priority liquidated uranium mines and uranium processing;
2. Some uranium mines and uranium processing are built without monitoring networks for radiation control and do not conduct departmental monitoring;
3. Compromised are already committed liquidation and reclamation works, due to the poor quality of their design and / or implementation and insufficient maintenance of already built facilities;
4. Radiological risk exists due to unresolved issues with management and complex purification of contaminated with radionuclides natural water flowing from the mining sites.

### 4. Literature:

1. A. Antonov, G. Belev, V. Zhuchko and others., Precision semiconductor spectrometer in nuclear physics laboratory "Microtron accelerator" at PU "P. Hilendarski" BgNS. Transactions of Item 2 pcs. 1 July 1997.
2. The yearer of the state of the environment in Republic of Bulgaria 1992, Ministry of environment and water, Sofia, 1993.
3. Studying the radiation status of sites related to uranium mining in Plovdiv and Smolyan regions, Report of Contract №518 / 2002 NRA Sofia.
4. Examination of the natural and technogenic radiation status of regions along the river Gorna Arda, the report is titled F-633/1996, fund "Research", MONT.
5. Setting the radiation status over the areas related by uranium yield in the region of Narechenski ore, report on the topic №552 / 2003 NRA Sofia.

6. Conduction of radiation monitoring of sites related to uranium mining near Belocherkovski hill, Statement of contract № 588/2004, NRA Sofia.

7. Ordinance for basic standards for radiation protection BSRP-2004, SG. 73, 2004.

8. PMS № № 3 / 15.01.2014g. For allocation of funds for programs under technical liquidation and conservation of objects from the mining sector for 2014.

# RADIATION EFFECT ON HUMAN AND LIVING NATURE

## ВЛИЯНИЕ НА РАДИАЦИЯТА ВЪРХУ ЧОВЕКА И ЖИВАТА ПРИРОДА

Ass. eng. Dolchinkov N. T., Karaivanova-Dolchinkova B. E.

National Military University „Vasil Levski“, Veliko Tarnovo, Bulgaria

n\_dolchinkov@abv.bg, bonka\_vt@abv.bg

**Abstract:** *Radioactive and biochemical researches prove that after big reactor breakdowns nuclear explosions pastures and vegetation get polluted with radioactive iodine 131. High level of radioactive contamination has been established lucerne and other grasses, which required the prohibition of feeding farm animals with green fodder from the first slope. Milk is the most affected by the radioactive contamination of food of animal origin. Caught up in the human body radionuclides distributed in various organs, tissues and systems, they have complex kinetics, which depends on the nature of the metabolic processes. The distribution in the body depends on the manner of introduction of the radionuclide.*

**Keywords:** RADIOACTIVE ELEMENTS, HUMAN, RADIATION EFFECT , RADIONUCLIDE, FOOD PRODUCT, ISOTOPES

### 1. Introduction

Cosmic rays that reach the Earth's surface can create radioisotopes decay but compared to other naturally occurring radionuclides is extremely low and not particularly important.

With the importance of biological standpoint are thus formed in the atmosphere of carbon-14 and tritium. Carbon-14 is formed by irradiation with neutrons, nitrogen-14, and the three - of hydrogen. Radio hydrocarbon included in the organic world, follows the path of stable isotope and it helps to learn a number of processes, such as photosynthesis, decomposition of organic matter, determine the age of organic formations and others. It passes in the coal, oil, etc., and also in the inorganic carbon compounds (carbonates) and others. Tritiated also be mixed with hydrogen into the water, and other organic compounds, which enter as a component and is involved in the circulation of the substances, but its half-life is much shorter. Much of tritium and carbon-14 accumulates in ocean waters.

It is believed that the content of radioactive elements is the result of nuclear reactions in the atmosphere and in recent years 1000 constantly present in it. Naturally there is no question of radionuclides as a result of the testing of nuclear weapons and other human activity, but natural cosmogeneous radionuclides. Interest is established depending on the content of radionuclides in the atmosphere not only by the altitude but also the latitude of the globe. It was found that with the distance from the equator to the north intensity of cosmic radiation is uvelichava. Tova binds to the influence of magnetic fields on the planet.

Soil is the main source of radioactive pollution got into the biosphere through the atmosphere and in other ways. It is proved that the air radioactive pollution of plants has main significance the first days and weeks after the radioactive blast even more when plans are in the status of active vegetation. Later on when the atmosphere gets partially or fully cleansed from the radioactive particles, soil becomes the main provider of pollution to vegetation and therefore to people and animals. This phenomenon has been constituted after the period of intense testing of nuclear weapons in air in the beginning of 60's and after the stop of the tests according to Moscow contract of 1963. Polluted water continues to nourish plants with radioactive particles in those areas. This happens as result of the radioactive particles and compounds being included in the biological components of the lithosphere and soil.

### 2. Materials for Production of Prototype Parts

Radioactive and biochemical researches prove that after big reactor breakdowns nuclear explosions pastures and vegetation get polluted with radioactive iodine 131. The most polluted this this isotope milk cannot be drunk after that. In those occasions, milking animals must immediately be removed from pastures and fed only

with provender from the warehouses. As in similar occasions, milk is the most affected product by radioactive pollution.

From all kinds of meat the one with highest levels of radioactive pollution is mutton. In other eatables from vegetarian and animal origin – tomatoes, pepper, cucumbers, potatoes, carrots, cabbage, beans, apples, pears, watermelons, mushrooms, cans, sausages, baby foods, etc...have been detected lower levels of radioactive pollution. This has served as reason to the Committee on the Peaceful Uses of Atomic Energy to state that main part of foods used within population doesn't seem to be radioactive and to suppose risk to health is as its lower levels. Highest levels of pollution within researched plants have been detected with leaf vegetables – salads, lettuce, green onion, parsley.

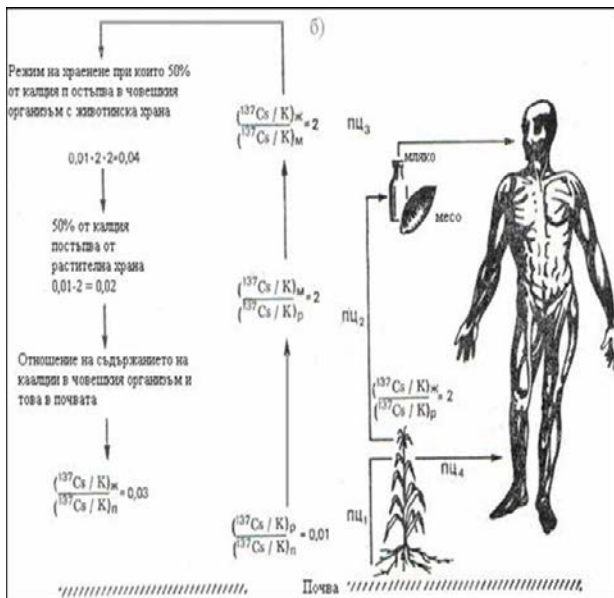
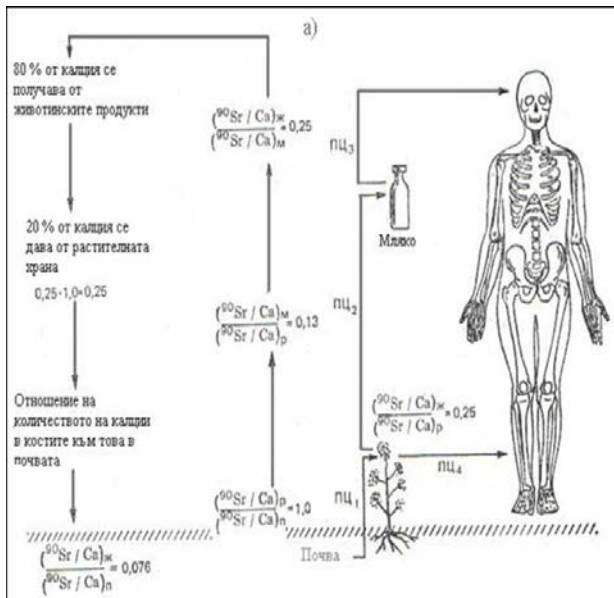
High level of radioactive contamination has been established lucerne and other grasses, which required the prohibition of feeding farm animals with green fodder from the first slope. In straw cereals is measured several times higher activity than in the classes. In the measured activity was significant participation of radio-caesium.

Radioactive contamination of plants and plant products is associated mainly with air route of administration of radionuclides and their attachment on the soil and plant organs and a further shift in the chain - food for animals and humans. Milk is the most affected by the radioactive contamination of food of animal origin.

In some cases, it can be applied and biological decontamination of radioactively contaminated areas, ie extraction of radionuclides with plants that can accumulate and neutralize them.

Picture of the path of radioactive pollution in the human food chain gives us Fig.1. It appears that up to 80% of the calcium in the human body is obtained from foods of animal origin (Figure 1), but the most radioactive element strontium -90 (Sr90), is obtained in the radioactive contamination of the soil. The ratio of calcium and strontium in the bones of a person is equal to that of the elements in the soil.

From the figure it is clear that in terms of Sr-90 the most dangerous radioactive pollution is in the milk (a). The products of plant and animal origin have equal contribution to the pollution of the human body with Cs-137 (fig.1b). The ratio of Sr-90 / Ca is equal in the tissues of plants and soil. The organisms of animals use more quickly calcium than strontium, and this ratio is less than one. At the same time it should be noted that the contribution of Cs-137 in the food chain is extremely diverse. On one hand, plants extract more potassium from the soil than cesium, at the same time in animals the accumulation of cesium is more intense than calcium, and the ratio between their concentrations is above unity.



**Fig.1.** Passage of Sr-90 and Cs-137 in the human food chain, the most sensitive to pollution with these radioactive elements (in Langkam, 1965).

The internal exposure of the human body is due to the radionuclides that have fallen into the (incorporated). Incorporation may be done in several ways, in which purposes of radioecology rights are the most important two:

- oral ingestion of food or water (oral incorporation);
- inhalation of radioactive gases and aerosols (inhalation incorporation). Caught up in the human body radionuclides distributed in various organs, tissues and systems, they have complex kinetics, which depends on the nature of the metabolic processes. Some radionuclides have selective uptake, such as iodine in the thyroid gland, radium and strontium – in bones ; others distributed more evenly, such as cesium and potassium muscle tissue, etc.

At some point, the body has a certain activity  $A$  [Bq], which is distributed on the body mass  $m$  [kg], determined with specific activity [Bq / kg]. But  $C$  varies with time not only in body as a whole, but in different organs and tissues. This is due to the fact that the radionuclide is allocated in the body (especially in initial stages after arrival), but even is considered as a whole,  $C$  is changing because that given radionuclide decays with a physical half-life  $T_f$ , but is also appears in the body to the strong of it is a chemical element that is involved in metabolic processes. That departure is a purely biological process and is characterized by the so-called biological half-life  $T_b$ .

The distribution in the body depends on the manner of introduction of the radionuclide. For example, after ingestion of plutonium-239 in the body is held only about 0,003%, whereas after inhalation retained part is 25%. It is seen and the complex distribution in various organs of the body. These organs, in which he goes and accumulates respective radionuclide are called critical organs.

Radioactive isotopes of any chemical element, which falls in the body are involved in the exchange of substances in the same way as the stable isotopes of an element. Biological activity of radioactive isotopes is determined by the parameters of ionizing radiation which they emit.

The radiotoxicity is called the property of radionuclides that cause various degrees pathological changes in their entry into the human body. Pure radiotoxicity cannot be separated from the chemical toxicity of a chemical element and compound and a typical example of this is uranium, which belongs to the so-called heavy metals.

Toxic effects of radionuclides caught up in the human body is determined by:

- solubility and absorption of the compounds in which they are found;
- The way of incorporation;
- character of the allocation in organs and tissues;
- speeds of input and output of the body
- Physical characteristics of emitted ionizing radiation: type of radiation, energy, etc.;
- Age of the person, in which has fallen the radionuclide and other individual characteristics.

As a result of human exposure with large doses of some symptoms showing changes in normal physiology, may occur within days, hours or minutes. On the other hand, the body can react to irradiation of clinical events after years or decades. In this connection, radiation-induced effects in humans are divided into:

- Early somatic effects, with periods of manifestation from minutes to days. They are called acute and comprise a very wide range of phenomena, starting from the radiation erythema and lead to death of the organism. Somatic name comes from the Greek word soma, which means body.
- Late somatic or somatic-stochastic, with development period of years and decades. These include radiation the induced malignancies (commonly referred to as cancer).
- Inherited or genetic effects that occur in the progeny of exposed individuals: children, grandchildren, great-grandchildren, etc. In human radiobiology or otherwise, radiation in medicine, principally define two types of effects due to the effects of ionizing radiation on humans that medicine defined as diseases:
- deterministic effects, as all of them are somatic and are characterized by a threshold of radiation impact (threshold dose of radiation), under which these effects were not observed, and above this threshold the severity (level) of the clinical expression of the effect depends on the dose;
- stochastic effects, ie somatic (cancer) or hereditary (genetic) effects that occur in the irradiated person years after exposure or in subsequent generations. These effects (diseases) have a probability (stochastic) nature; for them it is assumed that there is no threshold on the radiation dose and the their gravity is independent of dose. Stochastic effects are not specific in nature, they can not be distinguished from other similar effects induced by other factors of non-radiation nature.

This principally separation of radiationthe induced effects in humans is a result of multi-year study of the effects of ionizing radiation on both human and experimental animals (mainly mammals), starting from the molecular level through to level body as a whole and population level. On the other hand, a number of problems, both theoretical and practical, has a number of unclear incomplete data on specific patterns on the formation and progress of the corresponding radiation-induced effect.

### ***3. Conclusions:***

1. Radioactive contamination of plants and plant products is associated mainly with air route of administration of radionuclides and their attachment on the soil and plant organs and a further shift in the chain - food for animals and humans .;
2. Milk is most affected by radioactive pollution food product of animal origin and flesh at high overlay of radioisotopes was observed in sheepmeat;
3. The highest contamination of vegetation is found in leafy vegetables - spinach, salads, lettuce, green onions, parsley, etc .;
4. The most widespread isotopes that have an impact on the human body are I-131, Sr-90 and Cs-137.

### ***4. Literature:***

1. Vasilev D., Radioecology, Titus Consult, Sofia 2005.
2. Marinov V. Agricultural radioecology Zemizdat, Sofia, 1989.
3. Ordinance on basic safety standards, BSRP-2004, SG. 73, 2004.
4. Yarmonenko S., Radiobiology per person and Animals, Vysshaya School, Moscow, 1988.
5. Nechev Hr., Salovski P. Protection against radiation hazard, Medicine and Sports, Sofia, 1987.

# ПРОГНОЗИРАНЕ СКОРОСТТА НА ДВИЖЕНИЕ ПО МАРШРУТ И ВРЕМЕТО ЗА ПРИСТИГАНЕ ПО УЧАСТЪЦИ

Eng. Pavel Stoyanov

Faculty of Transport, Department of Transport – University of Ruse, Bulgaria

E-mail: pstoyanov@uni-ruse.bg

**Abstract:** Prediction of bus speed on an urban route: A new method to inform the passengers for the time of arrive of buses from urban transport is the modern system for information. It is necessary to predict the bus speed between two points, including any delay at stops, to get this information. This article presents some models to investigate the running bus speed. They include different parameters of the traffic conditions therefore they are with different degrees of complexity.

**Keywords:** running speed, exponential speed model, commercial bus speed, traveler information systems, advanced public transportation systems, arrival time estimation methods

## 1. Въведение

В съвременните условия на работа на градският транспорт и особено при използване на системи за информация на пътниците за времето на пристигане на автобусите по спирките, се налага да се прогнозира скоростта им на движение между определени точки от маршрута или по целия маршрут, като се отчитат условията за движение по него. влияние върху средната скорост на движение на транспортни средства в градски условия оказват редица фактори (задръжки по кръстовищата, брой на спиранията, брой на лентите за движение, интензивност на движението, типов състав на транспортния поток и други), които могат да бъдат отчетени и чрез подходящ модел да се прогнозира скоростта на движение за всяка точка от маршрута. Редица изследователи предлагат модели за предсказване на скоростта на движение, в които се отчитат по-малко или повече фактори [1,3,4], оказващи влияние върху скоростта на движение на отделното транспортно средство по маршрут.

При макромоделите скоростта на движение е функция на някакъв по обобщаващ фактор и служат за оценка качеството и ефективността на пътническите превози [2].

При микромоделите се използват фактори за по-детайлно описание на режима на движение и се използват за оперативно управление на движението на транспортните средства по маршрут [3,4]. Тази група модели се прилага в системите за информация на пътниците (в транспортното средство и на спирките), за проектантски транспортни средства цели по избора и оценка на режима на движение по маршрута, разхода на гориво и замърсяването на околната среда, за оценка решенията от проекти по организация на движението на транспортните потоци по метода “преди и след”.

## 2. Изложение

### 2.1. Методи за прогнозиране скоростта на движение на транспортните средства по градски маршрут (статични модели).

В практиката най-често се налага да се използва модел за предсказване на средната скорост на движение по целия маршрут, наричана още като съобщителна (маршрутна) скорост или средна скорост по отделни участъци от маршрута – участъкова скорост.

Популярният експоненциален модел, при който сравнително лесно става формалното представяне на отделните фактори, влияещи върху скоростта на движение на транспортното средство по маршрут.

Един от методите за прогнозиране на скоростта е експоненциалния модел е даден в работи [3,4], където е представена корелационна зависимост между маршрутната скорост и броя на спирките по маршрута

$$V_m = V_n e^{-\alpha S_{\text{общ}}} \quad (1)$$

където  $V_m$  е маршрутната скорост,  $km/h$ ;

$V_n$  – номиналната (установената) скорост, която се постига за конкретния маршрут,  $km/h$ ;

$\alpha$ – коефициентът за отчитане влиянието на всяко спиране;

$S_{\text{общ}}$ – броят на спиранията по маршрута на километър (поради всякаква причина),  $броя/km$ .

Този вид на модела дава най-груби оценки за скоростта по маршрута за различните условия на движение (интензивност на движението и типов състав на транспортния поток, с или без отделна лента за движение и интензивност по нея, време за слизване и качване на пътниците и други), параметрите  $V_n$  и  $\alpha$  имат отделни стойности.

В друга работа [5] моделът (1), отчита характера на спиранията по маршрута – служебно спиране на спирката и спиране свързано с организацията на пътното движение.

$$V_m = V_n e^{-(\alpha S_{\text{сп}} + \beta S_{\text{од}})} \quad (2)$$

където  $\beta$  е коефициентът, отчитащ влиянието на всяко допълнително спиране свързано с организацията на пътното движение;

$S_{\text{сп}}$ – броят на спиранията по маршрута на километър на спирки,  $броя/km$ .

$S_{\text{од}}$ – броят на спиранията по маршрута на километър, поради организацията на пътното движение,  $броя/km$ .

Параметрите на този вариант на модела имат същата интерпретация както в модела (1), но тук с коефициента  $\beta$  може да се отчете влиянието на допълнителните спираня и техния характер, свързани с организацията на пътното движение по маршрута – брой кръстовища по маршрута с предимство и без предимство или със и без светофари, разрешено или забранено паркирането по трасето на маршрута, висока плътност на транспортния и пешеходния поток и други.

Очевидно е, че влиянието на тези фактори на организацията на пътното движение оказват в различна степен влияние, което означава различни тегла на всеки един фактор за конкретния маршрут.

Друг вариант на модела (2) се разглежда в работите [1,2], където влиянието на отделните фактори (освен броя на спиранията по спирките) се представят с един интегрален фактор – време за престой или задръжки в движението по маршрута:

$$V_M = V_H e^{-(\alpha S_{ОБЩ} + \beta T_{ОД})} \quad (3)$$

където  $\beta$  е коефициентът (параметър), който отчита влиянието на времето на престоя според организацията на пътното движение;

$S_{ОБЩ}$  – броят на спиранията по маршрута на километър (поради някаква причина), броя/км.

$T_{ОД}$  – броят на спиранията по маршрута на километър, поради организацията на пътното движение, броя/км.

Напоследък някои автори [8] включват в експоненциалния модел времето за престой, за да се усъвършенства изследването на вредните емисии от градския транспорт. Моделът показва добра чувствителност на променливите характеристики като: посока на пътуването; период на пътуването и технически характеристики на транспортното средство.

Параметрите на този модел са показани в следната формула:

$$V_M = \left( V_H + V_H' \delta_H + V_H'' \delta_B \right) e^{[(\alpha + \alpha' \delta_A) S_{ОБЩ} + (\beta + \beta' \delta_M) T_{ОД}]} \quad (4)$$

където  $\delta_H$  е направление на пътуване, като в близост до центъра на града  $\delta_H = 1$ ; извън града  $\delta_H = 0$ ;

$\delta_B$  – коефициентът за времето на пътуване, като във върховете интервали -  $\delta_B = 1$ , а в невърховете интервали -  $\delta_B = 0$ ;

$\delta_A, \delta_M$  – коефициенти отчитащи техническите характеристики на автобуса ( $\delta_A, \delta_M = 1$  (за автоматична предавателна кутия);  $\delta_A, \delta_M = 0$  (за степенна предавателна кутия));

$V_H'$  – увеличението на номиналната скорост, ако автобусите пътуват в близост до центъра на града;

$V_H''$  – увеличението на номиналната скорост при върхов интервал;

$\alpha'$  и  $\beta'$  – коефициенти, отчитащи всяко спиране (на автобусни спирки или от организацията на движението).

Коефициентите  $V_H, \alpha$  и  $\beta$  имат същото значение като във модела (2).

Автоматичната предавателна кутия поражда плавно ускорение и намаляване на скоростта, така че ефектът от всяко спиране нараства, а времето за престой е намалено защото на водачите им отнема по-малко време да потеглят.

Ако в описанието на модела се добави допълнителната фиктивна променлива, може да се покаже ефектът от отделна (BUS)лента. Моделът добива следният вид:

$$V_M = \left( V_H + V_H' \delta_H + V_H'' \delta_B + V_H''' \delta_L \right) e^{[(\alpha + \alpha' \delta_A) S_{СП} + (\beta + \beta' \delta_M) T_{СП} + (\gamma + \gamma' \delta_A) S_{ОД} + (\sigma + \sigma' \delta_M) T_{ОД}]} \quad (5)$$

където:  $S_{СП}$  – броят спирания на автобусните спирки, броя/км;

$S_{ОД}$  – броят спирания поради организацията на пътното движение, броя/км

$T_{СП}$  – времето за престой на автобусните спирки, с/спиране;

$T_{ОД}$  – задръжките, поради организацията на пътното движение, с/спиране;

$\delta_L$  – коефициент за отделните видове пътища;

$\delta_{Ax}, \delta_{Mx}$  – коефициент за техническите характеристики на автобуса, при спиране ( $x = s$  – на автобусни спирки;  $x = p$  – поради организацията на пътното движение), ( $\delta_{Ax}, \delta_{Mx} = 1$  (за автоматична предавателна кутия);  $\delta_{Ax}, \delta_{Mx} = 0$  (за степенна предавателна кутия)).

Следващата стъпка е как се използва този модел, за предсказване на маршрутна скорост в реални условия, или за оценка на хипотетични ситуации. В реални условия стойностите на параметрите  $S_{СП}, S_{ОД}, T_{СП}$  и  $T_{ОД}$  могат да бъдат получени експериментално и чрез симулация.

Много автори използват линейната връзка между времето прекарано на спирките и броят на качащите се и слизащи пътници от всеки автобус съответства добре на резултатите от изследването. Следователно времето за спиране на автобусните спирки може да бъде представено с израза:

$$T_{СП} = T_{НИ} + \max_i \{ T_K \Pi_{Ki} + T_{СЛ} \Pi_{СЛи} \} \quad (6)$$

където е  $T_{СП}$  е време за обслужване на пътниците на спирката, с/спиране;

$\Pi_{Ki}$  – среден брой на пътниците качващи се през врата  $i$ , брой/транспортното средство;

$\Pi_{СЛи}$  – среден брой на пътниците слизащи през врата  $i$ , брой/транспортното средство;

$T_{НИ}$  – неизползвано време за слизание и качване, с/спиране;

$T_K$  – време за качване на всеки пътник, с/пътник;

$T_{СЛ}$  – време за слизание на всеки пътник, с/пътник.

При експоненциалния модел като разновидност на макроскопичния модел за маршрутна скорост, броят качващи се и слизащи пътници за всяко транспортно средство, може да бъде получен от по-обобщени данни.

Експоненциалният модел има различни приложения. Например във [6,7] са разгледани някои критерии за определяне ефективността на работата на градския пътнически транспорт.

## 2.2. Методи за прогнозиране на времето на пристигане на транспортните средства на градските спирки с използване на GPS данни (динамични модели)

Оценките за местоположението на транспортно средство от GPS за движението от сегмент  $i$  в  $j$ , ще се определи в една предварително определена матрица от времена, представляващи оценките за времето на движение от  $i$  до  $j$ . Времето за движение на  $k$ -тото транспортно средство в сегмента  $i$  е означено като, а прогнозираното време на пристигане в сегмент  $j$  като.

Следователно прогнозираното време за пристигане на  $k$ -тото транспортно средство в сегмент  $j$  ще бъде:

$$t_K(j|i) = t_K(i) + \tau(i, j) \quad (7)$$

Данните за матрицата за движението на транспортно средство във всяка точка от маршрута може да бъде изготвено от разписанието за движение по маршрута.

Ако за сегментите  $i$  и  $j$  в границите на двете спирки  $m$  и  $n$  се означаи времето на пристигане на транспортно средство по разписание с  $i$ , то времето за придвижване от  $i$  до  $j$  е

$$\tau(i, j) = \frac{l_{ij}}{l_{mn}} [t_p(n)t_p(m)] \quad (8)$$

където  $l_{ij}$  е разстоянието между двата съседни сегмента.

Метод, основан на реални данни от GPS и разписанието за движение на превозното средство.

В този подход, когато транспортно средство е далеч от следващата спирка  $n$  (сегмента  $j$ ), корелацията между закъснението (отклонението) за пристигане в текущата спирка  $m$  (в сегмент  $i$ ) е толкова малко, че може да бъде пренебрегнато. Обратно, корелацията става толкова по-силна, колкото транспортно средство се доближава до  $j$ . Прогнозираното време за пристигане на  $k$ -тото транспортно средство в участък  $j$  е:

$$t_k(j|i) = \begin{cases} t_{cn}(j) & \text{при } i \leq \rho \leq j \\ t_k(i) + \tau(i, j) & \end{cases} \quad (9)$$

където  $\rho$  е прагова стойност, получена от опитни изследвания и се свързва с времето за движение от  $i$  до  $j$ , колкото времето нараства от  $t_{cn}(i)$ , толкова и  $\rho$  нараства.

Още по-голяма точност дава метода за прогнозиране, който включва и допълнителни данни за закъснението.

Разписанието на транспортно средство по маршрута е направено за някаква постоянна средна скорост за участък  $m$  и  $n$ . Първите два метода се базират на предположението, че транспортното средство се движи с такава скорост, независимо от закъснението.

Практически, ако по разписание транспортно средство следва да пристигне на спирка в  $i$ -тия сегмент в момента  $t_p(i)$  и то е със закъснение  $t_k(i) - t_p(i)$ , то водачът на транспортно средство се стреми да компенсира закъснението, чрез увеличаване на скоростта и намаляване на престоя на спирката. Прогнозираното време за пристигане в този случай е

$$t_k(j|i) = t_k(i) + \lambda(t_p(i) - t_k(i)) + \tau(i, j) \quad (10)$$

където:  $\lambda$  е в границите 0 до 1, и ако  $\lambda = 0$ , то този метод става като първия (2.32).

Логично е  $\lambda$  да бъде намаляваща функция на разстоянието между  $i$  и  $j$ , т.е. колкото по-близо е транспортно средство до следващата спирка, толкова по-силно ще влияе закъснението, т.е. трудно може да се компенсира от водача на транспортно средство.

В някои работи [9,10]  $\lambda$  се представя като отношение на  $l_{ij} / l$  (където:  $l_{ij}$  е останалото разстояние до  $j$ , а  $l$  е дължината на маршрута). Друг метод, който предлага още по-голяма точност е методът за прогнозиране на времето на пристигане на транспортно средство на спирката, включващ и контролни времена на потегляне от някои спирки по маршрута. За прогнозиране на времето на пристигане на следващата спирка е важно да се знае времето на тръгване от предходната спирка. Закъснението може да намалява по посока на движение на транспортно средство с отдалечаване от контролната спирка.

Ако  $n=1,2,\dots$  сегмента за маршрута, а контрола по спирките е  $c(m)$ , като  $m=1,2,\dots,M$ , то времето за пътуване от  $i$  до  $j$  случаите, когато няма контрол на спирките за потеглянето, се определя от матрицата  $\{\tau(i, j)\}$ , а времето за пътуване между две последователни контролирани спирки е  $\tau[c(m), c(m+1)]$ . В случая когато между два сегмента  $i$  и  $j$  попада една контролна спирка, то времето от контролната спирка по посока на движението на транспортно средство е  $c_n$

( $i$ ) и за обратната посока на движение  $c_o(i)$ . Следователно времето за пристигане на сегмент (спирка)  $j$ , прогнозирано на сегмент  $i$  за  $k$ -тото транспортно средство е

$$t_k(j|i) = \begin{cases} t_k(i) + \tau(i, j) \\ \max \left\{ \begin{aligned} & t_k(i) + \tau[i, c_n(i)] + \\ & + \sum_{c_n(i)}^c \tau[c(m), c(m+1)] + t_p(c_o) \end{aligned} \right\} + \tau[c_o(j), j] \end{cases} \quad (10)$$

При сравняване на отделните модели се използва грешката на прогнозиране  $\delta_{k,m}$ , която представлява разликата между действителното и прогнозираното време за пристигане на сегмента (спирката)  $j$  за  $k$ -тото транспортно средство за  $m$ -тата извадка, т.е.

$$\delta_{k,m} = t_k(j|i) - t_k(j) \quad (11)$$

### 3. Заключение

В заключение може да се каже, че представените модели за прогнозиране на времето за пристигане на транспортно средство на спирка са подходящ инструмент за реализиране на разновидностите интелигентни информационни системи в транспорта.

Следователно разгледаните по-горе варианти на динамичния модел е подходящ за оценяване на фактическа средната скорост на ТС от ГПТ във всеки момент от движение по маршрута, тъй като данните в този модел се актуализират в реално време с отчитане на всички особености по маршрута.

Този модел с неговите варианти се използва в съвременните информационни и управляващи системи за ГПТ и информирание на пътниците.

*Докладът отразява резултати от работата по проект No 2016 - ФТ - 03 на тема „Изследване на симулатор за обучение на водачи за подобряване безопасността на пътното движение“, финансиран от фонд „Научни изследвания“ на Русенския университет.“*

### Литература

- [1] CITRA (1990) Analysis of level of services for public transport – the conception. Commission of Urban Transport, VIII Region, Concepcion, Chile.
- [2] CITILABS - TRIPS (Transport Improvement Planning System) Demo, www.citilabs.com. CITILABS Ltd, Surrey, UK, 2001.
- [3] Cohen, S. Indicateurs d'allure et de consommation d'un autobus en exploitation. Recherche Transport Securite – Janvier, 1984, 16-22.
- [4] Gibson, J., I. Baeza and L.G. Willumsen Bus-stop, congestion and congested bus-stops. Traffic Engineering and Control 30(6), 1989, 291-302.
- [5] Fernandez, R. (1996) Evaluation Ex-Post de la Operacion de la Via Exclusiva para Buses de Avenida Grecia. Informe Final, Comision de Planificacion de Inversiones en Infraestructura de Transporte, Secretaria Ejecutiva (SECTRA), Santiago.
- [6] Fernandez, R. (1999) Design of bus-stop priorities. Traffic Engineering and Control 40(6), 335-340.



[7] Fernandez, R and N.A. Tyler (1999) Design of bus stops as part of bus priorities. Proceedings of the European Transport Conference 1999. Seminar D: Traffic Management, Safety and ITS, 187-200, PTRC, London.

[8] Fernandez, R., M. Osses and E. Valenzuela, A model to predict bus commercial speed to estimate public transport emissions. Presented at the 11th International Symposium on Transport and Air Pollution, Grazer, Austria, June 2002, 19-21.

[9] Gomez, A., F. Zhao, and L. D. Shen, Benefits of Transit AVL and Transit AVL Implementation in the U.S., Annual Transportation Board Meeting, 1998, Transportation Research Board, Washington, D.C., 1998

[10] Schweiger, C. ,TCRP Synthesis 48, Real-Time Bus Arrival Information Systems, Transportation Research Board, 2003

**За контакти:**

ас. инж. Павел Стоянов, асистент към катедра “Транспорт”,  
Русенски университет “Ангел Кънчев”, тел.: 082 888 515, e-mail: pstoyanov@uni-ruse.bg

# SAFETY OF INFORMATION-MANAGEMENT SYSTEMS IN RAILWAY TRANSPORT

## БЕЗОПАСНОСТЬ ИНФОРМАЦИОННО-УПРАВЛЯЮЩИХ СИСТЕМ НА ЖЕЛЕЗНОДОРОЖНОМ ТРАНСПОРТЕ

Prof., Dr. Technical Science Moiseenko V. I., Postgraduate. Kotov M. O.  
 Ukraine State University of Railway Transport – Kharkov, Ukraine  
 E-mail: mvi53@ukr.net, kotov.mykyta@gmail.com

**Abstract:** in the article is considered questions of the organization structure of the software of information-management systems in railway transport. A new approach based on matching software structure with functions and their level criticality by safety. Received results allow to implement the synthesis of structures of systems with regard to their purpose and the functions they perform.

**KEYWORDS:** SYSTEMS STRUCTURE, SAFETY, SOFTWARE AND HARDWARE.

### 1. Introduction

Railway transport is one the most intensively developing sectors in the global economy. Modern train control systems is a difficult complex software and hardware. Besides the usual technological tasks assigned to them a very important function - providing traffic safety and continuity the transportation process. Most of the functions of information-management systems implemented at the software level. In connection with this question of improving the software of these systems are timely and relevant.

Problems of safety and reliability of the application software of railway automation has traditionally been considered from the standpoint of classical reliability theory, as evidenced by the work [1-3]. Usually authors in the process of synthesis of software and hardware structure not take into account the specifics of the technology of functioning of the control object. Often enough the software structure is tied to the structure of the hardware. Some few authors, try to link the structure of software and hardware complex with the singularity technology work of the control object, as that can be a railway station.

This work is a logical continuation of this direction. The objective is to formulate the basic principles of synthesis of software and hardware systems considering the specifics of the functions information and control system.

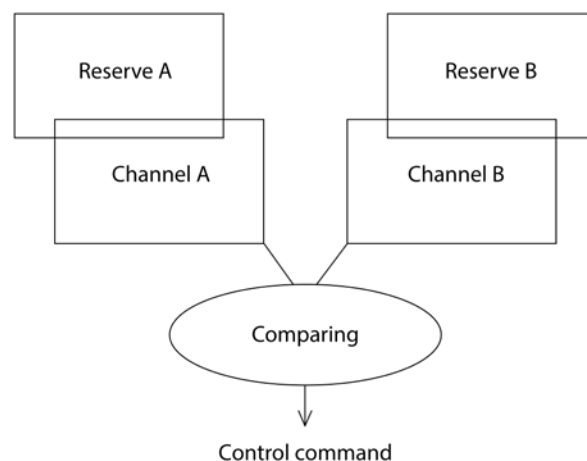
If we consider from this positions functions automated train control system on the station, in accordance with [4], it is possible to allocate:

- responsible functions, implementation of which ensures the functioning of the control system and its safety factor;
- functions related to ensuring of the system which are not critical to safety;
- service functions.

Regulatory documents of the EU and Ukraine (IEC 61508) sets different levels of risk dangerous events, as well as qualitative and quantitative indicators of the safety of functioning management systems.

### 2. Preconditions and means for resolving the problem

With this in mind, let us consider options for organization of software structure with classical two-channel reserve of station microprocessor control system, pic.1.

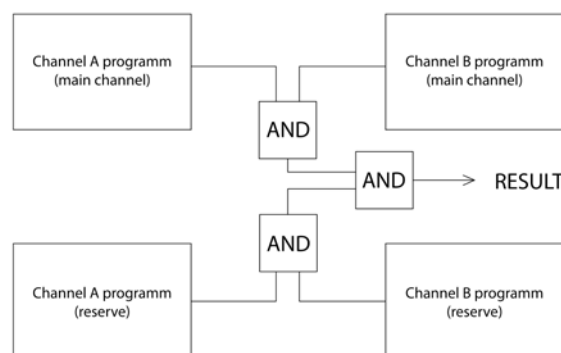


Pic.1. Block diagram of a hardware-software complex of the station information management system.

According to the scheme in picture 1, channels interact in scheme logical "AND", and reservation in each channel is carried on scheme "OR". Obviously, all the functions of control and management will be implemented by this logic.

After this we transform the scheme on picture 1, keeping in mind all the responsible functions, which are most critical to safety. In a case of failure, the system must go into the condition, so-called "the deffensive condition", wherein it's functioning is limited.

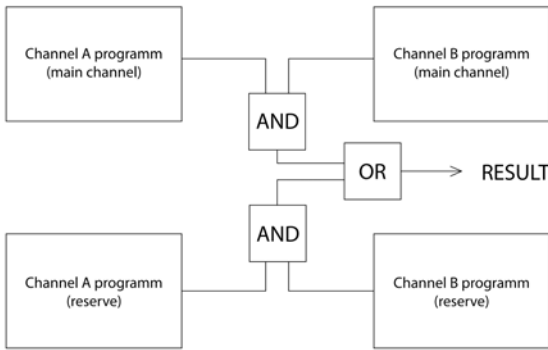
Basing on this limits, we have no need in reservation. And the main task consists find and to block mistake. For a software implementation of such functions, mostly fits the logical structure "AND"—"AND", pic.2.



Pic.2 The structural scheme of realisation of responsible functions.

The output signal can be created only with full identical work of A and B programs of both channels. A priori, such a structure loses in reliability, but can have good safety parameters. With the help of this structure, can be realized functions of object blocking, artificial opening, enabling of inviting light etc.

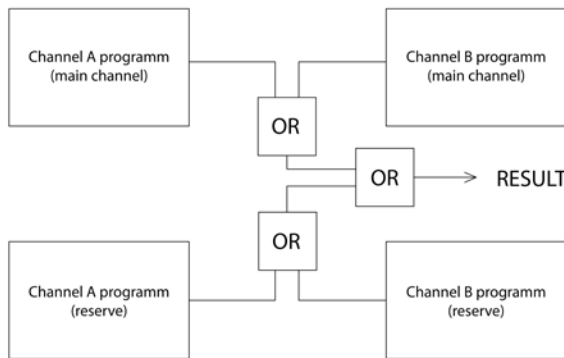
The structurally-logic scheme "AND"—"OR" can be used for realisation of functions, which are not so critical to safety, pic.3.



Pic.3 The structural scheme of realisation of management functions, which are not critical to safety.

Such a structure is designed for the realisation of the main system commands, which are linked with the setting of the route, and also with locking and automatic unlocking. At the expense of the balance between the indicators of safety and reliability, it can provide an effective work of the hardware and software complex under the influence of destabilizing factors.

Failure operation serves as a main indicator of success for the service functions of information-management systems. According to this requirement, it's logical to suggest usage of operation "OR", pic.4.



Pic.4 The structural scheme of realisation service functions.

In this approach, some ambiguity is not excluded if one of the programs will crash. But it doesn't matter in two reasons. The first one, is that information is provided to the human operator. And the second one. It's not critical to the railway traffic safety.

### 3. The solution of the considered problem

The successful work or the crashing of the system can be described with help of the combination of final events, which are united into the composite tree of all dangerous conditions of system. We can determine the parameters of probability for the all system for their further comparing.

The simultaneously pairwise coincidence of refusal in main and reserve channels A, A', B and B' of system software are the criterion of refusal at performing control functions for the

scheme on picture 2. Let's mark by  $\Psi$  the parameter of condition of system which characterizing refusal, . then for the scheme in pic.2, it can be represented by a function of the form:

$$\Psi_1 = (A \& B) \& (A' \& B') \tag{1}$$

In the same way for the structure, which is not so critical for safety on pic.3. :

$$\Psi_2 = (A \& B) \parallel (A' \& B') \tag{2}$$

The structural function of refusal for service functions has a form of classical scheme "OR"

$$\Psi_3 = (A \parallel B) \parallel (A' \parallel B') \tag{3}$$

According to this logic, the conditions of element or the whole system determine by auxiliary binary variable parameter of function of probability refusal component  $Y_i$  [5]. Obviously, event occurs if  $Y_i = 1$ , and conversely, doesn't occur, if  $Y_i = 0$ . Accordingly, similarly for the systems of realization in general  $Z_1, Z_2, Z_3$ .

A publication analysis [6-9] makes it possible to formulate a hypothesis about the independence of primary events, and to suggest the presence of exponential law distribution. The latter hypothesis is supported by the majority of researchers, working in this field [10-13]. A list of the main indicators of reliability and safety is set by normative documents, particularly in the evaluation of software according to ISO/IEC 9126, ISO/IEC 12207, GOST 28195-89. The issues of provision computational formulas required statistical data reflecting the reliably behavior of the system and with sufficient sample objects, is the main problem, faced by researchers.

We're going to use a maximum value for  $Z_0 = 9 \cdot 10^{-9}$  1/hour in following discussions.

### 4. Results and Discussion

Taking into account the above the functions of probability of failure, for each of the proposed structures:

$$Z_1 = Y_1 \cdot Y_2 \cdot Y_3 \cdot Y_4 \tag{4}$$

$$Z_2 = 1 - [1 - Y_1 \cdot Y_2][1 - Y_3 \cdot Y_4] = Y_3 \cdot Y_4 + Y_1 \cdot Y_2 - Y_1 \cdot Y_2 \cdot Y_3 \cdot Y_4 \tag{5}$$

$$Z_3 = 1 - [1 - Y_1][1 - Y_2][1 - Y_3][1 - Y_4] = Y_4 + Y_3 - Y_3 \cdot Y_4 + Y_2 - Y_2 \cdot Y_4 - Y_2 \cdot Y_3 + Y_2 \cdot Y_3 \cdot Y_4 + Y_1 - Y_1 \cdot Y_4 - Y_1 \cdot Y_3 + Y_1 \cdot Y_3 \cdot Y_4 - Y_1 \cdot Y_2 + Y_1 \cdot Y_2 \cdot Y_4 + Y_1 \cdot Y_2 \cdot Y_3 - Y_1 \cdot Y_2 \cdot Y_3 \cdot Y_4 \tag{6}$$

where are  $Y_1, Y_2, Y_3, Y_4$  – parameters characterizing of refusal component of the system A, B, A', B', respectively.

Based on the fact that control system an arbitrary time  $t$  implements only a single function, and in the range  $[t; t+\Delta t]$  system may implement a row of basic functions. Then the function of refusal of the whole system is written like:

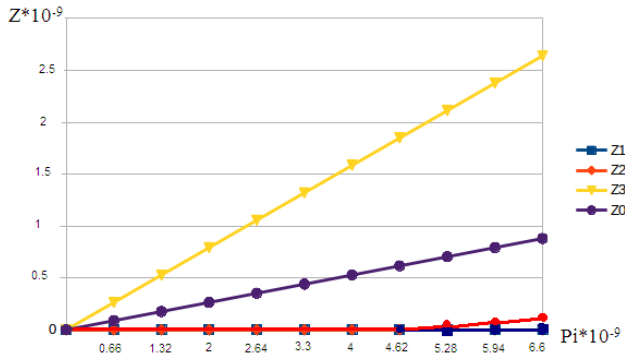
$$Z_0 = Z_1 \parallel Z_2 \parallel Z_3 \tag{7}$$

We assume that the intensity of refusal of programs A, A', B and B' are the same,  $\lambda_1 = \lambda_2 = \lambda_3 = \lambda_4$ . This assumption may have a right to exist in connection with the setting task of comparison potential capabilities of different structures of the organization of the software.

To simplify further change of the last expression, considering previously adopted assumptions about the equality of the intensities of refusals components A, B, A', B', we make the change of variables  $Y_1 = Y_2 = Y_3 = Y_4 = X$ . Then in the final form the function of refusal of system can be represented by the equation:

$$Z_0 = 4X - 4X^2 - 4X^3 + 11X^4 - 8X^5 + 8X^7 - 11X^8 + 4X^9 + 4X^{10} - 4X^{11} + X^{12} \tag{8}$$

Figure 5 shows the probability of refusal  $Z_0, Z_1, Z_2, Z_3$  from the refusal of individual component  $P_i$ .



Pic.5 The structural scheme of realisation of safety functions  
Exterior view of implementation schedules Z1, Z2, Z3, and of whole system Z0 confirms the prospects of the proposed approach.

## 5. Conclusion

The considered embodiments structure of hardware and software do not exhaust all the possible implementations. This is most likely just a basic configurations, icombining and extending them will allow to get considerable quantity of different modifications. The choice of a particular type is determined by the requirements for the overall system and for its individual functions.

Also it should be noted that to obtain the expected properties in reliability and safety it is advisable to allocate a hardware implementation of the programs A and B in the main and standby channels. Otherwise, malfunctions and failures on the general reasons may significantly to worse the expectation of developer.

## 6. Literature

1. РТМ 32 ЦШ 1115482.02-94. Безопасность ЖАТ. Методы расчета показателей безотказности и безопасности СЖАТ [Текст].
2. ГОСТ Р 51901.5-2005. Менеджмент риска. Руководство по применению методов анализа надежности [Текст].
3. Викторова, В. С. Анализ программного обеспечения моделирования надежности и безопасности систем [Текст] / В. С. Викторова, А. С. Степанянц // Надежность. – 2006. – No 4 (19). – С. 46-57.
4. ГОСТ Р 51901.14-2005 (МЭК 61078:1991). Менеджмент риска. Метод структурной схемы надежности [Текст].
5. ДСТУ 4178-2003 Комплексы технических средств систем управления и регулирования движением поездов. Функциональная безопасность и надежность.
6. MIL-HDBK-217F Military handbook. Reliability prediction of electronic equipment.
7. Надежность и эффективность в технике [Текст] : справ. в 10 т. Т. 3. Эффективность технических систем / под общ. ред. В. Ф. Уткина, Ю. В. Крючкова. – М. : Машиностроение, 1988. – 328 с.
8. Джон фон Нейман «Вероятностная логика и синтез надёжных организмов из ненадёжных компонентов».
9. Baun C. Cloud Computing. Web-Based Dynamic IT Services // C. Baun / Springer-Verlag, Berlin. - 2011. - 108 p.
10. René J. Chevance Server Architectures. Multiprocessors, Clusters, Parallel Systems, Web Servers, and Storage Solutions // J. René / Elsevier Digital Press USA. - 2005. - 709 p.
11. EN 50126 Европейский стандарт спецификация и доказательство надежности, эксплуатационной готовности, ремонтпригодности и безопасности (RAMS) для использования на железных дорогах.
12. Косолапов А.А. Исследование тенденций развития архитектуры информационных систем на сортировочных станциях.
13. Надежность технических систем и оценка риска. Автор: Хенли Э., Куэмамото Х

# NEW MATERIALS FOR IMPLANTS OF THE HUMAN HIP JOINT AND TECHNOLOGY OF THEIR MACHINING WITH THE ACHIEVEMENT OF HIGH PRECISION AND QUALITY OF SPHERICAL SURFACES

Doctor of science, Prof., Turmanidze R.<sup>1</sup>, Undergraduate student Popkhadze G.<sup>2</sup>  
Faculty of Transportation and Mechanical Engineering<sup>1,2</sup> – Georgian Technical University, Tbilisi, Georgia, inform@gtu.ge

**Abstract:** In view of the fact that the endo-prosthesis heads of human hip-joint are operated in extreme conditions, in respect of load, the selection of corresponding material and also increase of precision and quality of machining of spherical surfaces is rather topical task.

In the submitted work are reviewed the problems connected with definition of the influence degree of orientation of the sapphire crystal on its workability during diamond grinding with a butt of the ring and elaboration of the perspective, original scheme of formation of the incomplete spherical surface, particularly, of the sapphire head of endo-prosthesis of the human hip-joint.

**KEYWORDS:** SINGLE CRYSTAL SAPPHIRE, ANISOTROPY, GRINDIBILITY, ENDOPROSTHESIS, PRECISION GRINDING FORMING, SPHERICAL SURFACE.

## 1. Introduction

Endo-prosthetics is effective and often the only method of the function restoration of the human joint. It is established that every year in the world are made about a million operations of exchange of the human hip-joint.

The endo-prosthesis heads of the human hip-joint from the point of view of the character and value of load are operated in extreme conditions. The contemporary joint endo-prostheses consist of acetabular (cup) and hip component (leg) and also the head from metals or ceramic materials on their base. At present there is an acute problem of creation of wear resistant inert materials for implantology.

Therefore, in each specific case the selection of the necessary material with corresponding physical – mechanical characteristics and also increasing of precision and quality of the most significant part of endo-prosthesis – spherical surfaces is rather actual task the acuteness of which intensively grows in recent years. The number of used endo-prostheses is some tens of millions of pieces a year and the statistics shows that unfortunately this number increases every year.

The production of implants from bio-ceramic materials is rather profitable direction. Up to now a powerful industry of fabrication of implants, tools and accompanying materials has been created and the western market of this product is evaluated in 2,5-3 billion Dollars a year. The basic developing and producing countries of implants are: USA, Japan, Germany, France, Great Britain, Russia, Italy, South Korea, countries of Asia region and other countries.

It is conditioned by the fact that if earlier the necessity of similar operations was caused by the age factor of the man or traumatology fractures in recent two decades abruptly increased the number of patients at young age of 30-40 years of both men and women without any injuries and fractures. In opinions of physicians the principal reasons of it are non-active way of life of youth, composition of contemporary artificial food products and metabolic disorder. All the above-mentioned reasons determine the number of used endo-prostheses in some tens of millions of pieces a year.

The medical practice proves that the repeated prosthetics of the human hip joint is connected with big problems. In many cases the implementation of such operations becomes practically impossible. Therefore, the durability of the endo-prosthesis of the human hip joint to the end of the patient's life especially at young age has especially significant meaning.

The contemporary elaborations of the endo-prosthesis structure are directed to exchange of chirulen by ceramic material that leads to the change of the endo-prosthesis structure, development of new ceramic materials with the improved physical and mechanical characteristics, development of processing of internal and external spherical surfaces, development of diamond tools providing the high quality of the

machined surface, definition of the optimal wear resistance of the pair of materials for manufacture of the endo-prosthesis etc.

For nowadays in the world practice these heads are manufactured from various alloys, composite materials and ceramics which mainly are isotropic materials. Therefore, the data of the above-mentioned works do not give the necessary information on machining of anisotropic materials, particularly artificial crystal of sapphire (Fig. 1).

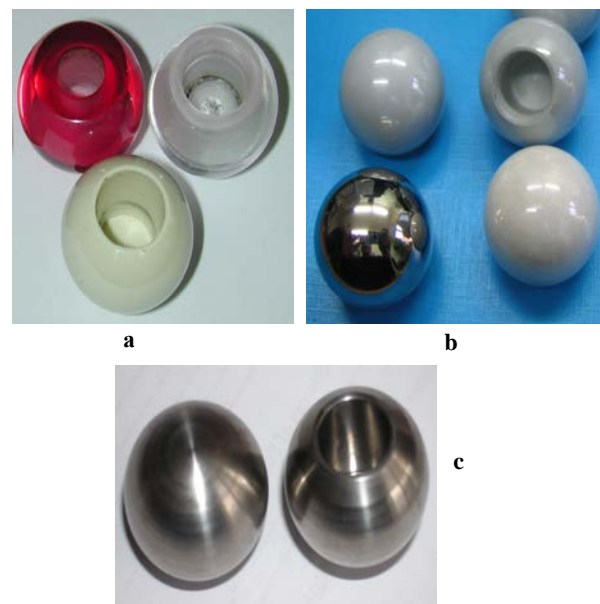


Fig. 1. Hip heads from sapphire (a), Zirconium ceramics (a), b - Stainless steel, c - Biologically pure titanium alloy.

Together with indisputable positive qualities the contemporary structures of endo-prostheses from metal, ceramics polymers have certain defects. Among them there is an insufficient biological inertness and redundant wear of components of the friction pair that lead to short duration of work of the artificial hip-joint. Besides that as the result of wear of the material in the friction pair of endo-prosthesis hinge toxic and onco-dangerous products of the dissociation in various organs and tissues accumulate that in 30-40% leads to hard complications and requires complex disabling interferences.

The circle of materials that satisfy the criterion of biological compatibility is rather limited. Because of it and requirements of the resource of articles in condition of action of alternating loads, corrosion active environment titanium and its alloys as the material for fabrication of endo-prostheses have the advantage over Co-Cr-Mo alloys.

The wear of heads from zirconium ceramics is 7-9 nm a year while titanium 105 nm a year. Coming out of this the fabrication of implants from bio-ceramic materials is a perspective direction of development of the science intensive technologies of creation of materials and their machining. Most bio-compatible with the human organism, wear resistant and durable material for fabrication of the above-mentioned article is the artificial mono-crystal of sapphire.

For nowadays basically the circle of materials for fabrication of pairs of bearing surfaces of endo-prostheses of joints with minimally possible number of products of wear has been determined. Such pairs of bearing surfaces with excellent characteristics of wear resistance are the friction pairs of ceramics-ceramics, metal-metal and polyethylene with a high degree of cross-section links in combination with ceramics or metal. Together with that the basic unresolved problem of the last decade was the development of bearing surfaces that could endure much higher loads with young and movable patients. The surfaces that are being investigated at present in laboratory conditions due to their hopeful characteristics of wear are ceramic matrix (82% of aluminum oxide, 17% of zirconium dioxide, 0,3% chrome oxide), zirconium dioxide and ceramics in pair with cobalt-chrome alloy.

Together with that sapphire representing the mono-crystal of aluminum oxide as a material for bearing surfaces possesses unique inertness including electrolyte passiveness, perhaps the best of the well-known materials, bio-compatibility, corrosion resistance and hardness. Resistance of sapphire towards any acids and alkali is rather higher than that of metals and even poly-crystalline oxide of aluminum. Probably because of it sapphire doesn't change the immune status of the patient. If metals and poly-crystalline materials used for the bearing surfaces have different speed of wear of the micro-sites it leads to the coefficient increase of the pair friction and wear increase then this effect with sapphire is absent.

Tribological investigations of the friction pairs of materials were conducted by the scheme of rotational friction with the contact geometry of "ball on disk" type. The flat disk was manufactured from the investigated material and the ball from the material of counter body (Fig. 2).

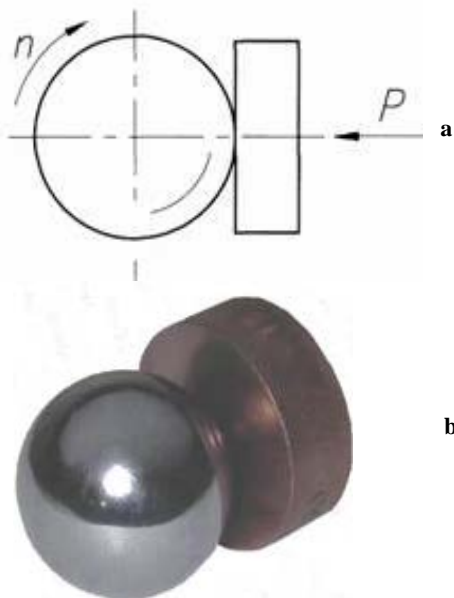


Fig. 2. Schematic arrangement of rotational friction – a, and example of counter bodies – b.

The obtained dependencies of the friction force of pairs: sapphire-sapphire, sapphire-ruby from the time of tests (number of cycles) has mainly non-monotonous abrupt character. From them one can mark out three stages of wear, namely: running-in wear – creation of the work roughness and necessary supporting

surface on frictional surfaces. At the moment of beginning of work the contact of bodies takes place in the point, accordingly the specific load is sufficiently high that leads to the abrupt growth of the friction force and as a consequence of wear of the surface material.

Normal wear is after achievement of the surface wear meaning, at which the optimal meanings of characteristics of supporting surface are reached, the stable process of friction of bodies has place with gradually decrease force of friction.

Catastrophic wear is in the process of friction of counter bodies of the wear products which fill the pockets on the friction surface and because of the weak (drop) feeding of the Ringer solution into the area of friction the wear products accumulate occupying all the vacant place in the pockets and as a result of this take part in the process of wear of the investigated surfaces as a free abrasive.

The pointed out above stages of wear can have different length of time or generally to be absent in the wear process.

From the dependencies follows that the best results in relation of the friction force to the pressing force shows the friction pair of sapphire-sapphire with orientation of the crystalline lattice on flatness 0001, linear wear of the friction pair of sapphire-sapphire with the orientation of the crystalline lattice on the flatness 0001 and sapphire-ruby.

Titanium and alloys on its basis are widely used in medicine as implants and other articles. From the point of view of bio-compatibility for the implants working for a long time in the live organism the use of titanium is preferable that unlike alloys does not contain alloying additives harmful for the live organism. However, titanium in its usual state has low mechanical properties in comparison with its alloys. This problem was solved by means of formation of nano - and composition structure in technically pure titanium.

The use of the friction pairs of sapphire/titanium consisting of non-toxic materials would help us to solve the pointed out problem. However, for nowadays it is considered that from titanium and its alloys is impossible to manufacture a friction pair because of their high inclination to a contact snatch and as a consequence increased wear during friction. This property makes dangerous the use of titanium in the friction pairs (Fig. 3).



Fig. 3 Experimental specimens of titanium head and sapphire cup for endo-prosthesis of the hip-joint.

Thus, the work objective is the creation of a new bearing connection of endo-prosthesis of the hip-joint having the improved quality at the expense of use of hardened sapphire and biologically inert technically pure titanium with modification of the surface layer of IPD and subsequent

nitriding as materials improving tribological properties of the connection.

For conduct of investigations of machinability of the sapphire crystal the method of Low Temperature Precision Grinding (LPG) has been chosen developed at the Department of Mechanical Engineering of the Georgian Technical University as a version of progressive methods of diamond grinding of hard and brittle non-metallic materials.

In Fig.4a the machined parts set on the cassette in separators or by other method of mounting, for example, gluing carry out rotational movement with angular speed of  $\omega_2$  and the grinding ring with speed of  $\omega_1$  in the same direction. In the cutting area the pressing is carried out by force P of the machined surfaces of parts to the work surface of the grinding ring.

The experimental investigations were conducted on the laboratory setting equipped with the special precision head (Fig. 4b).

By the data analysis of complex, all-round experimental investigations conducted by us one can make the following conclusion:

By other equal conditions of machining the most intractable is orientation 0001. For all the tested diamond rings the ration of meanings of the linear removal of material q is within  $q_{0001}/q_{1010} = 0,25...0,5$ , at that,  $q_{1012}/q_{1010} = 0,75...1$ .

The productivity of machining grows in the range of cutting speed of  $V=1...6$  m/sec while at the further increase of the cutting speed to 12m/sec it remain constant.

With increase of the pressing force P in all the investigated range the productivity of machining grows, however, in the interval of  $P=1000...1500$  kPa the productivity growth considerably decreases.

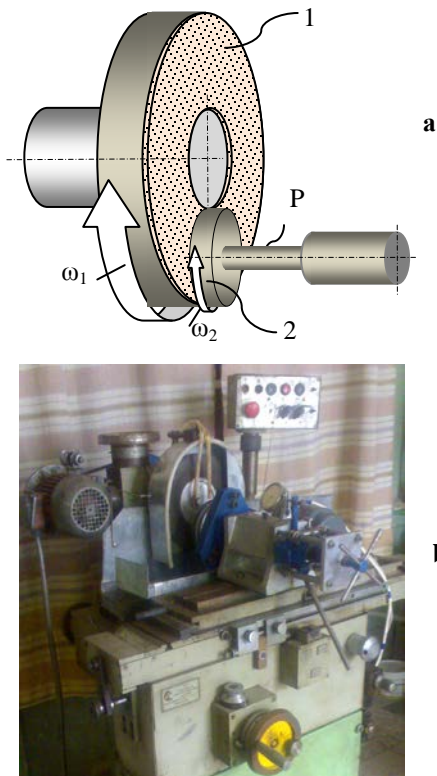


Fig. 4. a- Schematic arrangement of LPG: 1- Grinding ring, 2 - Cassette with parts, b- Laboratory setting for LPG.

From characteristics of the diamond tool on productivity by the prevailing way influence granularity and bunch of the diamond tool. The concentration influence is insignificant. With the increase of the grain size within  $d_3=14/10...28/20$  the productivity grows 1.5...2.5 times. The maximum productivity of machining is provided by the tool on ceramic bunch ( $\{0001 -$

$130\text{mkm/min}$ ;  $\{1010\} - 300\text{mkm/min}$ ;  $\{1012\} - 250\text{mkm/min}$ ), then on metallic ( $\{0001\} - 50$  mkm/min;  $\{1010\} - 200\text{mkm/min}$ ;  $\{1012\} - 170\text{mkm/min}$ ) and organic ( $\{0001\} - 30\text{mkm/min}$ ;  $\{1010\} - 120\text{mkm/min}$ ;  $\{1012\} - 110\text{mkm/min}$ ). The tool on the ceramic bunch works in the mode of self-grinding.

From characteristics of the diamond tool the granularity and material of the tool bunch influence in prevailing way on the surface quality. With the grain increase in the investigated range the height of unevenness  $R_z$  grows within 1...1.5 classes and the depth of the violated layer H 1.5...2 times. In other equal conditions of machining on orientation (0001) higher quality of the surface is reached than on the rest two. The difference is in 1...1.5 classes of roughness. By this indication the best results are shown by the diamond rings on organic bunch. So, for example, on the diamond rings on bunches BC-11 and organic special are obtained the following results:  $R_z=0,25$  mkm;  $t_{p03}=35...45\%$ ;  $H=2...5$  mkm. At that the meaning of parameter  $R_z$  is in order below than parameter  $t_{p03} - 1,5$  times higher of parameter H- 3...5 fewer than the meanings of corresponding parameters that are obtained on the diamond rings on ceramic and metallic bunches.

The influence character of the process factors on output parameters for the chosen orientations of the sapphire crystal ((0001), (1010), (1012)) is constant.

By study of morphology of the machined surface the possibility of cutting the sapphire material by plastic deformation of the removed layer at low cutting speeds  $V=1...3$  m/sec with the least depth of the violated sub-relief layer has been proved (Fig. 5).

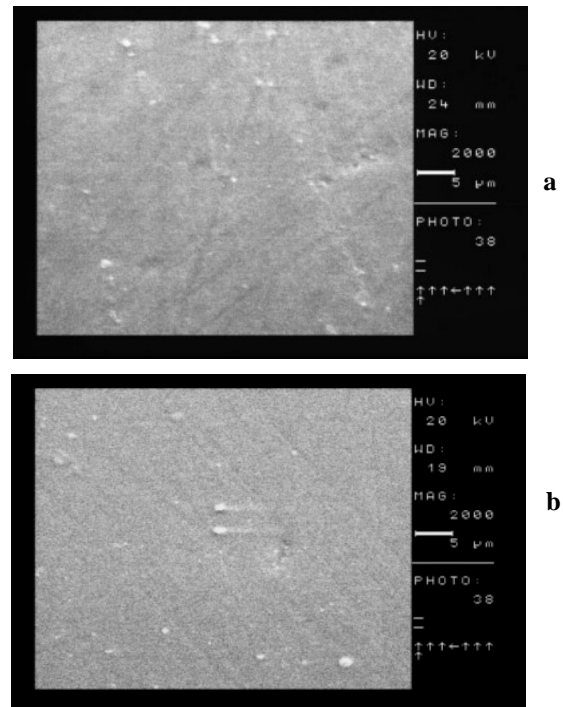


Fig. 5. Micro-photographs of surfaces of experimental specimens of sapphire machined by the LPG method: a - Orientation 1010, b - 1012. Diamond ring-ACM 14/10, bunch organic special, 50%. Cutting modes:  $V=1\text{m/sec}$ ,  $P=750$  kPa.

It is known that machining of vitreous materials, particularly, the sapphire crystal by means of plastic deformation of the removed layer instead of fragile destruction – dispersion, the pledge of acquisition of the machined surface practically without hereditary defect – without sub-relief layer. Value H appeared to be the least namely on these specimens of sapphire. The obtained meaningful result requires individual investigations the conduct of which is being planned.

The development of a new or updating of the existing technological process of machining of the sapphire head sets the actual task of creation of new highly effective schemes of formation. The optimization criteria of technological operations such as productivity, indices of the surface quality and precision of machining determine the place of new schemes-methods of formation in technological process taking into account their advantages.

The schematic arrangement of the spherical head of endo-prosthesis is shown in Fig.6. The partial sphere is determined by its radius and angle  $\beta$  of spherical segment. There are several ways of machining of the spherical head.

The closest to the LPG process in kinematics is the scheme of grinding of the partial sphere with use of the end grinding ring. The machined part rotates with angular speed of  $\omega_2$  and  $\omega_3$  around axes 2 and 3 subsequently (Fig. 7). This kinematics forming the incomplete surface of the sphere is taken as the basis of development and possible realization of more effective schemes of grinding of spherical heads of endo-prosthesis taking into account the kinematics and other positive features of the LPG method [1 – 6].

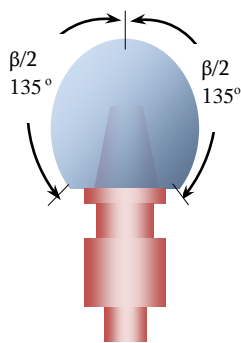


Fig. 6 Endo-prosthesis heads:  
 $\beta$  – Angle of spherical segment.

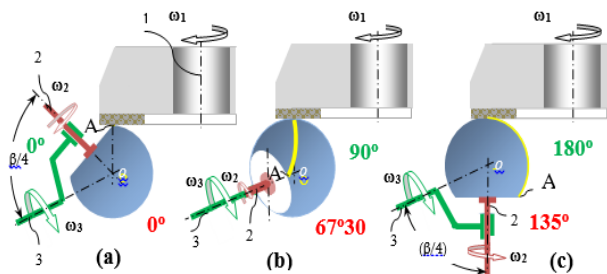


Fig. 7. The scheme of forming a partial spherical head of endoprosthesis by face grinding: (a), (b) and (c) are successive relative positions of a ground head while axis 2 turns around the axis 3 within  $180^\circ$ .

The end grinding ring rotates with the angular speed of  $\omega_1$  removing the tightness for machining from sphere with the required speed of cutting and rate of feeding. For full machining the spherical head must rotate simultaneously around axes 2 and 3 with the angular speed of  $\omega_2$  и  $\omega_3$ . Axes 2 and 3 intersect in the centre of sphere in the point  $O$ . As it is seen in Fig.4 the angle between axes 3 and 4 must be equal to  $\beta/4$  but for to machine the whole surface of partial sphere angular speeds  $\omega_2$  and  $\omega_3$  must cinematically correlate as the both of them specify the values of components of the feeding rate. The linear speed on the ring/ball juncture and correlation of angular speeds  $\omega_2/\omega_3$  will determine the surface texture of the half-complete or complete head of endo-prosthesis. The detailed analysis of kinematic connections between rotational speeds and other relative parameters of the grinding process are out of the Report and this will be discussed in the following publications. One of the formation schemes of

the incomplete spherical surface with the forming grinding ring is shown in Fig. 8.

The partial spherical head rests on the forming grinding ring consisting of internal and external cones with abrasive layers (Fig. 8 a, b) and rotates around axes 2 and 3 with angular speeds of  $\omega_2$  and  $\omega_3$  in the same manner as it was described above in Fig.8. The machined part by means of a strong spring  $P$  is pressed to the forming ring and is continuously fed to the required depth in direction of the ring. The applied pressing is equally distributed on the end of the ring work i.e. in points A and B (Fig. 8 b).

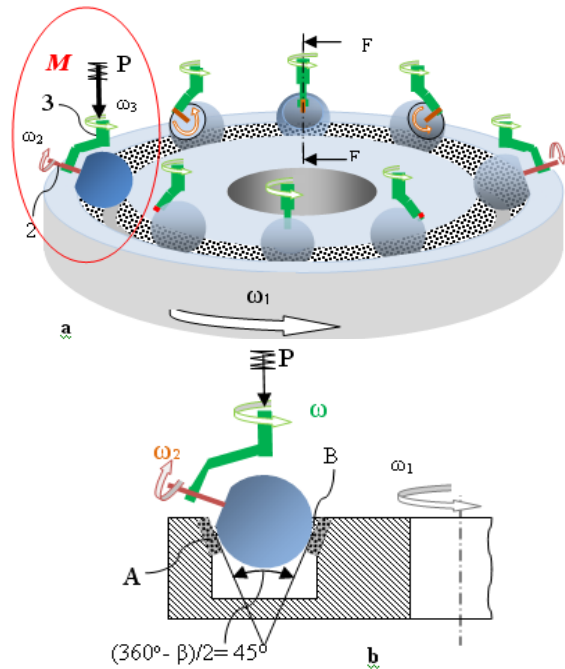


Fig. 8. Scheme of forming of a partial spherical head by shaped grinding wheel (based on LPG method).

In Fig. 8a are shown eight subsequent positions of the spherical head in one cycle. For clarification all the positions are equally distributed along the ring although such subsequent positions are in the same place  $M$ . This scheme enables also carry out machining in “machining stations” around the ring.

The main defect of this scheme is a complexity of the grinding ring and difference of speeds in points A and B. The latter can be compensated in the same way as in the LPG process. Comparatively simple schemes of formation of the spherical heads of endo-prosthesis with the use of commercially available shapes of the ring are shown below in Fig.9 a, b, c and d. The schemes presented in Fig.9 a, b and c differs only by the shape of used rings. The kinematics of formation of the partial spherical head is the same as the first scheme presented in Fig. 7 and 8.

As for the case described in Fig.8 the partial spherical head rests between two grinding rings but preferable are three (Fig. 9d) that accordingly consist of two or three terminally located elements. For effective use of full space of abrasives on the used rings is suggested the implementation of coordinated in time harmonic movement of rings and machined sphere within the required distances as it is shown in Fig. 9 with arrows.

The diameters of grinding rings are unlimited when the grinding mode is carried out with two rings. In case of grinding with three heads the sphere radius ( $r$ ) and maximum radius of the ring ( $R$ ) are interdependent. The mode of three rings provides a high stability of the grinding process. In subsequent studies will be seen more detailed development of structural schemes of



formation of spherical heads and carried out experiments with the real spherical heads for endo-prosthesis.

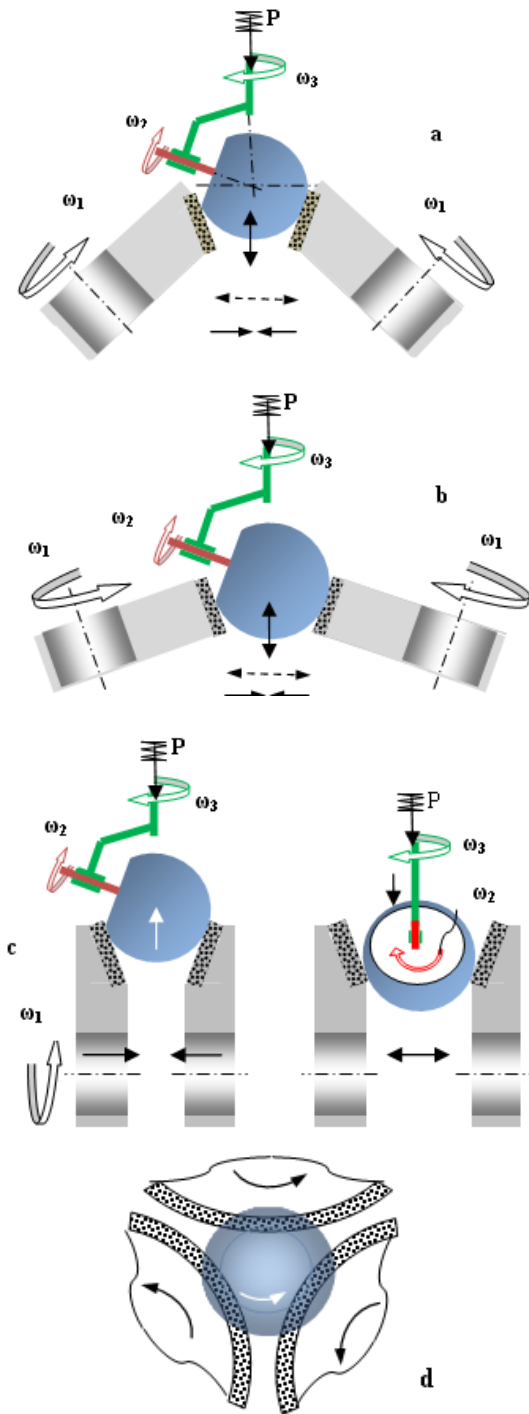


Fig. 9. Possible versions of grinding of the endo-prosthesis during the use of commercially available usual rings.

## 2. Conclusion

1. Scale of influence of single-crystal sapphire of the crystallographic flat orientation and the grinding conditions in the mode of removal of material, surface finishing and the state of sub-surface layer studied during low-temperature precise grinding have revealed that workability of single-crystal sapphire considerably depends on the crystallographic flat orientation. The relative values of removal of the material against the specimen with crystallographic flat orientation (1010) are within  $q_{0001}/q_{1010}=0.25\dots0.5$ , and  $q_{1012}/q_{1010}=0.75\dots1$ . In other equal conditions of the LPG process the high quality of the ground surface is achieved for crystal

orientation (1010). The difference with two other orientations of the crystallographic flatness is within 1...1.5 class of roughness.

2. By the studies of morphology of the ground surface was proved the grinding possibility by single-crystal sapphire in compliant mode, i.e. removal of the deformed layer by cutting without cracks at the low speed of cutting. In such conditions of machining was detected the least depth of the faulty sub-surface layer.
3. The structural schemes of formation of the partial spherical heads of endo-prosthesis for human hip-joint need a further analysis and optimization with the aim of designing of advanced technological processes and the prototype of grinding machines.

## 3. Literature

1. Batiashvili B.I., Butskhrikidze D.S., Mamulashvili G.A., Turmanidze R.S., Kromp K., Mills B., Mgaloblishvili O. *Technological Possibilities of Low Temperature Precision Grinding Process when Machining Hard and Brittle Materials. Fractography of advanced ceramics, International Conference, Stará Lesná, High Tatras, May 2001.*
2. Turmanidze R.S., Butskhrikidze D.S., Kromp K., Mills B., "Low temperature precision grinding of hard and brittle materials". *Problems of mechanics and physico-chemistry of the process of abrasive machining, Kiev 2002, pp. 490-499.*
3. Rozenberg O.A., Sokhan S.V., Vozny V.V., Mamalis A.G., Gavlik J., Kim D-J. *Trends and Development in the Manufacturing of Hip Joints: An Overview Int. J. Adv. Manuf. Technology (2006) 27: pp. 537-542.*
4. Lieberman J R, *Two Alternative Bearings for Total Hip Arthroplasty: More Data Are Needed. J Am Acad Orthop Surg 2009; pp. 61-62.*
5. Dobrovinskaya E., Litvinov L., Pishchik V. *Mono-crystals of corundum – K: Science, 1994. – 256 p.*
6. Turmanidze R.S. *Implants of the human hip joints and peculiarities of their manufacture with the high precision and quality of machining of the work surfaces. Proceedings of the 13th International Conference on Tools, ICT 2012. 27-28 march 2012. University of Miskolc, Hungary. Session (B).*

# OPTIMIZATION OF GEOMETRIC PARAMETERS OF HARD METAL MICRO DRILLS TO INCREASE TOOL LIFE AND PERFORMANCE OF DRILLING PACKAGE OF PRINTED CIRCUIT BOARDS

Doctor of science, Prof., Turmanidze R.<sup>1</sup>, Senior laboratory Bachanadze V.<sup>2</sup>, Undergraduate student Popkhadze G.<sup>3</sup>  
Faculty of Transportation and Mechanical Engineering<sup>1,2,3</sup> – Georgian Technical University, Tbilisi, Georgia, inform@gtu.ge

**Abstract:** In the presented work investigated the changes of power characteristics of deep drilling package of printed circuit board's hard metal micro drills depending on the drilling depth, cutting data and geometry of the drill. In particular studied the nature of changes in axial efforts and torque depending on the drilling depth drill with different inclinations of the spiral grooves using specially designed highly sensitive devices, enabling direct measurement method. Based on the analysis of the results of the study, changes in the geometry of existing standard drills. Proposed new construction of micro drills vary-angle spiral grooves in such a way that the angle is the maximum value at the top of the drill and uniformly decreases towards the end of the working parts. The drills are manufactured with different inclinations of the spiral grooves. Based on the experiments of them chosen more for its near standing power rates to the standard drill bit and its comparative test with a standard drill bit, bringing them up to the breakage, thanks to which the proven advantages of drills new design. Taking into account the results of the experiments proposed drill elongated structures to improve performance by increasing the processing drilling depth and accordingly the number of plates in the package of printed circuit boards.

**Keywords:** DRILL, GRADIENT OF SPIRAL GROOVE, VARIABLE ANGLE, DEVICE.

## 1. Introduction

It is impossible to imagine modern equipment without electronic knots, starting from household and ending with space equipment. Printed circuit board's production, basic parts of electronic equipment associated with drilling process vast quantities of small diameter holes (about 1mm or less). Carry out drilling of micro carbide drill geometry, which has multiple experiments an experiences relevant production. In particular: the optimum cutting angle and spiral angle grooves respectively is 300, and the rear angle 180. They are refaced through each hole and 1000 are designed for 3-4 regrinding costs.

Production of printed circuit boards is mass production, where performance is carried out with the aim of increasing the drilling package, composed of several plates, it has a place of deep-hole drilling, where the drill depth exceeds the diameter of 8-10 times.

Downtimes of expensive technological equipment, especially in mass production are associated with significant economic losses. In the production of printed circuit boards easy connected not only with the replacement of the tool with the aim of reshaping, but unexpected, caused by fragile destruction even before the first reshaping. Probability of brittle fracture grows significantly during deep drilling package of printed circuit boards. When this zone is located in the near destruction of the end of the spiral grooves.

Providing the best mass production processes for manufacture of printed circuit boards, at least a slight increase in resistance, including fragile resistance micro drills and consequently increasing productivity processes, can provide significant economic benefits.

## 2. The Main Part

Research work with a view to enhancing the resistance of tungsten carbide micro drills and deep hole drilling process performance package of printed circuit boards were held in the laboratory precision micro instrumental Department "Industrial Technologies Engineering Mechanics", Georgian Technical University in close cooperation with specialists of the Institute of Manufacturing Technology and Quality Management (IFQ) Magdeburg University Otto-von-Guericke (Germany).

Studies were initiated the study of the nature of the change of power indicators-torque and axial reinforcement depending on the depth of cutting and drilling printed circuit board package from fiberglass.

To measure the axial effort was the appliance is made on the basis of known methods and existing analogs, measuring element, which is the system of strain gauges mounted on the elastic casing (see fig. 1).

As for measurement of a torque, in our case the existing indirect method at which measurement is carried out by means of measurement of power of process of cutting is unsuitable as we deal with very low indicators. That is why it is necessary to use this method, which will make it possible to measure directly the torque with high precision. To this end, we have designed and manufactured a special device (see fig. 2), in which table for drilling is equipped with rotating lever mechanism. As the measuring element, elastic element applies here too with the system of load cells, only the higher strain measure (0.2 g).



Fig. 1. Instrument for measuring axial efforts.



Fig. 2. The device for measurement of torque.

Experiments were conducted with drills from solid alloy VK60M diameter  $\varnothing$  0,9mm long spiral groove  $l=10$ mm. Rake angle and spiral angle grooves respectively  $\omega=30^{\circ}$ , rear angle was  $18^{\circ}$ .

Drilling was carried out a package of printed circuit boards of fiberglass thickness 1.6mm composed of 5 plates with a total thickness of 8mm (see fig. 3).

Drilling of blanks is carried out on different modes of cutting depth up to 7 mm and 1 mm the depth of the recorded testimony

every depth controlled readings. Experimental results are shown in fig. 4 and 5.

From this results, clearly shows that the load power with increasing depth progressively increasing. If the axial thrust is growing, approximately 1.5 times the amount of torque is increased 3-4 times.

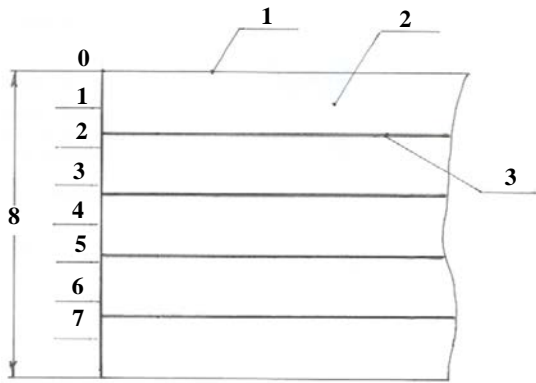


Fig. 3. Package diagram printed circuit boards of 5 plates. 1-copper foil, 2-fiber, 3-double layer of copper foil.

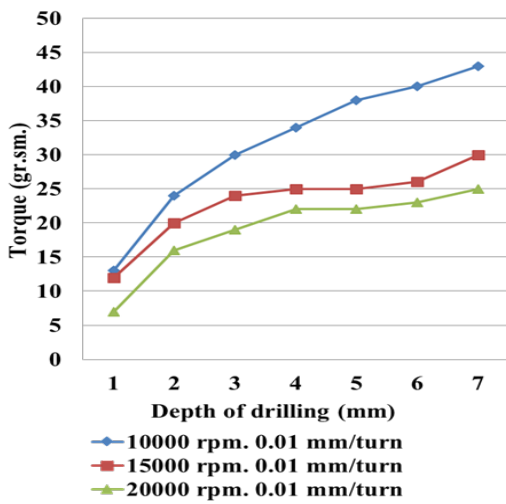


Fig. 4. The chart for standard drills  $\omega = 30^\circ$ .

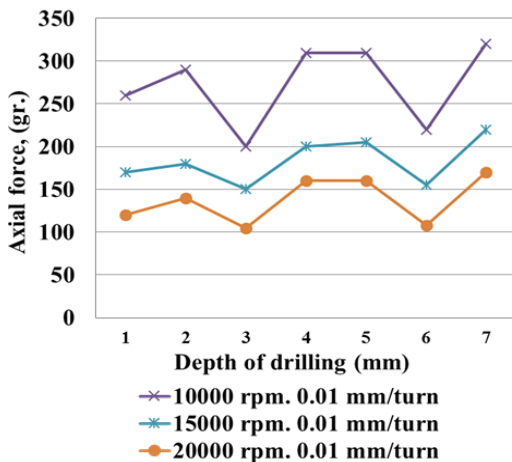


Fig. 5. The chart of axial efforts for standard drill  $\omega = 30^\circ$ .

Question, what caused this increase in power? Cutting conditions at the cutting edge of drills with increasing depth does not change. The only reason for this could be the increased contact area abrasive chips with the surface of the hole and emerged from it frictional forces.

You need to note that the sharp fall in axial efforts on areas of depth 2-3 and 5-6 (see fig. 5.) on these sites due to the lack of the work piece (fig. 3.) the copper layer.

The main factor increase the likelihood of brittle fracture of the cutting tool of these two power indicators may not increase the axial effort and more progressive increase in torque because the strength properties of carbide materials on the compression significantly exceed indicators of torsion.

Accelerating the process of chips from the cutting zone would contribute to the reduction of the force of friction and, consequently, improve the reliability of the drilling process. The problem of removal of chips when drilling deep hole in different cases decide in different ways. For example, when drilling drills dimensions solid this exercise method of leaching using a coolant, which is supplied, into the hole through, done in the body of the drill. In other cases, when the drill bit sizes do not give possibility of coolant above method to remove shavings used drilling method intermittent, where after a certain depth drilling is carried out periodically by the disqualification of drills from holes fast running.

The application of these techniques in our case nepriemlim. In the first case we have with micro drills. The use of coolant in the manufacture of printed circuit boards is not allowed. Design and method of intermittent drilling, because it led to the strong performance. When processing deep eyelet micro drills accelerating factor could be an increase in chip removal step spiral grooves, i.e. reducing the angle, but it would have led to a deterioration of the cutting conditions, so-as will decrease the cutting angle drills.

In the design of the drills carried out in a way that at the top of the save the desired cutting angle, and toward the end of the spiral grooves reduce its angle, IE a spiral groove cut into a vary-angle [1, 3, 4, 5, 6] and gradually increase its step, it would accelerate the process of chip and facilitate conditions for drilling.

Fig. 6 shows the scheme of drills with vary-angle spiral grooves where the angle of the grooves at the top of the drill  $\omega_0$ , and at the end of the working part of  $\omega_1$ . The width of the grooves in the normal section  $B_n$  on all length does not change, but the change in the front section and at the top is  $B_{T0} = \frac{B_n}{\cos \omega_0}$ , and at

the end of the working parts  $B_{T1} = \frac{B_n}{\cos \omega_1}$ .

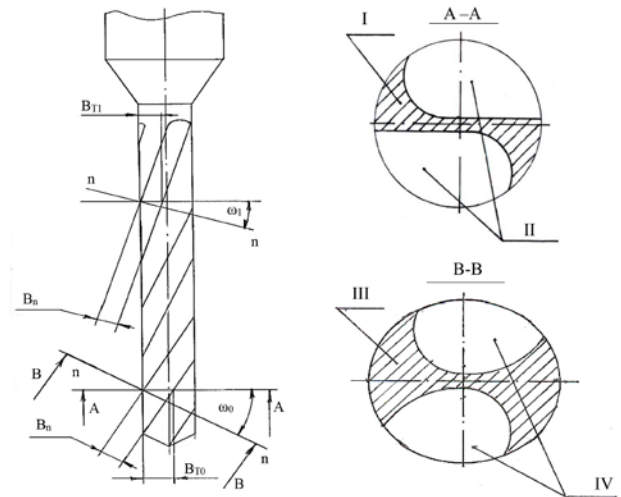


Fig. 6. Drill scheme with vari-angle spiral grooves, I – The useful mechanical section of the drill, II – Face section of the groove, III – Useful normal section of the drill, IV – Normal section of the groove.

Changing and useful mechanical drill section. Useful section at the top:  $S_o = \frac{\pi d^2}{4} - \frac{2S_n}{\cos \omega_0}$ , and at the end of the working

parts:  $S_1 = \frac{\pi d^2}{4} - \frac{2S_n}{\cos \omega_1}$ , where  $S_n$  - square grooves in the normal section,  $d$  - is the diameter of the drill.

If you take into account that  $\omega_0 > \omega_1$ , it turns out that toward the end of the working part of the useful cross-section drills intensifies. Then there are drills compared to standard must withstand stress.

Production of such drills associated with certain difficulties. At production of standard drills with a constant tilt angle of a spiral flute the special adaptation carries out the mutually agreement two movement – rotations of preparation of a drill and its movement in the axial direction at a size of a step of a spiral flute. Thus, this interrelation is defined by linear function. In case of a variable step, this interrelation is defined by difficult tangential function. Because of it was necessary to modernize the equipment and its mechanism of axial giving of an element with the Archimedean spiral to replace elements with a tangential spiral, made by our special calculations [2, 3, 4, 5].

Besides, because of a variable tilt angle of a spiral flute, at you - polishing of these flutes should change orientation of a grinding wheel relatively to an axis of preparation of a drill respectively to change of a tilt angle of a flute. It can be carried out in two ways: at a motionless axis of a grinding spindle to turn a preparation spindle axis round a point of intersection of these axes at a corner size  $\omega = \omega_0 - \omega_1$  (see figs. 7), or motionless to leave an axis of a spindle of preparation and to turn an axis of a grinding spindle (see figs. 8) [7].

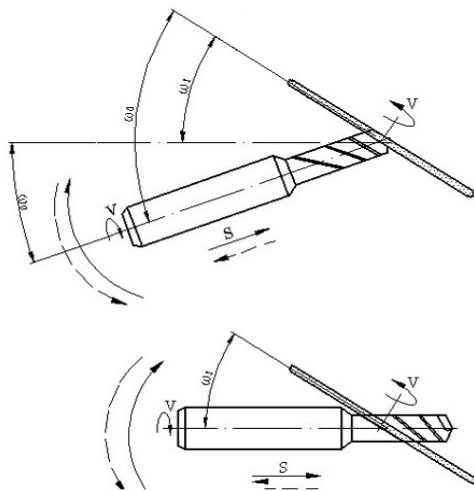


Fig. 7. Schemes of change of orientation of axes of a spindle of preparation of a drill and grinding spindle. Method of turn of an axis of a spindle of preparation.

Proceeding from constructive reasons the preference was given by us to the first option (figs. 7) and in the course of modernization of the equipment it was equipped with the additional mechanism of turn providing when cutting spiral flutes, turn of an axis of preparation of a drill relatively to an axis of a grinding spindle at a corner size  $\omega = \omega_0 - \omega_1$  thus depending on are long the cutting part of a drill turn is carried out by the linear law:  $\omega_x = \ell_x \cdot K_\omega$ , where  $\omega_x$  - the current size of an angle of rotation of an axis of preparation,  $\ell_x$  - the current coordinate of length of the cutting part of a drill,  $K_\omega$  - the size of change of a tilt angle of a spiral flute per unit length the cutting part of a drill.

We have designed constructed prototypes of drills with vary-angle  $\omega = 30 - 17^\circ$ ,  $\omega = 35 - 20^\circ$ ,  $\omega = 40 - 22^\circ$  and  $\omega = 43 - 23^\circ$ .

All of these included circuit boards same experiments as the standard. Experimental results for drills  $\omega = 30 - 17^\circ$  and  $\omega = 35 - 20^\circ$  are shown on fig. 9 - 12.

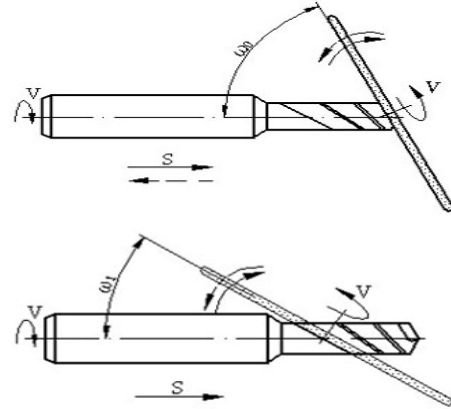


Fig. 8. Schemes of change of orientation of axes of a spindle of preparation of a drill and grinding spindle. Method of turn of a grinding spindle.

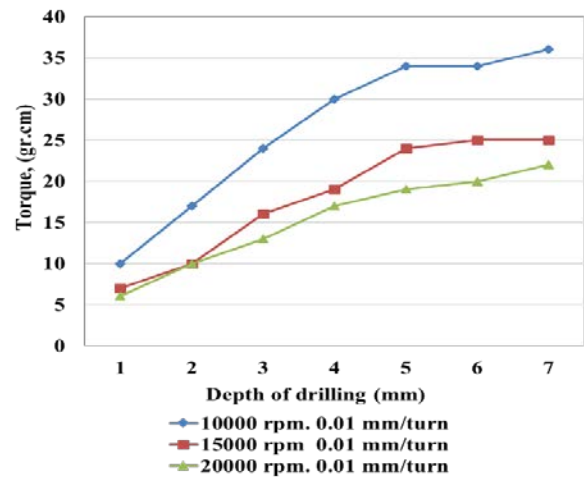


Fig. 9. The chart of change of a torque for drills  $\omega = 30 - 17^\circ$ .

Analysis of these graphs shows the following: for drills  $\omega = 30 - 17^\circ$  performance of axial efforts almost indistinguishable from a standard drill bit  $\omega = 30^\circ$ , so, it was expected, because these same drill front angle and cutting conditions respectively at the cutting edge. With regard to indicators of torque, they drill  $\omega = 30 - 17^\circ$  depending on the cutting was understated by 12-16%.

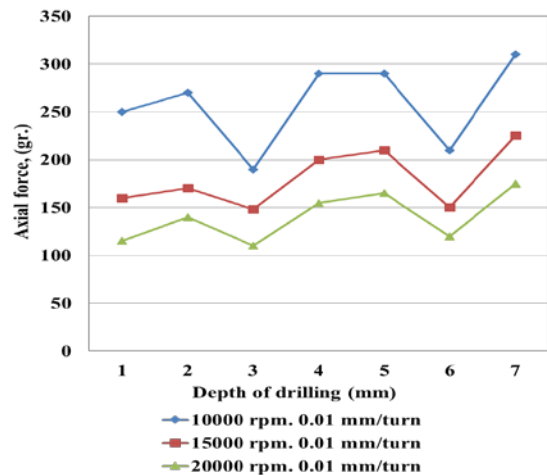


Fig. 10. The chart of changes of axial efforts for drills  $\omega = 30 - 17^\circ$ .

For drills  $\omega = 35 - 20^\circ$  performance of axial efforts relatively understated, as rake angle increased by 5% and this facilitated the process of cutting, but indicators of torque with increasing depth drilling grows more intensively and exceed indicators of both previous designs. It is clear that the understatement of torque to drills  $\omega = 30 - 17^\circ$  compared with standard drills  $\omega = 30^\circ$ , due to the gradual increase in step spiral grooves and accordingly reduced contact area formed by chips with processed apertures. Increasing the angle of inclination and therefore a decrease in pitch of spiral drills  $\omega = 35 - 20^\circ$  again causes the reverse-torque figures intensively promoted.

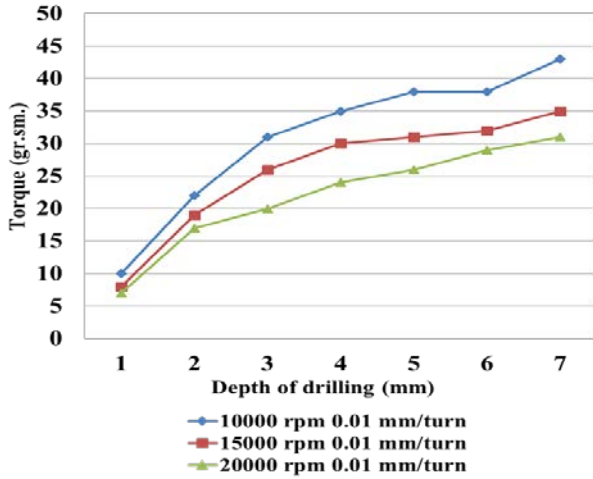


Fig. 11. The chart of torque for drills  $\omega = 35 - 20^\circ$ .

When drilling by drills of  $\omega = 40 - 22^\circ$  and  $\omega = 43 - 23^\circ$  these power indicators are rather underestimated (see figs. 13-16) that is explained by improvement of conditions of cutting because of considerable (5-8%) increases in a forward corner at the cutting edge. However, reduction of a corner of a point at further operation causes increase in intensity of wear, and they without repoint reach only 600-800 openings.

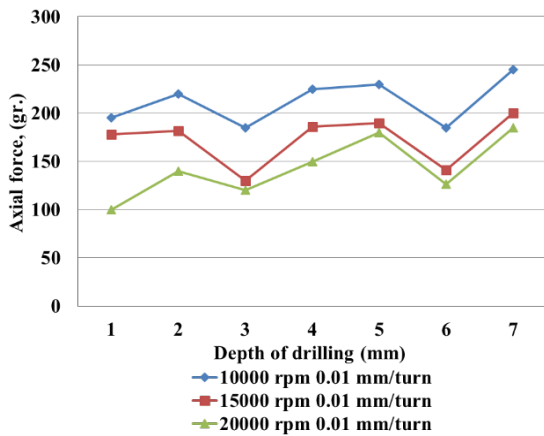


Fig. 12. The chart of changes of axial efforts for drills  $\omega = 35 - 20^\circ$ .

Obviously, to get a clearer picture further experiment need to keep standard drills  $\omega = 30^\circ$  and drills with vari-angle spiral grooves  $\omega = 30 - 17^\circ$ . Experiments were continued until the breakdown drills. Through each hole 200 checked power indicators, with increasing cutting edge wear gradually increases. After 1000 holes check carried out through every 100 holes, as increasing the likelihood of breakage of drill. Throughout a series of experiments for both types of drills,  $\omega = 30^\circ$  nearly identical indicators remain innovative wear and axial efforts. As for torque,

its value on the standard drills always exceed the value of drills with variable angle of the spiral grooves  $\omega = 30 - 17^\circ$ .

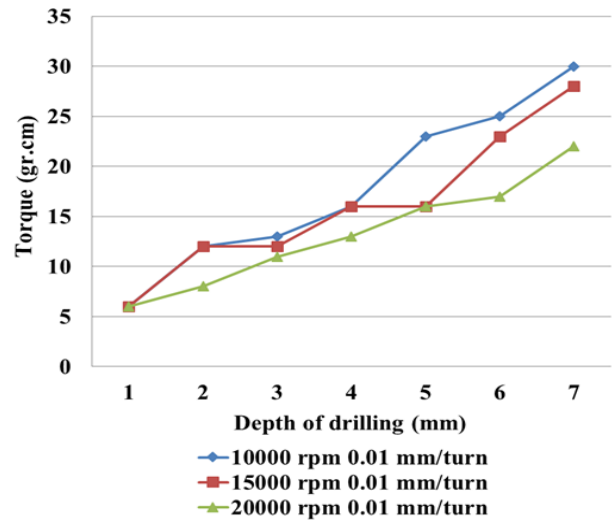


Fig. 13. The chart of change of a torque for a drill  $\omega = 40 - 22^\circ$ .

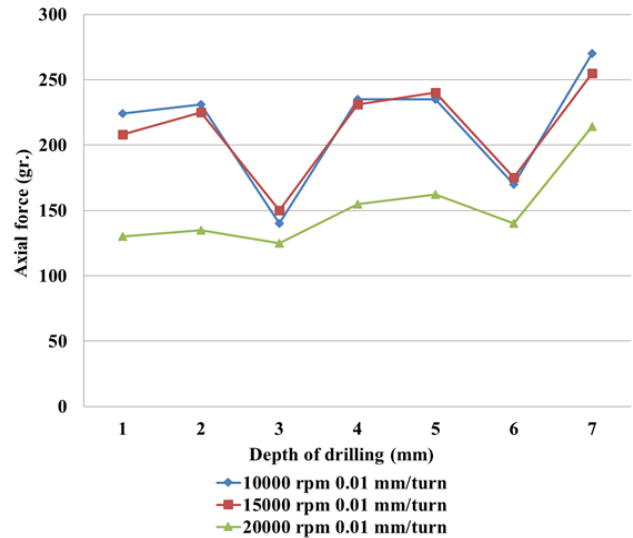


Fig. 14. The chart of change of axial effort for drills  $\omega = 40 - 22^\circ$ .

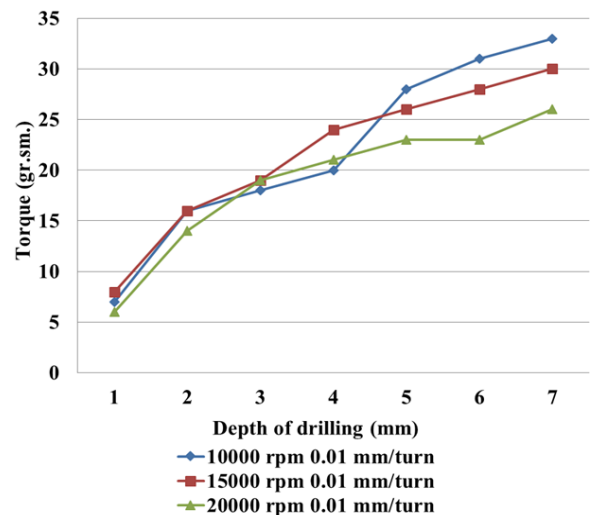


Fig. 15. The chart of change of a torque for drills  $\omega = 43 - 23^\circ$ .

Statistics showed that the breakage of the standard drills  $\omega = 30^\circ$  going from 1200 to 1300 holes and drill with vari-

angle  $\omega = 30 - 17^\circ$  from  $-1400$  to  $-1500$ . Performance torque values before breakdown indicating the number of drilled holes  $N$  traversed the path  $L$  and size of wear on back surface drills  $f$  shown in Fig. 17 and 18.

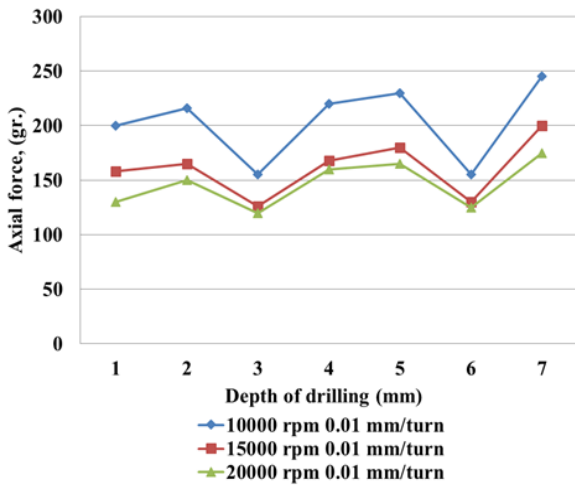


Fig. 16. The chart of change of axial effort for drills  $\omega = 43 - 23^\circ$ .

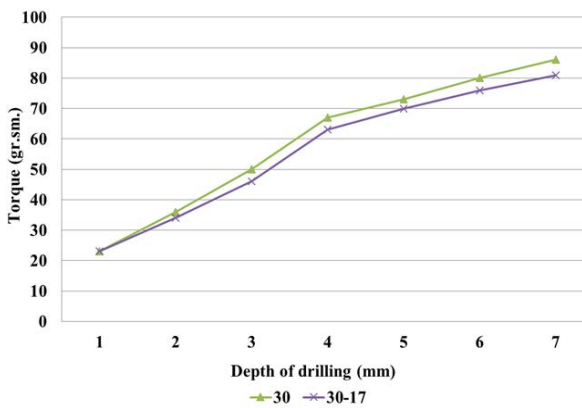


Fig. 17. The chart of torque graph for drills  $\omega = 30^\circ$  and  $\omega = 30 - 17^\circ$  before the breakdown drills  $\omega = 30^\circ$ .

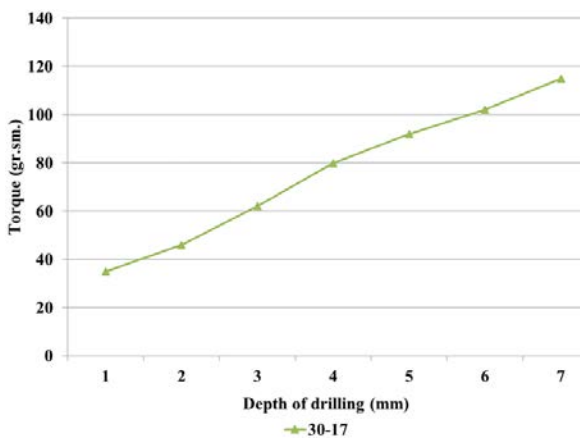


Fig. 18. The chart of change the torque diagram for drills  $\omega = 30 - 17^\circ$  before its breakdown.

### 3. Conclusions

Solid Carbide micro drills with vary-angle spiral grooves in deep drilling package provides improved chip control process intensity of hole, promoting this underestimates the force of friction and consequently the torque on the axis of the drill.

Implementation of the spiral grooves with a gradual lowering of the  $\omega$ -angle from the top of the drill toward the end of the working part provides useful cross-section reinforcement drills, increasing the reliability of the brittle.

On the basis of the foregoing, it becomes possible to manufacture drills with elongated working part at 2-2, 5mm and in the package circuit boards add another plate, which will make it possible to improve the performance of drilling process on 20%.

### 4. Literature

1. B.Karpushewski, R.Turmanidze, L.Dübner, O.Kushnarenko. Erhöhung der standzeit und prozesssicherheit von mikrobohrern durch die entwicklung neuer werkzeuggeometrien. Collection of scientific works "Modern technologies in mechanical engineering", publishing house of the Kharkov national technical university "KPI". Release 2. Kharkov, 2008 year. Pages 27-32.
2. D.Adamia, Z.Gviniashvili, V.Bachanadze. Peculiarities of formation of shavings grooves of spiral drill of hard alloy with variable inclination. Scientific technical journal "Transport and Machinebuilding" 2009 year. Edition No. 3(15). Publishing house "Transport and Machinebuilding". Pages 133-140.
3. R.Turmanidze, O.Kushnarenko, D.Adamia, Z.Gviniashvili. Small-sized hard metal spiral drills with variable angle of inclination chip grooves. Collection of scientific works "Modern technologies in mechanical engineering", publishing house of the Kharkov national technical university "KPI". Kharkov, Release 5, 2010 year, Pages 318-327.
4. R.Turmanidze, D.Adamia, Z.Gviniashvili. Peculiarities of Manufacture and Tests of Fine-Sized hard-metal Spiral Drills with Variable Setting Angle of Chip Grooves. Proceedings of the 17th international scientific and technical conference "Mechanical Engineering and Technical Sphere of the XXI century", 13-18 September 2010 year, in Sevastopol. Donetsk National Technical University. Volume 3. Pages 181-184.
5. R.Turmanidze, O. Kushnarenko, D. Adamia, Z. Gviniashvili. Fine-sized hardmetal spiral drills with variable setting angle of chip grooves. 10th International scientific conference "New Ways in Manufacturing Technologies – NWMT 2010. 17-19 June 2010year. Prešov, Technical University of Košice, Faculty of Manufacturing Technologies, Košice, Slovak Republic. Pages 217-226.
6. R. Turmanidze, Z. Gviniashvili. Fine-sized hard metal spiral drills with variable setting angle of chip grooves. Selected, peer reviewed papers from the 6th International Congress of Precision Machining ICPM 2011. 13th-15th September 2011year. Liverpool John Moores University, Day 1. Liverpool. Pages 253-258.
7. D. Adamia, Z. Gviniashvili, L. Tediashvili, V. Bachanadze. Destination of swing-out mechanism on special device for chip groove fluting with variable angle of spiral. Scientific technical journal "Transport and Machinebuilding" #1(23), 2012 year. Publishing house "Transport and Machinebuilding". Pages 196-205.

# EXAMINATION OF ACOUSTIC PROPERTIES OF A GEAR PUMP AFTER TOOTH ROOT UNDERCUTTING USING THE INDUCTION OF DECISION TREES

PhD., M.Sc. Deptuła A.<sup>1</sup>

Faculty of Production Engineering and Logistics – Opole University of Technology, Opole<sup>1</sup>

a.deptula@po.opole.pl

**Abstract:** Among cavity pumps used in hydraulic drive systems as energy generators, gear pumps are the most widespread. Apart from their numerous advantages from the point of view of noisiness and the delivery fluctuation coefficient, they are inferior to others. Steps are undertaken to decrease the noisiness. According to the research results, own acoustic parameters of the pump depend on the technology and performance quality as well as on the geometrical features of the tooth profile. The paper is restricted to the analysis of acoustic properties of an innovative gear unit after tooth root undercutting. Acoustic properties have been described with taking into consideration induction of decision trees and decision rules.

**Keywords:** ACOUSTIC PROPERTIES, GEAR PUMP, INDUCTION TREES, OPTIMIZATION

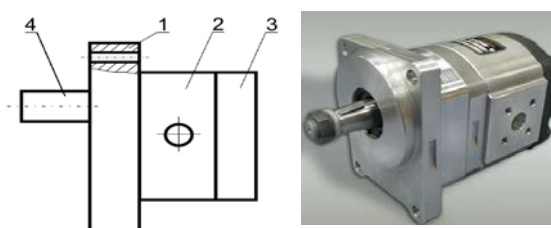
## 1. Introduction

Hydraulic machines are one of the most widespread machine classes, without which it would be hard to imagine the functioning of modern industry and of society today. These machines can be divided into pumps, water turbines, hydrokinetic drives, mixers, water-jet drives, propellers etc., but also hydraulic transport, hydraulic drive and hydraulic steering, etc. [1-4]. Overflow machines form a wide group of systems. The work of overflow machines is most frequently based on two states: transient state (in which values of the system functions change in time) and steady state (the functions values do not change in time or change periodically). If the pump is the heart of a hydraulic system then the valve is the brain. Valves are used to perform a large variety of governing and controlling functions.

The noise is most effectively reduced through a combination of the two ways (the active way being the most effective of the two). Detailed studies have shown that the noisiness of the displacement pump is due to the flow of the working medium (Fluid Born Noise) and to the vibrations of its structural components (e.g. the unbalance of the rotating parts, excessive clearance in the moving joints, improper workmanship and assembly). The main causes of noise generation, having the most significant bearing on the sound pressure emission level, are the pressure fluctuation on the delivery side and the trapping of the fluid in gear wheel tooth spaces. In order to avoid such adverse phenomena, relief grooves and dampers are used to at least partially reduce the fluctuations generated by the pump (the passive method) [4, 12, 13]. Such measures, however, entail additional costs. The authors' own research has shown that the pump's acoustic parameters depend on the manufacturing technology, the quality of workmanship and the tooth profile geometry. The present study is limited to the analysis of the acoustic properties of a novel gear pump with tooth root relief, in particular with the use of a induction trees.

## 2. Tested pump

The designed and built prototype pump has a three-plate structure shown schematically in Fig. 1. The front plate (1) is used for mounting the pump on the drive unit. The middle plate (2) contains gear wheels, slide bearing housings and suction and forcing holes for connecting to a hydraulic system. The whole construction is closed with a rear plate.



**Fig. 1** Three-plate design of gear micropump with external meshing.  
1 – front (mounting) plate, 2 – middle (rest) plate, 3 – rear plate, 4 – driving shaft

The tested prototype unit was designed in-house and manufactured by the Hydraulic Pumps Manufacturing Company Ltd. in Wrocław. The pump was designed having in mind the technological capacities of this company [10, 11]. The novelty of the prototype pump consists in the modification of the involute profile in its upper part through the so-called tooth root relief (undercut). The main meshing parameters for the pump with unit delivery  $q = 40 \text{ cm}^3$  are listed in the table below (Table 1).

**Table 1:** Meshing parameters

	Symbol	Unit	Value
Number of teeth	$z$	-	9
Modulus	$m_o$	[mm]	4.5
Pressure angle	$\alpha_o$	[°]	20
Gear wheel width	$b$	[mm]	32.2

## 3. Measuring rig

The reverberation chamber (3) for acoustic testing meets standard ANSI S1.21-1972 and standard PN-85/N-01334 and can be used for the vibration and noise certification of machines and equipment. The chamber's sound insulating power against external noise in a frequency range of 20-20 kHz amounts to 50 dB. This insulating power ensures the elimination of disturbances originating from the drive system and from the hydraulic system supplying the tested pump. Figure 2 shows a schematic of the rig for the testing of acoustic parameters. For measurements the tested pump together with a microphone array was placed in a reverberation chamber.

The chamber is made from two similar irregular polyhedrons, one of which is placed in the other. The walls of the chamber are made of solid brick while its inner plasters are made of cement mortar.

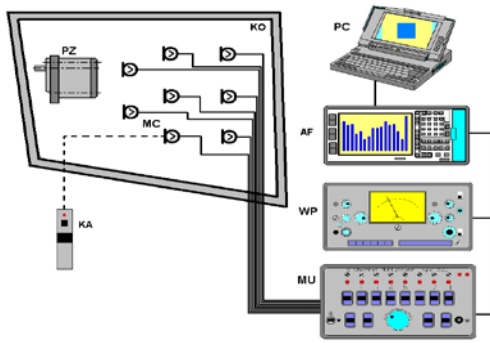


Fig. 2 Block diagram of gear pump noisiness measuring rig: KA-calibrator, MC-eight free sound field microphones, MU-multiplexer, WP-instrumentation amplifier, AF-two-channel frequency analyzer, PC-computer, PZ-gear pump, KO-chamber

### Reverberation chamber

The chamber is made from two similar irregular polyhedrons, one of which is placed in the other. The walls of the chamber are made of solid brick while its inner plasters are made of cement mortar (Figures 3). Standing waves have been eliminated owing to the different dihedral angles and the concrete plasters. The uniformity of sound field distribution in the chamber is good, being within acceptable limits starting with the octave midband frequency of 125 Hz. Eight constant measuring points have been fixed in the chamber on the basis of sound field distribution studies. In conformance with the above standards, the microphones have been fixed at a height of 1.3 m from the floor.

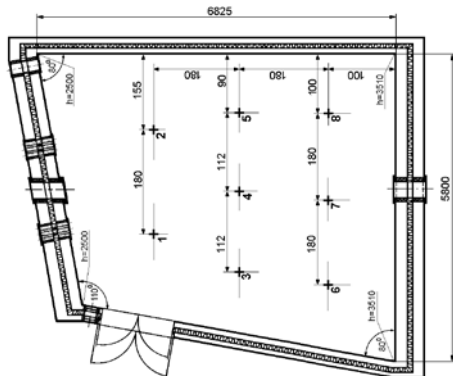


Fig. 3 Reverberation chamber

The equipment setup for measuring the noise of the gear pump placed in the diffusion sound chamber is shown in Fig. 4. Measuring microphones were positioned in eight points. The sound pressure level readings taken from them were averaged. For data reading the measuring microphones were selected by means of the multiplexer, and the sound pressure level with the spectrum was stored in the two-channel analyzer memory. The data were edited using a PC and the B&K type 5306 software.



Fig. 4 A gear pump in the acoustic chamber

## 4. Acoustic research

Acoustic measurements of an experimental version of the pump respectively for the value of discharge pressure  $p_t$ : 0, 2, 4, ..., 30 [MPa] and the frequency  $f$ : 25÷20k [Hz] have been obtained in the analysis. Table 2 shows exemplary acoustic measurements of a gear pump after tooth root undercutting for  $p_t = 12$  MP. Figure 5 presents the value of the acoustic pressure level  $L_m$ , corrected acoustic pressure level  $L_A$ , acoustic power level  $L_p$  and corrected acoustic power level  $L_{pA}$  in the function of discharge pressure  $p_t$  at a constant rotational speed of a pump shaft  $n = 1500$  rpm.

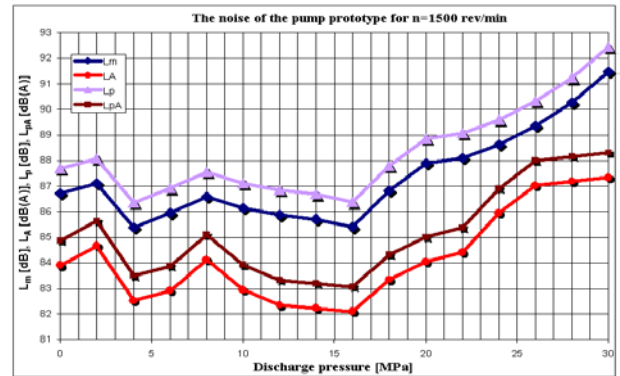


Fig. 5 The noise of the gear pump after tooth root undercutting for nominal rpm.

Figures 6 and 7 present a tertian and an octave spectrum of the gear pump after tooth root undercutting for nominal discharge pressure and nominal rotational speed.

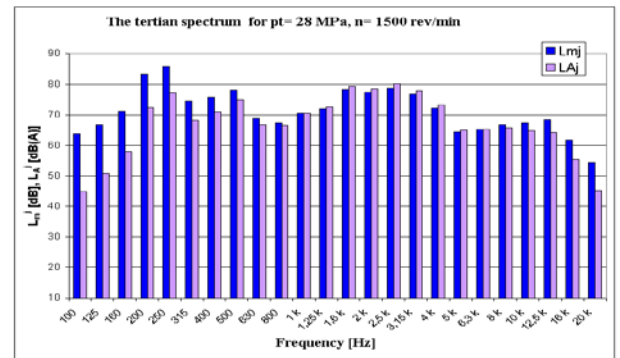


Fig. 6 The tertian spectrum of an experimental unit for nominal pressure and rotational

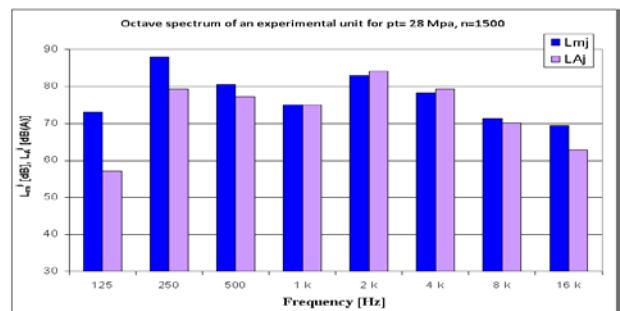


Fig. 7 The octave spectrum of an experimental unit for nominal pressure and rotational speed

The dominant level in the whole scope of discharge pressures is present in case of an octave of the centre frequency equal to 2k Hz. Table 2 compares data gathered for an experimental unit and the pump PZ4-32 TKs 186.



Table 2: Meshing parameters.

$p_t$ [MPa]	Pump test $L_{A(1)}^{2000}$	PZ4-32 TKs 186 $L_{A(2)}^{2000}$	$\Delta L_A^{2000}$
6	74,7 [dB]	79,5 [dB]	4,8 [dB]
12	74,8 [dB]	79,5 [dB]	4,7 [dB]
18	78,2 [dB]	83,6 [dB]	5,4 [dB]
24	81,0 [dB]	83,0 [dB]	2,0 [dB]
28	82,9 [dB]	83,6 [dB]	0,7 [dB]

Figure 8 compare a corrected level of the acoustic pressure  $L_A$ , and the corrected level of the acoustic power  $L_{pA}$  of an experimental unit and pump PZ4-32 TKs 186.

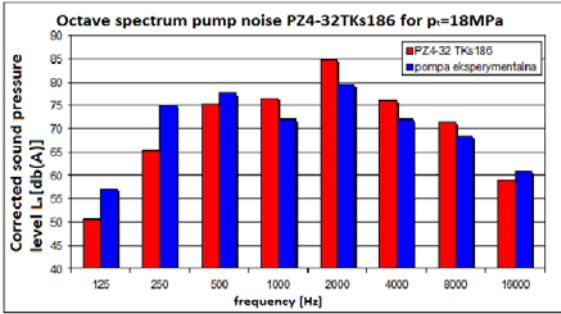


Fig. 8 The octave spectrum of an experimental unit and pump PZ4-32 TKs 186

### 5. Discrete methods of identification and classification of acoustic signal

The classification is an important stage in the analysis of acoustic properties. In this stage, properties characteristic for signals of particular microphones are compared with each other. On the basis of obtained results a decision concerning the classification of the signal properties to a given group is made [5]. Among the most often applied methods of recognising acoustic signals are: HMM (Hidden Markov Models), VQ (Vector Quantization), LVQ (Learning Vector Quantization), SOM (Self-Organising Maps), ANN (Artificial Neural Network), GMM (Gaussian Mixture Models) [14, 16], SVM (Support Vector Machines). In addition, there are classifiers based on the induction of decision trees, ML-HMM (Maximum Likelihood Hidden Markov Model) [6, 7, 8]. In a general case, the classification includes two stages: creating of patterns for recognition and identification.

#### Tree induction as classifiers of acoustic signals

A decision tree is a structure which has ordinary properties of trees in the meaning assigned to the tree in the information technology, so it is a structure composed of nodes from which branches come to other nodes or leaves. It is convenient to define tree structures in a recursive way. Assuming that a given branch  $X$  on which attributes  $a_1, a_2, \dots, a_n$  and the set of notions  $C$  of the category  $C$  are determined:

1. The leaf containing any category label  $d \in C$  is a decision tree.
2. If  $t: X \rightarrow R_t$  is a test made on the values of attributes of examples with a set of possible results  $R_t = \{r_1, r_2, \dots, r_m\}$  are decision trees, then the node containing the test  $t$ , from which  $m$  branches come out, given that for  $i = 1, 2, \dots, m$  branch  $i$  corresponds to the result  $r_i$  and leads to the tree  $T_i$ , is a decision tree.

For any node of  $n$  decision tree, by  $t_n$  we mean a test connected with it, and for each of its possible results  $r \in R_t$  by  $n[r]$  node or child leaf, to which the  $n$  branch related to the  $r$  result leads from the node. The notation described above is presented in Figure 9.

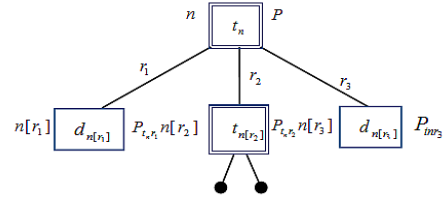


Fig. 9 A sample query "query-by-example" to the decision-making system

Information included in the set of training examples is equal to:

$$I(E) = - \sum_{i=1}^{|E|} \frac{|E_i|}{|E|} \cdot \log_2 \left( \frac{|E_i|}{|E|} \right)$$

where:

$E$  - the set of training examples

$|E_i|$  - the number of examples which describe  $i$  object

$|E|$  - the number of examples in the training set  $E$

The expected value of information after the division of the set of examples  $E$  into subsets  $E^{(m)}, m = 1, \dots, |V_a|$ , for which the attribute  $a$  has the value  $V_m$ , determined as [15]:

$$I(E, a) = \sum_{m=1, K, |V_a|, E^{(m)} \neq \emptyset} \frac{|E^{(m)}|}{|E|} \cdot I(E^{(m)})$$

where:

$|E^{(m)}|$  - the number of examples after the division of the set  $E$  in relation to the value  $m$  of a given attribute,

$|E|$  - the number of examples in the training set  $E$ .

Figure 10 presents preliminary signals processing without a filter for 8 microphones in the whole range of values of discharge pressure that is 2-30 MPa.

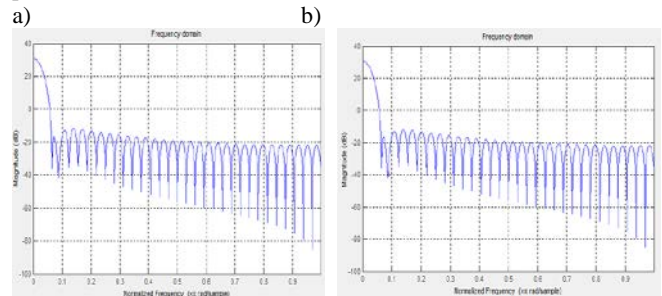


Fig. 10 Initial processing of the signals for the four microphones: a) 1, b) 3

A method of analysing a frequency spectrum has been chosen as a parametrisation method. The method using this rule is called the Burg method, the implementation of which is included among others in the range "Signal Processing Toolbox" of the Matlab programme [9]. The figure 11 shows the spectrogram for 2 microphones.

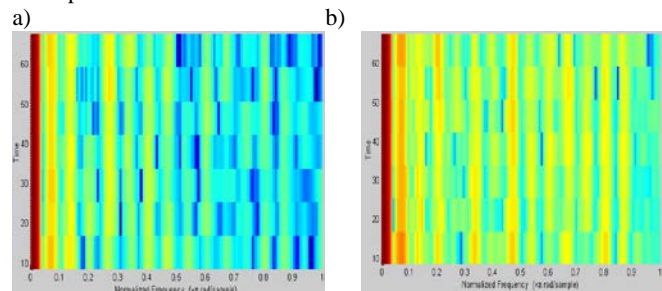


Fig. 11 The spectra of acoustic signals of four microphones a) 1 b) 3

The classification by means of induction trees has been made separately for acoustic pressure  $L_m$ , frequency  $kHz$  and discharge pressure  $MPa$ , as output attributes (wy):  $L_m(wy)$ ,  $kHz(wy)$ ,  $MPa(wy)$ . Input attributes (we) are the values of acoustic measurements registered from 8 microphones:  $microphones1(we)$ ,  $microphones2(we)$ ,  $microphones3(we)$ ,  $microphones4(we)$ ,  $microphones5(we)$ ,  $microphones6(we)$ ,  $microphones7(we)$ ,  $microphones8(we)$ . As a result of the analysis, induction trees have been generated for each parameter  $L_{mj}$ ,  $p_t$  [Mpa],  $f$  [Hz].

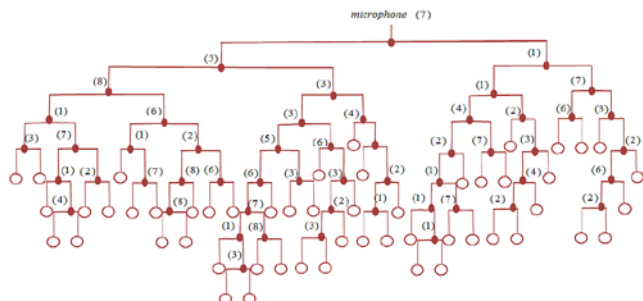


Fig. 12 The induction tree for the acoustic pressure  $L_m$  – without trimming

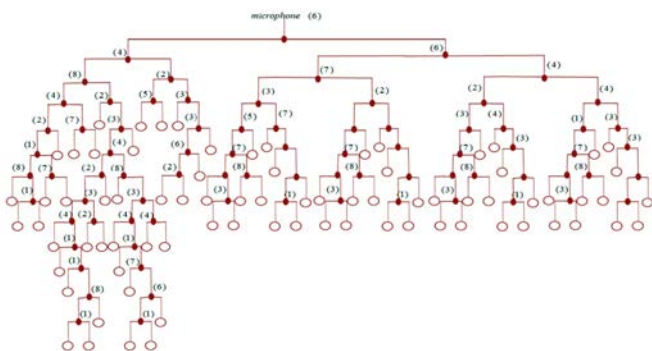


Fig. 13 A simplified induction tree for the frequency  $f$  [Hz]- the number of examples forming the tree graph- 4, tree trimming- 40%

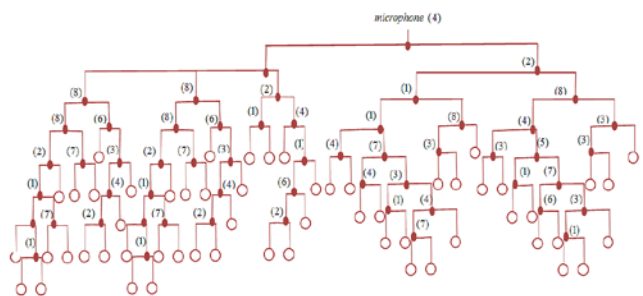


Fig. 14 A simplified induction tree for the discharge pressure  $p_t$  [Mpa]- the number of examples forming the tree graph-4, tree trimming-25%

The induction tree determines the degree of importance of the attribute from the most important one placed in the root, through classification of any example. The most important acoustic signal generated by the value of the discharge pressure is present in the microphone 4- in accordance with the tree from Figure 14 whilst the most important acoustic signal influenced by the change of frequency is generated on the microphone 6- in accordance with the tree from Figure 13. In accordance with the tree from Figure 12, the most important signal influencing the value of the acoustic pressure is the signal registered on the microphone 7.

## 6. Conclusions

In a decision tree, nodes store tests checking values of example attributes and leaves store categories assigned to them. For each of possible test results, there is one branch coming from a node to a subtree. In this way, it is possible to represent any attributes of the

hypothesis admissible for a given set. All operations were made in the real time during normal exploitation of the gear pump. On the basis of the results received from the inference mechanism, resulting from the correlation between acoustic signals measured in a continuous manner and model signals placed in the data base, there would be identification of the influence of particular signals from microphones on the chosen parameters of the gear pump after tooth undercutting

## 7. Bibliography

- [1] Barelli L., Bidini G., Buratti C., Mariani R.: *Diagnosis of internal combustion engine through vibration and acoustic pressure non-intrusive measurements*, Applied Thermal Engineering 29, 1707–1713, 2009.
- [2] Carlucci A.P., Chiara F.F., Laforgia D.: *Analysis of the relation between injection parameter variation and block vibration of an internal combustion diesel engine*, Journal of Sound and Vibration, 295, 141–164, 2006
- [3] Collective work, Techbook - OBD II & Electronic Engine Management Systems, Haynes, 2005.
- [4] Deptuła A.: *Application of multi-valued weighting logical functions in the analysis of a degree of importance of construction parameters on the example of hydraulic valves*, International Journal of Applied Mechanics and Engineering, vol.19, No.3, University Press Zielona Góra, pp. 539-548, ISSN 1425-16554, 2014.
- [5] Deptuła A., Osiński P., Radziwanowska U.: *Decision support system for identifying technical condition of combustion engine*, Archives of Acoustics, Vol. 41, No 3, 2016 [in print]
- [6] Deptuła A., Partyka M. A.: *Decision optimization of machine sets with taking into consideration logical tree minimization of design guidelines*. International Journal of Applied Mechanics and Engineering, vol.19, No.3, University Press Zielona Góra, pp. 549-561 ISSN 1425-16554, 2014.
- [7] Kirpluk M.: *Fundamentals of acoustics (in Polish)*, Wyd. NTL-M, Warszawa, 2012.
- [8] Learner, in IEEE Transactions on Evolutionary Computation, vol. 9, no.1, Feb. 2005, pp. 31–43.
- [9] Luft S.: *Basics of Engines Construction (in Polish)*, Wyd. WKŁ, Warszawa, 2010.
- [10] Osiński P., Deptuła A. Partyka M. A. : *Discrete optimization of a gear pump after tooth root undercutting by means of multi-valued logic trees*, Archives of Civil and Mechanical Engineering, vol. 13, nr 4, pp. 422-431, 2013.
- [11] Osiński P., Kolllek W.: *Assessment of energetic measuring techniques and their application to diagnosis of acoustic condition of hydraulic machinery and equipment*, Archives of Civil and Mechanical Engineering. 2013.
- [12] Wu J.D., Chen J.Ch.: *Continuous wavelet transform technique for fault signal diagnosis of internal combustion engines*, NDT&E International 39, 304–311, 2006
- [13] Wu J.D., Kuo J.M.: *An automotive generator fault diagnosis system using discrete wavelet transform and artificial neural network*, Expert Systems with Applications, No. 36, pp. 9776-9783, 2009.
- [14] Wu J.D., Kuo J.M.: *An expert system for fault diagnosis in internal combustion engines using wavelet packet transform and neural network*, Expert Systems with Applications, No. 36, pp.4278-4286, 2009.
- [15] Quinlan J. R.: *Induction of Decision Trees*, Machine Learning, 1, pp. 81-10, 1986
- [16] Xuo L., Jelinek F.: *Probabilistic classification of HMM states for large vocabulary*, [in:] Proceedings of ICASSP, 2044–2047, Phoenix, USA, 1999.

# DIRECTIONS OF DEVELOPMENT MECHATRONIC DEVICES TO MOVE IN PIPELINES

## НАПРАВЛЕНИЯ РАЗВИТИЯ МЕХАТРОННЫХ УСТРОЙСТВ ДЛЯ ПЕРЕМЕЩЕНИЯ В ТРУБОПРОВОДАХ

Аврука И. С.

Национальный университет водного хозяйства и природопользования – Ровно, Украина

e-mail: irina.avruka@mail.ru

**Abstract:** Mechatronic devices are one of the most important innovative devices to achieve automated operation of process pipelines, including their inspection, cleaning, repair, etc. In order to determine what kind of technology is recommended for a particular pipeline, it is necessary to conduct research and analysis of existing types of mechatronic devices.

Known mechatronic devices can be divided into 8 types of robotic system, namely "spider", "worm", with automotive principle "engine - wheel", crawler, "feet", snakelike ("micro snake"), spiral, cylindrical.

In this paper analyzed the known types of mechatronic devices, based on what is selected, according to the author, the most universal, the principle of operation is based on a prototype bionic-worm (Lumbricidae family). Proposed innovation to elaborate mechatronic device that can perform multi-functional tasks in the maintenance and repair of sewer pipes and process piping.

**KEYWORDS:** MECHATRONIC DEVICE, BIONIC PROTOTYPES, MAINTENANCE AND REPAIR OF PIPELINES.

Нами проведен сравнительный анализ различных типов мехатронных устройств (МУ), которые могут перемещаться в трубопроводах для наиболее часто встречающихся диаметров труб, результаты которого приведены в следующей таблице.

**Таблица 1**

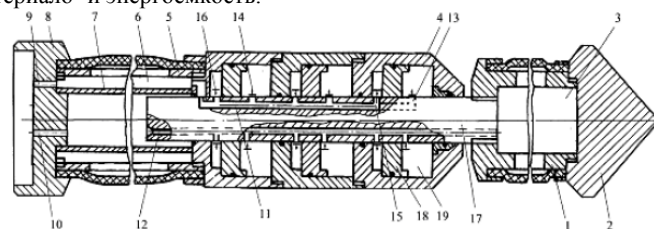
Сравнительные характеристики мехатронных устройств

Тип мехатронного устройства	Преимущества и недостатки					Размер трубопровода (мм)
	Автономность	Ревёрсивность	Значительные тяговые усилия	Возможность установок оборудования	Передвижения в трубах с углом 90°	
Паук [4, 5, 6]	+	+	-	+	-	25-100
Червяк [1, 2, 3]	+	+	+	+	+	50-300
Двигатель-колеса [7, 8]	+	-	-	+	+	>300
Гусечные [10]	-	-	-	-	+	300-600
Ноги [11, 12]	+	-	-	-	-	>150
Змееподобные [13]	-	+	-	+	+	18-100
Спиральные [9]	+	-	-	-	-	40-170
Цилиндрические [14]	+	+	-	-	-	80-1000

Исходя из анализа представленного в таблице, нами выбран червякоподобный тип МУ для дальнейшей доработки, поскольку он отличается возможностью создания высоких тяговых усилий, реверсивностью и применимостью для широкого диапазона диаметров трубопроводов.

Известно реверсивное подземно-подвижное устройство, которое используется для образования полостей в почве и создания линейно-протяженных объектов [1]. Недостатком подземно-подвижного устройства является недостаточная гибкость, не позволяющая двигаться по криволинейной

траектории, а также конструктивная сложность и высокая материало- и энергоёмкость.



**Фиг. 1.** 1 - носовая часть, 2 – гидродвигатель, 3 - перфорированный цилиндр, 4 - эластичная оболочка, 5 - рабочее тело, 6 – поршень, 7 – шток, 8 – соленоид, 9 – сердечник, 10 - опоры кочения, 11 - электрический кабель, 12 – блок, 13 – пружина, 14, 15 - ограничитель хода, 16 – переключатель, 17 - подшипник скольжения, 18 - гофрированный цилиндр, 19 - пружина растяжения, 20 - задняя стенка носовой части.

Принцип работы реверсивного подземно-подвижного устройства изображенного на фиг. 1 заключается в следующем.

При поступлении энергоносителя по патрубку 9, поскольку радиальные каналы 15 открыты, а каналы 13 закрыты, то под действием последнего увеличиться в объеме эластичная оболочка задней фиксирующей камеры 6 до упора в стенку предварительно образованной почвенной полости, в результате чего корпус подземно подвижного устройства фиксируется. Одновременно с этим, энергоноситель давит на левую плоскость поршней 18, в результате чего носовая часть 1, преодолевая сопротивление почвы, переместится вперед на отрезок пути, равный ходу поршня. При поступления по патрубку 10 увеличиться в объеме эластичная оболочка передней фиксирующей камеры (задняя, при этом уменьшится в объеме к предыдущему размеру). В результате этого зафиксируется носовая часть 1, одновременно с этим энергоноситель будет действовать уже на правую плоскость поршней 18, которые вместе со штоком удерживаются передней фиксирующей камерой, и на дно каждого из силовых модулей 19. Это приведет к тому, что корпус устройства подтянется к зафиксированной носовой части. В результате этого данное устройство переместится вперед на отрезок, названный "шагом", а периодическая смена шагов приведет к дискретному движению вперед.

В случае необходимости, можно подать команду на обратное перемещение подземно-подвижного устройства [2].

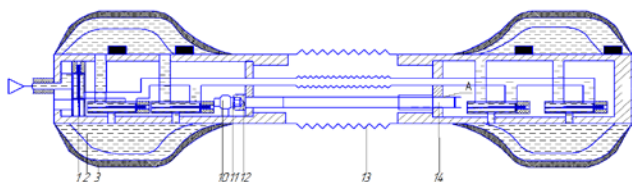
Fang Н.В. и др. [5] разработали серводвигатель, основанный на исполнительном механизме, который имитирует альтернированное удлинение и сокращение одного дождевого червячного сегмента. Сервопривод с приводом от двигателя, провода и ленты из пружинной стали применяются в каждом сегменте робота для имитации продольных и круговых мышц дождевого червя. Каждый сегмент робота соединенных последовательно способен сокращаться и расслабляться, как сегмент тела дождевого червя.



**Фиг. 2.** Мехатронное устройство червячного типа:  
а) сравнительный разрез дождевого червяка и одного сегмента МУ;  
б) конструкция МУ.

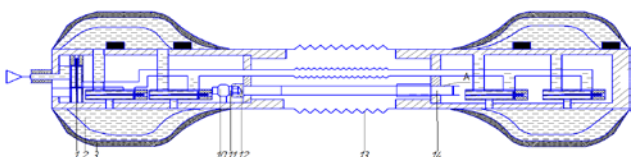
Одиночный сегмент этого робота состоит из двух прозрачных акриловых пластин, а именно пластины головки и концевой пластины, серводвигатель с управлением рожка, два сервопривода с приводом от двигателя и восемь пружинных стальных лент. Каждый сегменты могут быть приведены в действие независимо друг от друга. Недостатком является то, что при наличии загрязнений и наростаний в трубе устройство может зацепиться за выступы и прекратить дальнейшее движение. Недостатком данного серводвигателя является невозможность возвращения назад.

Нами предложен свой вариант МУ для перемещения технологического оборудования в трубопроводах. Контактным сегментом, которого являются пневматические подушки, каждая из которых рассчитана на определенный диаметр трубы. Ниже приведен рисунок и описание мехатронного устройства.



**Фиг. 3.** Мехатронное устройство для перемещения в трубопроводах.

Мехатронное устройство для перемещения в трубопроводах состоит из носовых 15, 16 и хвостовых 2, 4



фиксирующих пневмокамер, поверх которых смонтировано упругую оболочку 3 для дополнительной защиты и средней части которая находится в гофрированном корпусе 13. Для перемещения устройства по горизонтали используется гибкая муфта 12, которая вращается реверсивным двигателем постоянного тока 10 и вкручивается в гайку 14. Для передачи крутящего момента вала двигателя используется муфта 11.

Разработан модернизированный тип МУ является более гибким, надежным и пригодным для применения в загрязненных средах. Данное мехатронное устройство, способное выполнять осмотр, чистку и техническое обслуживание труб для чего дополняется платформой для быстрой замены наборов сенсоров состояния трубопровода и оборудованием для его ремонта.

#### Литература:

1. Патент України на корисну модель No42104, E02F 5/18. Реверсивний підземнорухомий пристрій / Древецкий В. В., Кованько В. В., Кованько О. В. –Опубл. 25.06.09, Бюл. 12.
2. Аврука І. С. Мехатронний пристрій для переміщення в трубопроводах / І. С. Аврука, С. В. Уманець // Вісник інженерної академії України. –Київ, 2015. –Вип. 2/2015. –С. 40-43.2.
3. R. Bischoff and T. Guhl, "The strategic research agenda for robotics in Europe," IEEE Robotics & Automation Magazine, vol. 17 (1), pp. 15-16, 2010.
4. <http://www.pub.gov.sg/dtss/PublishingImages/>, November 2014
5. H. Fang, C. Wang, S. Li, J. Xu, and K. W. Wang, "Design and experimental gait analysis of a multi-segment in-pipe robot inspired by earthworm's peristaltic locomotion," Proc. of SPIE, vol. Vol. 9055, 90550H, 2014.
6. W. Neubauer, "A spider – like robot that climbs vertically in ducts or pipes", Proc. IEEE RSJ International Conference on Intelligent Robots and Systems, 1994, pp. 1178-85.
7. M. Maramatsu, N. Namiki and R. Koyama, "Autonomous mobile robot in pipe for piping operations", Proc. IEEE RSJ International Conf. on Intelligent Robots and Systems, 2000. pp. 2166-71.
8. J. F. Archila and M. Becker, "Study of Robots to Pipelines, Mathematical Models and Simulation," IEEE Latin American Robotics Symposium, pp. 18-23, 2013.
9. M. Horodincea, I. Dorftel, E. Mignon and A. Preumont, "A simple architecture for in – pipe inspection robots", Proc. International Colloquium on Mobile and Autonomous Systems, 2002, pp. 61-4.
10. N. Truong-Thinh, N. Ngoc-Phuong, and T. Phuoc-Tho, "A study of pipe-cleaning and inspection robot," IEEE International Conference on Robotics and Biomimetics, 7-11 December 2011.
11. [http://www.bostondynamics.com/robot\\_bigdog.html](http://www.bostondynamics.com/robot_bigdog.html), November 2014.
12. M. Raibert, K. Blankespoor, G. Nelson, R. Playter, and t. B. Team, "BigDog, the Rough-Terrain Quaduped Robot," 2008.
13. C. Walter, J. Saenz, N. Elkmann, H. Althoff, S. Kutzner, and T. Stuerze, "Design Considerations of Robotic System for Cleaning and Inspection of Large-Diameter Sewers," Journal of Field Robotics vol. 29(1), 2012.
14. L. A. Mateos, M. R. y. Dominguez, and M. Vincze, "Automatic Inpipe Robot Centering from 3D to 2D Controller Simplification," 2013 IEEE/RSJ International Conference on Intelligent Robots and Systems (IROS), 3-7 November 2013.

# MATERIALS FOR ELECTROMAGNETIC INTERFERENCE SHIELDING

Ass.prof. PhD Kamelia Ruskova<sup>1</sup>, Assos. Prof. PhD Ljudmila Taneva<sup>2</sup>, Assos. Prof. PhD Alexandar Lirkov<sup>1</sup>  
 Technical University, Sofia, Bulgaria<sup>1</sup>, South-West University "Neofit Rilski", Blagoevgrad, Bulgaria<sup>2</sup>

e-mail: kruskova@tu-sofia.bg

**Abstract:** The electronic devices are everywhere in our life and for their proper performance it is very important to have them protected from Electromagnetic Interference (EMI). Sources of EMI could be some components of the device, nearby conductors, other devices, high voltage lines, atmosphere static discharges, etc. One of the main methods for protection from external EMI is by shielding the whole device and for this purpose are used various materials. In this paper are presented two types of materials used for EMI shielding - polyester silk with electrolysis metal coating and nitrile butadiene based compounds (NBR) containing as a filler natural magnetite. For both materials is investigated the EMI absorption for electromagnetic waves in the band (8-12 GHz) and at 2380 MHz.

**Keywords:** ELECTROMAGNETIC INTERFERENCE, SHIELDING, FILLED ELASTOMERS, PLASTIC ELECTROMAGNETIC INTERFERENCESHIELDING

## 1. Introduction.

Shielding from EMI is a complex process associated with propagation of electromagnetic waves in environments with various electromagnetic properties and their interaction with the object, characterized with reflection, refraction, scattering and absorption. For quantitative evaluation of the effectiveness of the protection is used shielding coefficient (S) equal to the ratio of the amplitude of the intensity of the electric or magnetic field at any point in the shielded area compared to the amplitude of the intensity of the field at the same point in the absence of the shield:

$$(1) S_E(\text{dB}) = 20 \lg \frac{E_{\text{oe}}}{E_o} \quad (2) S_H(\text{dB}) = 20 \lg \frac{H_{\text{oe}}}{H_o}$$

When an electromagnetic wave reaches the shield, one part of it is reflected and another penetrates it undergoing absorption and multiple internal reflections (MIR) as ultimately some portion of it passes through the shield. All processes of reflection and absorption lead to loss of electromagnetic energy:

$$(3) A/dB = A/refl. + A/abs. + A/MIR$$

The energy loss from absorption (absorption loss) does not depend on the type of the electromagnetic waves (electric or magnetic field) and goes up with increasing the waves frequency and the thickness of the shield, as well as with increasing the magnetic permeability of the material from which it is made. [1] The energy loss from reflection (reflection loss) depends on the ratio of the impedance of the waves and the impedance of the shield material. It is larger for electric fields, decreases with increasing waves frequency, and does not depend on the thickness of the shielding material. Multiple internal reflections always reduce the shielding effect because each reflection inside the screen allows a small amount of energy to pass through it.

## 2. Shielding methods.

Electromagnetic interference (EMI) is emitted by every wire or electronic device associated with electrical energy transferring, sun radiation, high voltage atmosphere discharge and other sources. The rapid development of the electronic industry during the second half of XX century resulted in implementation of electronic devices everywhere. Each of them is a source of EMI, jeopardizing the normal functionality of the electronic devices, thus bringing out in the foreground this problem.

Basically the protection from undesired signals emitted from electronic devices could be achieved by three methods:

proper design; electromagnetic shielding of separate device modules; shielding of the whole device. The last method is the easiest for realization and economically profitable especially because of the possibility for plastic shielding realization. The frequency interval above 10 GHz is radio frequency and is the most common in the everyday life.

For electromagnetic shielding are used various materials - metal foils, metal grid, cloth with metal knitted fibers, materials with electro conductivity fibers and absorbents - wood pulp, micro porous rubber, polyvinylchloride resins with fillers, silicon rubber, graphite filled textolite, etc. (tab.1)

**Table 1:** Characteristics of some shielding methods

Method	Width, $\mu\text{m}$	Resistance, $\Omega/\square$	Shielding, dB
Arc sputtering of zinc	15-25	0,03	50-60
Spraying of molten zinc	25	4,0	50-60
Acrylic paint with nickel powder	50	0,5-2,0	30-75
Acrylic paint with silver powder	25	0,04-0,1	60-70
Acrylic paint with copper powder	25	0,5	60-70
Paint with graphite filler	25	7,5-20	20-40
Cathode sputtering	0,75	1,5	70-90
Galvanic metalizing	0,75	0,1	85
Chemical metallization /copper-nickel/	1,25	0,03	60-70
Chemical metallization /silver/	1,25	0,5	70-90
Vacuum metalizing	1,25	5-10	50-70
Ion deposition of copper	1,0	0,01	50
Conductive plastic /nylon containing 40% carbon/	-	75-100	40-60

Nowadays microwave absorbers are mainly used for:

-protection of the environment and people from the adverse influence of high frequency electromagnetic radiation due to industrial and other sources;

-technical purposes like eliminating undesired signals and noise in radio and television technique; in anechoic chambers; antiradar camouflage of mobile and fixed military structure and objects for reducing or altering the radar signature.

The main microwave absorbers' requirements are minimum reflection and maximum absorption of the electromagnetic energy. The ideal absorber has broad frequency range of the absorbing energy, excellent weather stability, light weight, characteristic reliability and capability to work in a broad temperature range.

### 3. Measurement of the attenuation coefficient of metalized fabrics

The measurement of the attenuation or shielding effect of the metalized fabric was conducted within 8-12 GHz band. The samples were installed between two coaxial waveguides for this frequency range - R100 (3x10mm) and pressed with equal force. The signal was transmitted from sweep generator HP 8620C and its changes were monitored on spectrum analyzer HP 8559A (both sets - Hewlett Packard make). The fabric samples size is 50mmX50mm. They are pressed with equal force between the two waveguides fully covering their openings.

The attenuation of the tested sample is calculated as follow:

$$(4) A = 10 \lg P_{pass} / P_{out}, \text{ where}$$

$P_{pass}$  - power of the electromagnetic waves that passed through the shield;  $P_{out}$  - power of the electromagnetic wave outside the shield;  $P_{out} = 4 - 5 \text{ mW}$ .

### 4. Experimental results.

The paper presents two types of shielding materials. The first one is made of 100% polyester silk (K167 dtex.) with electrolysis metal coating - "sandwich" type construction - Cu/Ni-P [1].

Data was collected according BDS – specific area mass 84 g/m<sup>2</sup>, breaking strength on the basis 74,7 daN, weft-72,2 daN, extensibility of the base and by weft - 400 n/10 cm, filling 77%, coefficient of drape 23%. With appropriate combination of thickness EMI attenuation above 50 dB is achieved in the band of the civil radiolocation (8-12 GHz) and at 2380 MHz. The received data of the experiments is given on tab.2, tab.3, tab.4 and tab.5.

**Table 2:** Electrical resistance of a square ( $\Omega/\square 10\text{cm}$ ) depending on the conditions of the chemical metallization

Chemical metallization	Direction of the measurement	Duration (min)				
		10	20	30	45	60
Coppering	by base	0,12	0,09	0,075	0,05	0,03
	by weft	0,24	0,12	0,08	0,055	0,045
Coppering +10min nickel-plating /Ni-P/	by base	0,36	0,06	0,045	0,03	0,03
	by weft	0,56	0,07	0,06	0,04	0,04

**Table 3:** Shielding effectiveness (attenuation, dB) depending on the chemical metallization type. Signal level 10mW, 10GHz

Chemical metallization	Duration (min)				
	10	20	30	45	60
Coppering	42	62	65	67	67,5
Coppering +10min nickel-plating /Ni-P/	57	65	66	71	72

**Table 4:** Shielding effectiveness (dB) depending on the duration of the nickel-plating of fabric A

Electrolyte for nickel-plating	Frequency, GHz	5min	10min	20min	30min
alkaline pH=9,0	8,06		39,5	51,4	55,5
	9,46	29,1	38,1	47,8	52,3
	12,06	26,1	36,0	44,5	49,3
acid pH= 5,0	8,06	38,5	47,6	58,6	-
	9,46	36,8	43,8	49,6	-
	12,06	36,1	40,2	46,8	-

**Table 5:** Shielding effectiveness (dB) depending on the duration of nickel-plating on fabric B (calendered)

Electrolyte for nickel-plating	Frequency, GHz	5min	10min	20min	30min
alkaline pH=9,0	8,06		35,4	50,6	55,6
	9,46	25,8	34,9	48,1	52,3
	12,06	24,5	33,6	42,9	46,8
acid pH= 5,0	8,06	25,3	35	49,3	51,2
	9,46	24,3	33,8	46,7	49,4

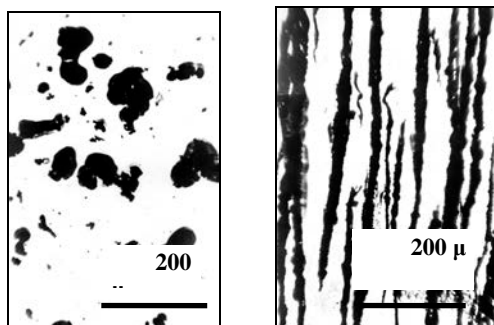
There were also investigated the properties of thin elastomeric microwave absorbers. The samples were built on the basis of nitrile rubber, containing natural magnetite (particle size below 10 $\mu$ ) as absorption active filler.

The mixing process of the rubber with the filler was carried out by Brabender Plasticorder at 50 °C. The rubber-filler ratio was 10-60 phr. The films (average thickness of 100  $\mu$ ) were prepared from 2mass% 1,2-dichloroethane solution of the rubber-filler composition. Magnetic field with induction of 0,60T was applied for the period of 20 minutes during the film formation process. The magnetic field induction was controlled by teslameter. The samples were placed parallel and perpendicularly to the magnetic field lines of force.

The optical microscopy pictures give us information about the structure of non modified magnetite filled samples and another one modified with EMF. (Fig.1.) In presence of magnetic field we can

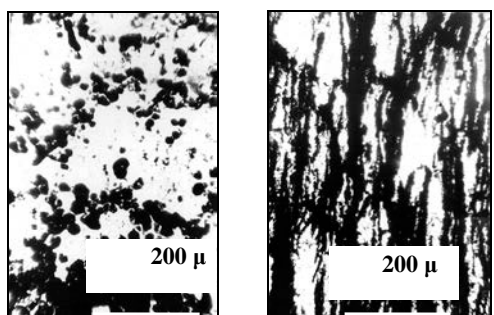
see an organization in filler particles ordering, which increases the probability the propagating wave to meet on its way a filler particle instead of polymer matrix material. This probability in the absence of EMF, when the structure has the usual disordered nature and the filler particles are situated chaotic is considerably less.

**Fig.1:** Optical microscope pictures ( $\times 70$ ) of nitrile rubber films, containing different concentrations of magnetite ( $H=0$ , without magnetic field application;  $H>0$ - with magnetic field application)



a) 10 phr  $Fe_3O_4$ ,  $H=0$

b) 10 phr  $Fe_3O_4$ ,  $H>0$



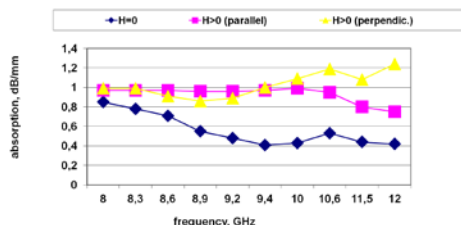
c) 50 phr  $Fe_3O_4$ ,  $H=0$

d) 50 phr  $Fe_3O_4$ ,  $H>0$

Fig. 2 shows the absorption of electromagnetic waves in the range 8-12 GHz for our samples. The effects concern the influence of the magnetic field on the magnetite distribution in the rubber matrix. The material is magnetically soft and its particles orientation is highly dependent on external magnetic fields.

The measurements were performed in a waveguide line. There were three measured absorbing samples - one control and two magnetically modified. For the first modified sample the direction of the external magnetic field is parallel with the wave in the waveguide. For the second sample it's perpendicular. The absorption of the no modified sample is the lowest. The sample modified with a perpendicular magnetic field has the highest absorption.

**Fig. 2.** Absorption of electromagnetic waves in the 8-12 GHz range by films based on nitrile rubber and natural magnetite filler.



The application of magnetic field during sample preparation affects the filler particles ordering causing secondary structures formation guided by the direction of the magnetic field lines of force.

The change in absorption of the electromagnetic waves of the elastomeric microwave absorbers under the influence of an external magnetic field is due to the orientation phenomena in the elastomeric matrix, as well as the arrangement of the particles of the absorption-active filler in a favorable manner for better interaction between it and the electromagnetic waves falling on the shield [2].

## 5. Conclusions.

The researched materials were tested for effectiveness of the shielding effect. The attenuation was measured after application of magnetic field to the elastomeric microwave absorbers in both ways of operation of the electromagnetic field - perpendicularly and parallel to the sample in the range 8-12 GHz. The experiments proved that the tested materials have better shielding effect, compared to the control sample. For both materials the absorption in both directions was higher for the whole range 8-12GHz than the one of the sample. The observed improvement of the shielding effect is due to the interaction of the electromagnetic waves and the filler-magnetite. The oriented arrangement and resulting structure of the particles of the active compound under EMF influence leads to increase of the effect of shielding [3,4].

## 6. Literature.

- [1] Lirkov Al., Dobreva E., (1994), Method for plastic electromagnetic interference shielding, Patent of R. Bulgaria №43790/23.02.1994.
- [2] N.Dishovski, K. Ruskova, I. Radulov (2001), 36, 35-45, „In situ” magnetic modification of polar elastomers, Materials Research Buletin
- [3] Alexeev, A., Kornev, A. (1987), Magnetic elastomers, Khimia, Moscow.
- [4] Emerson & Cuming, (1987), Microwave Absorbers Guide.

# ИЗСЛЕДВАНЕ НА ПОДАВАТЕЛНИ ЕЛЕКТРОЗАДВИЖВАНИЯ ЗА КЛАС МЕТАЛОРЕЖЕЩИ МАШИНИ

## STUDY OF FEED ELECTRIC DRIVES FOR A CLASS OF MACHINE TOOLS

### ИССЛЕДОВАНИЕ ЭЛЕКТРОПРИВОДОВ ПОДАЧИ ОДНОГО КЛАССА МЕТАЛЛОРЕЖУЩИХ СТАНКОВ

Гл. ас. д-р инж. М. Жилевски, Проф. д-р инж. М. Михов  
Технически университет – София, България  
E-mail: mzhilevski@tu-sofia.bg, mikhov@tu-sofia.bg

**Abstract:** This paper examines the features of feed electric drives for a class of milling machines with digital program control. The requirements that should be met with these electric drives are formulated. Practical settings of the represented DC and AC electric drives have been carried out. Experimental studies have been conducted showing that the selected AC drive with permanent magnet synchronous motor satisfies the necessary requirements. The research carried out and the results obtained can be used in the development of such electric drives for the studied class of machine tools.

**KEYWORDS:** MILLING MACHINES, FEED ELECTRIC DRIVE, DC DRIVES, AC DRIVES

#### 1. Въведение

Подавателните електрозадвижвания се използват за позициониране на режещия инструмент и обработвания детайл на желаното място и участват в процеса на машинна обработка. По тази причина, тяхната позиционна точност и скорост влияят съществено върху качеството и производителността на метало-режещите машини [1].

Към тези задвижвания се предявяват високи изисквания, които може се формулират по следния начин [2], [3]:

- широк диапазон на регулиране на скоростта;
- добри динамични показатели;
- плавно регулиране на скоростта в двете посоки;
- точност при зададени траекториите на движение;
- осигуряване на необходимият въртящ момент;
- сигурност;
- икономичност и други.

При разработването на подавателни електрозадвижвания за метало-режещи машини е необходимо да се отчетат редица съществени фактори, такива като:

- особеностите на технологичния процес;
- вида на обработваните материали;
- параметрите на използваните инструменти;
- избраните механични предавки.

Методики за избор на линейни и ъглови подавателни електрозадвижвания, приложими както за постояннотокови, така и за променливотокови системи е описана в [4], [5].

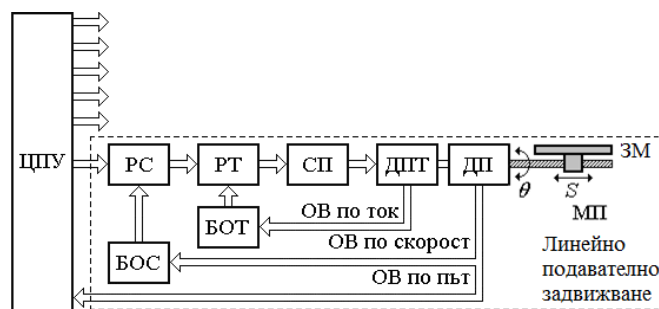
Математическото моделиране и компютърно симулиране предлагат ефективни начини за изследване на системите за задвижване при различни динамични и статични режими на работа, особено когато не е възможно или е неудобно да се извършват такива тестове в лабораторни или промишлени условия. Резултати от изследване посредством компютърно симулиране на подавателни електрозадвижвания са отразени и анализирани в [6], [7], [8].

В тази статия са представени резултати от изследвания на подавателни електрозадвижвания с двигатели за постоянен ток, предназначени за един вид фрезови машини с ЦПУ, които имат 3 линейни и 2 ъглови подавателни координатни оси [9]. Направен е и сравнителен анализ по основните показатели.

#### 2. Постояннотокови електрозадвижвания

Блоковата схема на едно от изследваните линейните пода-

вателни електрозадвижвания с двигатели за постоянен ток (ДПТ) за една координатна ос е дадена на фиг. 1. Използваните означения са следните: ЦПУ – система за цифрово-програмно управление; РС – регулатор на скорост; РТ – регулатор на ток; СП – силов преобразувател; ДПТ – двигател за постоянен ток; ДП – инкрементален датчик на път; МП – механична предавка; ЗМ – задвижван механизъм;  $\theta$  – ъгъл на завъртане на вала на двигателя;  $S$  – линейно преместване по съответната координатна ос. Схемата е триконтурна, с подчинено регулиране на променливите котвен ток, ъглова скорост и ъглов път.



Фиг. 1. Подавателно електрозадвижване с ДПТ.

Разработването на подходящо подавателно електрозадвижване се осъществява в следната последователност:

1. Създаване на методика за избор на базата на поставените изисквания към задвижването, като се отчитат особеностите на процеса фрезване, вида на обработвания материал, параметрите на използваните инструменти и типа на механичните предавки [10], [11].
2. Провеждане на съответните изчислителни процедури по методиката.
3. Извършване на технико-икономически анализ на възможните варианти за електрозадвижване с отчитане на каталожните данни от фирми производители [12], [13], [14].
4. Съставяне на модел на електрозадвижването за компютърно симулиране.
5. Разработване на стенд за експериментални изследвания.
6. Експериментално уточняване на параметрите, необходими за моделирането.
7. Оптимизация и настройка на регулиращите контури.
8. Провеждане на изследвания посредством компютърно симулиране при различни настройки, задаващи и смущаващи въздействия.



9. Подробни експериментални изследвания в съответните динамични и статични режими на работа за оценка на действителните показатели.

Оптимизацията на регулиращите контури и настройката на съответните регулатори на системата се извършва, като се започне от най-вътрешният контур (по тока в котвата). След това се преминава към следващия контур (по скоростта) и накрая се оптимизира най-външния контур, който е по основната координата (по позицията) [15].

Получената предавателна функция на регулатора на котвения ток, осигуряваща пререгулине под 5%, е следната:

$$(1) \quad W_{pm}(p) = \frac{R_{a\Sigma}(T_{a\Sigma}p + 1)}{K_n K_{om} a_m T_{um} p},$$

където:  $R_{a\Sigma}$  е сумарно активно съпротивление на котвената верига;  $T_{a\Sigma}$  – сумарна електромагнитна времеконстанта;  $K_n$  – коефициент на усилване на силовия преобразувател;  $K_{om}$  – коефициент на обратната връзка по ток;  $a_m$  – коефициент, влияещ върху показателите на контура;  $T_{um}$  – малката времеконстанта на токовия контур, неподлежаща на компенсиране.

Предавателната функция на регулатора на скорост в този случай е получена в следния вид:

$$(2) \quad W_{pc}(p) = \frac{1}{\frac{a_c T_{mc} p (T_{mc} p + 1)}{K_m K_{oc} R_{a\Sigma} / K_{om}} + T_{mc} p} = \frac{K_{om} T_{m\Sigma}}{K_m K_{oc} R_{a\Sigma} a_c T_{mc}},$$

където:  $T_{m\Sigma}$  е сумарна електромеханична времеконстанта;  $K_m$  – предавателен коефициент на двигателя;  $K_{oc}$  – коефициент на обратната връзка по скорост;  $a_c$  – коефициент, влияещ върху показателите на контура;  $T_{mc}$  – малката времеконстанта на скоростния контур, неподлежаща на компенсиране.

Предавателната функция на регулатора на път се представя с израза:

$$(3) \quad W_{pn}(p) = \frac{2K_{oc} \varepsilon_{cn \max}}{K_{on} \omega_{nom}},$$

където:  $\varepsilon_{cn \max}$  е максималния темп на намаляване на скоростта;  $K_{on}$  – коефициент на обратната връзка по път;  $\omega_{nom}$  – номиналната скорост на двигателя.

При конкретната настройка на позиционното електрозадвижване, заложеното максимално бързодействие може да бъде ограничено по технологични причини.

### 3. Променливотокови електрозадвижвания

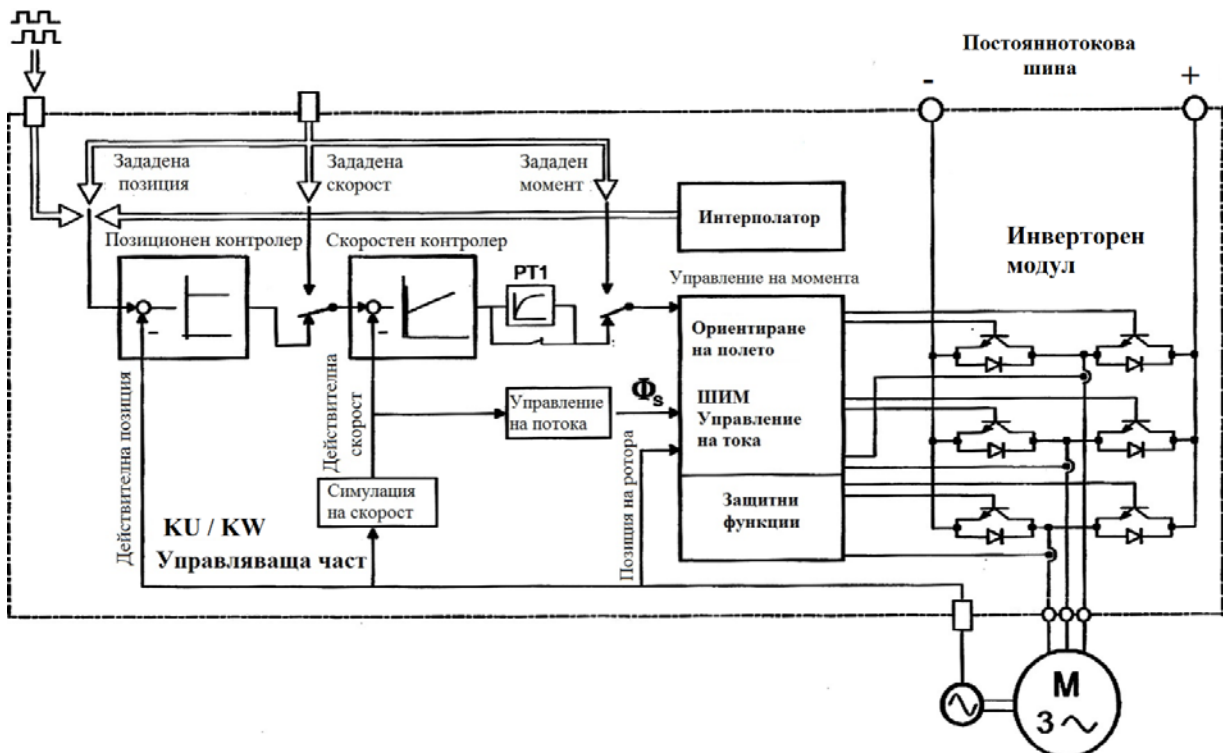
На базата на формулираните изисквания, посредством осъществените изчислителни процедури по разработената методика [4], е избрана променливотокова система за подавателно електрозадвижване на фрезова машина с ЦПУ.

Функционалната схема на изследваното променливотоково електрозадвижване със синхронен двигател, възбуден с постоянни магнити (СДПМ) [12], [13] е дадена на фиг. 2.

Използваният двигател е от високо-моментната серия синхронни мотори ДТ на фирмата АМК с вграден енкодер за обратна връзка. Тези двигатели осигуряват широка гама от въртящи моменти и мощности, имат висока претоварваща способност и много добра динамика. Двигателите от посочената серия са подходящ вариант за подавателни електрозадвижвания за разглеждания клас фрезови машини.

Сериите на АМК - КУ и КЕ/КВ се използват за управление на променливотокови двигатели, като те са идентични помежду си като конструкция и функционалност. Управляващата част се реализира чрез контролерска карта, която осигурява изцяло цифрово управление. Със съответни параметри се оказва типа на използвания променливотоков двигател и се извършват всички необходими оптимални настройки за конкретно избраното електрозадвижване.

Основните функции, които осигурява представената от АМК управляваща част, са следните: векторно управление, честотно управление, оценка и наблюдение на енкодера, управление по момент, скорост и позиция и други [12].



Фиг. 2. Подавателно електрозадвижване със СДПМ.

Основният елемент в управляващата част на изследваното променливотоково електрозадвижване е микропроцесорът, който изчислява периодично моментните стойности на необходимите токове, които след това се подават в трите статорни намотки чрез инверторния модул, като се отчитат зададената стойност, действителните стойности на фазните токове, както и позицията на ротора.

Управляващите контури по скорост и позиция са реализирани посредством микропроцесор. Системата за управление определя действителните стойности за скоростта и позицията от сигналите на енкодера на двигателя [14]. Осъществява се векторно управление с ориентиране на полето по роторното потокосцепление.

#### 4. Експериментални изследвания и анализ

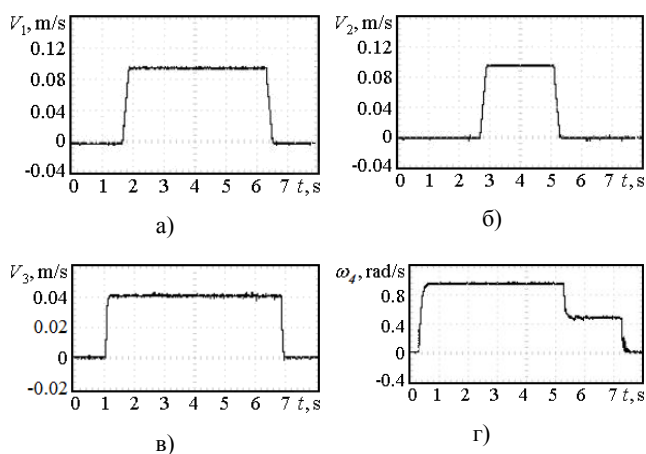
За осъществяване на необходимите експериментални изследвания е разработен стенд за настройка и изследване на системите за електрозадвижване.



Фиг. 3. Настройка на подавателно електрозадвижване.

Провеждане на експериментално изследване и оптимална настройка на едно електрозадвижване за подавателно движение е илюстрирано на фиг. 3.

На фиг. 4 са представени някои осцилограми от изследванията на подавателни постояннотокови електрозадвижвания, получени експериментално при различни настройки на регулиращите контури за съответните линейни и ъглови координатни оси.



Фиг. 4. Осцилограми на електрозадвижвания с ДПТ.

Траекторията на движение, показана на фиг. 4а е снета за първата координатна ос (x) при зададена линейна скорост

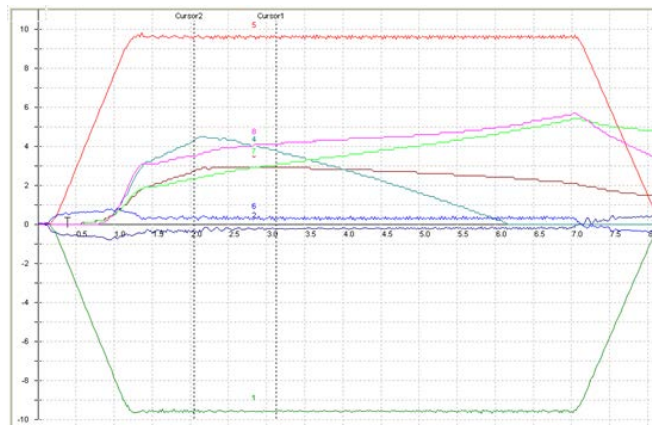
$$V_{13} = 1 \text{ m/s} .$$

На фиг. 4б е представена траектория на движение при изследване на втората координатна ос (y).

На фиг. 4в е дадена траектория, получена експериментално за третата координатна ос (z) при движение със зададена скорост  $V_{33} = 0.04 \text{ m/s}$  .

На фиг. 4г е показана осцилограма на скоростта за четвъртата координатна ос (въртящата се маса), получена при преминаване от зададена скорост на въртене  $\omega_{431} = 1 \text{ rad/s}$  към по-ниска стойност  $\omega_{432} = 0.5 \text{ rad/s}$  .

На фиг. 5 са представени някои от получените резултати при експериментално изследване на променливотокова система за електрозадвижване със СДПМ. Илюстрирано е осъществяването на позиционен цикъл със зададено разстояние на преместване от  $S_3 = 0.49 \text{ m}$  и въртане със същата скорост в изходната позиция.



Фиг. 5. Осцилограми на електрозадвижване със СДПМ.

Снемането на показаните характеристики се извършва на базата на използвания програмен продукт APEX PRO, който е интегриран към електрозадвижванията на фирмата АМК и дава възможност за подробни изследвания с високо качество на резултатите.

По абсцисната ос е представено времето за извършване на изследванията, а по ординатата – скалата е във волтове. Със зелена и червена линии са представени сигналите за обратните връзки по скорост за едната и другата посока съответно, с тъмносива линия е показан сигналът за обратната връзка по момент, а с кафява и синя линии са представени кривите на претоварване на двигателя и инвертора.

Системите за електрозадвижване със синхронни двигатели, възбуждани от постоянни магнити са особено перспективни. В сравнение с асинхронните двигатели с накъсо съединен ротор, които също имат много добри показатели, СДПМ притежават редица предимства, обусловени от следните техни специфични особености:

- липса на загуби в ротора;
- високо съотношение на въртящия момент към инерционния момент;
- голяма мощност в малък обем;
- компактна форма.

Като недостатък, на този етап може да се посочи по-висока цена на представеното променливотоково електрозадвижване, която е свързана с по-специалната конструкция на СДПМ и с по-сложното реализиране на векторното управление.

Направеният сравнителен анализ показва, че съответните динамични и статични показатели на изследваното променливотоково електрозадвижване със СДПМ са високи и напълно съизмерими с тези на постояннотоковото подавателно електрозадвижване. Същевременно трябва да се отбележи значително по-лесната експлоатационна поддръжка на променливотоковия

вариант, поради липсата на колекторно-четков апарат, който е характерен за задвижванията с ДПТ.

## 5. Заключение

Формулирани са изискванията към подавателните електрозадвижвания на един вид фрезови машини с цифрово-програмно управление.

Извършена е оптимизация на регулиращите контури и практическа настройка на използваните електрозадвижвания за постоянен и за променлив ток.

Осъществени са експериментални изследвания, показващи, че представеното променливотоково електрозадвижване с векторно управление удовлетворява поставените изисквания.

Проведените изследвания и получените резултати от тях може да се използват при избор на подавателни електрозадвижвания за разглеждания клас металообработващи машини.

## Литература

[1] Altintas, Y., A. Verl, C. Brecher, L. Uriarte, G. Pritschow, Machine Tool Feed Drives, *CIRP Annals - Manufacturing Technology*, vol. 60, No. 2, pp. 779 -796, 2011, ISSN: 0007-8506.

[2] Kiel, E., *Drive Solutions*, Springer, 2008, ISBN 978-3-540-76704-6.

[3] Михов, М., *Системи за електрозадвижване*, Технически университет – София, София, 2011, ISBN 978-954-438-922-2.

[4] Жилевски М, М. Михов, Методика за избор на подавателни задвижвания за фрезови машини, *Годишник на Технически университет - София*, т. 64, № 1, 33-42, София, 2014, ISSN 1311-0829.

[5] Zhilevski M., M. Mikhov, Study of Electric Drives for Rotary table of Milling Machines, *Journal of Multidisciplinary Engineering Science and Technology*, Vol. 2 No. 4, pp. 607-611, 2015, ISSN

3159-0040.

[6] Михов, М., М. Жилевски, Възможности за подобряване на показателите на позиционно електрозадвижване за фрезови машини, *Годишник на Технически университет - София*, т. 62, №. 2, 269-278, София, 2012, ISSN 1311-0829.

[7] M. Mikhov and M. Zhilevski, Computer simulation and analysis of two-coordinate position electric drive system, *Proceedings of the International Scientific Conference on Information, Communication and Energy Systems and Technologies*, pp. 251-254, V. Tarnovo, Bulgaria, 2012, ISBN 978-619-167-002-4.

[8] M. Mikhov and M. Zhilevski, Performance improvement of a type of milling machines, *Proceedings of the International Conference "Research and Development in Mechanical Industry"*, Vol. 1, pp. 218-227, Kopaonik, Serbia, 2013, ISBN 978-86-6075-042-8.

[9] Жилевски М, М. Михов, Алгоритъм за съгласуване на задвижванията на фрезови машини с цифрово-програмно управление, *Годишник на Технически университет - София*, т. 65, № 1, 41-50, София, 2015, ISSN 1311-0829.

[10] Sandvik Coromant, *Metalcutting Technical Guide: Turning, Milling, Drilling, Boring, Toolholding*, Sandvik, 2005.

[11] Sandvik Coromant, *Tool Selection Guide, Selected Assortment in Turning-Milling-Drilling*, Sandvik, 1997.

[12] AMKASYN, Servo Drives KE/KW, *AMK Catalogue*, 2014.

[13] DYNASYN, Servo Motors DT and DP, *AMK Catalogue*, 2014.

[14] AMKASYN, Device description, Controller cards, KU-R02/ -R03/ -R03P, KW R02/ -R03/ -R03P / -R04, *AMK Catalogue*, 2013.

[15] Михов М., *Системи за управление на електрозадвижванията*, Технически университет - София, София, 2007, ISBN 978-954-438-628-3.

# АВТОМАТИЗИРАНО УПРАВЛЕНИЕ НА ФИКСИРАЩ МОДУЛ ЗА ФРЕЗОВИ МАШИНИ

## AUTOMATED CONTROL OF FIXING UNIT FOR MILLING MACHINES

### АВТОМАТИЗИРОВАННОЕ УПРАВЛЕНИЕ МОДУЛЕМ ФИКСАЦИИ ДЛЯ ФРЕЗЕРНЫХ СТАНКОВ

Маг. инж. М. Жилевска  
Технически колеж– Ловеч, България  
E-mail: mzhilevska@mail.bg

**Abstract:** This paper examines the features of additionally introduced fixing unit for milling machines with digital program control. The requirements that should be met with this unit are formulated. Opportunities for its control have been carried out and features of the developed ladder diagram are indicated. The research held and the results obtained can be used in the development of such fixing unit for the studied class of machine tools.

**KEYWORDS:** MILLING MACHINES, FIXING UNIT, AUTOMATED CONTROL

### 1. Въведение

Фрезевите машини са изградени от различен набор от линейни и въртящи се координатни оси, чрез които се осъществява позициониране на детайла и инструмента, както и те участват в процеса на механична обработка. Тези оси се обслужват и задвижват от различни постояннотокови и променливотокови електрозадвижвания [1, 2, 3].

Въртящите се координати значително разширяват функционалните възможности на фрезевите машини, увеличават производителността и осигуряват достигане на желаните параметри при обработка. Тези оси осъществяват ъглово позициониране на детайла и дават възможност за обработка с висока точност на различни винтови канали, корпусни детайли, червячни колела и други. Обикновено ъгловото позициониране на детайла се реализира чрез въртящи се маси, кръгли делителни маси и универсални делителни апарати [4, 5].

Добавянето на управляеми въртящи се оси към фрезевите машини, изисква и внедряване на съответни електрозадвижвания. Това води до значително оскъпяване на цялата машина поради наличието на допълнително използвани двигатели, силови преобразуватели, датчици на път, както и необходимост от сложна система за цифрово-програмно управление [6, 7, 8].

Нуждата за твърдо позициониране на детайла на строго фиксиран ъгъл, доведоха до търсене на по-евтини и надеждни решения с практическо приложение.

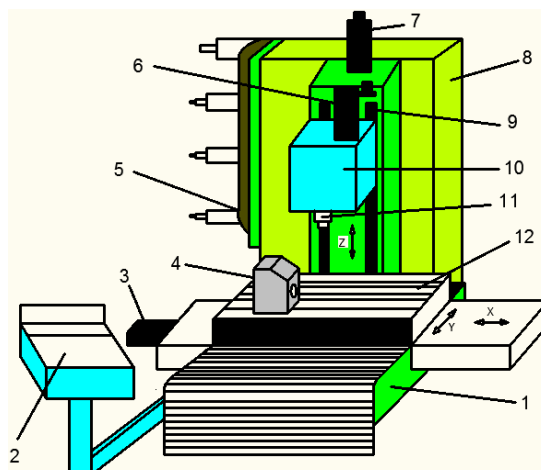
При модернизацията на клас фрезови машини се въвежда допълнителен фиксиращ модул. Целта е да се увеличат производителността и функционалните възможности на машините, да се осигури възможност за обработка на детайли със значително по-сложна геометрична форма и да бъде осигурен значително по-евтин вариант от въртящите се маси [9].

В тази статия са формулирани изискванията към добавения фиксиращия модул за фрезови машини, изследвани са начините за неговото управление, посочени са особеностите на разработената логическа схема и са представени резултати от проведените експериментални изследвания.

### 2. Изисквания към фиксиращия модул

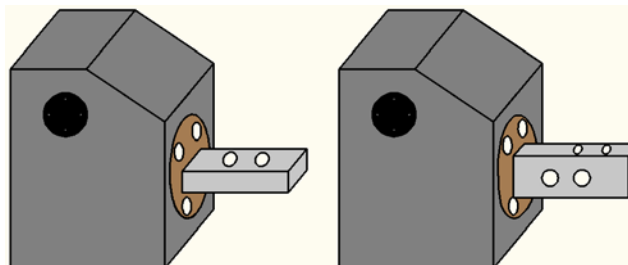
Разглежданият клас машини принадлежи към многокоординатните машини с ЦПУ. Те са съставени от три линейни подавателни оси и шпиндел. На фиг.1 е представена машина от разглеждания клас, като използваните означения са следните: 1 – тяло на машината; 2 – пулт за управление; 3 – двигател за ос x; 5 – инструментален магазин; 6 – двигател за главното движение; 7 – двигател за ос z; 8 – метален шкаф, в който са разположени системата за ЦПУ и съответните части от електрозадвижванията по съответните координатни оси и шпиндела; 9

– направляващи; 10 – скоростна кутия; 11 – фрезови инструмент; 12 – хоризонтална маса, извършваща линейни движения по координатните оси x и y. При модернизацията е добавен допълнителен фиксиращ модул, извършващ ъглово позициониране на детайла, означен с 4 на фигурата. Използваният фиксиращ модул осигурява възможност за твърдо позициониране на дванадесет позиции, през тридесет градуса.



Фиг. 1. Машина от разглеждания клас.

На фиг. 2 е показана възможността за позициониране на детайла на ъгъл от 90 градуса, с което се осигурява перпендикулярност на обработката.



Фиг. 2. Позициониране на детайла от 0 на 90 градуса.

Представеният модул се задвижва от асинхронен двигател с накъсо съединен ротор чрез механична предавка. Механичната част се състои от механизъм, който избутва напред въртящия диск, представляващ триходов винт. При въртенето си в посока "напред" той предизвиква преместване в аксиална посока на диска, при което се отцепва хиртовия съединител. При реверс

на електродвигателя става обратното- хиртовият съединител се зацепва, което гарантира, че е фиксирана точната позиция на въртящия диск, респективно на допълнително въведения модул.

Изискванията, които се поставят към добавения фиксиран модул, може да се формулират по следния начин:

- твърдо позициониране на детайла на ъгъл от тридесет градуса;
- позициониране с висока точност;
- възможност за лесно приспособяване към металообработващата машина;
- реализация чрез сравнително евтино управление.

### 3. Възможности за управление

Възможностите за управлението на представения фиксиращ модул са: неавтоматизирано и автоматизирано, посредством системата за ЦПУ. При първия случай е разработен допълнителен пулт, който осигурява независимо задвижване и управление на модула [9]. Като основен недостатък на такъв вид управление се явява липсата на автоматизирано управление от системата за цифрово-програмно управление. Това значително усложнява технологичния процес, тъй като не може да бъде постигната пълна автоматизация, както и води до увеличаване времето за обработка на детайла.

С добавянето на системата за ЦПУ за управлението на фиксиращия модул, се осигурява възможност за:

- автоматизиране на технологичния процес;
- намаляване времето за обработка на детайла;
- повишаване на точността;
- достигане на изисквания като успоредност и перпендикулярност на детайлите;
- увеличаване производителността на машината.

Използването на системата за ЦПУ като управляващ елемент, изисква разработка на ладер диаграма и добавяне на точно определено място в общата релейна част на цялата машина. Разработването на логическа схема изисква детайлно познаване на особеностите на механизмите и тя преминава през няколко етапа, като за целта е разработен алгоритъм [10].

Като входни данни се задават: изисквания за избор на съответната позиция чрез М команда; отчитане използвания механизъм в фиксиращия модул.

Началните етапи са свързани с избор на конкретна система за ЦПУ и проблемно-ориентиран език. Избира се система за ЦПУ- Fanuc и се отчитат свободните позиции във входните, изходните сигнали и междинните условия [10].

В табл. 1 са представени някои от входните сигнали, които се отнасят за допълнително въведения фиксиращ механизъм, като хоризонтално са разположени адресите, а вертикално са съответните битове в системата за ЦПУ. Те са свързани със задаване на команда за избор на позиция, декодирани с M11÷M22, както и Qsm – ключ, използван от фиксиращия модул. Сигналите се разполагат на свободните места от таблицата, без да бъдат засегнати останалите управляеми периферни устройства, които изграждат металообработващата машина.

Табл. 1. Таблица с входните сигнали, свързани с фиксиращия модул.

	7	6	5	4	3	1	0
032				Qsm			
033				M22			
034				M21			
037				M20			
040	M14	M15	M16	M17	M18		
042						M12	M11

Изходните сигнали, свързани с фиксиращия модул, са представени в табл. 2 като хоризонтално са разположени адресите, а вертикално са съответните битове в системата за ЦПУ. Те са свързани с: включване и изключване на релета за движение на модула съответно напред и назад; включване и изключване спирачката на двигателя.

Табл. 2. Таблица с изходните сигнали, свързани с фиксиращия модул.

	7	...	4	3	2	1	0
07				K12	K13	K14	K15

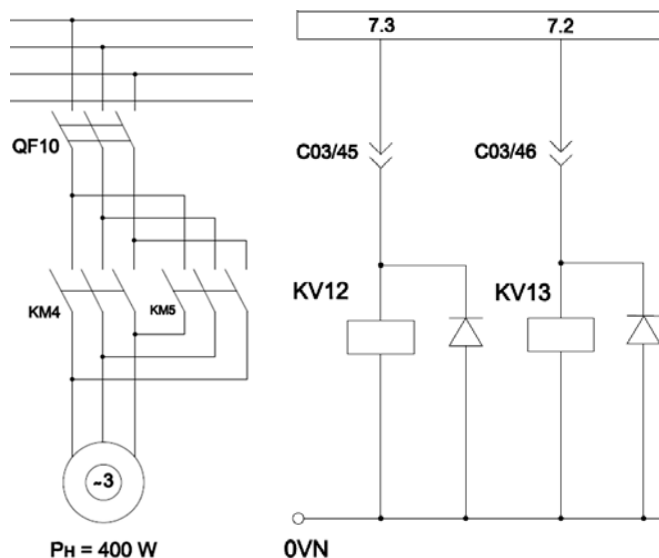
В табл. 3 са представени съставените междинни условия, свързани с отчитане действителната позиция на фиксиращия модул от галетата и използваните таймери, които подобряват работата на устройството и увеличават експлоатационния живот на механизма.

Табл. 3. Таблица с междинните условия, свързани с модула.

	7	6	5	4	2	1	0
204	M11A	M12A	M13A	M14A	M16A	M17A	M18A
205	M19A	M20A	M21A	M22A	M15A	R30	R31
206							R32
210	TM17			TM09	TM10	TM07	TM08

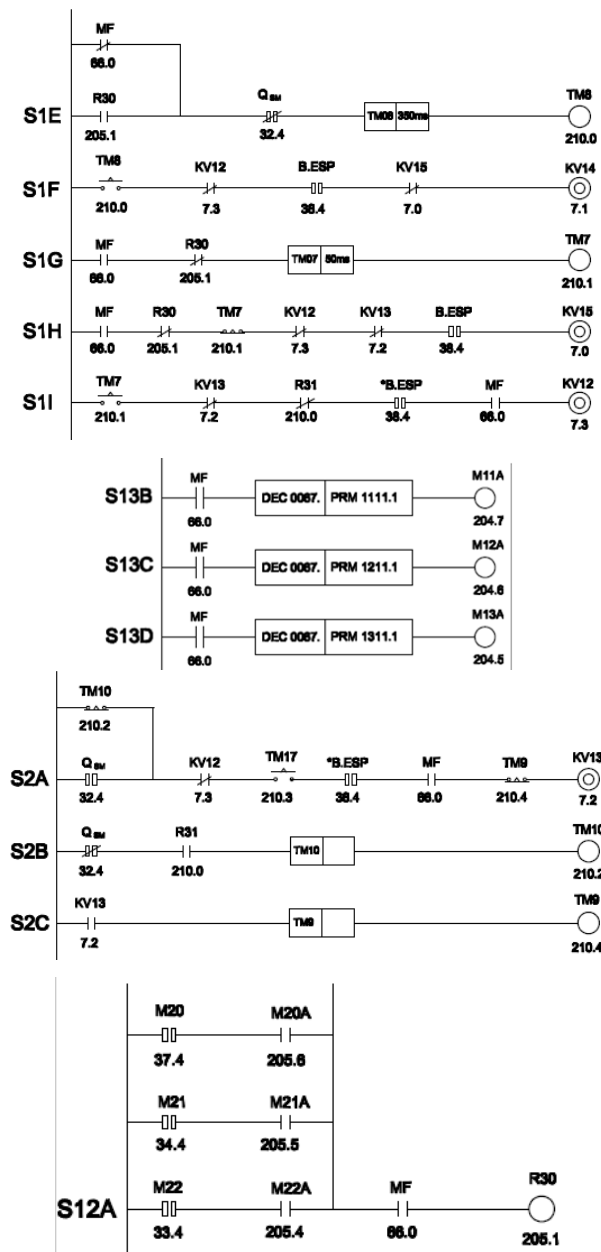
След преминаване на всички последователни стъпки от алгоритъма за разработка на ладер диаграма [10]: съставянето на блоковата схема на фрезовата машина; уточняването на изискванията и избор на СЦПУ; избор на проблемно ориентиран език; уточняването на базови, входни/изходни сигнали и междинни условия; се осъществява изчертаване на разработената релейна схема и съответната таблична част.

На фиг. 3 са представени част от електрическите схеми, свързани с фиксиращия модул.



Фиг. 3. Електрически схеми, свързани с фиксиращия модул.

На фиг. 4 е представена част от разработената логическа схема на фрезовата от фиг. 1, която обслужва допълнително въведения модул.



Фиг. 4. Логическа схема, свързана с фиксиращия модул.

След уточняването на ладер диаграмата, се извършва и таблично представяне, като малка част е показана в табл. 4. Представената таблица се отнася за условията на работа на фиксиращия модул, декодирането на М командите; избора на позиция и създаване на защити, които увеличават неговия експлоатационния живот.

Табл. 4. Таблица с условията за работа на фиксиращия модул.

20	RD.NOT	66.0	MF	Базов сигнал PC→NC „зададена М функция“
21	OR	205.1	R30	Междинно условие
22	AND.NOT	32.4	Qsm	Входен сигнал „ключ на допълнителния модул“
23	TM8			Таймер, свързан с допълнителния модул“
24	WRT	210.0	TM8	Междинно условие
25	RD	210.0	TM8	Междинно условие
26	AND.NOT	7.3	KV12	Изходен сигнал „движение на модула напред“
27	AND	38.4	*B.ESP	Входен сигнал „аварен стоп“

#### 4. Изследване на логическата схема

При съставяне на логическата схема на работа за определено периферно устройство от металорежещата машина, от съществено значение се явява необходимостта от подробно познаване на механизма, който го изгражда.

Използваният допълнителен модул се управлява от трифазен асинхронен двигател с две посоки на въртене (права и реверс), като към вала на двигателя е куплирана електромагнитна спирачка.

Исходните сигнали, водещи до включване на съответните релета, са свързани с въртене на двигателя са съответно KV12 и KV13, а тези които включват и изключват електромагнитната спирачка са KV14 и KV15.

Допълнителният модул избира всяка отделна позиция като се задава някоя от М- функциите (M11÷M22). Декодирането за всяка от М функциите се осъществява по строго определена последователност (задаване на базовия сигнал MF, команда за декодиране с задаване на желанния номер и запис в определено-то междинно условие).

При задаване на съответна М команда, асинхронният двигател се завърта в права посока. Първоначално подвижната част на модула се измества аксиално напред до освобождаване на хиртовото съединение, след което започва въртене на подвижната част, достига избраната позиция, като я подминава. След това двигателят се реверсира до връщане на подвижната част в изходно положение, осигуряващо се от хиртовото съединение.

Аксиалното изместване на подвижната част се следи от датчик Qsm, а текущата позиция се следи от галетен превключвател.

За стартиране избора на позиция трябва да се изключи електромагнитната спирачка, която е включена в нормално състояние, чрез изход KV14. Изключването на спирачката се осъществява чрез изход KV15.

С въвеждането на таймери се осигурява:

- повишаване на експлоатационния живот на механизма;
- сигурно и твърдо позициониране на модула на зададената позиция;
- предпазва се двигателя от претоварване.

Приемането на завършена М команда от системата за ЦПУ (FANUC), е необходимо активиране на сигнала FIN - след приключване на избора на позиция. Това се осъществява чрез активиране на няколко последователни междинни условия, което води до активиране на сигнала FIN.

С предложеното автоматизирано управление, посредством системата за ЦПУ, се осигурява възможност:

- пълна автоматизация на технологичния процес;
- повишаване експлоатационния живот на механизма;
- надеждна и значително по-евтина реализация.

#### 5. Експериментални изследвания

Практическата реализация на въведения модул е свързана с възможности за обработка на детайли със значително сложна геометрична форма и изисквания за успоредност и перпендикулярност, които се предявяват към тях.



Фиг. 5. Обработени детайли с помощта на фиксиращия модул.

На фиг. 5 са показани детайли, получени след фрезова обработка, посредством използване на допълнително въведения фиксиращ модул.

Разработеното и внедрено устройство с автоматизирано управление на базата на система за ЦПУ допринася за повишаване на производителността и подобряване на качеството на работа при обработката на детайли с металоурежещи машини.

Същевременно разработената логическа схема повишава експлоатационния живот на механизма и позволява автоматизация на технологичния процес.

## 6. Заключение

Въведен е допълнителен фиксиращ модул, който разширява възможностите, подобрява точността и осигурява по-висока производителност на разглеждания клас машини.

Реализирано е автоматизирано управление на фиксиращия модул, посредством системата за ЦПУ, с което се осигурява възможност за позициониране на детайла през тридесет градуса.

Изследвана е логическата схема за управление на допълнителния механизъм.

Осъществени са експериментални изследвания, показващи, че внедрения фиксиращ модул удовлетворява поставените технологични изисквания.

Разработени са гама фрезови машини, в които са приложени резултати от представената ладер диаграма. Машини от разглеждания клас са внедрени в редица фирми.

## Литература

[1] Михов М., М. Жилевски, Въвеждане на допълнителна регулируема координатна ос при клас металоурежещи машини

с цифрово-програмно управление, *Годишник на Технически университет - София*, т. 63, №. 2, 41-48, София, 2013, ISSN 1311-0829.

[2] Михов М., М. Жилевски, Възможности за подобряване на показателите на позиционно електрозадвигване за фрезови машини, *Годишник на Технически университет - София*, т. 62, №. 2, 269-278, София, 2012, ISSN 1311-0829.

[3] Zhilevski, M., M. Mikhov, Study of Electric Drives for Rotary Table of Milling Machines, *Journal of Multidisciplinary Engineering Science and Technology*, Vol. 2, Issue 40, pp. 607-611, 2015, ISSN: 3159-0040.

[4] Hoffman, P., J., E. S. Hopewell, B. Janes, K. M. Sharp, *Precision Machining Technology*, Cengage Learning, 2011, ISBN 9781435447677.

[5] Mattson, M., *CNC Programming, Principle and Applications, Second Edition*, Cengage Learning, 2009, ISBN 978-1-4180-6099-2.

[6] Жилевски, М., Многокоординатни системи за електрозадвигване на клас металоурежещи машини, *Технически университет – София*, Дисертация, 2015.

[7] AMKASYN, Servo Drives KE/KW, *AMK Catalogue*, 2014.

[8] DYNASYN, Servo Motors DT and DP, *AMK Catalogue*, 2014.

[9] Дочев М., М. Жилевска, Св. Тонкова, Модернизиране на металоурежещи машини чрез въвеждане на автономно управление на позициониране на ножодържаща с фиксирани деления, *23 МНТК*, София, АДП – 2014, стр. 452-456.

[10] Zhilevska, M., M. Zhilevski, Algorithm for development of ladder diagram for machine tools, *Unitech - Gabrovo*, т. 1, 387-391, 2015, ISSN 1313-230X.

# AUTOWAVES OF LOCALIZED PLASTIC DEFORMATION ON THE YIELD PLATEAU AND ON THE WORK HARDENING STAGE

## АВТОВОЛНЫ ЛОКАЛИЗОВАННОЙ ПЛАСТИЧЕСКОЙ ДЕФОРМАЦИИ НА ПЛОЩАДКЕ ТЕКУЧЕСТИ И НА СТАДИИ ДЕФОРМАЦИОННОГО УПРОЧНЕНИЯ

Prof. Dr. Phys.-Mat. Sci. Danilov V.<sup>1,2</sup>, Cand. Phys.-Mat. Sci. Gorbatenko V.<sup>1</sup>, Prof. Dr. Phys.-Mat. Sci., Zuev L.<sup>1,3</sup>  
Institute of Strength Physics and Material Science Siberian Branch of Russian Academy of Sciences<sup>1</sup>,  
Tomsk Polytechnic University<sup>2</sup>, Tomsk State University<sup>3</sup> – Tomsk, Russia  
dvi@ispms.tsc.ru, gvv@ispms.tsc.ru, lbz@ispms.tsc.ru

A study was made of the macro-scale plastic flow non-homogeneities, which occur in metals in the form of Luders bands or Portevin-Le Chatelier effect. The motion kinetics was investigated for the mobile fronts of Luders bands observed for the yield plateau as well as localized plasticity fronts traveling in the course of serrated plastic flow behavior (Portevin-Le Chatelier effect). It is shown that the propagation of the above two kinds of band fronts can be regarded as macro-scale auto-wave processes of switching and excitation, respectively, which frequently occur in active media of different kinds.

**KEYWORDS:** INSTABILITY OF PLASTIC FLOW, LUDERS BANDS, PORTEVIN-LE CHATELIER EFFECT, AUTOWAVES OF LOCALIZED PLASTIC DEFORMATION

### 1. Introduction

Investigations of the plastic deformation in solids have been carried on for 25 years. On the macro-, meso- and micro-scale levels the plastic flow is found to exhibit a non-uniform behavior from the yield limit to the fracture of material [1-4]. In the course of plastic flow development a changeover in the modes of localized plasticity auto-waves would occur, with each mode corresponding to the respective flow stage on the loading curve plotted for deforming material. Thus the phase auto-waves would form at the stage of linear hardening; a stationary dissipative structure would emerge at the stage of parabolic hardening (Taylor stage); collapse of the auto-wave would occur at the pre-fracture stage where the onset of necking takes place [4]. The phase auto-wave is represented by a set of equidistant localized deformation nuclei moving in a concerted manner in one and the same direction. The phase auto-waves have been considered in greater detail; the spatial period (wave length) and propagation rate can be determined for this kind of autowaves [4-6]. In a particular case, the number of moving nuclei might be no more than four; hence, the motion of these nuclei would exhibit no spatial periodicity. However, a correlation has been established for the motion rates of nuclei propagating at the yield plateau. The latter stage is characterized by plastic flow instability, which is generally referred to as Luders band (LB) propagation [7]. The plastic deformation is also known to exhibit another type of space-time non-homogeneity, the so-called effect of Portevin-Le Chatelier (PLC) or serrated flow, which would change the traditional shape of the deformation curve due to the appearance of peaks [8]. The both types of plastic flow instabilities and their formation and development in the deforming medium are addressed herein in the frame of auto-wave approach. The deforming medium undergoing self-organization and structuring is analyzed in the frame of concept proposed in [9].

### 2. Materials and experimental procedures

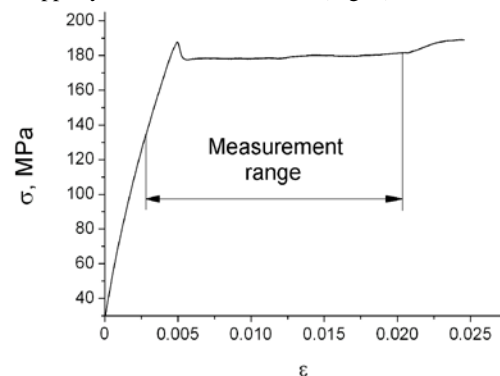
The LB propagation was studied for the test samples of low carbon hot rolled steel, which had near ferrite structure and average grain size  $\sim 20 \mu\text{m}$  (steel composition 0.05...0.11 % C; 0.35...0.65 % Mn; 0.05...0.17 % Si). The PLC effect was studied for naturally aged duralumin containing Al-based solid solution having grain size  $\sim 30 \mu\text{m}$  and hardening particles having submicron size (duralumin composition 3.8...4.8 % Cu; 0.4...0.8 % Mn; 0.4...0.8 % Mg). Note: alloy composition is in mass percent. The test samples having dog-bone shape were cut out of steel plates; the sample gauge had dimensions  $50 \times 10 \times 3 \text{ mm}$ . The samples were tested in tensile loading in the testing machine Walter+Bai AG LFM-125 at the rate  $V_{mach} = 3.3 \cdot 10^{-6} \text{ m/s}$  (deformation rate  $\dot{\epsilon} = 6.6 \cdot 10^{-5} \text{ s}^{-1}$ ) and at the temperature 300 K.

In conformity with the requirements of the experimental technique, the test samples had flat diffuse reflecting gauge. Using

the method of digital statistical speckle photography, the visualization and nuclei kinetics registration was performed for the localized plasticity zones occurring on the sample surface [10]. The sample was illuminated by the coherent light of a semi-conductor laser having wavelength 635 nm and power 15 mW. The speckle pattern superimposed on the respective image was registered, digitized with the aid of video camera PixeLink PL-B781 having frequency 10 Hz and then stored. A sequence of counts was formed for each image point, which characterized variation of image brightness with time. Then the dispersion and mathematical expectancy were calculated; the ratio of the values obtained was used for mapping deformation localization zones. The above technique makes feasible *in situ* registration of material zones in which deformation localization occurs for a given increment in tensile sample length. It can be seen that the localized deformation zones show up in the video images as bright bands.

#### 2.1. Development of Luders bands

It was found that the micro-plasticity stage will be invariably realized in the deforming samples of low carbon steels [11]. Therefore, the registration of localized plasticity zones was started before the upper yield limit was attained (Fig. 1).

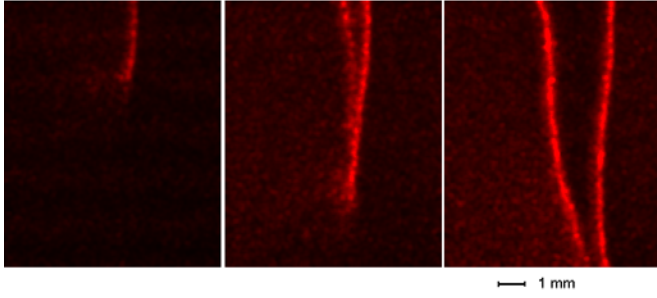


**Fig. 1.** The yield plateau on the deformation curve plotted for the test sample of low carbon steel

Speckle image recording was terminated as soon as the yield plateau was over and the deformation hardening stage began. It was established experimentally that the plastic deformation would first localize in the form of LB nucleus emerging at the micro-plasticity stage. The appearance of LB nucleus might be traced from acoustic emission signals [12]. As is seen from Fig. 2, a narrow wedge of deformed material would advance crosswise through the test sample at the rate  $V_{nuc1} \approx (0.4...1.2) 10^{-3} \text{ m/s}$ . The diagram  $\sigma(\epsilon)$  represents the nucleus growth as a fairly sharp yield point having an ascending and a descending branch (Fig. 1). As soon as the LB nucleus traverses the sample cross-section, the formation of LB is completed and its widening would begin (band widening observed in the diagram  $\sigma(\epsilon)$  corresponds to the yield plateau). Now that the

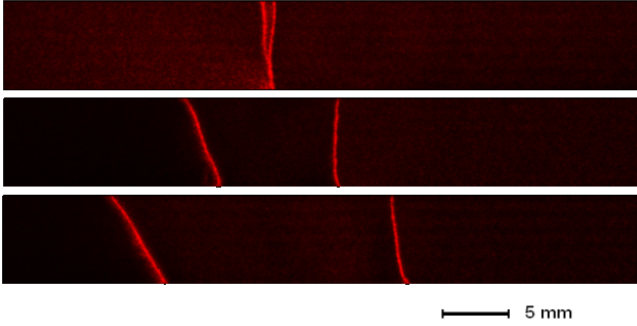


LB formation is over, one front would emerge at the LB foreground and the other at the rear. The both fronts start traveling in the opposite directions along the sample axis at rate  $\pm V_f$  (Fig. 3). Sometimes a LB band and its two fronts would form at the clamp of the testing machine; then one of the fronts would almost immediately leave the clamp and become immobilized.



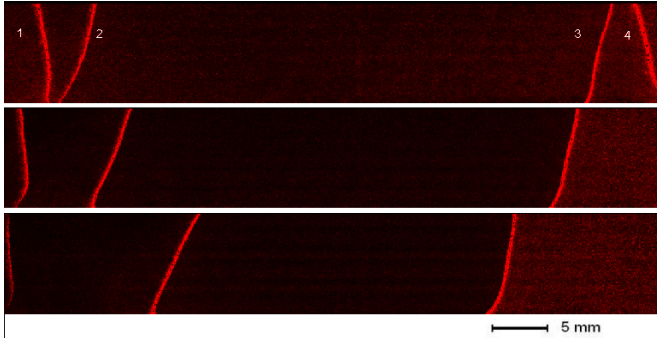
**Fig. 2.** The nucleation of LB; the images were obtained at time intervals of 7 s

The motion rate of LB fronts is an important characteristic of the process. As soon as a single LB appears (see Fig. 3), two its fronts start moving in opposite directions at practically the same rates, i.e.  $V_f \approx \pm 8 \cdot 10^{-5}$  m/s; hence,  $|V_f| \approx 0.1 V_{nuct}$ . As one of the fronts approaches the clamp of the testing machine, its rate drops down to zero, while the rate of the other front increases up to  $(1.3 \dots 1.5) \cdot 10^{-4}$  m/s.



**Fig. 3.** The ingrowth and propagation of LB; the images were obtained at time intervals of 60 s

When a couple of LBs forms simultaneously, four fronts start traveling at practically the same rate  $\pm (3 \dots 5) \cdot 10^{-5}$  m/s, which is somewhat lower than in the former case (see Fig. 4). As soon as fronts 1 and 4 approach the testing machine clamp, their rate drops off and, both fronts would finally become arrested. Fronts 2 and 3 continue moving in the opposite directions at the rate which is almost twice that of the original rate. The fronts of two neighboring LBs would become annihilated on meeting. The original fronts are inclined to the extension axis at the angle  $\sim \pi/3$ ; however, in the course of front motion towards the clamp the inclination would drop off to  $\sim \pi/2$ .



**Fig. 4.** The propagation of two LBs; the images were obtained at time intervals of 60 s

Thus in the case of mobile LB front, which emerges in the deforming sample at the yield plateau at the pre-assigned value  $M_{ach}$ , the following rule holds true:

$$\sum_{i=1}^N |V_f^{(i)}| = \langle V_f \rangle = const, \quad (1)$$

where  $|V_f^{(i)}|$  is the modulus of the motion rate of  $i$ th LB front;  $N$  is the number of fronts traveling in a concerted way and  $\langle V_f \rangle = 1.6 \cdot 10^{-4}$  m/s is the generalized rate of growth of the plastically deforming zone, which emerges at the yield plateau in the test sample. The relationship between the velocities  $V_{mach}$  and  $\langle V_f \rangle$  is found from the equality of the time it takes for the given plasticity zone to cover sample gauge length,  $L$ , and of the time of it takes for a given sample to acquire ultimate elongation at the yield plateau,  $\delta L$ ,

$$\frac{L}{\langle V_f \rangle} \approx \frac{\delta L}{V_{mach}}. \quad (2)$$

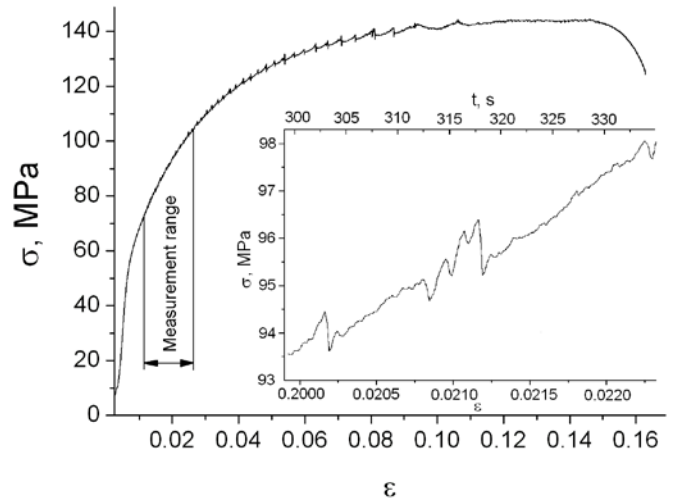
The above suggests that such is indeed the case: the generalized growth rate of deformed zone area is by about one order greater than the rate of the movable clamp of the testing machine, i.e.

$$\langle V_f \rangle = \frac{L}{\delta L} V_{mach} > V_{mach}. \quad (3)$$

Generally, yield plateau length expressed in terms of deformation ( $\delta L/L$ ) varies in the range from 1% to 10% [12]; hence,  $\langle V_f \rangle = (10 \dots 100) V_{mach}$ .

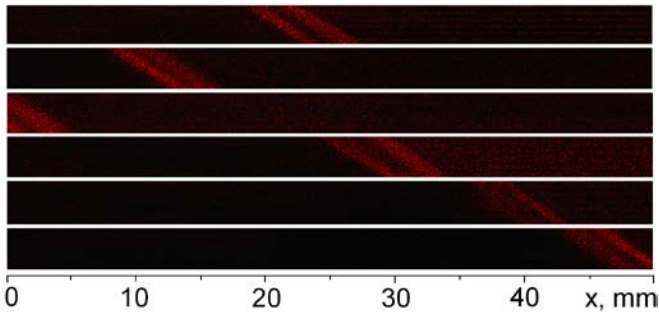
## 2.2. Development of serrated flow

The PLC effect is manifested in duralumin at room temperature in the course of deformation up to necking (see Fig. 5).



**Fig. 5.** The serrated flow observed for the test sample of duralumin; the insert shows toothing observed for the studied range of stresses

It can be seen from the diagram  $\sigma(\varepsilon)$  that the intermittent flow is characterized by the appearance of type A, B and C toothing, with the type of toothing varying with sample elongation [14]. Thus the occurrence of a C type tooth corresponds to a single sharp decrease in the deformation, while the appearance of A type tooth is suggestive of working stress drops alternating with constant or weak increase in the stress. The deformation diagram was obtained for the linear work hardening stage in the test sample of duralumin for the strain range  $0.01 \leq \varepsilon \leq 0.03$ . It shows mostly C type toothing, which can be attributed to separate localized deformation bands corresponding, in terms of morphology, to non-complex material areas. The PLC bands will originate in the middle of the sample gauge or on the lateral side of the sample in the vicinity of the clamp of the testing machine. The bands occurring in the tensile sample would expand throughout the sample cross-section. The rate of growth of PLC nuclei is  $\sim 1$  m/s, which is three times that of the LB nuclei. The band having an ingrown nucleus has a forefront and a rear-front with  $\sim 2 \dots 3$  mm separation in between (Fig. 6); it is inclined to the extension axis at an angle  $\sim \pi/4$ . The band would travel along the sample to the testing machine clamp at a rate  $\pm V_{sb}$ .



**Fig. 6.** The localized deformation bands observed in the course of serrated flow; the images were obtained at time intervals of 5 s

The modulus of band propagation rate is  $1.3 \cdot 10^{-3} \leq V_{sb} \leq 1.8 \cdot 10^{-3}$  m/s, which is ten times that of the PLC fronts' propagation rate or even higher. A sharp drop of the working stress is observed in the diagram  $\sigma(\varepsilon)$ ; it corresponds to the process of nucleus ingrowth, while the motion of the PLC band (single C-type tooth) corresponds to an increase in the working stress up to the nominal value. As soon as the PLC band reaches the clamp of the testing machine, a drop in the working stress would occur, with resultant emergence of a new band in the middle of the sample. The new band would start traveling along the extension axis in the opposite direction relative the former band (see Fig. 6). As soon as the new band reaches the clamp of the testing machine, the same process is repeated once again. Thus, the serrated flow behavior has a characteristic feature: the PLC bands of deformation localization would travel repeatedly along the sample gauge, with each run of a PLC band over half the gauge length corresponding to a single C-type tooth in the diagram  $\sigma(\varepsilon)$ . The same periodic motion of PLC band fronts would occur at the stage of parabolic deformation hardening; however, the motion rate of fronts would drop off gradually and at the onset of necking the fronts would become immobilized.

### 3. Discussion of results. Matching of the localized deformation behavior at the LB fronts and the PLC effect

The studies were performed on the base of experimental evidence. The kinetics of mobile LB and PLC fronts suggests that they have both similar and dissimilar features. Thus the plastic deformation tends to localize within narrow zones of material; hence, the both types of band fronts are macro-scale manifestations of this tendency. In both cases the kinetics of band emergence is similar, since localized plasticity nuclei would form on the lateral surface of the sample gauge to grow finally through the sample cross-section. As soon as the ingrowth of nuclei is completed, a sharp distinction between the two kinds of processes becomes manifest. Thus the evolution of LB is in point of fact its widening within the sample gauge, with the entire plastic deformation becoming localized within the mobile fronts traveling in opposite directions, with their intricate shape varying in the process. The LB fronts would move independently of one another; however, their motion rates would vary in such a way that the sum of moduli of the fronts' rates remains constant (Eqn. 1). In case two or more LBs start broadening, their fronts are liable to annihilate on meeting.

Due to the PLC effect, the plastic flow would become localized within a single band, which excludes the possibility that bands would annihilate on meeting. We are reminded that the LB fronts would propagate over the sample gauge only once, while the PLC front would travel repeatedly along the sample gauge. This is an added reason to state that the effects in question differ significantly.

The above distinctions are considered in the frame of auto-wave model of plastically deforming medium by the workers in [4]. One of the main assumptions of the model is that the deforming medium is an active one; hence, it must contain energy sources distributed in the material volume [13]. By addressing the problem of plasticity, it might be reasonable to consider elastic stress carriers

as energy sources, which are capable of relaxation when crystal lattice defects are formed in the deforming solid.

In the frame of well-known microscopic models of LBs [6, 10], the medium within the mobile front would pass from an elastically stressed state to a plastically deformed state due to the relaxation of stress carriers. The both states are stable ones; however, the elastically stressed state is a metastable one and the plastically deformed state, an absolutely stable one; hence, no transition is feasible from the latter state back to the former. In point of fact, the microscopic models of LB have nothing to do with the auto-wave theory [13]. However, the relaxation of stress concentrators occurring in the medium enables one to place the given medium into the category of trigger type (bistable) systems. Hence, the perturbation front might be regarded as a switching auto-wave. The acts involving a changeover in the medium's states are irreversible ones, which precludes repeated passing of perturbation fronts over one and the same area. For this reason, two switching auto-waves traveling in opposite directions would generally annihilate on meeting, which is the case with the LB fronts.

The PLC effect and the micro-mechanisms involved have been studied in detail [7, 12]. The results suggest that the components of the active medium might be in a different sequence of states. At the PLC front the components may also pass from the metastable elastically stressed state to the plastically deformed state. However, the latter state is never absolutely stable, since the PLC effect development occurs at the hardening stage. As the stress level increases up to the nominal value, which is manifested by the formation of C type tooth, the active elements of the deforming medium will return to the original metastable elastically stressed state. In conformity with the theory of auto-wave processes, such elements and such active media is excitable to occur.

The excitable element is modeled by a three-state cycle. Thus an excitable element, which is fully recovered from any previous excitation, is in state A (at rest); state B is the excited state of the excitable element and state C is the refractory state of the excitable element. By way of illustration, let us consider the stress carrier as an excitable element. State A is a meta-stable elastically stressed state of the stress carrier; state B is the gradual disappearance of stresses from the stress carrier and state C is the refractory state of the stress carrier with the stresses increasing. A perturbation will excite the quiescent stress carrier, which would become excited at random times following an external stimulus, e.g. when subjected to external periodic forcing by another excitable element or due to thermal fluctuations. The transition from a refractory state to rest takes place in the excitable element at the hardening stage due to the steadily increasing level of external stresses. So long as the stress carrier is in a refractory state, it would remain inactive. As the localized deformation front travels along the sample, all the stress carriers would become excited following an external stimulus and the medium would acquire a refractory state. The stress concentrators would pass into the state of rest after the lapse of refractory time; then another deformation front would propagate in the sample. The above events summate to produce the macroscopic dynamics of the whole system [13]. In view of the above, the PLC effect is attributed to the propagation of excitation auto-waves in the deforming medium.

### 4. Conclusions

1. It is shown that the LBs and the deformation bands related to the PLC effect are initiated in the deforming medium via one and the same mechanism, i.e. nucleus ingrowth throughout the sample section on the lateral sample side.
2. It is found that the rate of deformation bands which form due to the PLC effect is three times that of LB.
3. LB fronts and deformation bands related to the PLC effect are switching and excitation auto-waves, respectively, which form in deforming active media.

The study was performed in the frame of fundamental scientific research program of Russian Federation state academies of science for the period 2013-2020 with partial support of the RFBR Grant

No. 14-08-00299. The experimental studies were conducted on the equipment made available by the courtesy of the Nanotech Center at the ISPMS SB RAS.

## 5. References

- [1] Kuhlmann-Wilsdorf, D. The low energetic structures theory of solid plasticity, in *Dislocations in solids*. Ed. by F.R.N. Nabarro and M.S. Duesbery. Amsterdam, Boston: Elsevier, 2002, pp. 213-338.
- [2] Panin, V.E. Nonlinear wave processes in a deformable solid as in a multiscale hierarchically organized. / V.E. Panin, V.E. Egorushkin, A.V. Panin. - *Physics Uspechi*, 55, 2012, pp. 1260-1267.
- [3] Zuev, L.B. On the waves of plastic flow localization in pure metals and alloys. - *Ann. Phys.*, 16, 2007, pp. 286-310.
- [4] Zuev, L.B. Autowave model of localized plastic flow of solids. / L.B. Zuev, V.I. Danilov, S.A. Barannikova, V.V. Gorbatenko. - *Phys. Wave Phenom.*, 17, 2009, pp. 66-75.
- [5] Zuev, L.B. Autowave mechanics of plastic flow of solids. - *Phys. of Wave Phenom.*, 20, 2012, pp. 166-173.
- [6] Pelleg, J. *Mechanical Properties of Materials*. Dordrecht: Springer, 2013, 633 p.
- [7] Rizzi, E. On the Protevin-Le-Chatelier effect: theoretical modeling and numerical results / E. Rizzi, P. Hähner. - *Int. J. Plasticity*, 2004, 20, pp. 121-165.
- [8] Seeger, A. *Non-Linear Phenomena in Material Science*. / A. Seeger, W. Frank. - New York: Trans. Tech. Publ., 1987, pp. 125-138.
- [9] Zuev, L.B. Elaboration of speckle photography techniques for plastic flow analyses. / L.B. Zuev, V.V. Gorbatenko, K.V. Pavlichev. - *Measurement Science and Technology*, 2010, 21, pp. 054014-18.
- [10] Dudarev, E. F. *Microplastic deformation and yield limits in polycrystals*. Tomsk: Tomsk University Publisher, 1988, 255 p.(in Russian).
- [11] Plekhov, O.A. Elastic-plastic transition in iron: Structural and thermodynamic features. / O.A. Plekhov, O.B. Naimark, N. Saintier, T. Palin-Luc. *Technical Physics*, 2009, 54, pp 1141-1146.
- [12] Cuddy, L.J. Some aspects of serrated yielding in substitutional solid solution of iron. / L.J. Cuddy, W.C. Leslie. - *Acta Met.*, 1972, 20, pp. 1157-1167.
- [13] Mikhilov, A.S. *Foundations of Synergetic I: Distributed Active Systems*. Berlin: Springer-Verlag, 1994, 270 p.

# ДИНАМИЧЕСКАЯ УСТОЙЧИВОСТЬ ТРУБОПРОВОДА С КОНЦЕНТРИРОВАННЫМИ МАССАМИ

## DYNAMIC STABILITY OF A PIPE WITH CONCENTRATED MASSES

гл.ас. д-р инж. Лолов Д.<sup>1</sup>, проф. д-р инж. Лилкова-Маркова Св.<sup>2</sup>  
 Университет по Архитектуре, Строительству и Геодезии, София, Болгария <sup>1</sup>  
 E-mail: dlolov@yahoo.com, lilkovasvetlana@gmail.com

**Abstract:** A pipe with a static scheme of a simply supported beam with attached concentrated masses is investigated in the paper. The spectral method of Galerkin is applied in order to determine the critical velocity of the fluid. A great influence of concentrated masses on the critical velocity of the fluid is observed.

**Keywords:** PIPE, DYNAMIC STABILITY, CRITICAL VELOCITY

### 1. Введение

Трубы с протекающим флюидом являются одним из часто встречающихся элементов в различных областях промышленности. Развивающиеся колебания – предмет исследования многих ученых. Трубопроводы в ядерной и нефтяной промышленности имеют клапаны и соединения, которые могут быть смоделированы в виде концентрированных масс. Очень важно учитывать их воздействие в исследовании динамического поведения трубопроводов.

Исследование таких труб сделано впервые Хилом и Свенсоном и представлено в [2]. Чтобы решить дифференциальное уравнение для функции поперечного перемещения применяется метод Галёркина. Было обнаружено, что, когда труба консольная концентрированные массы снижают критическую скорость флюида. Это скорость флюида, при которой труба теряет устойчивость.

Чен и Йендрейчик [1] проводят эксперименты и исследования для труб с протекающим флюидом в двух случаях опор: Q - устройство и опора, позволяющая перемещение вдоль оси, а также и консольные трубы. На свободном конце труб прикреплена концентрированная масса. В экспериментах использовали трубы из двух материалов: полиэтилен и акрил. Исследована потеря устойчивости. Определены круговые частоты свободных колебаний, функции формы и критическая скорость флюида.

Ву и Ражи в [6] представляют метод исследования колебаний трубы с концентрированной массой. Скорость флюида меньше чем критическая. Для труб с различными опорами получены функции формы. Исследовано влияние концентрированной массы в середине трубы типа простой балки на круговую частоту свободных колебаний.

### 2. Постановка задачи

Исследован трубопровод с длиной  $l$  и жесткость на изгибе  $EI$ . Поток жидкости имеет постоянную скорость  $V$ . Вязкость жидкости и гравитационные силы игнорируются. На трубопроводе расположены и концентрированные массы. Исследуется устойчивость системы.

Расчётная модель системы труба-жидкость представлена на рисунке 1.

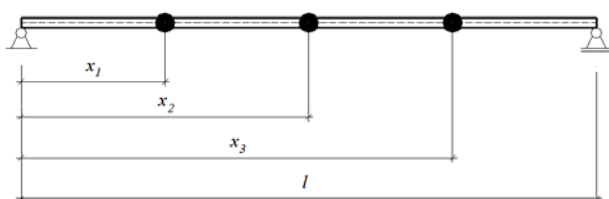


Рис. 1 Труба с концентрированной массой.

Дифференциальное уравнение, описывающее поперечные колебания трубопровода (в горизонтальной плоскости), имеет следующий вид [3]:

$$(1) \quad EI \frac{\partial^4 w}{\partial x^4} + \left( m_f + m_p + \sum_{j=1}^m m_j \delta(x - x_j) \right) \frac{\partial^2 w}{\partial t^2} + 2m_f V \frac{\partial^2 w}{\partial x \partial t} + m_f V^2 \frac{\partial^2 w}{\partial x^2} = 0$$

$w(x, t)$  - функция поперечных перемещений;

$m_f$  и  $m_p$  - соответственно масса транспортируемой жидкости и масса трубы на единице длины трубопровода;

$m_j \quad j = 1, \dots, m$  -  $j$ -тая сосредоточенная масса на оси трубы;

$x_j$  - отстояние  $j$ -той сосредоточенной массы от левого конца трубы (рис.1).

$\delta$  - функция Дирака, для которой в соответствии с [4] есть зависимости:

$$(2) \quad \begin{aligned} \delta(x - x_j) &= 0 \quad \text{при} \quad x \neq x_j \\ \delta(x - x_j) &= \infty \quad \text{при} \quad x = x_j \end{aligned}$$

$$\int_a^b f(x) \delta(x - x_j) dx = f(x_j) \quad \text{за} \quad a < x_j < b$$

В большинстве трудов о трубах с протекающим флюидом вводят следующие безразмерные параметры:

$$(3) \quad \eta = \frac{w}{l}; \zeta = \frac{x}{l}; \zeta_j = \frac{x_j}{l}; a_j = \frac{m_j}{l(m_f + m_p)}; \beta = \frac{m_f}{(m_f + m_p)};$$

$$\tau = \sqrt{\frac{EI}{m_f + m_p}} \frac{t}{l^2}; v = Vl \sqrt{\frac{m_f}{EI}}$$

Тогда уравнение (1) принимает следующий вид:

$$(4) \quad \frac{\partial^4 \eta}{\partial \zeta^4} + \left( 1 + \sum_{j=1}^m a_j \delta(\zeta - \zeta_j) \right) \frac{\partial^2 \eta}{\partial \tau^2} + 2\sqrt{\beta} v \frac{\partial^2 \eta}{\partial \zeta \partial \tau} + v^2 \frac{\partial^2 \eta}{\partial \zeta^2} = 0$$

Определение критической скорости флюида осуществляется спектральным методом Галёркина. Надо искать приближение к точному решению краевой задачи (4):

$$(5) \quad \eta(\zeta, \tau) = \sum_{i=1}^n W_i(\zeta) a_i(\tau)$$

В (5)  $W_i(\zeta)$  - функции формы трубы без сосредоточенных масс и без флюида в ней. Эти функции удовлетворяют граничные условия трубы.  $a_i(\tau)$  - неизвестные функции параметра  $\tau$ .

Выражение (5) не является точным решением дифференциального уравнения (4). Поэтому после подстановки в (4) получается функция ошибок  $R(\zeta, \tau)$ :

$$(6) \quad R(\zeta, \tau) = \left( 1 + \sum_{j=1}^m a_j \delta(\zeta - \zeta_j) \right) W_i \ddot{a}_i + 2\sqrt{\beta} \nu W_i^I \dot{a}_i + (W_i^{IV} + \nu^2 W_i^{II}) a_i$$

В методе Галёркина для функции ошибок  $R(\zeta, \tau)$  в области  $\zeta \in [0; 1]$  должно быть удовлетворено:

$$(7) \quad \int_0^1 R(\zeta, \tau) W_k(\zeta) d\zeta = 0 \quad \text{за } k = 1, \dots, n.$$

Условие (7) является требованием функция ошибок  $R(\zeta, \tau)$  быть ортогональной к всем основным функциям  $W_k(\zeta)$ . Выражение (6) подставляется в (7) и получается система дифференциальных уравнений с неизвестными функции  $a_i(\tau)$ . Эта система следующая:

$$(8) \quad \sum_{i=1}^n \int_0^1 \left[ \left( 1 + \sum_{j=1}^m a_j \delta(\zeta - \zeta_j) \right) W_i \ddot{a}_i + 2\sqrt{\beta} \nu W_i^I \dot{a}_i + (W_i^{IV} + \nu^2 W_i^{II}) a_i \right] W_k(\zeta) d\zeta = 0, \quad \text{за } k = 1, \dots, n$$

Это можно записать в виде матрицы так

$$(9) \quad [M] \ddot{a}_i + [C] \dot{a}_i + [K] a_i = 0$$

Принимая во внимание ортогональность функций  $W_i$  и  $W_k$  для шарнирно опёртой трубы на двух концах, каждый член матриц в (9) получается с использованием следующих формул [3]:

$$(10) \quad M_{ik} = 0.5 \delta_{ik} + \sum_{j=1}^m [a_j W_i(\zeta_j) W_k(\zeta_j)]$$

$$(11) \quad C_{ik} = 2\nu \sqrt{\beta} \frac{\lambda_i \lambda_k [1 - (-1)^{i+k}]}{\lambda_k^2 - \lambda_i^2} \quad \text{при } i \neq k \text{ и } C_{ik} = 0 \quad \text{при } i = k$$

$$(12) \quad K_{ik} = 0.5 (\lambda_i^4 - \nu^2 \lambda_i^2) \delta_{ik}$$

Здесь

$$(13) \quad \lambda_i = i\pi; \quad i = 1, 2, 3, \dots, n$$

$$(14) \quad W_i(\zeta) = \sin(\lambda_i \zeta);$$

$\delta_{ik}$  - символ Кронекера;

$$k = 1, 2, 3, \dots, n$$

Систему уравнений (9) можно записать в следующем виде:

$$(15) \quad [A] \{\dot{q}\} + [B] \{q\} = 0$$

Здесь

$$(16) \quad \{q\} = \{\dot{a}_i(\tau) \quad a_i(\tau)\}^T$$

$$(17) \quad A = \begin{bmatrix} [O] & [M] \\ [M] & [C] \end{bmatrix}$$

$$(18) \quad B = \begin{bmatrix} -[M] & [O] \\ [O] & [K] \end{bmatrix}$$

(15) умножается слева с  $[A]^{-1}$ . Получается:

$$(19) \quad [I] \{\dot{q}\} + [A]^{-1} [B] \{q\} = 0$$

где  $[I]$  - единичная матрица.

Для функции  $a_i$  принимается:

$$(20) \quad a_i = A_i e^{i\Omega\tau}$$

где  $i$  показателе является мнимая единица.

$A_i$  - константы, а  $\Omega$  - безразмерный параметр круговой частоты трубы  $\omega$ .

$$(21) \quad \Omega = \sqrt{\frac{(m_f + m_p) l^2 \omega}{EI}}$$

Тогда из (16) и (20) получается следующее выражение для  $\{q\}$ :

$$(22) \quad \{q\} = \{\dot{a}_i(\tau) \quad a_i(\tau)\}^T = e^{i\Omega\tau} \{u\}$$

В элементах вектора  $\{u\}$  участвуют константы  $A_i$ .

(22) подставляется в (19) и получается следующее уравнение:

$$(23) \quad i\Omega [I] \{u\} + [A]^{-1} [B] \{u\} = 0$$

Система (23) представляет задачу о собственных числах и о собственных векторах. Потом для конкретной скорости флюида могут быть определены значения  $\Omega$ . Если одно или несколько из этих значений имеет отрицательные мнимые части, то при соответствующей скорости система неустойчива. Это условие позволяет определить критическую скорость протекающего флюида. Если  $\text{Im}\Omega < 0$  и  $\text{Re}\Omega \neq 0$  то потеря устойчивости будет флаттером. Когда  $\text{Im}\Omega < 0$  и  $\text{Re}\Omega = 0$ , то потеря устойчивости - в дивергентной форме.

### 3. Численные исследования

Предметом исследования в данной работе является трубопровод (рис 1). Поперечное сечение - с внешним радиусом 0,1m и внутренним радиусом 0,095m. Модуль упругости трубы  $E = 2.1 \times 10^8 \text{ kN/m}^2$ , масса трубы на единице длины  $m_p = 0.02404 \text{ t/m}$ , а длина трубы  $l = 6 \text{ m}$ .

Исследована труба со статической схемой простой балки. С шестью одинаковыми сосредоточенными массами она разделена на семь равных отрезков. Сделаны исследования для трёх видов флюида с плотностями  $\rho_f = 0.8 \text{ t/m}^3$ ,  $\rho_f = 1 \text{ t/m}^3$ ,  $\rho_f = 1.2 \text{ t/m}^3$ . Полученные результаты представлены на графике на рис.2.

Исследования показывают, что для всех флюидов с увеличением сосредоточенной массы  $m_j$  до 0.15t критическая скорость флюида уменьшается. Когда масса выше этого значения, наоборот - критическая скорость флюида увеличивается.

В случае трубы без концентрированных масс критическая скорость флюида очень высока,  $V = 155 \text{ m/s}$  Для результатов, представленные на рисунке, критическая скорость достигается при флаттерной потери устойчивости.

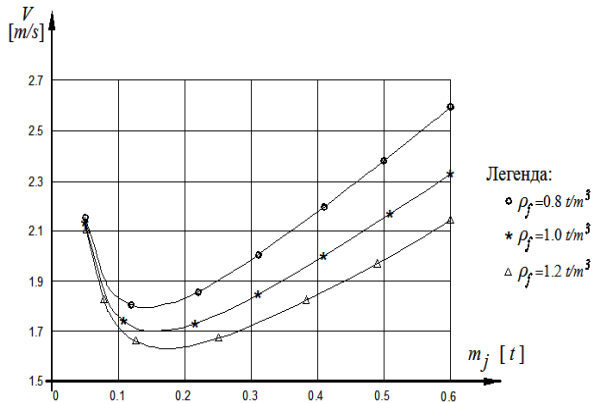

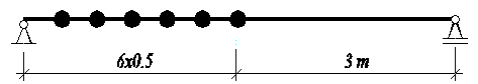

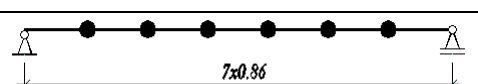


Рис. 2 Зависимость критической скорости флюида от значения  $m_j$  для трубы с шестью концентрированными массами для трёх типов протекаемых жидкостей.

Исследования показали, что при 1, 2, 3, 4 или 5 сосредоточенных масс, расположенных на равных расстояниях друг от друга вдоль оси трубы, для трех жидкостей ( $\rho_f = 0.8 \text{ t/m}^3$ ,  $\rho_f = 1 \text{ t/m}^3$ ,  $\rho_f = 1.2 \text{ t/m}^3$ ) и в пределах значений  $m_j < 0.6 \text{ t}$  потеря устойчивости трубы в дивергентной форме. Это соответствует очень высокой скорости флюида  $V = 155 \text{ m/s}$ . Такая скорость не достигается при транспортировке флюидов в трубопроводах.

Исследована труба с двумя шарнирами в концах. В таблице 1 показаны различные расположения шести масс. Определена критическая скорость протекающего флюида. Интересным является близость между значениями этой скорости в первом и в последнем случае. Потеря устойчивости для всех труб флаттером.

Таблица 1: Критическая скорость протекаемого флюида с  $\rho_f = 1.2 \text{ t/m}^3$  при различном расположении масс вдоль трубы ( $m_j = 0.2 \text{ t}$ ).

Статическая схема	Критическая скорость
	$V_{cr} = 1.67 \text{ m/s}$
	$V_{cr} = 8.41 \text{ m/s}$
	$V_{cr} = 6.68 \text{ m/s}$
	$V_{cr} = 1.64 \text{ m/s}$

#### 4. Выводы

Выполненные численные исследования показывают большое влияние концентрированных масс на критическую скорость флюида. Игнорирование масс может привести к аварии исследованных трубопроводов.

#### 5. Литература

[1] Chen S.S., J.A.Jendrejczyk. General Characteristics, Transition and Control of Instability of Tubes Conveying Fluids, Journal of Acoustical Society of America, 77, 887, 1985.

[2] Hill, J.L., C.P.Swanson. Effects of Lumped Masses on the Stability of Fluid Conveying Tubes, Transactions ASME, Journal of Applied Mechanics, 37, 494, 1970.

[3] Kang, M.G. Effect of rotary inertia of concentrated masses on the natural vibration of fluid conveying pipes, Journal of the Korean Nuclear Society, Vol. 31, Number 2, 1999, pp. 202-213.

[4] Chakraborty S. Some Applications of Dirac's Delta Function in Statistics for more Than One Random Variable, Applications and Applied Mathematics, Vol.3, Issue 1, 2008, pp. 42-54.

[5] Païdoussis, M.P. Fluid-Structure Interactions: Slender Structures and Axial Flow, Volume 1, Second edition, Elsevier, London, 2014.

[6] Wu, T.T., P.P.Raju. Vibration of a Fluid Conveying Pipe Carrying a Discrete Mass, Transactions ASME, Journal of Pressure Vessel Technology, November, 154, 1974.

# CONTENTS

## TRANSPORT TECHNIQS AND TECHNOLOGIES. SECURITY AND ECOLOGY.

### CREATION OF ACCUMULATION AND STORAGE OF ELECTRICAL ENERGY FOR DRIVERLESS ELECTRIC VEHICLES OF RUSSIAN PRODUCTION

Ph.D., Ass. Prof. Kurmaev R.Kh., Ph.D. Karpukhin K.E., Ph.D. Terenchenko A.S., D.Sc. Saykin A.M. 4, Struchkov V.S. .... 4

### ALTERNATIVE FUELS FOR DIESEL ENGINES AND THEIR IMPACT ON ENGINE EMISSIONS. A LITERATURE REVIEW

Zbarcea O. PhD student, Prof. Scarpete D. .... 8

### THE PARAMETRIC OSCILLATIONS OF STEEL FRICTION PLATES FOR A MULTIPLATE CLUTCHES

Prof. Dr. Eng. Taratorkin I., Prof. Dr. Eng. Derzhanskii V., postgraduate Taratorkin A. .... 14

### ОЦЕНКА СКОРОСТНЫХ СВОЙСТВ ГУСЕНИЧНЫХ МАШИН ПО ФАЗОВО-ЧАСТОТНЫМ ХАРАКТЕРИСТИКАМ

проф., д.т.н., Держанский В.Б., проф., д.т.н. Тараторкин И.А., к.т.н., Гизатуллин Ю.Н., инж., аспирант Тараторкин А.И.  
инж., аспирант Волков А.А. .... 18

### SUBHARMONIC RESONANCES IN THE HYDROMECHANICAL TRANSMISSION OF THE WHEELED CHASSIS

Prof. Dr. Eng. Derzhanskii V., Prof. Dr. Eng. Taratorkin I., postgraduate Taratorkin A. .... 22

### A METHOD OF VEHICLE-PEDESTRIAN ACCIDENT RECONSTRUCTION

Eng. Lyubenov D.A., PhD ..... 27

### CLEANING OF WATER AND SAND BEACHES FROM OIL AND OIL PRODUCTS WITH GRAPHITE SUPERSORBENT. METHODS AND EQUIPMENT.

Bondarenko O., Dr. eng. Strativnov E., Dr. eng. Kozhan A., Dr. eng. Dmitriev V., Dr. eng. Khovavko A. .... 30

### SIMULTANEOUS RESONANCE CASES IN A PITCH – ROLL SHIP MODEL. PART 1: FIRST – ORDER APPROXIMATE SOLUTIONS

Assoc. Prof. Dr. Deleanu D. .... 34

### SIMULTANEOUS RESONANCE CASES IN A PITCH – ROLL SHIP MODEL. PART 2: NUMERICAL ANALYSIS

Assoc. Prof. Dr. Deleanu D. .... 38

### POSSIBLE WAYS FOR ECOLOGIC PROBLEMS LIMITING CONCERNING THE PRODUCTION AND USAGE OF PETROLEUM FUELS

Stoyanka Petkova – Georgieva – associate professor, PhD. .... 42

### CERTIFICATION AND QUALIFICATION OF TOOLS FOR CODE GENERATION IN AUTOMOTIVE INDUSTRY

Dipl. Eng. Nikolay Petev Brayanov ..... 45

### EFFECT OF ADDITIVES IN PHASE COMPOSITION OF CARBON CATALYSTS OTHER THAN ASC WHETLERITE TYPE CARBONS ON THEIR REMOVAL EFFICIENCY AGAINST HYDROGEN CYANIDE VAPORS IN THE AIR

Mag.-Eng. Manoilova L., Mag.-Eng. Chatzis A., Assist. Prof. Dr. Eng. Vladov D. Ass. Prof. Dr. Eng. Spassova Iv.  
Ass. Prof. Dr. Eng. Nickolov R. .... 49

### MODIFIED ACTIVATED CARBONS AS MATERIALS FOR A DECONTAMINATION OF TI POISONED WATER

Mag.-Eng. Chatzis A., Assist. Prof. Dr. Eng. Tzvetkova P., Mag.-Eng. Manoilova L., Assist. Prof. Dr. Eng. Gentsheva G.,  
Ass. Prof. Dr. Eng. Nickolov R. .... 54

### ИЗБОР НА ВАРИАНТ ЗА ТРЕТИРАНЕ НА УТАЙКИТЕ ОТ ПРЕЧИСТВАТЕЛНА СТАНЦИЯ ЗА ОТПАДЪЧНИ ВОДИ – В. ТЪРНОВО

доц. д-р инж. Пенчо Стойчев ..... 58

### ЭКОЛОГИЧЕСКАЯ БЕЗОПАСНОСТЬ ИСТОЧНИКОВ ВОДОСНАБЖЕНИЯ КЫРГЫЗСКОЙ РЕСПУБЛИКИ.

К.т.н., проф. Каримов Т.Х., доцент Байгазы кызы Н., преп. Канаев М.Дж. .... 62

### ОПРЕДЕЛЯНЕ РАЗХОДА НА ГОРИВО ПРИ ИЗМЕНЕНИЕ МОМЕНТА НА ПОДАВАНЕТО НА ГОРИВО

д-р инж. Иван Георгиев, д-р инж. Евгени Драголов, доц. д-р инж. Стоян Георгиев, доц. д-р инж. Илиан Лилев ..... 64

### ОПРЕДЕЛЯНЕ ФУНКЦИОНАЛНАТА ВРЪЗКА МЕЖДУ РАЗХОДА НА ГОРИВО И СЪСТАВА НА ОТРАБОТИЛИТЕ ГАЗОВЕ ПРИ ИЗПРАВЕН ДВИГАТЕЛ

д-р инж. Иван Георгиев, д-р инж. Евгени Драголов, доц. д-р инж. Стоян Георгиев, доц. д-р инж. Илиан Лилев ..... 66

### ПОДОБРЕНИЕ НА АНАЛИТИЧНИЯ МЕТОД ЗА РЕШАВАНЕ НА ТРАНСПОРТНА ЗАДАЧА ПО КРИТЕРИЙ ВРЕМЕ

доц. д-р инж. Лилев И. Н. .... 68

### INFLUENCE OF URANIUM MINES IN THE FORMATION OF NATURAL BACKGROUND RADIATION

Ass. eng. Dolchinkov N. T., Prof., Doctor of chemical sciences, eng. Haralampiev M. S. .... 72

<b>RADIATION EFFECT ON HUMAN AND LIVING NATURE</b> Ass. eng. Dolchinkov N. T., Karaivanova-Dolchinkova B. E. ....	76
<b>ПРОГНОЗИРАНЕ СКОРОСТТА НА ДВИЖЕНИЕ ПО МАРШРУТ И ВРЕМЕТО ЗА ПРИСТИГАНЕ ПО УЧАСТЪЦИ</b> Eng. Pavel Stoyanov .....	79
<b>SAFETY OF INFORMATION-MANAGEMENT SYSTEMS IN RAILWAY TRANSPORT</b> Prof., Dr. Technical Science Moiseenko V. I., Postgraduate. Kotov M. O. ....	83
 <b>MECHANICS, DYNAMICS, STRENGTH. ANALYSIS OF ELEMENTS.</b>	
<b>NEW MATERIALS FOR IMPLANTS OF THE HUMAN HIP JOINT AND TECHNOLOGY OF THEIR MACHINING WITH THE ACHIEVEMENT OF HIGH PRECISION AND QUALITY OF SPHERICAL SURFACES</b> Doctor of science, Prof., Turmanidze R., Undergraduate student Popkhadze G. ....	86
<b>OPTIMIZATION OF GEOMETRIC PARAMETERS OF HARD METAL MICRO DRILLS TO INCREASE TOOL LIFE AND PERFORMANCE OF DRILLING PACKAGE OF PRINTED CIRCUIT BOARDS</b> Doctor of science, Prof., Turmanidze R., Senior laboratory Bachanadze V., Undergraduate student Popkhadze G. ....	91
<b>EXAMINATION OF ACOUSTIC PROPERTIES OF A GEAR PUMP AFTER TOOTH ROOT UNDERCUTTING USING THE INDUCTION OF DECISION TREES</b> PhD. , M.Sc. Deptula A. ....	96
<b>DIRECTIONS OF DEVELOPMENT MECHATRONIC DEVICES TO MOVE IN PIPELINES</b> Аврука И. С. ....	100
<b>MATERIALS FOR ELECTROMAGNETIC INTERFERANCE SHIELDING</b> Ass.prof. PhD Kamelia Ruskova, Assos. Prof. PhD Ljudmila Taneva , Assos. Prof. PhD Alexandar Lirkov .....	102
<b>ИЗСЛЕДВАНЕ НА ПОДАВАТЕЛНИ ЕЛЕКТРОЗАДВИЖВАНИЯ ЗА КЛАС МЕТАЛОРЕЖЕЩИ МАШИНИ</b> Гл. ас. д-р инж. М. Жилевски, Проф. д-р инж. М. Михов .....	105
<b>АВТОМАТИЗИРАНО УПРАВЛЕНИЕ НА ФИКСИРАЩ МОДУЛ ЗА ФРЕЗОВИ МАШИНИ</b> Маг. инж. М. Жилевска .....	109
<b>AUTOWAVES OF LOCALIZED PLASTIC DEFORMATION ON THE YIELD PLATEAU AND ON THE WORK HARDENING STAGE</b> Prof. Dr. Phys.-Mat. Sci. Danilov V., Cand. Phys.-Mat. Sci. Gorbatenko V., Prof. Dr. Phys.-Mat. Sci., Zuev L. ....	113
<b>ДИНАМИЧЕСКАЯ УСТОЙЧИВОСТЬ ТРУБОПРОВОДА С КОНЦЕНТРИРОВАННЫМИ МАССАМИ</b> гл.ас. д-р инж. Лолов Д., проф. д-р инж. Лилкова-Маркова Св. ....	117